COMPUTER-AIDED STRUCTURAL ENGINEERING (CASE) PROJECT

TECHNICAL REPORT ITL-92-7

REFINED STRESS ANALYSIS OF MELVIN PRICE LOCKS AND DAM

by

H. Wayne Jones

Information Technology Laboratory

DEPARTMENT OF THE ARMY
Waterways Experiment Station, Corps of Engineers
3909 Halls Ferry Road, Vicksburg, Mississippi 39180-6199

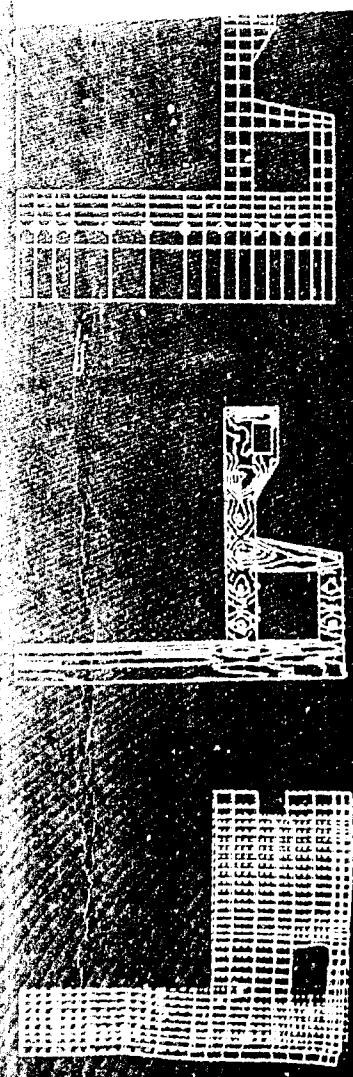

September 1992
Final Report

Prepared for US Army Engineer District, St. Louis
St. Louis, Missouri 63101-1986

Destroy this report when no longer needed. Do not return it to the originator.

The findings in this report are not to be construed as an official Department of the Army position unless so designated by other authorized documents.

The contents of this report are not to be used for advertising, publication, or promotional purposes. Citation of trade names does not constitute an official endorsement or approval of the use of such commercial products.

REPORT DOCUMENTATION PAGE

Form Approved
OMB No. 0704-0188

1. AGENCY USE ONLY *(Leave blank)*	2. REPORT DATE	3. REPORT TYPE AND DATES COVERED
	September 1992	Final report

4. TITLE AND SUBTITLE

Refined Stress Analysis of Melvin Price Locks and Dam

5. FUNDING NUMBERS

DA Form 2544
No. ED87-30

6. AUTHOR(S)

H. Wayne Jones

7. PERFORMING ORGANIZATION NAME(S) AND ADDRESS(ES)

US Army Engineer Waterways Experiment Station,
Information Technology Laboratory,
3909 Halls Ferry Road, Vicksburg, MS 39180-6199

8. PERFORMING ORGANIZATION REPORT NUMBER

Technical Report ITL-92-7

9. SPONSORING/MONITORING AGENCY NAME(S) AND ADDRESS(ES)

US Army Engineer District, St. Louis
St. Louis, MO 63101-1986

10. SPONSORING/MONITORING AGENCY REPORT NUMBER

11. SUPPLEMENTARY NOTES

Available from National Technical Information Service, 5285 Port Royal Road, Springfield, VA 22161.

12a. DISTRIBUTION/AVAILABILITY STATEMENT

Approved for public release; distribution is unlimited.

12b. DISTRIBUTION CODE

13. ABSTRACT *(Maximum 200 words)*

The analysis and design of massive concrete structures have been the object of much interest and study by the engineering community for many years. Recent advances in computer technology coupled with the advances in numerical modeling and analysis techniques have provided ever increasing abilities to perform complex structural analyses. Nonlinear, incremental construction analyses with time-dependent material properties can now be realistically performed giving the designer more insight into the behavior of the structures.

This report provides information on the modeling, analysis, and results for the nonlinear, incremental construction of two monoliths of the Melvin Price Locks and Dam under thermal and gravity loadings. These monoliths were analyzed using a concrete material model which considers aging, creep, shrinkage, and temperature effects.

14. SUBJECT TERMS

Creep
Incremental construction
Pile loads
Shrinkage
Thermal loads

15. NUMBER OF PAGES

193

16. PRICE CODE

17. SECURITY CLASSIFICATION OF REPORT	18. SECURITY CLASSIFICATION OF THIS PAGE	19. SECURITY CLASSIFICATION OF ABSTRACT	20. LIMITATION OF ABSTRACT
UNCLASSIFIED	UNCLASSIFIED		

Contents

Preface

The investigation described in this report was conducted for the U.S. Army Engineer District, St. Louis. Authorization was given by DA Form 2544, No. ED87-30, dated 10 April 1987. Funds for publication of the report were provided from those available for the Computer-Aided Structural Engineering program managed by the Information Technology Laboratory (ITL) at the U.S. Army Engineer Waterways Experiment Station (WES).

The investigation was performed and this report was prepared at WES by Mr. H. Wayne Jones, Scientific and Engineering Applications Center, ITL, under the general supervision of Dr. N. Radhakrishnan, Director, ITL. The author acknowledges Mr. Anthony Bombich, Concrete Technology Division, Structures Laboratory, WES, and Mr. Barry Fehl, who was the technical monitor for the U.S. Army Engineer District, St. Louis, for their help during this investigation.

At the time of publication of this report, Director of WES was Dr. Robert W. Whalin. Commander and Deputy Director was COL Leonard G. Hassell.

Conversion Factors, Non-SI to SI Units of Measurement

Non-SI units of measurement in this report can be converted to SI units as follows:

Multiply	By	To Obtain
Btu (International Table) per pound (mass) · degree Fahrenheit	4,186.8	Joules per kilogram kelvin
Btu (International Table) · inch per hour · square inch · degree Fahrenheit	20.7688176	watts per metre kelvin
calories/g	0.007738283	*kilojoules/kilogram*
Fahrenheit degrees	5/9	Celsius degrees or kelvins[1]
inches	25.4	millimetres
kips	4.448222	kilonewtons
microinches per inch	1.0	micromillimetres/millimetre
pounds (force) per square inch	0.006894757	megapascals
pounds (mass) per cubic inch	27,679.899	kilograms per cubic metre

[1] To obtain Celsius (C) temperature readings from Fahrenheit (F) readings, use the following formula: C = (5/9)(F-32). To obtain Kelvin (K) readings, use: K = (5/9)(F-32) + 273.15.

1 Introduction

Background

In 1983, the U.S. Army Engineer Waterways Experiment Station (WES) was requested by the U.S. Army Engineer (USAE) District, St. Louis, to analyze the lower gate monolith (L-17) and one intermediate lock chamber monolith (L-13) of the Melvin Price Locks and Dam on the Mississippi River for thermal and construction induced stresses using the finite element method (FEM). Phase I of this thermal study (Bombich, Norman, and Jones 1987) addressed the following four principal issues:

a. Select the most effective finite element (FE) analysis program to perform the thermal stress analysis.

b. Verify the FE analysis program on problems with known results.

c. Perform two-dimensions (2-D) analysis of the L-13 and L-17 monoliths of Melvin Price Locks and Dam and compare with previous analysis method results.

d. Perform a three-dimensional (3-D) analysis of these monoliths.

The PHASE I study was a cooperative effort between the Information Technology Laboratory (ITL) and the Structures Laboratory (SL) of WES. Numerous coordination meetings were held during the life of the project between personnel of the USAE District, St. Louis, SL, ITL, the Lower Mississippi Valley Division, and Headquarters, U.S. Army Corps of Engineers, to review progress and address problems as they occurred.

Summary of Previous Study

The Phase I study resulted in the selection of the general-purpose structural and heat transfer FE program, ABAQUS (Hibbitt, Karlsson, and Sorensen, Inc., 1987). The ABAQUS program was selected because of it flexibility and capability to perform the desired heat transfer and thermal

stress analysis. ABAQUS also had good pre- and postprocessing capabilities and was readily available to USAE field offices. It has a broad range of finite elements in its library which may be used separately or in combination as necessary for the type of analysis performed. Although ABAQUS has several material constitutive models, it was necessary to use the added capability of a user-defined constitutive material model entered through a user-supplied subroutine. The user-defined material model subroutine used in this study was developed by Anatech, Inc. The ABAQUS program has the ability to perform both static and time-history stress analyses. Although not used in this study, reinforcement (rebars) can be added to most elements, if desired. The heat transfer analysis can be transient or steady-state. A wide variety of boundary conditions required for both the stress and heat transfer analyses performed in this study are available in the ABAQUS program.

The Phase I study then investigated whether or not ABAQUS could effectively perform an incremental construction analysis as required for both the temperature and stress analyses. In the method developed to perform this staged construction analysis, the structure is modeled continuously at specified stages during its construction, with stresses and temperatures accumulated during the entire construction sequence.

A series of verification problems were examined to ensure that ABAQUS was operating properly and that the analysts could adequately model all of the desired behavior characteristics expected within the structure during the incremental construction process. After some necessary modifications to ABAQUS, it was determined that the desired 2-D analyses could be performed satisfactorily.

Next, the 2-D analyses of L-13 and L-17 were performed. As a result of these analyses, it was further determined that the ABAQUS program could adequately model the phenomena that occur during the incremental construction process on a full-scale structure. However, it was also determined that certain refinements to the user-supplied constitutive model were necessary to accurately predict the stresses, deflections, and pile loads within the monoliths. The pile loads were observed to be particularly dependent upon the modulus and creep properties used in the user-supplied constitutive model. It was clear from this phase I study that the early-age modulus of elasticity predicted by the material model was higher than that of the actual Melvin Price Locks and Dam concrete. It was also evident that the creep and shrinkage numerical models used in the constitutive model should be more carefully examined and refined to ensure that they adequately represent the actual behavior of the concrete.

The 3-D analyses were not completed because computer costs became prohibitive. The grids and input data for these analyses were retained so that they could be completed at a later time when they proved to be more economically feasible.

Objective of Phase II Study

The objective of the portion of the Phase II study documented within this report is a reanalysis of monoliths L-13 and L-17 with a revised constitutive model that more accurately models the behavior of the concrete from Melvin Price Locks and Dam. Particular emphasis will be given to examining the stresses within the monoliths and the loads within the piles. The parameters used in the revised material model will be presented herein. However, another report (Bombich, Norman, and Garner 1991) from this Phase II study documents the testing, calibration, and verification procedures employed to develop this more accurate material model.

Revised Material Model for Phase II Study

As stated above, one part of the Phase II study was to calibrate the material model to more accurately reflect the behavior of the Melvin Price Locks and Dam concrete. Only the resulting parameters are reported in this report. A more comprehensive discussion of the procedure used to develop these parameters is presented by Bombich, Norman, and Garner (1991). It was evident that the material behavior was not known to the extent that single curves for modeling the material behaviors of adiabatic temperature rise, modulus of elasticity, creep, and shrinkage could be determined. It was decided that a more realistic approach would be to use bounds on these parameters which reflect the confidence with which each is known. Plots of the curves reflecting these bounds for adiabatic temperature rise, modulus of elasticity, creep, and shrinkage are shown in Figures 1 through 4, respectively. The revised user-supplied subroutine which defines the material constitutive model was used. The revised material input information necessary for the ABAQUS data file is given in Appendix A. No changes were made to the temperature analysis data input since all modifications were in the temperature rise subroutine.

Finite Element Models

The FE grids developed for the initial Phase I study (Bombich, Norman, and Jones 1987) were used in this reanalysis. The 2-D grid for monolith L-13 is shown in Figure 5. This temperature analysis model contains 160 elements for the structure and soil foundation. Figure 6 shows the 2-D grid for monolith L-17. This temperature analysis model contains 316 elements for the structure and soil foundation. The stress analysis models for both monoliths use the same grids but do not include the soil foundation elements.

Additional Input Parameters

The additional input data required for the analyses are boundary conditions, material properties, pile locations, pile properties, and load step information. These data are taken form the Phase I study and are detailed by Bombich, Norman, and Jones (1987). They will not be presented again in this report. The bulk data file for the stress analysis was modified slightly to reflect the new material model (Appendix A).

Loading Conditions

After the incremental construction temperature analysis is performed for the structural and soil foundation system, the resulting temperature history is then used as a loading for the incremental construction stress analysis of the structure. L-13 is analyzed through day 47, 7 days after placement of the last lift, while the L-17 analysis is carried through 5 days after placement of the last lift. Temperatures and stresses for L-13 and L-17 are examined at several stages throughout the construction process. Pile loads are presented only at the end of construction for each monolith.

The preliminary results from the second lock study (Truman, Petruska, and Fehri in preparation) indicated that it was neither practical nor necessary to analyze all possible load case combinations resulting from the use of the upper and lower bounds on the material parameters. It was determined that, for the purposes of this study, the load cases 1 and 5 shown in Table 1 would provide the desired bounds on the stresses and pile loads desired. This resulted in the heat transfer analysis only being performed for the upper bound adiabatic condition and all stress analyses using the upper modulus of elasticity values. Load case 0 (upper bound on temperature rise and modulus and no creep or shrinkage effects), although an unrealistic conditions, was included in the L-13 analyses. Load cases nts (upper modulus curve but no temperature effects) was analyzed for both

Table 1
Load Cases To Be Analyzed

Load Case[1] Name	Adiabatic Temperature	Modulus of Elasticity	Shrinkage	Creep
0	Upper bound	Upper bound	Not used	Not used
1	Upper bound	Upper bound	Upper bound	Upper bound
5	Upper bound	Upper bound	Lower bound	Lower bound
nts	Not used	Upper bound	Not used	Not used

[1] The load case numbers correspond to those used by Truman, Petruska, and Fehri (in preparation).

monoliths. All of these analyses were performed using the 2-D plane strain assumptions. An additional analysis was performed on monolith L-13 using 2-D plane stress assumptions for load case 5. The reason for including this analysis will be discussed along with the L-13 results.

2 Temperature Analyses of Monoliths L-13 and L-17

General

This section will describe and present the temperature analyses of monoliths L-13 and L-17. The FE models developed during the Phase I study are used in Phase II. Figure 5 shows the grid used in the temperature analysis of monolith L-13. Figure 6 shows the grid used in the temperature analysis for monolith L-17. Both the soil foundation and structure are included within these models. The analyses were performed with each lift being placed at 5-day intervals, until the entire structure was in place. Since the highest temperatures would create the most severe loading, it was decided to run the analyses for the upper adiabatic temperature rise curve only. The new adiabatic temperature rise model was developed as part of this Phase II study (Bombich, Norman, and Garner 1991) and is presented in Figure 1 as a set of bounding curves. The upper bound adiabatic curve which was used for this study is almost identical to the adiabatic curve used during the Phase I study.

Presentation of Results

Temperature results in the form of contour plots are presented in Figures 7a-7d for four stages of the construction of L-13. These stages are 5 days after placement of lifts 2, 4, and 5 and 7 days after placement of lift 9. Figures 8a-8d present contour plots of temperature results for four stages of construction of L-17. These stages are 5 days after placement of lifts 4, 7, 13, and 16. All of these analyses use the upper bound for adiabatic temperature rise.

Discussion of Results

The temperature results from this study are almost identical to the ABAQUS results from the Phase I study. This is to be expected since the upper adiabatic temperature rise (Figure 1) curve used in this study is almost the identical curve used in the Phase I study. Since the temperature rise curve is essentially the only change in these analyses from the Phase I study, the temperature contours obtained in this study and presented in Figures 7a-7d for monolith L-13 and Figures 8a-8d for monolith L-17 fall almost exactly on top of the Phase I contours. The numerical results from the two studies show the temperatures to vary by less than 1 deg F.[1] These results indicate that a good approximation of temperatures within the monoliths can be obtained for 2-D problems by the modeling procedure developed in the Phase I study, the ABAQUS program, and the material model refined during this Phase II study.

---

[1] A table of factors for converting non-SI units of measurement to SI units is presented on page v.

3 Stress Analyses of Monolith L-13

General

This section will describe and present the stress analyses of monolith L-13. The FE model developed during the Phase I study will be used in this Phase II study. Figure 5 shows the grid of L-13 to be used in the stress analyses; however, the soil foundation elements will not be included in the model. The piles will be included in the model as linear horizontal and vertical springs with stiffnesses described in the Phase I report. The analyses consist of placing (building) the monolith in lifts at 5-day intervals, until the entire structure is in place. The temperatures calculated during the heat transfer analysis performed earlier will be used as loading for the stress analyses which include temperature effects. The revised material constitutive model will be used. The four load cases described in Table 1 will be analyzed for plane strain conditions. Additionally, load case 5 will be analyzed using plane stress assumptions.

Presentation of Results For Monolith L-13

Stress contours are presented to show the stress distribution within the structure for the five loading conditions analyzed by ABAQUS. Contours of horizontal (stress 1), vertical (stress 2), out-of-plane (stress 3), and maximum principal stress are given. The displaced structure is also presented. These stresses and deflections are given at 5 days after placement of lifts 2, 4, and 5 and 7 days after placement of lift 9. Pile loads will also be presented at 7 days after placement of lift 9.

Load case nts gravity loading

The 2-D plane strain analysis was performed for the incremental construction of L-13. Only gravity loads were applied. Figures 9a-9d give

the horizontal stress contours within the structure at four stages of construction. Figures 10a-10d give the vertical stress contours within the structure at the same stages of construction; Figures 11a-11d give the corresponding out-of-plane stress contours; Figures 12a-12d give the maximum principal stress contours; and Figures 13a-13d give the deflected shapes.

Load case 0
gravity and thermal loading

The 2-D plane strain analysis was performed again for the incremental construction of L-13 with thermal loadings added but no creep or shrinkage considered. Figures 14a-14d give the horizontal stress contours within the structure at the four stages of construction; Figures 15a-15d give the corresponding vertical stress contours; Figures 16a-16d give the out-of-plane stress contours; Figures 17a-17d give the maximum principal stress contours; and Figures 18a-18d give the deflected shapes.

Load case 1
gravity and thermal loading

Again, the 2-D plane strain analysis was performed for the incremental construction of L-13 under gravity and thermal loads but with the upper bound on both creep and shrinkage included. Figures 19a-19d give the horizontal stress contours within the structure at the four stages of construction; Figures 20a-20d give the corresponding vertical stress contours; Figures 21a-21d give the out-of-plane stress contours; Figures 22a-22d give the maximum principal stress contours; and Figures 23a-23d give the deflected shapes.

Load case 5
gravity and thermal loading

The 2-D plane strain analysis was again performed for the incremental construction of L-13. This time the lower bounds on both creep and shrinkage were used while both gravity and thermal loads were applied. Figures 24a-24d give the horizontal stress contours within the structure at the four stages of construction; Figures 25a-25d give the corresponding vertical stress contours; Figures 26a-26d give the out-of-plane stress contours; Figures 27a-27d give the maximum principal stress contours; and Figures 28a-28d give the deflected shapes.

Load case 5PS
gravity and thermal loading

A 2-D plane stress analysis was performed for the incremental construction of L-13 for gravity and thermal loadings using the lower bounds for both creep and shrinkage. Figures 29a-29d present horizontal stress contours within the structure at the four stages of construction; Figures 30a-30d give the corresponding vertical stress contours; Figures 31a-31d give the out-of-plane stress contours; Figures 32a-32d give the maximum principal stress contours; and Figures 33a-33d give the deflected shapes.

Pile load summary

Table 2 presents a summary of the resulting pile loads at the end of construction (placement of lift 9 plus 7 days) for the five analyses performed. These may be compared to the pile loads reported in the Phase I study (Bombich, Norman, and Jones 1987).

Table 2
Vertical Pile Loads for Monolith 13 (7 Days After Placement of Top Lift)

	Gravity Only	Gravity and Thermal Loading (Upper Mod/Adiabatic)			
Pile No.	Load Case nts kips	Load Case 0 (No Creep/Shrink) kips	Load Case 1 (Upper Creep/Shrink) kips	Load Case 5 (Lower Creep/Shrink) kips	Load Case 5SP (Lower Creep/Shrink Plane Stress) kips
1	77.5	60.6	68.4	73.1	72.4
2	81.2	64.3	73.4	77.3	76.7
3	91.9	74.8	87.5	89.1	88.6
4	108.1	90.7	109.5	107.2	107.1
5	145.0	126.8	157.8	147.7	147.9
6	178.0	158.9	198.7	182.8	183.6
7	200.2	182.1	223.5	205.4	206.4
8	205.5	192.0	223.5	208.7	209.7
9	193.3	193.3	196.5	192.9	193.4
10	185.7	197.8	181.2	184.6	184.8
11	180.0	207.9	169.9	179.8	179.6
12	177.5	226.1	165.0	180.2	179.6

Discussion of Results for Monolith L-13

Load case nts

Load case nts stress contours show results expected for the incremental construction with gravity loading only. The horizontal stresses (Figures 9a-9d) show bending at the lock center line with stresses between -300 psi and 150 psi. Another stress concentration is located just inside the lock wall. Here the base slab, acting as a beam on an elastic foundation, bends under its own weight as the central portion deflects downward. Later, this bending is increased as the culvert and wall sections are placed. The maximum horizontal stress at this location is approximately 250 psi. The vertical (Figures 10a-10d) and out-of-plane (Figure 11a-11d) stresses did not display any unusual characteristic. The maximum principal stresses (Figures 12a-12d) follow a pattern similar to that of the horizontal stresses. The deflected shape plots (Figures 13a-13d) demonstrate the observation that the base slab initially deflects downward in the center. Later, as construction continues, the portion of the slab under the culvert and wall deflects downward almost the same amount. Very little horizontal deflection is indicated, as expected.

Load case 0

Load case 0 deflected shapes (Figures 18a-18d) indicate a substantial amount of positive horizontal movement along the base slab. This is due to the expansion of the concrete resulting from an increase in temperature. This expansion results in an excessive outward (to the right) and downward movement of the right end of the base slab. Also, the plane strain conditions (fixed against movement) at the out-of-plane faces cause very large compressive out-of-plane stresses (Figures 16a-16d) to develop as expansion in this direction is restricted. These stresses are in excess of 350 psi and correspond very closely in location to the high temperatures obtained in the heat transfer analysis. These stresses should be expected for the load case under consideration, however, this is not a condition which will actually exist in the real structure. Creep and shrinkage, along with small movements in this out-of-plane direction, would relieve most, if not all, of these stresses. The horizontal (Figures 14a-14d), vertical (Figures 15a-15d), and maximum principal (Figures 17a-17d) stress contours also reflect higher values than from load case nts. These higher values are the result of the thermal loads, which occur with no relief mechanism, and the Poisson effect from the very large out-of-plane stresses. This load case is unrealistic because stresses due to thermal loads will be reduced significantly by creep. Thermal expansion should be considered only if creep is also included.

Load case 1

The deflected shape plots (Figures 23a-23d) show that the thermal expansion in the previous load case are negated by the creep and shrinkage effects included here. The upper bounds for creep and shrinkage which were used here not only cancel the expansion, but actually cause an overall contraction (shrinkage) of the monolith in the out-of-plane direction. This creates the unusual condition of having the two out-of-plane faces of the monolith slice actually holding on to the monolith as it tries to shrink. This causes high tension stresses (Figures 21a-21d) to develop in this out-of-plane direction which are as large in magnitude as the corresponding compression stresses found in the previous load case. This effect, a monolith being held in tension by the two surrounding vertical construction joints, is not realistic. The idea of performing a plane stress analysis resulted form this finding, since the plane stress assumption would allow the two faces to move toward each other if the shrinkage was large enough. The horizontal (Figures 19a-19d), vertical (Figures 20a-20d), and maximum principal (Figures 22a-22d) stress contours reflected reasonable stresses within the structure for the given loadings. The deflected shape plots indicated that the inclusion of creep allowed the base slab to relax thereby causing the vertical deflections to be greatest underneath the outer wall section. The vertical loads tend to have a more localized effect when creep was included.

Load case 5

This load case has the same loadings as load case 1, except it used the lower bounds on creep and shrinkage. The deflected shape plots (Figures 28a-28d) are very similar to load case 1 with slightly smaller magnitudes. Since the creep and shrinkage effects are lower, the horizontal contraction of the base slab is less. The vertical deflection of the slab under the wall is also smaller than in load case 1. This reduction in shrinkage effects causes the contraction in the out-of-plane direction to be less, thereby causing a smaller tension stress (Figures 26a-26d) to develop in that direction. This out-of-plane stress, although smaller, is still unrealistic. The horizontal (Figures 24a-24d), vertical (Figures 25a-25d), and maximum principal (Figures 27a-27d) stresses also follow a similar pattern to load case 1, but again with reduced magnitudes.

Load case 5PS

This load case (same loading and material properties as load case 5, but with a plane stress assumption) was analyzed when it was found that the plane strain assumption created the very high tensile stresses in the out-of-plane direction when creep and shrinkage effects were used. It was determined that this may be a more realistic model since the out-of-plane restraint against shrinkage will not occur to this degree in the real structure. If the shrinkage effects are large enough to overcome the thermal

expansion and cause the overall length of the monolith to decrease, a plane stress analysis should be used in lieu of the plane strain analysis. Even if a 3-D analysis were available, some assumption would be necessary at the monolith faces which would still create essentially the same choices for the analyst.

The deflected shape plots (Figure 33a-33d) show the in-plane deflections of the plane stress and plane strain cases to be essentially identical. This was expected. The out-of-plane stresses (Figures 31a-31d) were reduced to almost zero. This reduction id due to the free movement in that direction. Although this may not be exactly what actually occurs, it is probably closer to reality than the plane strain analysis. The horizontal (Figures 29a-29d), vertical (Figures 30a-30d), and maximum principal (Figures 32a-32d) stresses are very similar to the plane strain stress results but are reduced very slightly. This reduction is caused by the reduced Poisson effect from the out-of-plane stresses. Essentially, the effect of going to the plane stress assumption was that the very high, unrealistic out-of-plane stresses were eliminated, and all other stresses and deflections remained unchanged.

Pile loads

The pile loads from all of the above load cases are presented in Table 2. These pile loads should be compared to the Phase I results (Bombich, Norman, and Jones 1987) to get a better understanding of the effects of the revised material model. This comparison shows that the new model gives somewhat similar pile load distributions but reduces the maximum pile loads predicted by the Phase I study. This is largely due to the reduced creep effect which caused the structure to over relax and allow the vertical loads to be carried mostly by the piles directly below them. The new model spreads the vertical loading out over the pile foundation more evenly.

This redistribution is demonstrated by the slight variation of pile loads observed in Phase I and those observed in load case nts of Phase II. The change is less than 3 kips per pile and shows a move toward a uniform pile loading. These results are as expected for the new constitutive model. The maximum pile load in this load case is 205 kips, similar to that of 208 kips from the Phase I study. These new results are even closer to the gravity turn-on analysis results which were used by USAE District, St. Louis, to design the pile. The design pile load was 200 kips.

Load case 0 gives the largest vertical pile loads toward the right end of the slab. This is caused by the thermal expansion (to the right) and the downward deflection of the right end of the slab due to thermal bending. This thermal bending is a result of constructing the slab in lifts which are at different temperatures. This layered thermal expansion effect of the composite slab causes it to bend downward at the right end. This is shown by examining the deflected shape plots for this load case. The

maximum pile load is 226 kips, higher than desired, while the Phase I study gave 230 kips as the maximum load. Again, it should be pointed out that this load case is unrealistic and gives a pile load distribution which over loads some piles and under loads others.

Load cases 1 and 5 will be discussed together since they are identical, except for the amount of creep and shrinkage included. The pile load distributions are similar to the Phase I study with the magnitudes of the heavily loaded piles being smaller in the new analyses. This is due mainly to the new material model containing a smaller creep effect. This reduced creep effect causes the vertical structural loadings to be more evenly distributed over the entire pile foundation. This is clearly shown when the upper creep (load case 1) and lower creep (load case 5) pile loads are compared. The maximum pile load reduces from 224 kips (load case 1) to 209 kips (load case 5) when the reduced creep effect is used. These maximum pile loads occur under the wall stem where the greatest vertical load is being applied to the slab. The lower creep effects are assumed to be more realistic for this concrete, therefore, the load case 5 results show the pile loads to be reasonably close to the 200-kip value used in the design.

The plane stress analysis (load case 5PS) was performed to see what effect the excessive out-of-plane stress due to shrinkage would have on the pile loads. As seen in the results, there was nominally less than a 1-kip difference in each pile. It was concluded, therefore, that there was no need to reanalyze any load case that was performed using the plane strain condition. The pile loads could be assumed to be the same for the plane stress case.

4 Stress Analyses of Monolith L-17

General

This section will describe and present the stress analyses of monolith L-17. The FE model developed during the Phase I study will be used in this Phase II study also. Figure 6 shows the grid of L-17 to be used in the stress analyses; however, the soil foundation elements will not be included in the model. The piles will be included in this model as linear horizontal and vertical springs with stiffnesses described in the Phase I report. The analyses consist of placing (building) the monolith in lifts at 5-day intervals, until the entire structure is in place. The temperatures calculated during the heat transfer analysis of L-17, performed earlier, will be used as loading for all stress analyses including temperature effects. The revised material constitutive model will be used. Three of the four load cases described in Table 1 will be analyzed for plane strain conditions. Load case 0 will not be analyzed since it is an unrealistic condition.

Presentation of Results For Monolith L-17

Stress contours are presented to show the stress distribution within the structure for the three loading conditions analyzed by ABAQUS. Contours of horizontal (stress 1), vertical (stress 2), out-of-plane (stress 3), and maximum principal stresses are given. The displaced structure is also presented. These stresses and deflections are given at 5 days after placement of lifts 4, 7, and 16. Pile loads will also be presented at 5 days after placement of lift 16.

Load case nts gravity loading

The 2-D plane strain analysis was performed for the incremental construction of L-17. Gravity loads only were applied. Figures 34a-34c give

the horizontal stress contours within the structure at three stages of construction; Figures 35a-35c give the vertical stress contours within the structure at the same stages of construction; Figures 36a-36c give the corresponding out-of-plane stress contours; Figures 37a-37c give the maximum principal stress contours; and Figures 38a-3c give the deflected shapes.

Load case 1
gravity and thermal loading

Again, the 2-D plane strain analysis was performed for the incremental construction of L-17 under gravity and thermal loads but with the upper bounds on both creep and shrinkage included. Figures 39a-39c give the horizontal stress contours within the structure at the three stages of construction; Figures 40a-40c give the corresponding vertical stress contours; Figures 41a-41c give the out-of-plane stress contours; Figures 42a-42c give the maximum principal stress contours; and Figures 43a-43c give the deflected shapes.

Load case 5
gravity and thermal loading

The 2-D plane strain analysis was again performed for the incremental construction of L-17. This time the lower bounds on both creep and shrinkage were used while both gravity and thermal loads were applied. Figures 44a-44c give the horizontal stress contours within the structure at the three stages of construction; Figures 45a-45c give the corresponding vertical stress contours; Figures 46a-46c give the out-of-plane stress contours; Figures 47a-47c give the maximum principal stress contours; and Figures 48a-48c give the deflected shapes.

Pile load summary

Table 3 presents a summary of the resulting pile loads at the end of construction (placement of lift 16 plus 5 days) for the three analyses performed. These may be compared to the pile loads reported in the Phase I study (Bombich, Norman, and Jones 1987).

Discussion of Results for Monolith L-17

Load case nts

The results from the gravity only load case show a more uniform vertical deflection (Figures 38a-38c) of the base slab than the L-13 analysis.

Table 3
Vertical Pile Loads for Monolith 17 (5 Days After Placement of Top Lift)

Pile	Gravity	Gravity and Thermal Loading (Upper Mod/Adiabatic)	
No.	Only kips	Lower Creep/Shrink kips	Upper Creep/Shrink kips
1	100.2	97.7	95.2
2	102.7	99.1	96.6
3	106.2	98.7	93.8
4	177.7	155.1	141.5
5	183.5	144.6	120.0
6	192.9	135.0	92.1
7	201.6	115.8	95.5
8	214.6	129.9	147.4
9	226.3	168.2	192.9
10	241.7	198.2	235.8
11	254.2	223.2	267.6
12	267.6	245.5	294.3
13	278.8	264.1	312.6
14	286.6	280.0	322.2
15	294.7	300.0	330.1
16	302.3	324.4	333.8
17	320.2	367.6	352.2
18	349.1	430.9	385.1
19	259.5	344.2	209.1

This is due in part to the pile distribution underneath the slab. At the end of construction, the vertical deflections increase almost linearly from the center line to the right end of the base slab. The horizontal stress contours (Figures 34a-34c) show the bending which occurs, as expected, at the center line. The vertical stresses (Figures 35a-35c) at any location are mostly the result of the concrete load directly overhead. The maximum principal stresses (Figures 37a-37c) follow the same general pattern as the horizontal stresses. The out-of-plane stresses (Figures 36a-36c) are very small since no thermal loading is included.

Load case 1

When thermal effects and the upper bounds on creep and shrinkage are included, several phenomena occur. First, as the horizontal (Figures 39a-39c) and maximum principal (Figures 42a-42c) stress contours and the deflected shape plots (Figures 43a-43c) are inspected, it is evident that a vertical crack in the base slab appears to begin with placement of the seventh lift. This crack is located at the top of the base slab, between the one-third and one-half points along the slab. It appears to propagate completely through the slab by the end of construction. This location is probably connected to a change in pile stiffness in this area. While this crack was not indicated by the Phase I study, there was evidence from the maximum principal stress plots for the load case considering thermal and gravity loading without creep and shrinkage using UMAT1, that a stress buildup was occurring in the same general location. Another phenomenon is an instability which occurred immediately above the culvert. This stress state was so sensitive that the form work supporting the top of the culvert had to be removed a couple of days early so the numerical disturbance they created would not cause the top of the culvert to crack. Once this form work was removed, no other substantial cracking in this area occurred.

Several points should be kept in mind when considering these cracks. First, the crack appears in the top of the slab and propagates slowly. The slab is reinforced for just such moment resistance. The constitutive model used here does not include the tensile strength of the rebars. The model will eventually include the rebars, but it has not yet been thoroughly tested with them included. It is obvious that once the rebars are available, they will carry this tension stress which the present concrete can not carry. Second, the smeared crack constitutive model used, coupled with the very coarse grid (with respect to crack propagation analysis), tend to be a poor way to attempt to predict crack propagation. To attempt to model the crack propagation with the present smeared crack model would require a much more refined grid, which is impractical to run due to prohibitive computer costs. The result of using this coarse grid is that there are only two or three elements through the thickness of a bending member. Once there is a tension stress of significant magnitude in the member and one element cracks, the remaining one or two elements must carry the entire tensile stress. This may lead to cracking in the adjoining elements, and the process continues until the entire cross section is cracked. If there were more elements across the section, the tensile stress could be redistributed in smaller increments to the remaining elements, thereby arriving at a stable solution.

The very large tensile stresses (Figures 41a-41c) in the out-of-plane direction once again occurred as a result of the plane strain assumptions. From the L-13 analyses, it was determined that these do not significantly affect the in-plane stresses. It was also determined that the pile loads are impacted very little by them. Once it is understood that the out-of-plane stresses will not occur to this degree, the remaining stresses and deflections

are realistic, with the exception of the crack. The occurrence of the crack still requires more investigation. However, if the reinforcement were included in the model, these rebars would carry the tensile load in the member. This would minimize, if not eliminate, the crack, thereby minimizing the significance of the crack in terms of the structural stability.

Load case 5

The lower creep and shrinkage parameters were used in this analysis. As in the L-13 analysis, the use of these smaller values gave similar results. Again, the horizontal (Figures 44a-44c) and maximum principal (Figures 47a-47c) stress contours indicate that a crack occurred in the base slab. The deflected shapes (Figures 48a-48c) clearly show the crack developing as in load case 1. The out-of-plane tensile stresses (Figures 46a-46c) were still present, but at a slightly smaller magnitude. The form work had to be removed early from the top of the culvert as in load case 1.

Pile loads

The pile loads from the gravity only loading are very close (within 3 percent) to the results from the Phase I study for the same load case. These maximum loads of 349 kips are well within the approximate 400 kips used in the design. For load cases 1 and 5 the maximum loads are 385 kips and 430 kips, respectively, and occur toward the right end of the slab. These compare to 360 kips from the Phase I study which occurred under the center of the wall. One concern in the Phase I study was that obviously too much creep was being included in the material model. These new analyses show that as less creep is included, the pile loads do tend toward a more uniformly distributed pattern with the maximum load moving to the right end of the slab. Since it is believed that the actual creep value is closer to the middle-to-low range of the values used here, the maximum pile load should be at or below the design value of 400 kips.

Another interesting point is that even with the crack through the base slab in load cases 1 and 5, the pile loads did not show large adverse effects. The two piles immediately around the crack did show a reduced load of about 25 percent between the lower and upper creep models. The adjacent piles in the upper creep model took this additional load. The redistribution in the lower creep model did not take place in such a pronounced manner. This is probably due to the fact that the crack did not go completely through the slab. Again, it is noteworthy that the pile loads did not show drastic changes, even with the structure substantially cracked.

5 Conclusions and Recommendations

It is shown that the analysis techniques developed in Phase I of this study, coupled with the revised constitutive model, can adequately predict stresses and displacements within a structure and loads in the supporting piles when gravity, thermal, and services loads are applied in a 2-D analysis. The limiting points discussed earlier should be kept in mind when these analyses are performed. Proper care should be exercised to ensure that any cracks are controlled and do not adverse'y affect the stability of the structural system. Proper grid sizes should be used (Truman, Petruska, and Fehri in preparation) to allow both an accurate temperature and stress analysis.

It is obvious from this study that more attention should be given to the use of reinforcement in the concrete to eliminate the very sensitive stability situations which occur when an unreinforced concrete element is on the verge of cracking. This would also eliminate the need for using a very refined mesh in analyses where this smeared crack model is used.

While these structures were originally analyzed as a plane strain problem, it was evident as the study proceeded that this may not be the best way to analyze the structure. The presence of significant shrinkage causes the out-of-plane boundary conditions for plane strain to put the structure into substantial tension it that direction. It is obvious that this does not actually occur in the real structure. It is also true that if the structure does not really shrink (when thermal expansion and shrinkage are combined) in the out-of-plane direction, the plane strain condition may be closer to what really happens. Addressing this problem with a 3-D analysis may not give the correct answer either, since some boundary conditions still must be applied to these faces. This question still should be investigated further, even though it is shown by comparing the plane strain and plane stress results that this out-of-plane activity does not significantly affect the in-plane stresses or pile loads. If substantial out-of-plane loadings are present, this behavior may be of far more importance and require a more thorough investigation.

References

Bombich, A. A., Norman, C. D., and Garner, S. B. (1991). "Evaluation of parameters affecting thermal stresses in mass concrete." Technical Report SL-91-2. U.S. Army Engineer Waterways Experiment Station, Vicksburg, MS.

Bombich, A. A., Norman, C. D., and Jones, H. W. (1987). "Thermal stress analysis of Mississippi River Lock and Dam 26(R)." Technical Report SL-87-21. U.S. Army Engineer Waterways Experiment Station, Vicksburg, MS.

Hibbitt, Karlsson, and Sorenson, Inc. (1987). "ABAQUS - structural and heat transfer finite element code." *User's Manual.* Providence, RI.

Truman, K. Z., Petruska, D. P., and Fehri, A. Evaluation of thermal and incremental construction effects for monoliths AL-3 and AL-5 of the Melvin Price Locks and Dam (in preparation). U.S. Army Engineer Waterways Experiment Station, Vicksburg, MS.

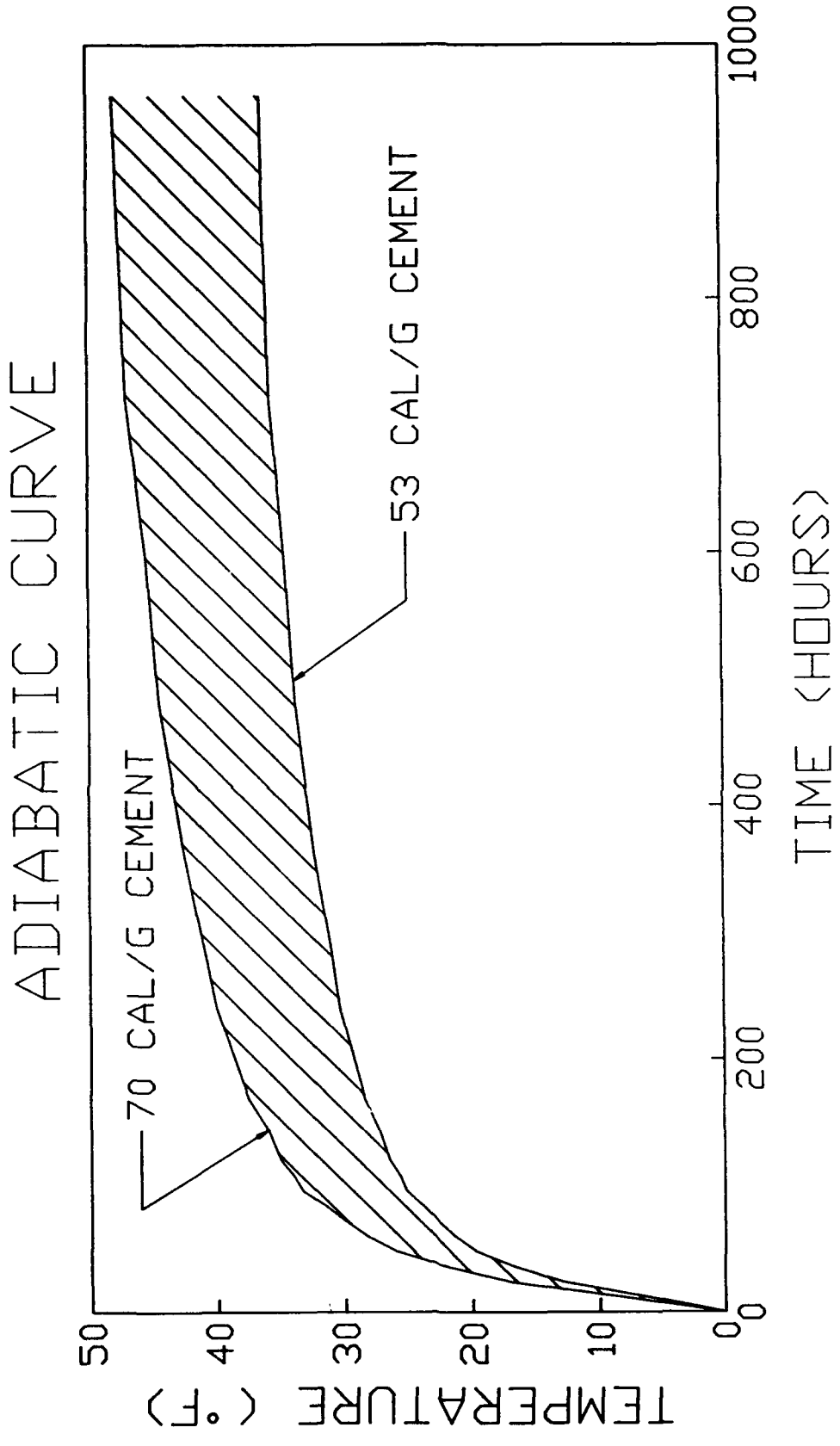

Figure 1 - Upper and lower bounds for adiabatic temperature rise used in 2D Phase II thermal study of Melvin Price Locks & Dam.

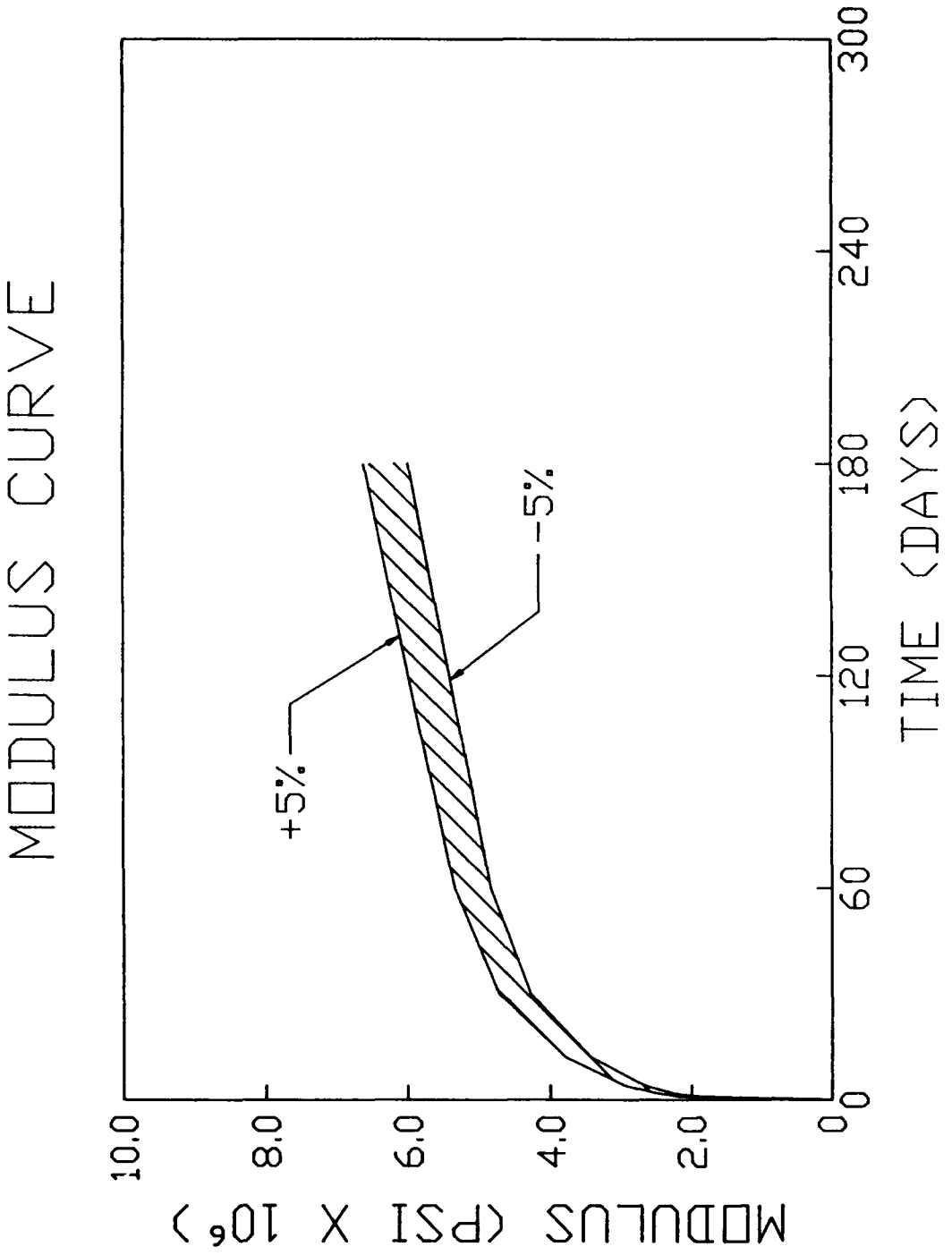

Figure 2 - Upper and lower bounds for Modulus of Elasticity used in 2D Phase II thermal study of Melvin Price Locks & Dam.

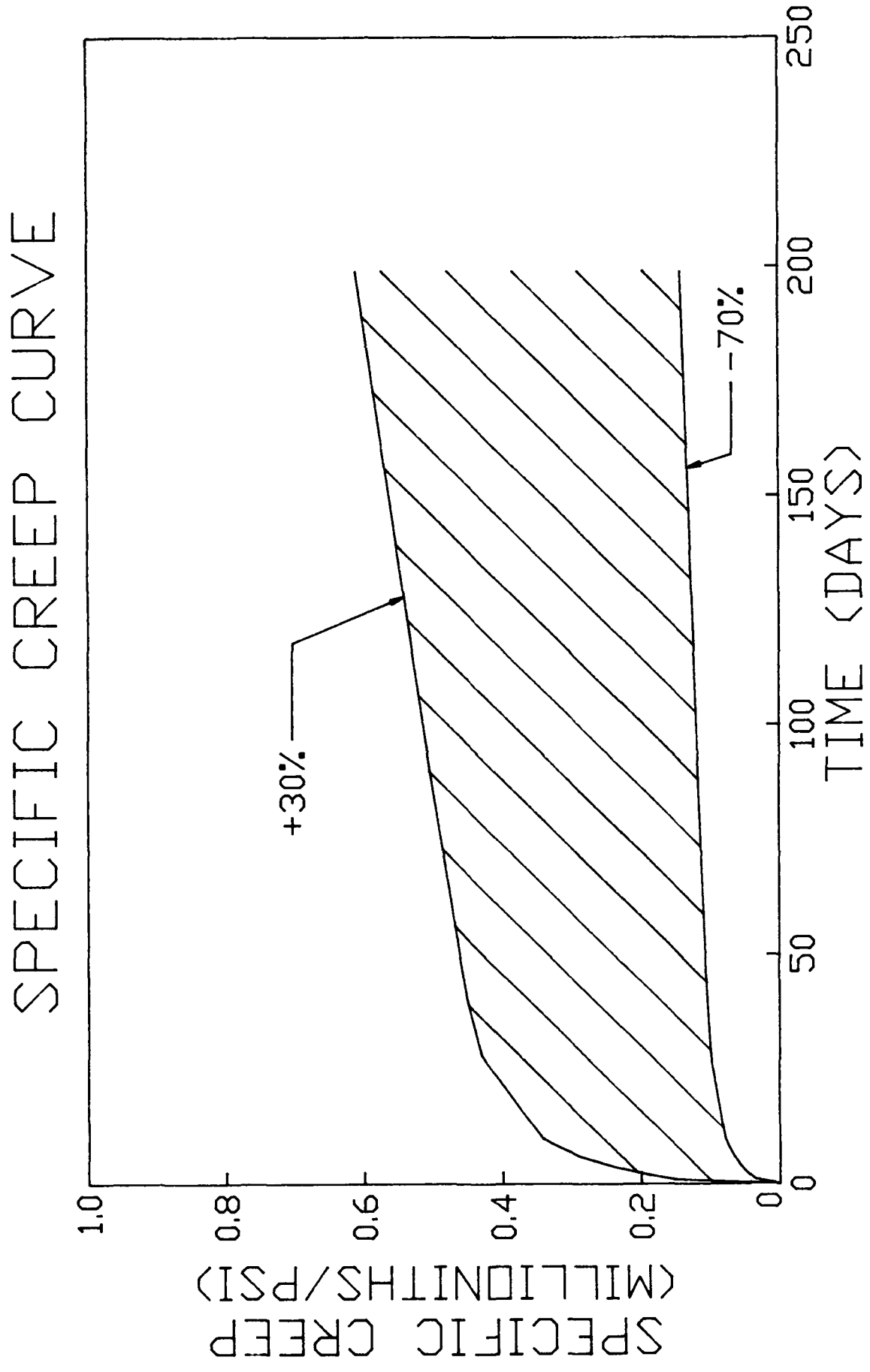

Figure 3 - Upper and lower bounds for creep model used in 2D Phase II thermal study of Melvin Price Locks & Dam.

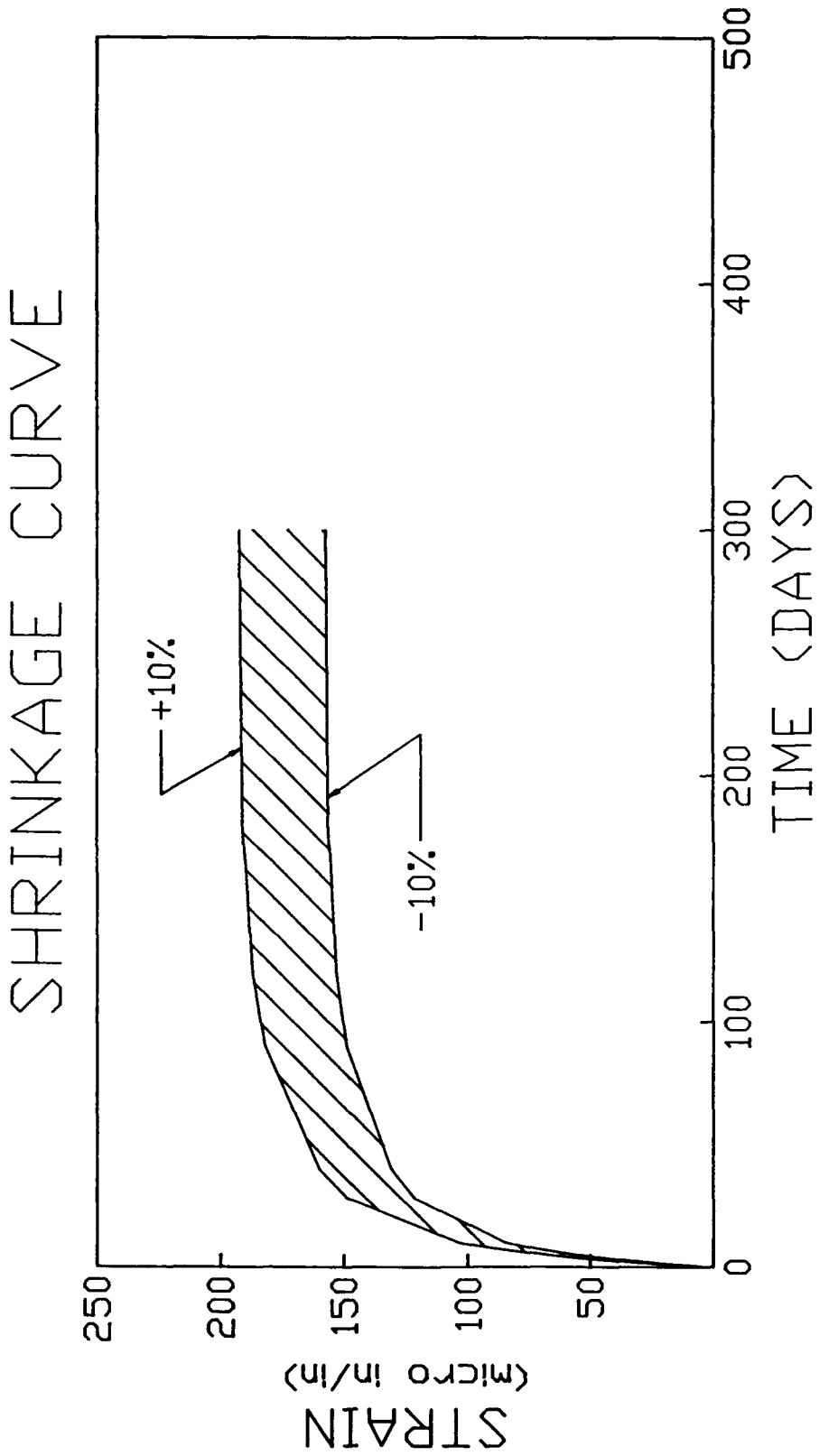

Figure 4 - Upper and lower bounds for shrinkage model used in 2D Phase II thermal study of Melvin Price Locks & Dam.

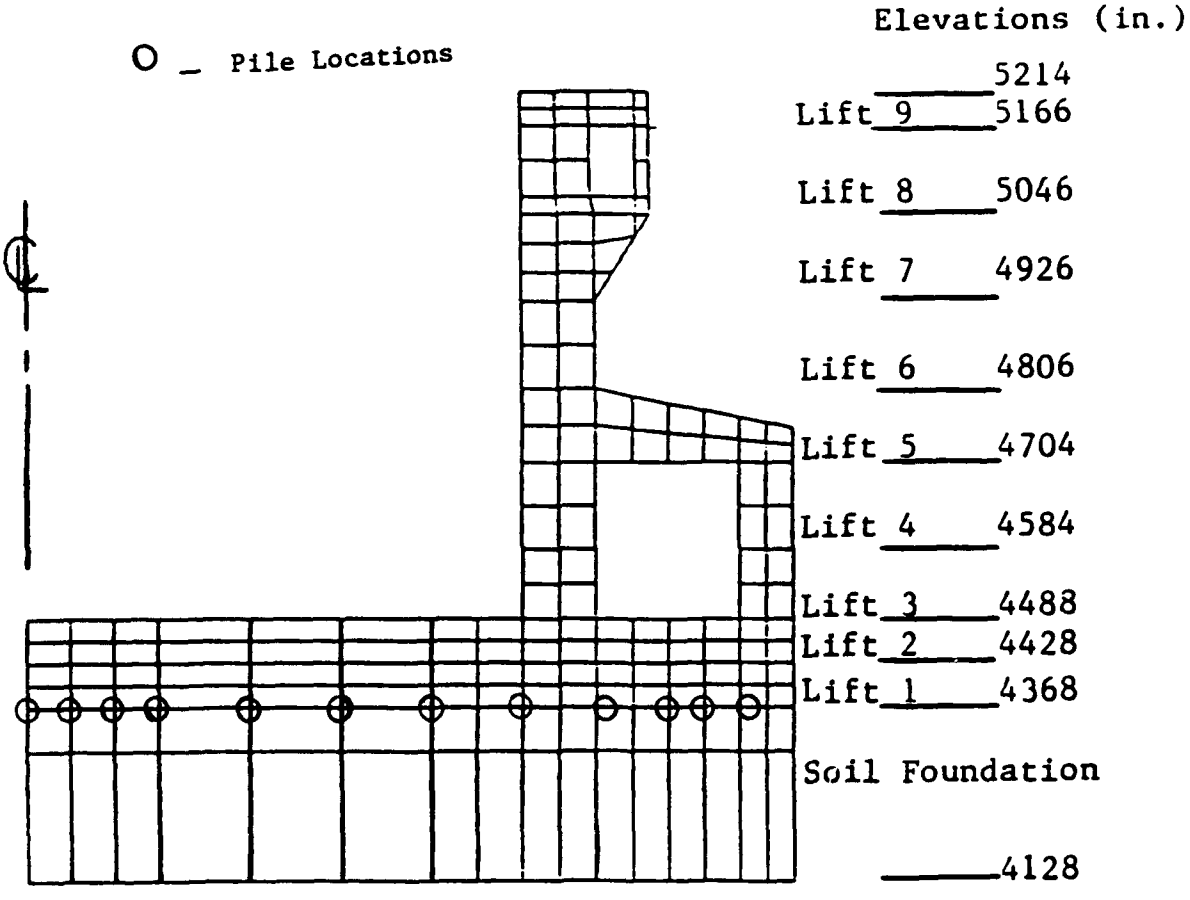

Figure 5 - Finite Element model of monolith L-13 (160 elements) used in 2D Phase II thermal study of Melvin Price Locks & Dam.

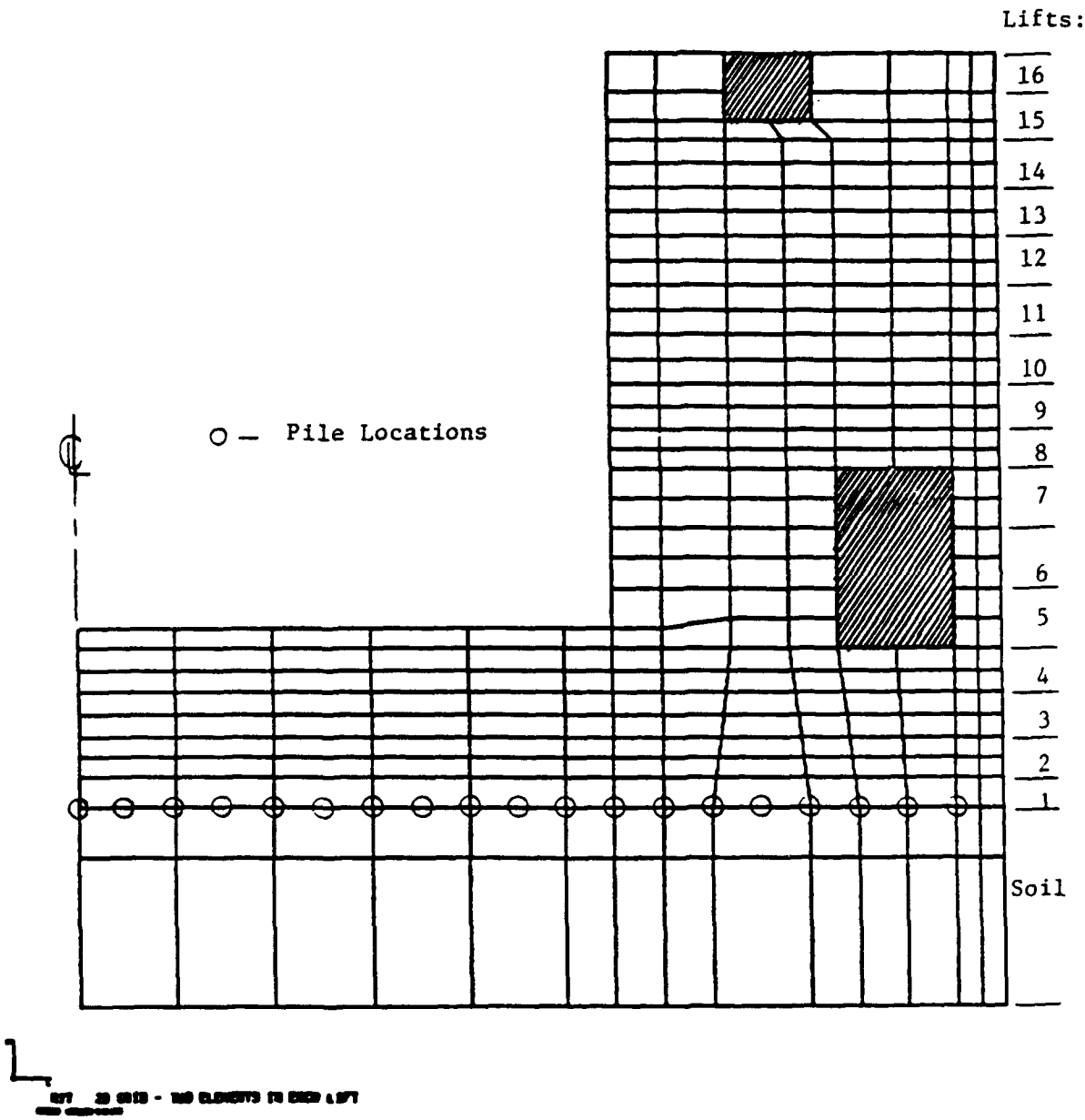

Figure 6 - Finite Element model of monolith L-17 (316 elements) used in 2D Phase II thermal study of Melvin Price Locks & Dam.

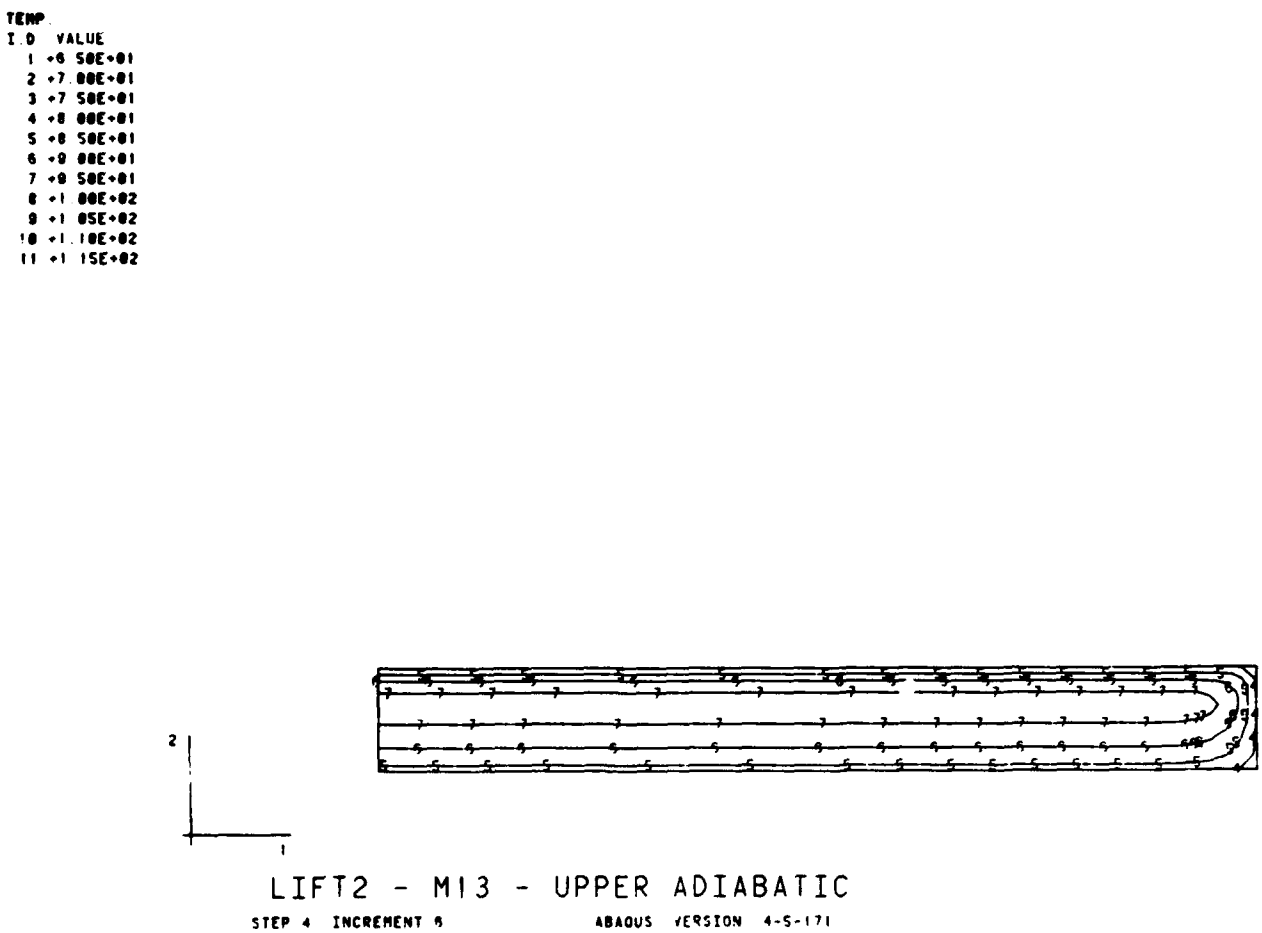

Figure 7a - Temperature distribution in L-13, 5 days after lift 2 is placed (upper adiabatic)

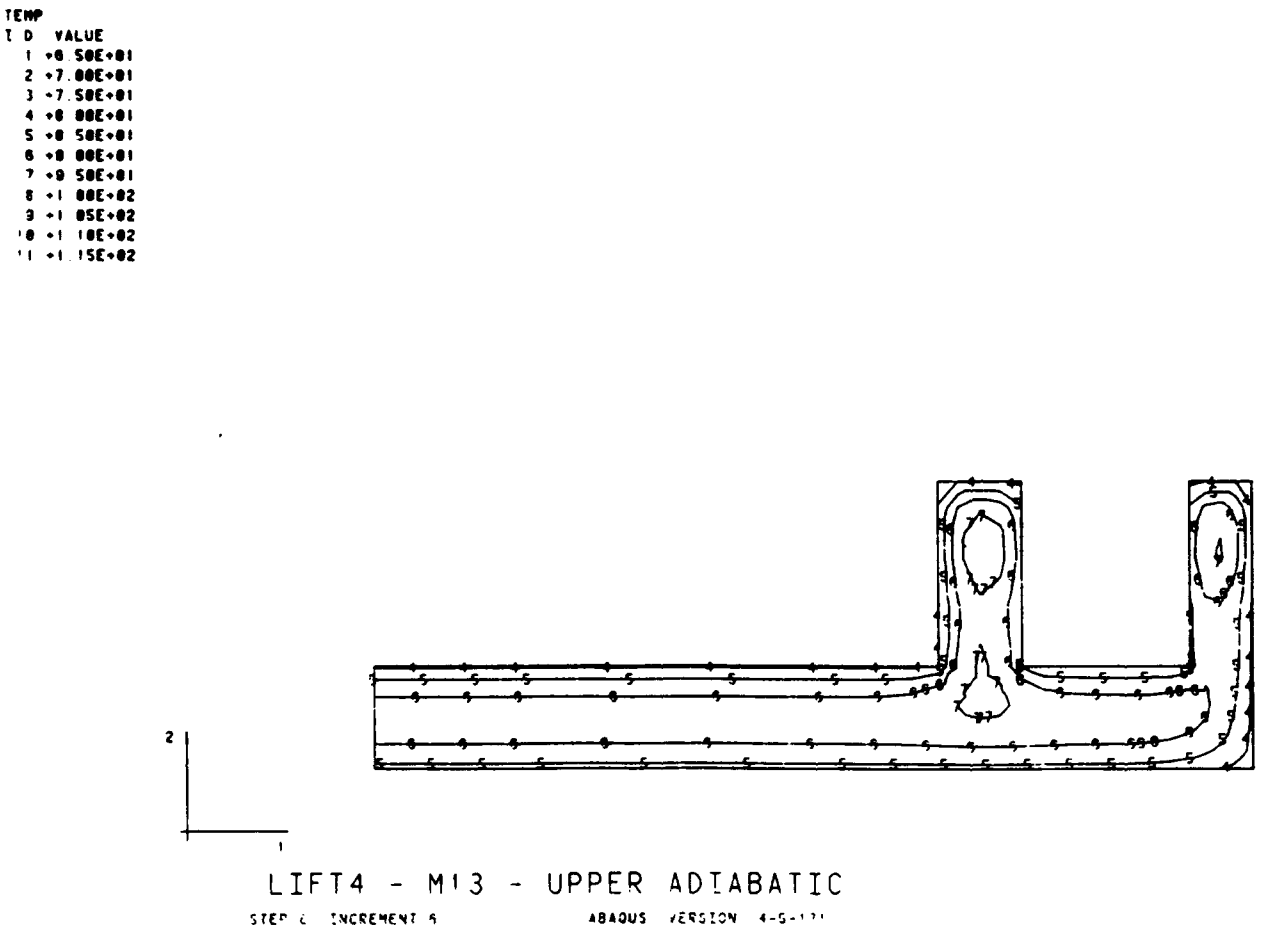

Figure 7b - Temperature distribution in L-13, 5 days after lift 4 is placed (upper adiabatic)

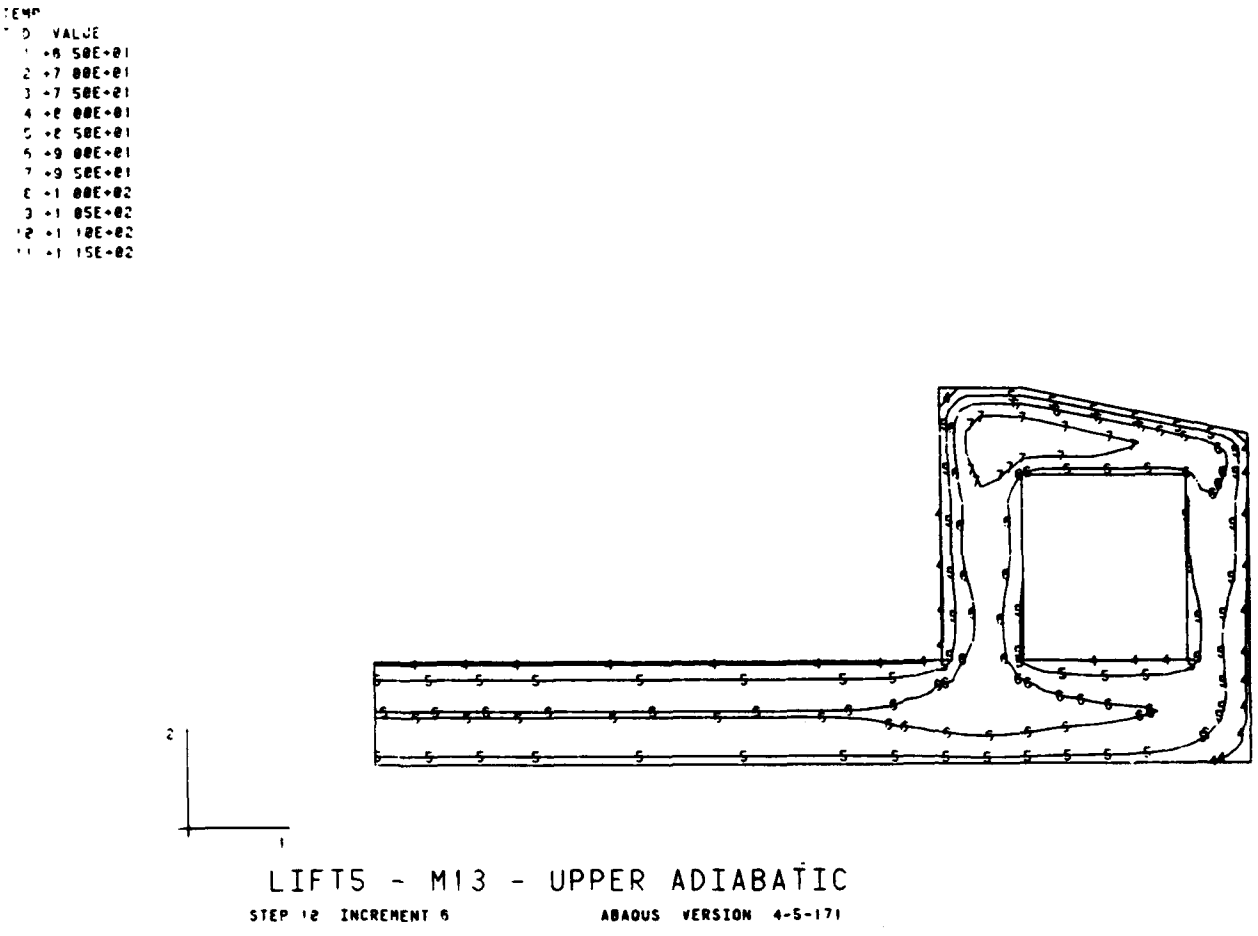

Figure 7c - Temperature distribution in L-13, 5 days after lift 5 is placed (upper adiabatic)

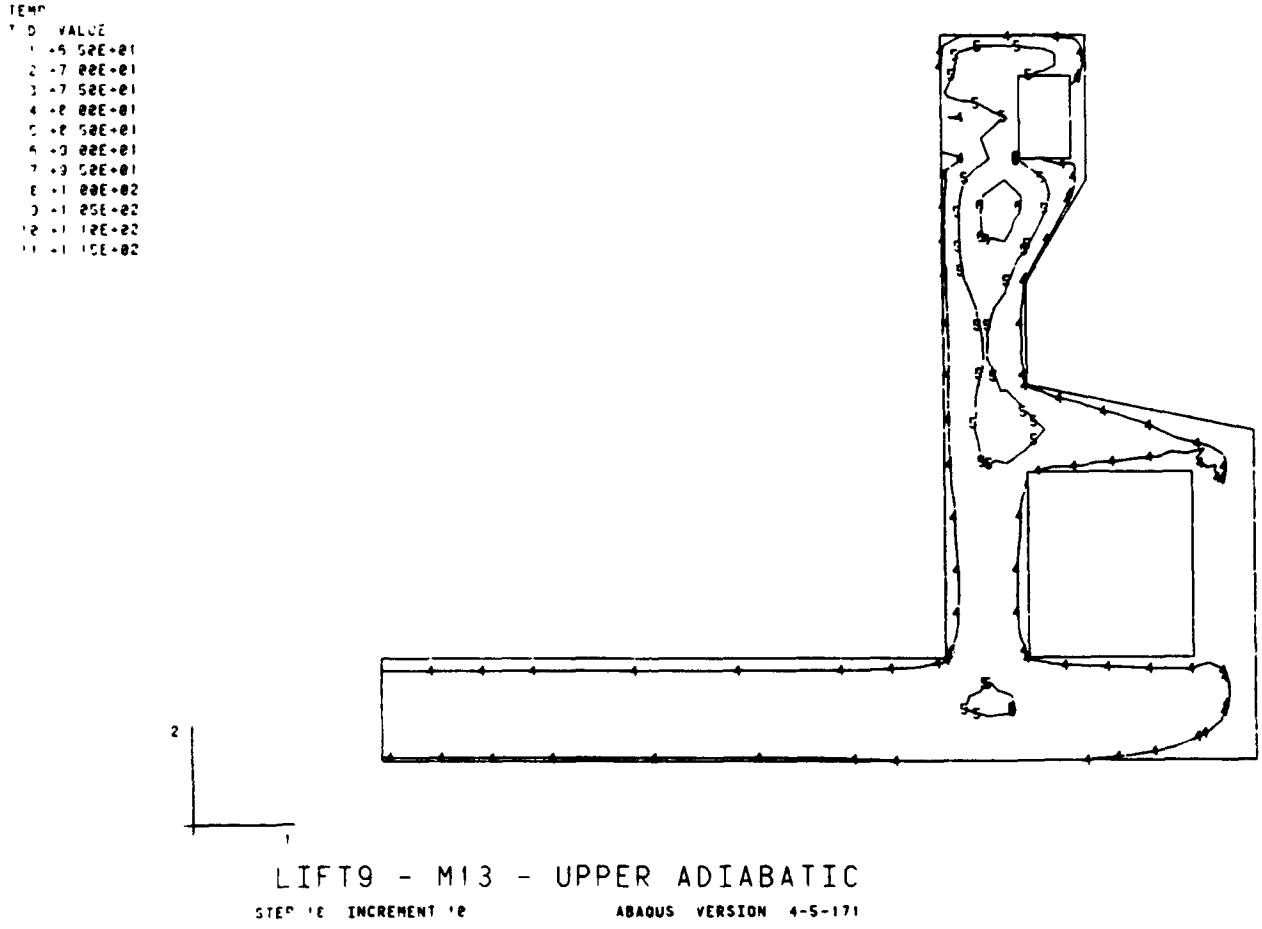

Figure 7d - Temperature distribution in L-13, 7 days after lift 9 is placed (upper adiabatic)

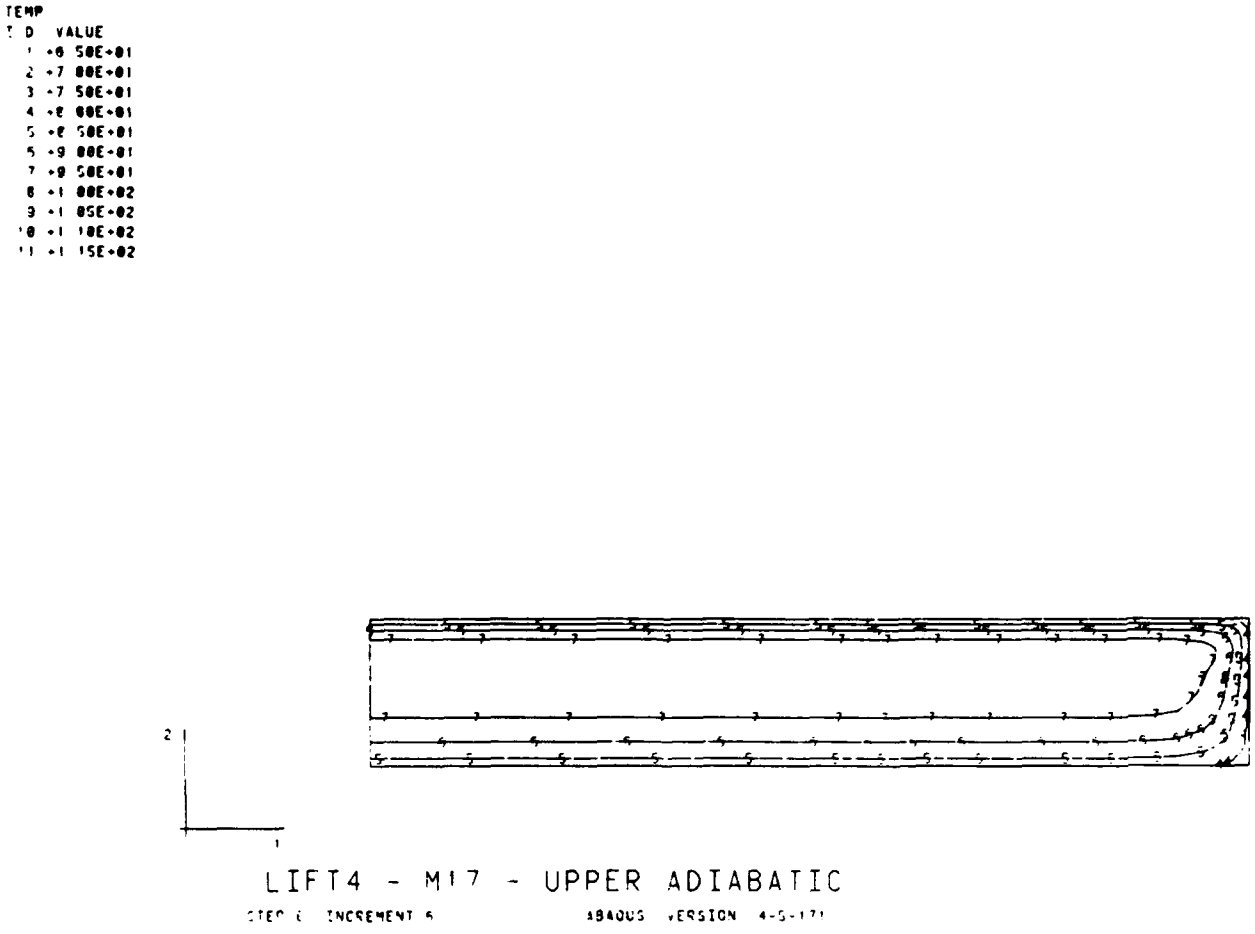

Figure 8a - Temperature distribution in L-17, 5 days after lift 4 is placed (upper adiabatic)

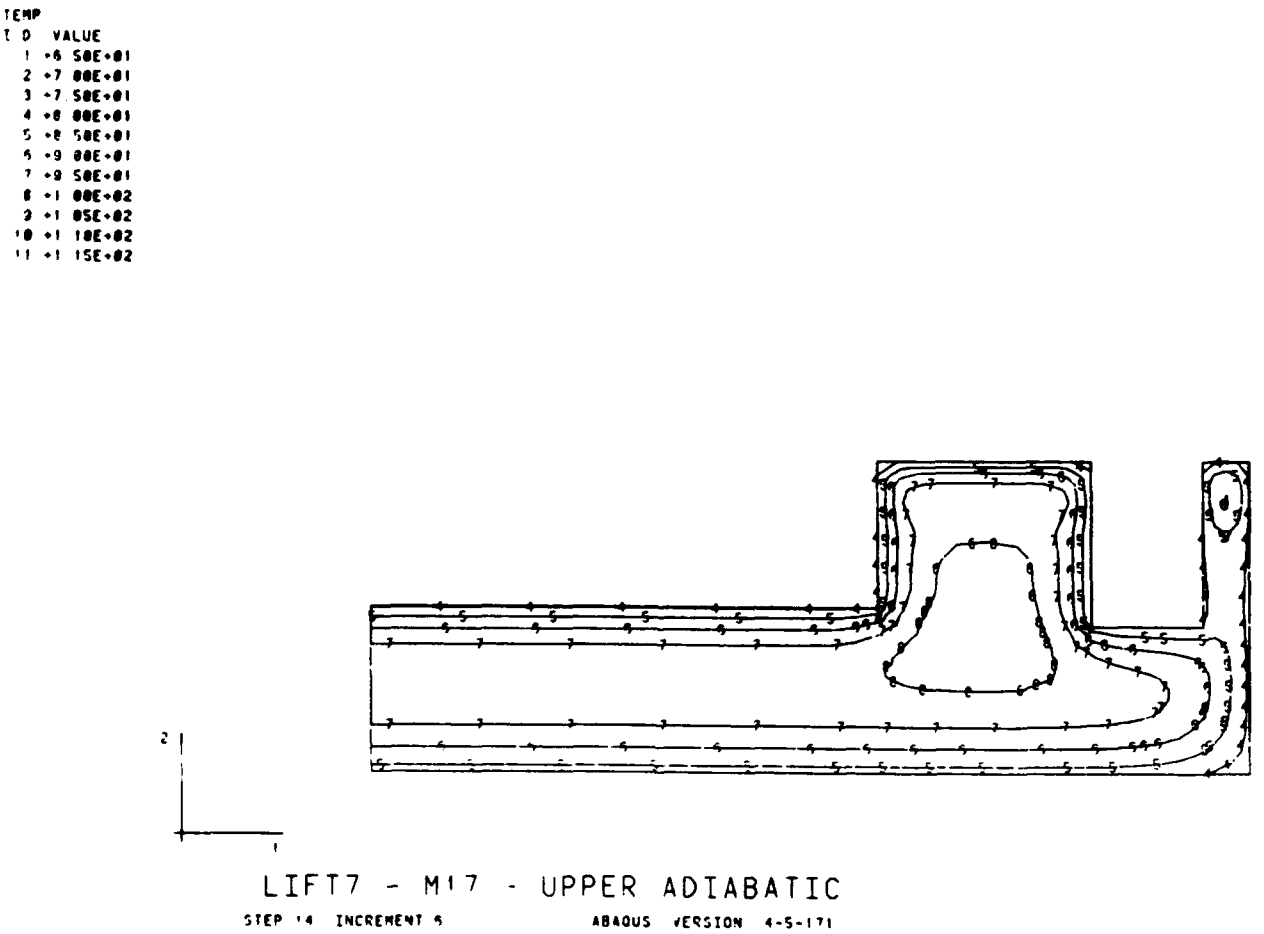

Figure 8b - Temperature distribution in L-17, 5 days after lift 7 is placed (upper adiabatic)

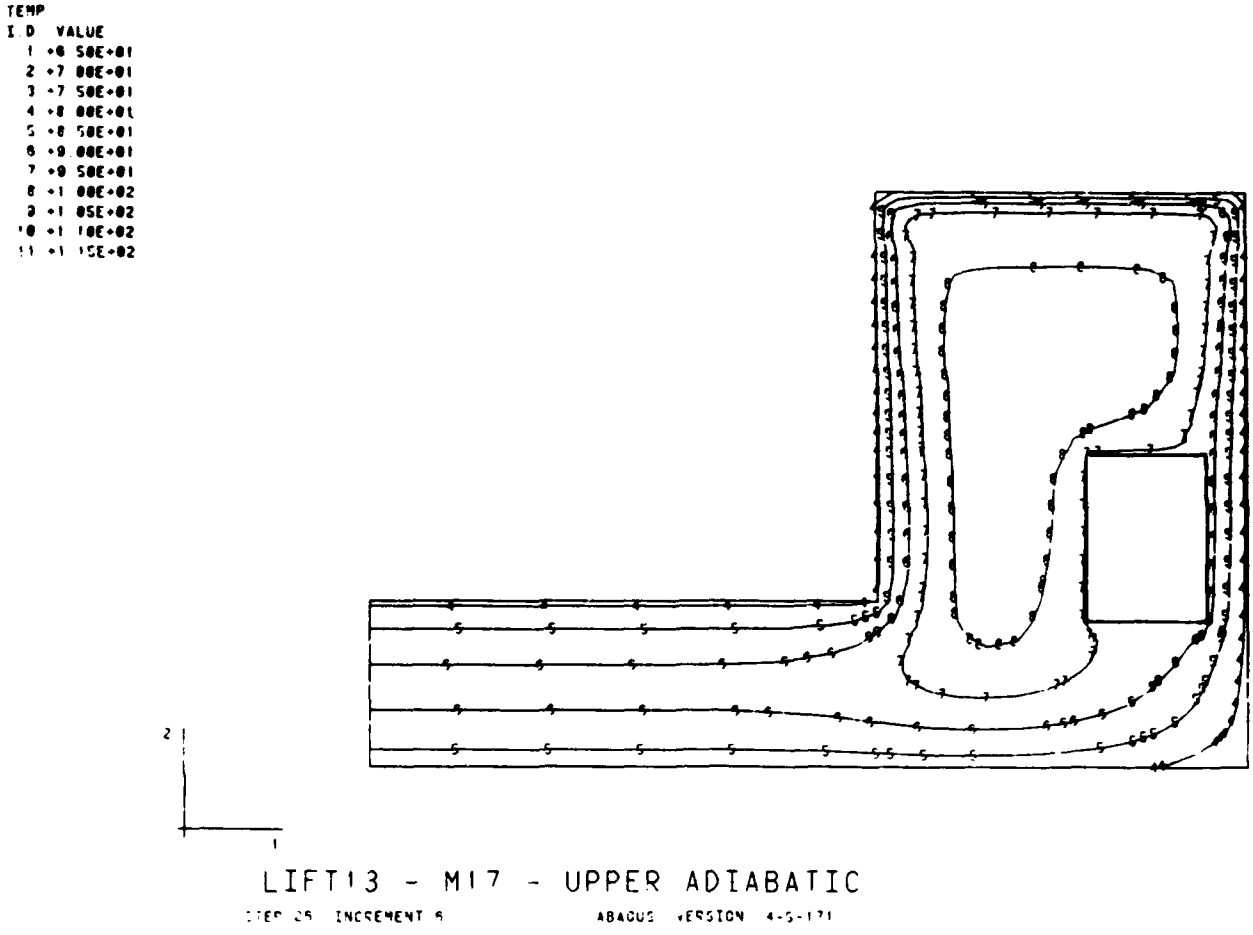

Figure 8c - Temperature distribution in L-17, 5 days after lift 13 is placed (upper adiabatic)

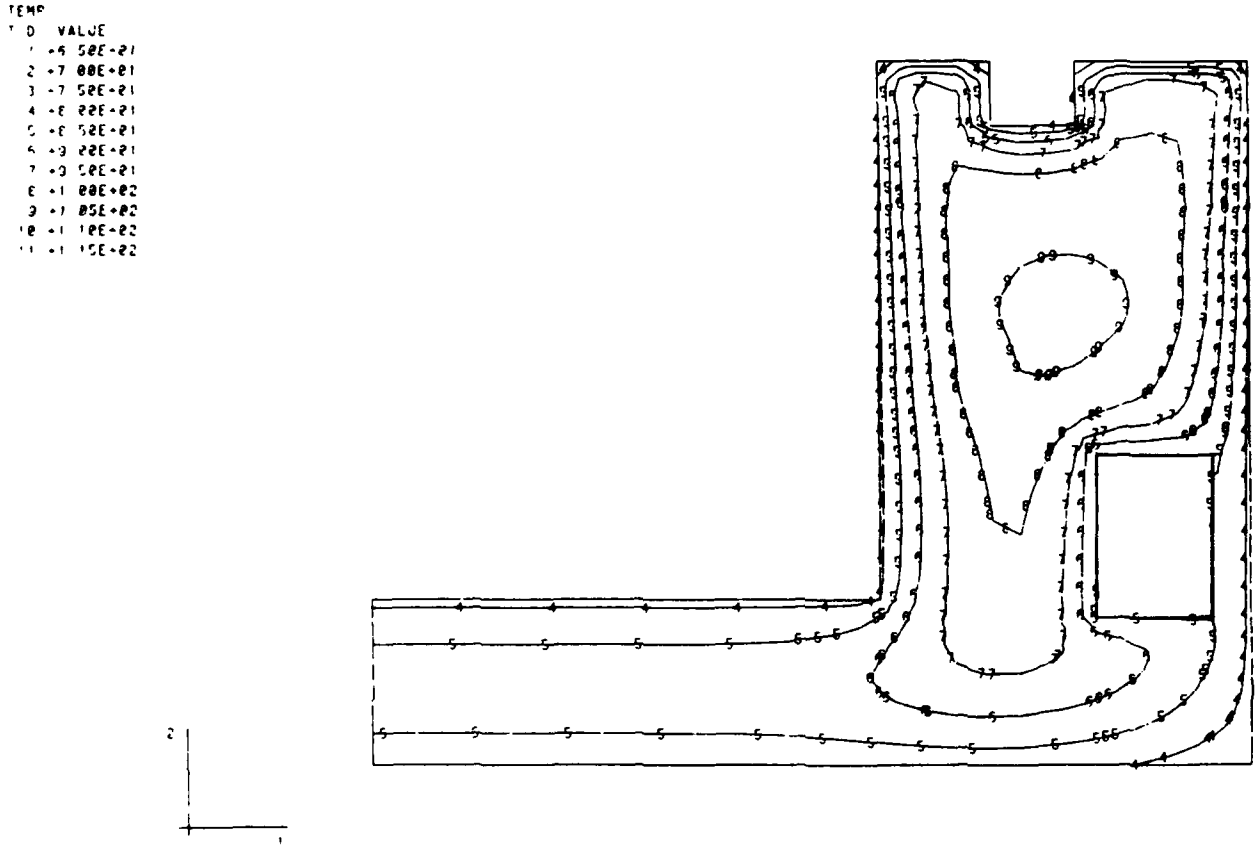

Figure 8d - Temperature distribution in L-17, 5 days after lift 16 is placed (upper adiabatic)

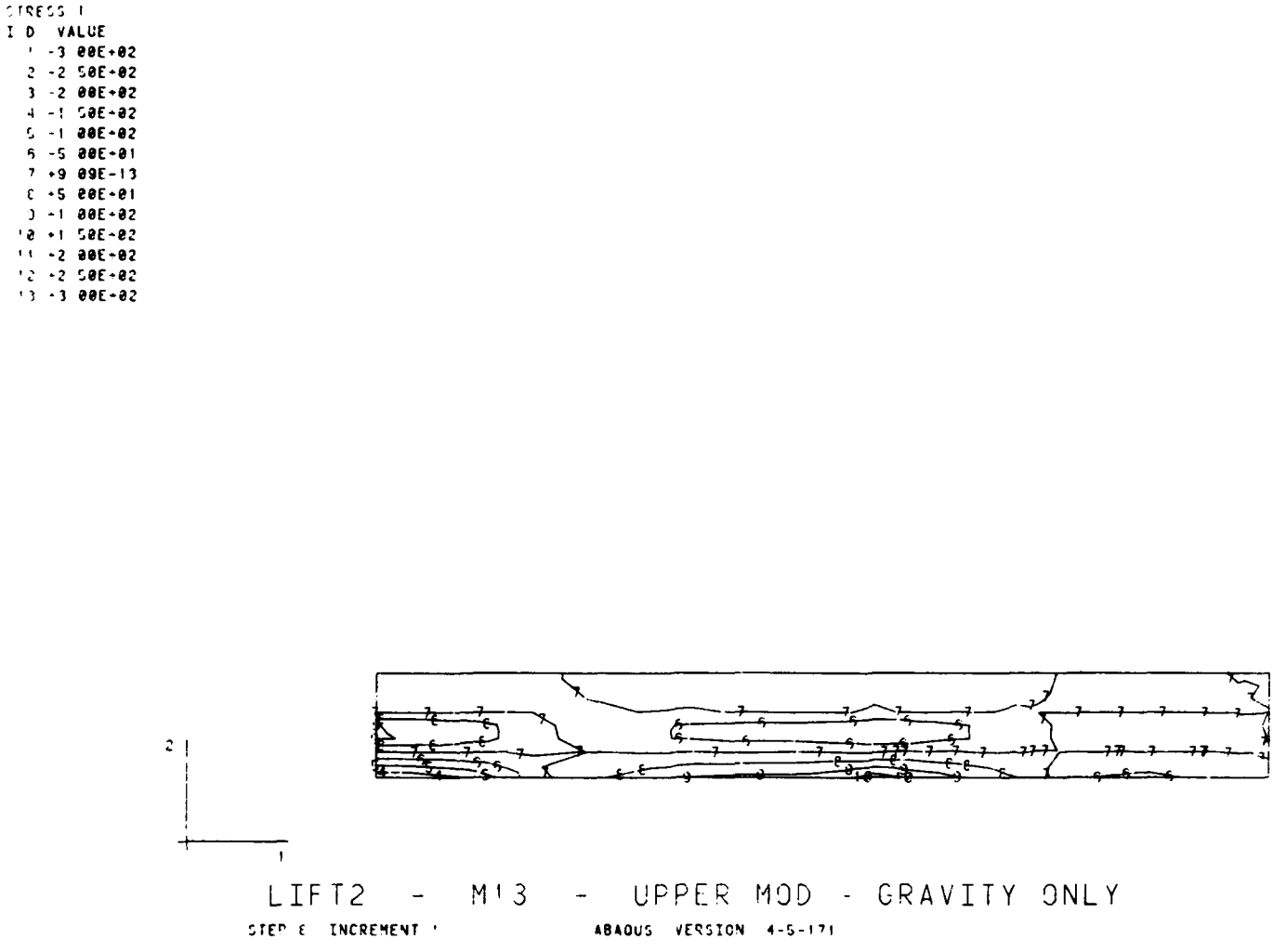

Figure 9a - Horizontal stress contours in L-13, 5 days after lift 2 is placed, Gravity loading only, No creep/shrinkage

STRESS 1

I D	VALUE
1	-3 00E+02
2	-2 50E+02
3	-2 00E+02
4	-1 50E+02
5	-1 00E+02
6	-5 00E+01
7	+9 09E-13
8	+5 00E+01
9	+1 00E+02
10	+1 50E+02
11	+2 00E+02
12	-2 50E-02
13	-3 00E-02

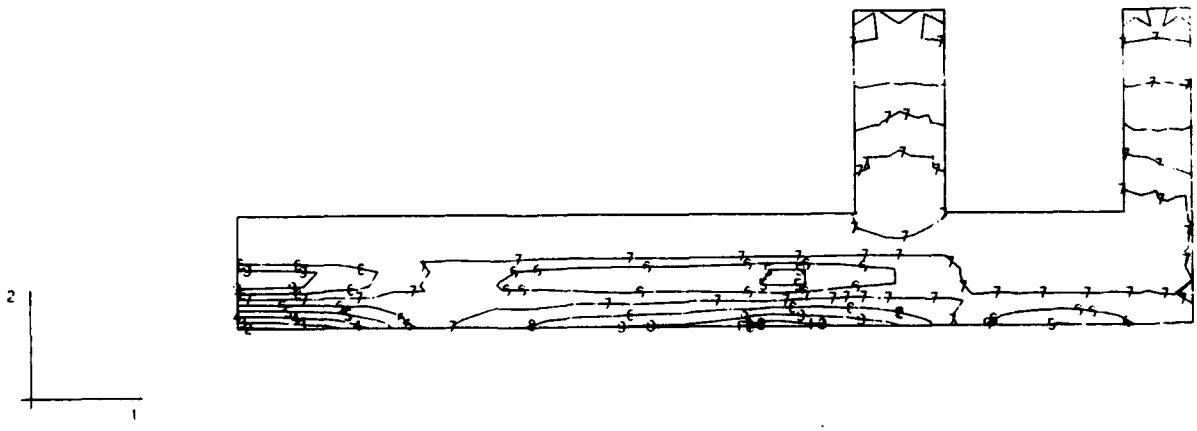

LIFT4 - M'3 - UPPER MOD - GRAVITY ONLY

STEP 15 INCREMENT 1 ABAQUS VERSION 4-5-171

Figure 9b - Horizontal stress contours in L-13, 5 days after lift 4 is placed, Gravity loading only, No creep/shrinkage

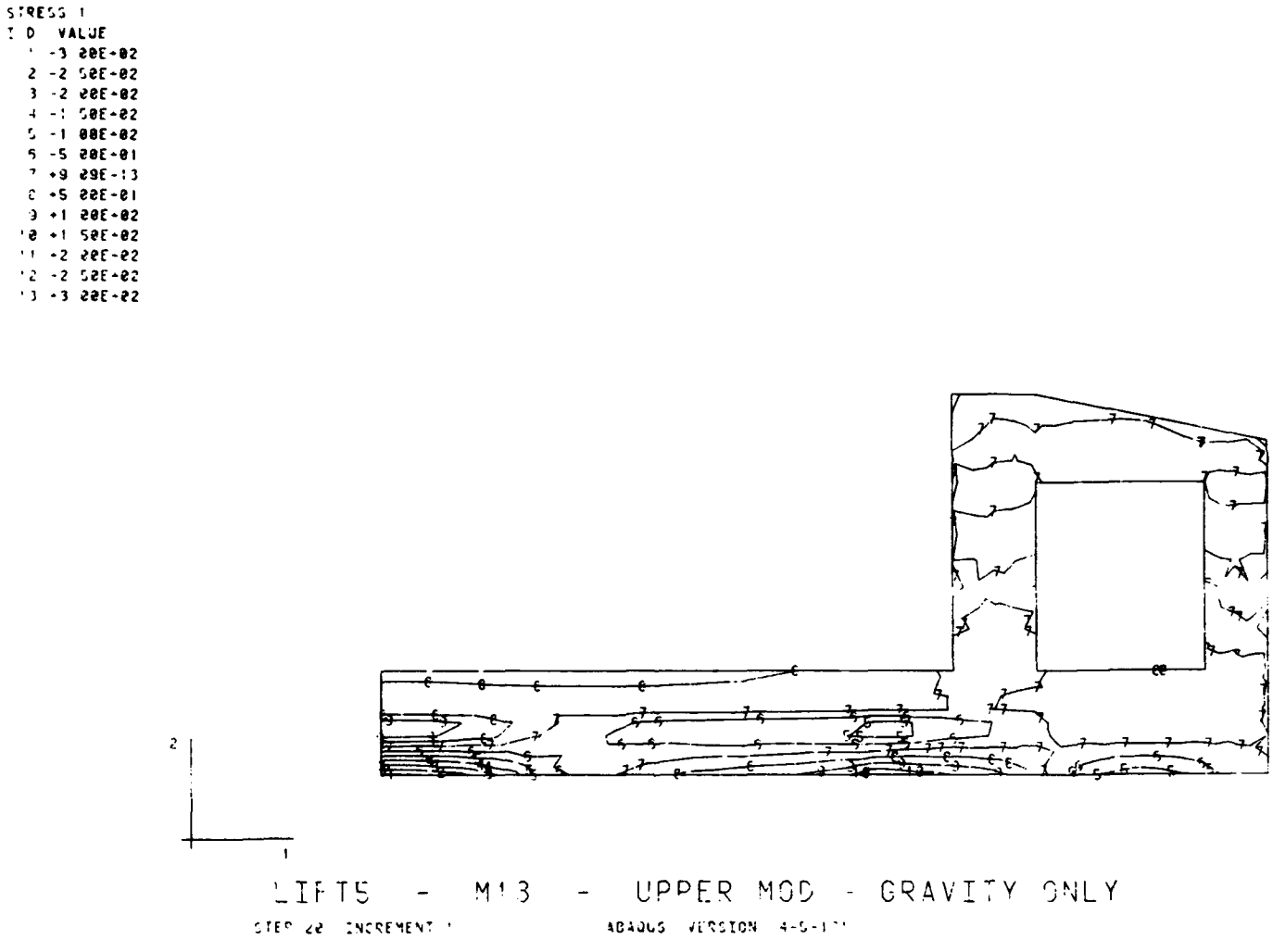

Figure 9c - Horizontal stress contours in L-13, 5 days after lift 5 is placed, Gravity loading only, No creep/shrinkage

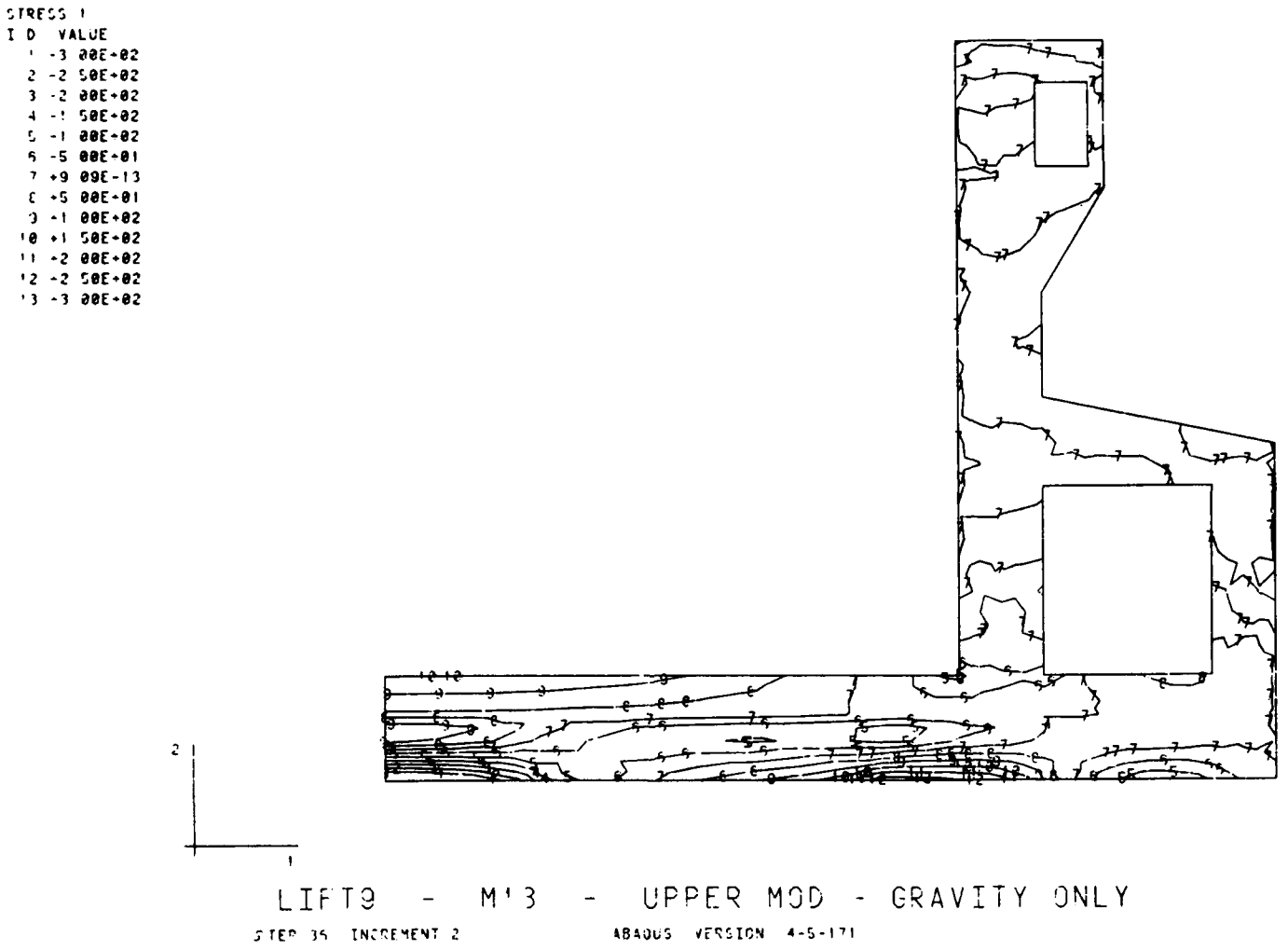

Figure 9d - Horizontal stress contours in L-13, 7 days after lift 9 is placed, Gravity loading only, No creep/shrinkage

STRESS 2

I D	VALUE
1	-3.00E+02
2	-2.50E+02
3	-2.00E+02
4	-1.50E+02
5	-1.00E+02
6	-5.00E+01
7	+9.09E-13
8	+5.00E+01
9	+1.00E+02
10	+1.50E+02
11	+2.00E+02
12	+2.50E+02
13	+3.22E+02

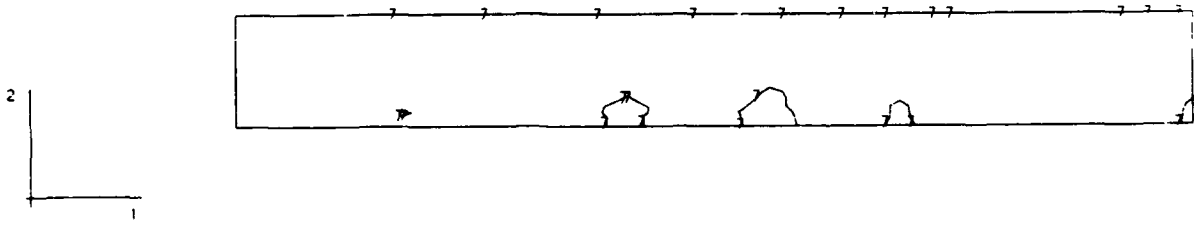

LIFT2 - M13 - UPPER MOD - GRAVITY ONLY

STEP 1 INCREMENT 1 ABAQUS VERSION 4-5-171

Figure 10a - Vertical stress contours in L-13, 5 days after lift 2 is placed, Gravity loading only, No creep/shrinkage

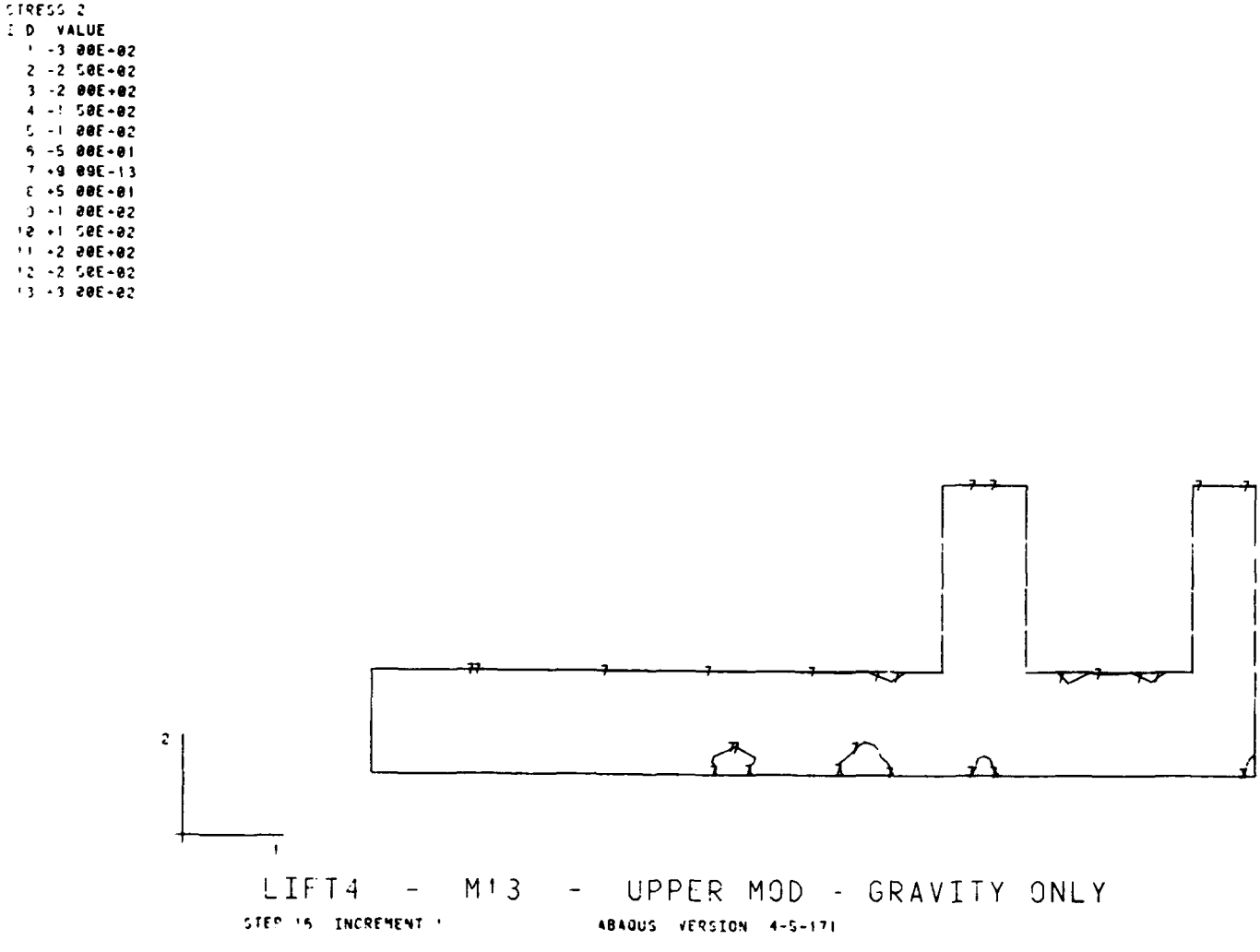

Figure 10b - Vertical stress contours in L-13, 5 days after lift 4 is placed, Gravity loading only, No creep/shrinkage

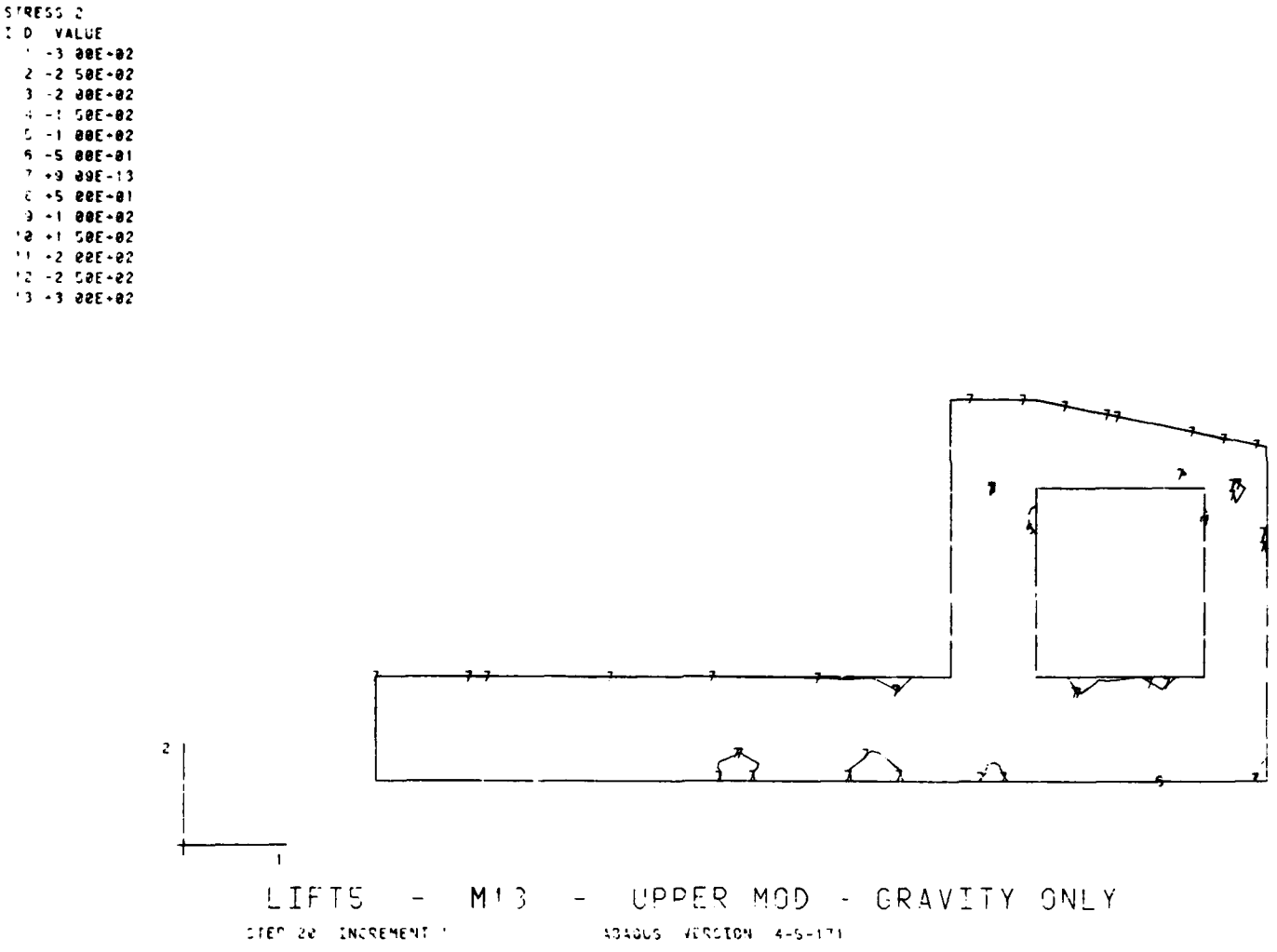

Figure 10c - Vertical stress contours in L-13, 5 days after lift 5 is placed, Gravity loading only, No creep/shrinkage

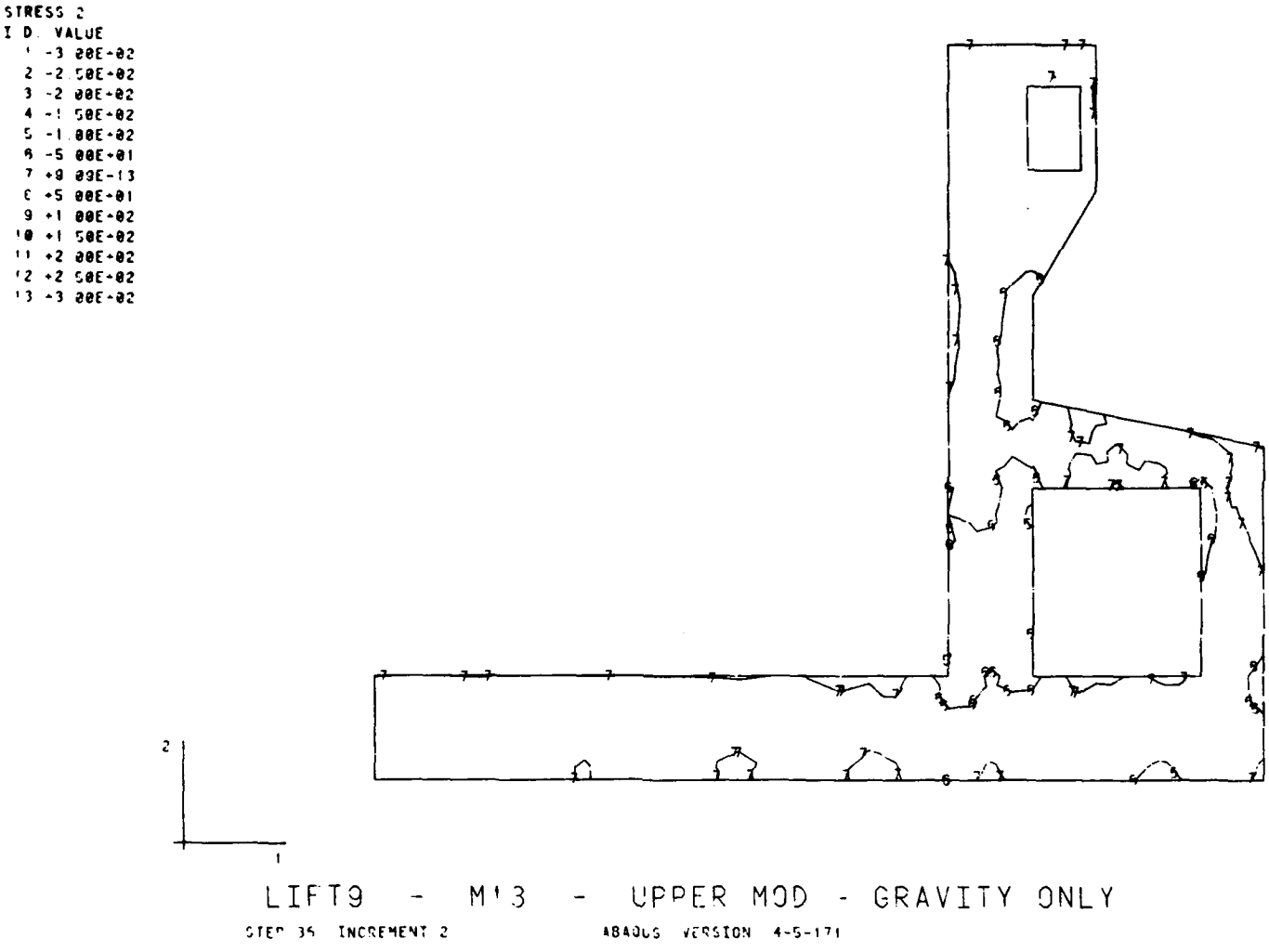

Figure 10d - Vertical stress contours in L-13, 7 days after lift 9 is placed, Gravity loading only, No creep/shrinkage

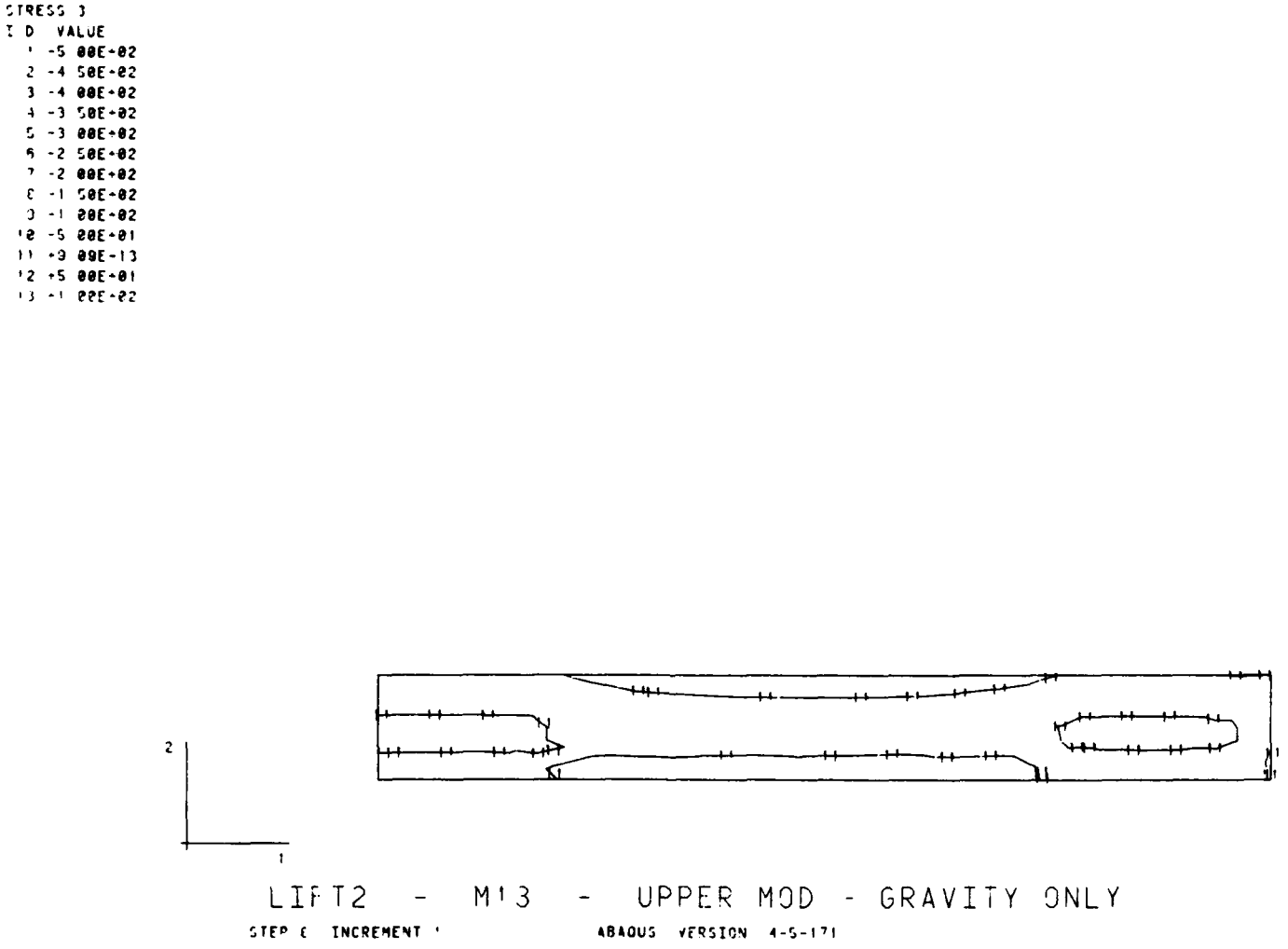

Figure 11a - Out-of-plane stress contours in L-13, 5 days after lift 2 is placed, Gravity loading only, No creep/shrinkage

STRESS 3
I D VALUE
1 -5.00E+02
2 -4.50E+02
3 -4.00E+02
4 -3.50E+02
5 -3.00E+02
6 -2.50E+02
7 -2.00E+02
8 -1.50E+02
9 -1.00E+02
10 -5.00E+01
11 +9.09E-13
12 +5.00E+01
13 +1.00E+02

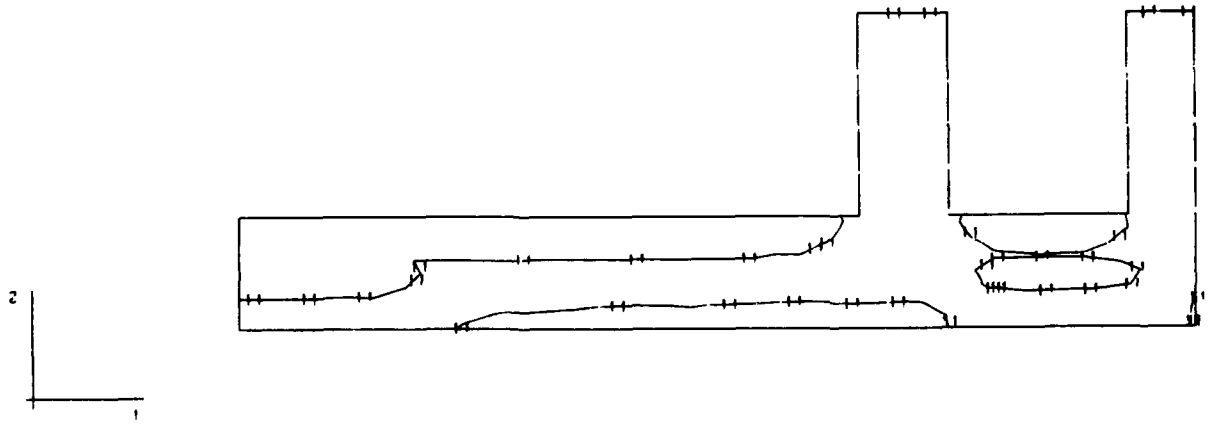

LIFT4 - M13 - UPPER MOD - GRAVITY ONLY

STEP 16 INCREMENT 1 ABAQUS VERSION 4-5-171

Figure 11b - Out-of-plane stress contours in L-13, 5 days after lift 4 is placed, Gravity loading only, No creep/shrinkage

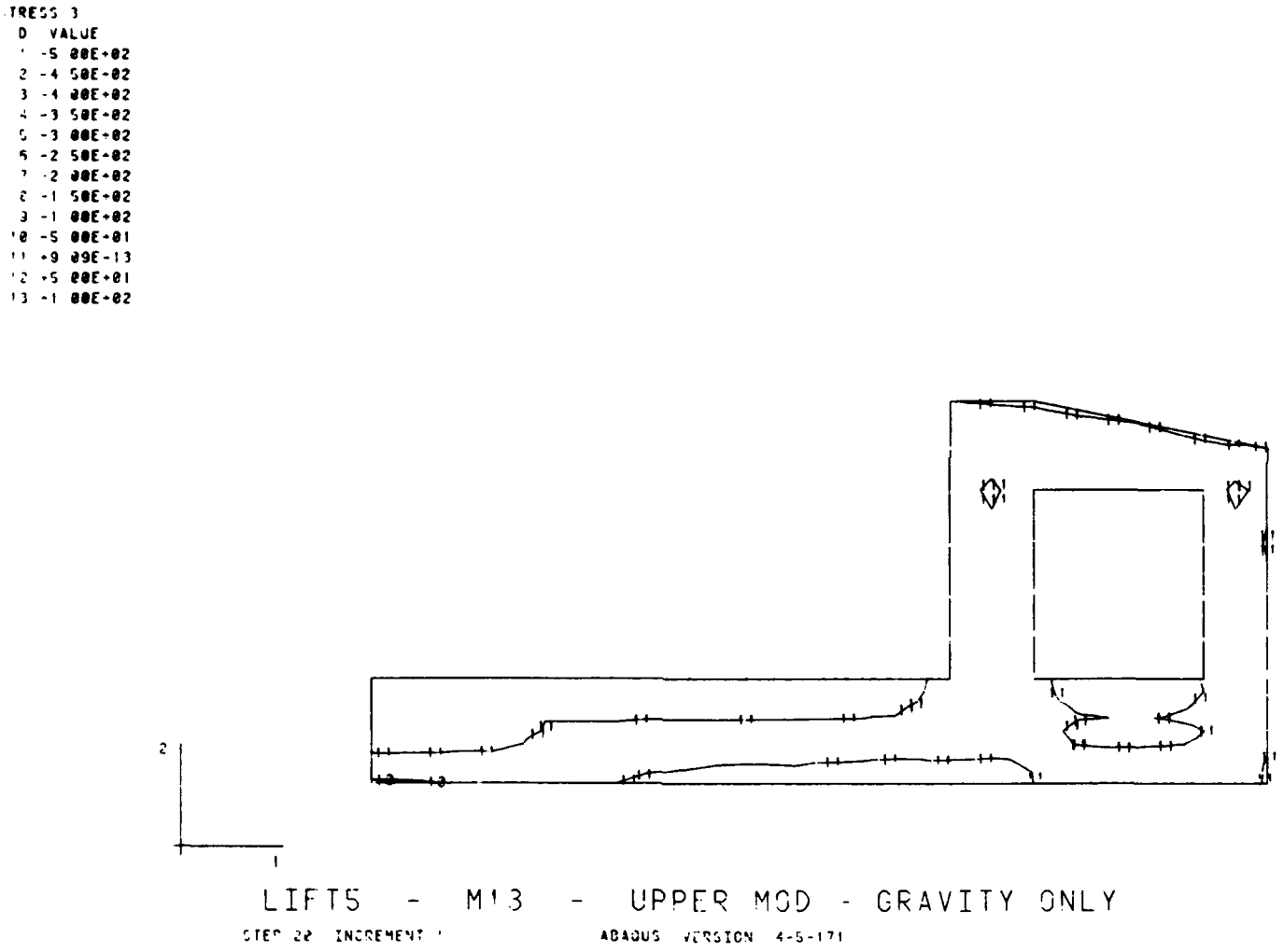

Figure 11c - Out-of-plane stress contours in L-13, 5 days after lift 5 is placed, Gravity loading only, No creep/shrinkage

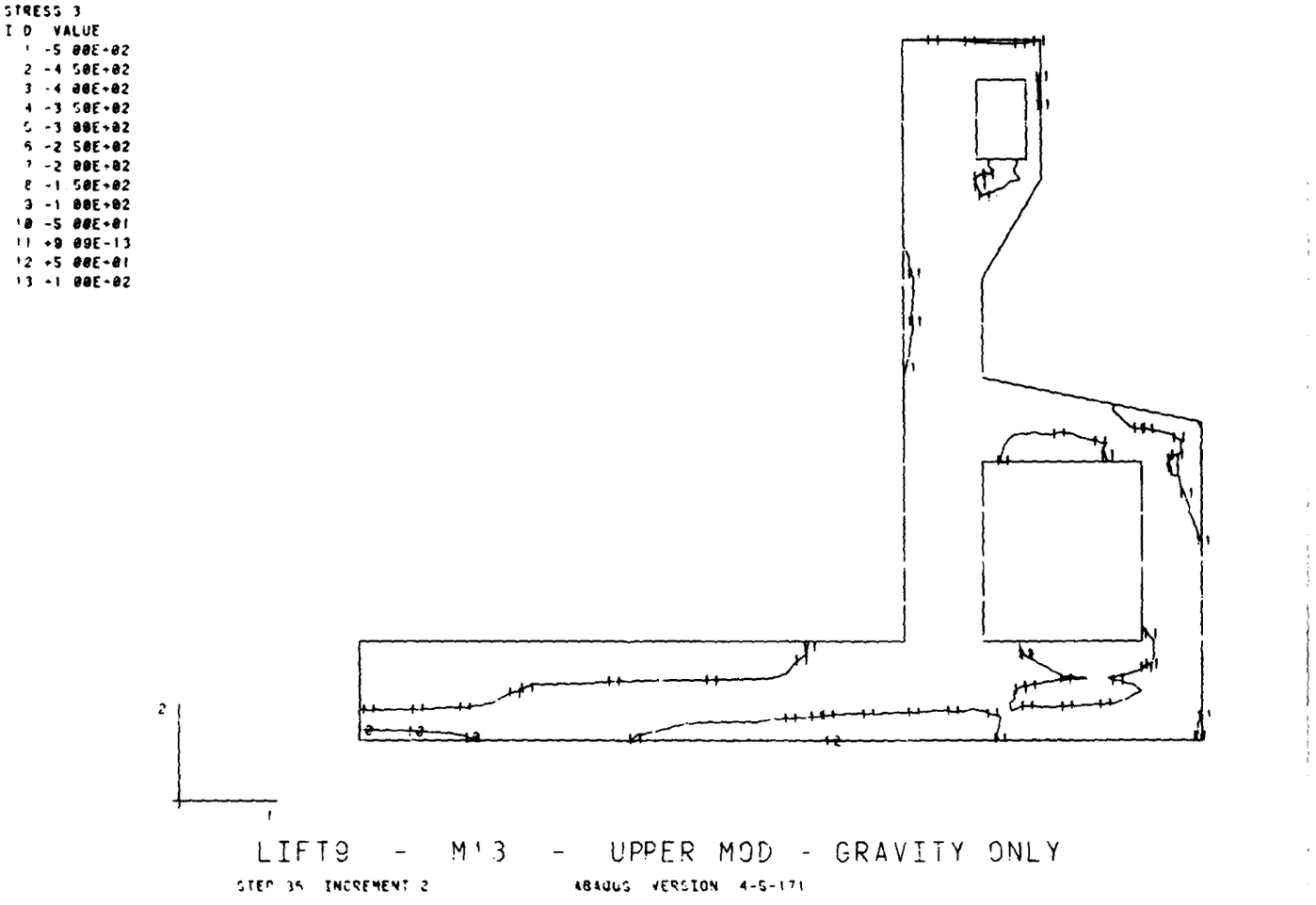

Figure 11d - Out-of-plane stress contours in L-13, 7 days after lift 9 is placed, Gravity loading only, No creep/shrinkage

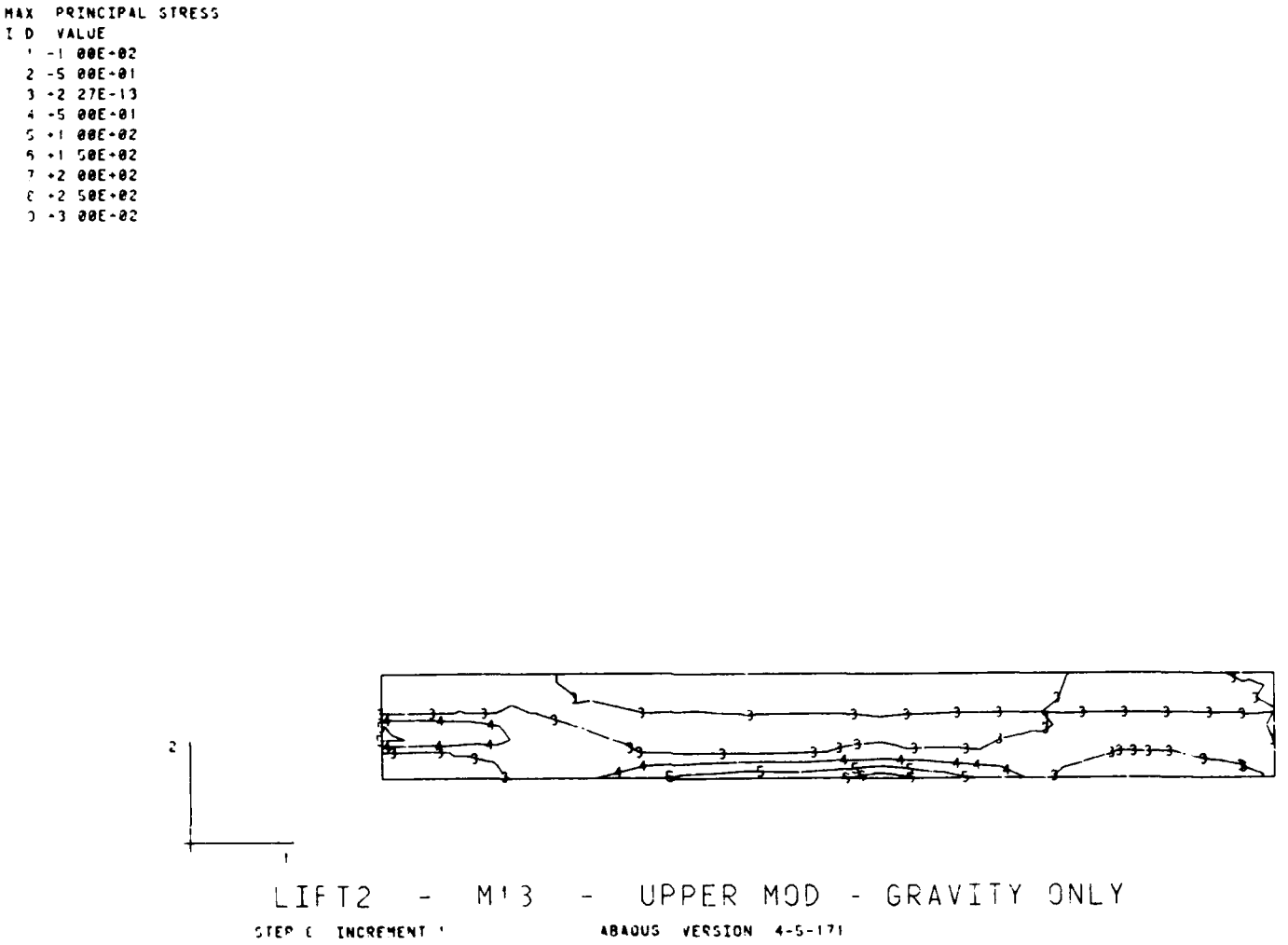

Figure 12a - Max. Principal stress contours in L-13, 5 days after lift 2 is placed, Gravity loading only, No creep/shrinkage

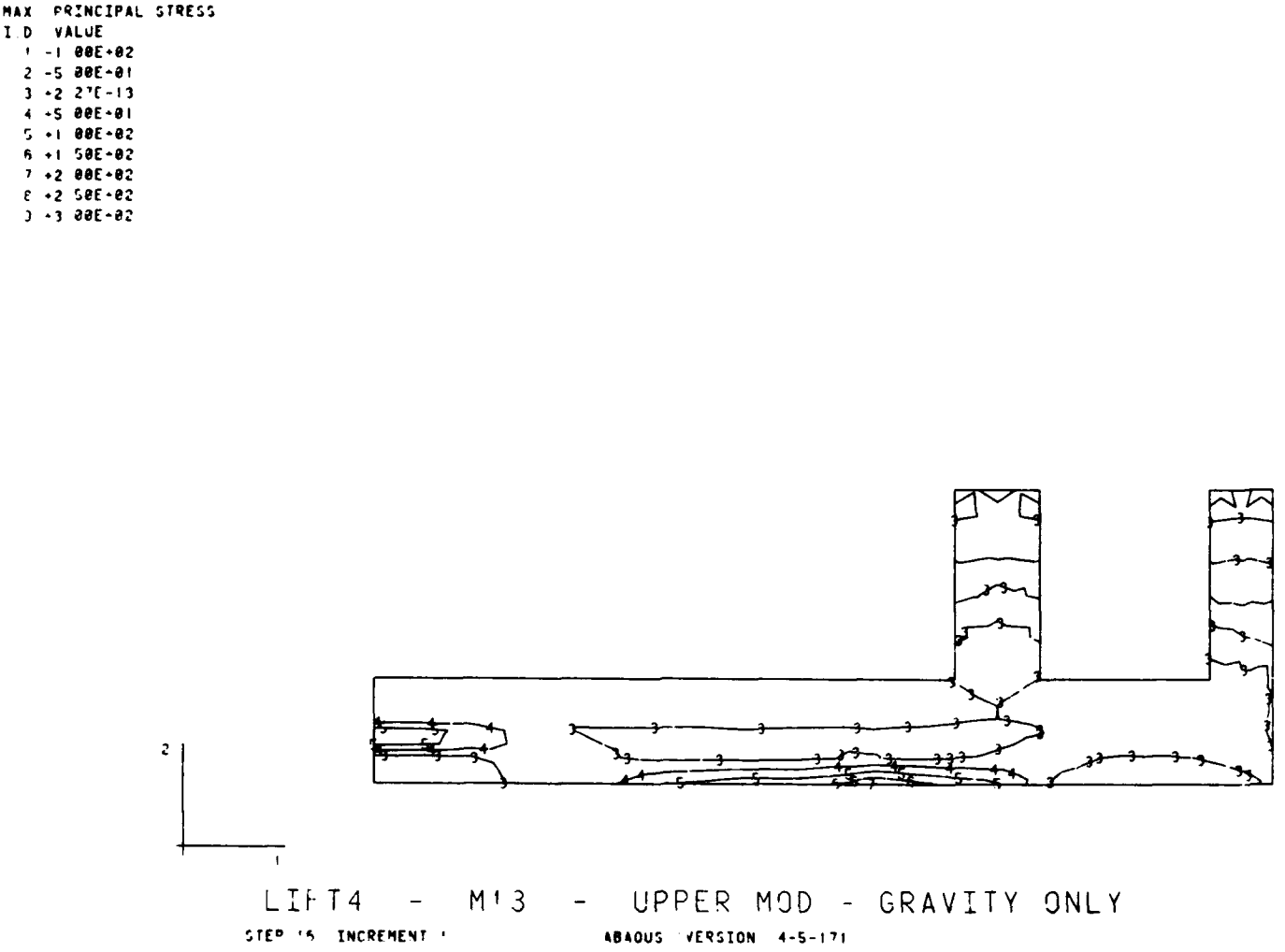

Figure 12b - Max. Principal stress contours in L-13, 5 days after lift 4 is placed, Gravity loading only, No creep/shrinkage

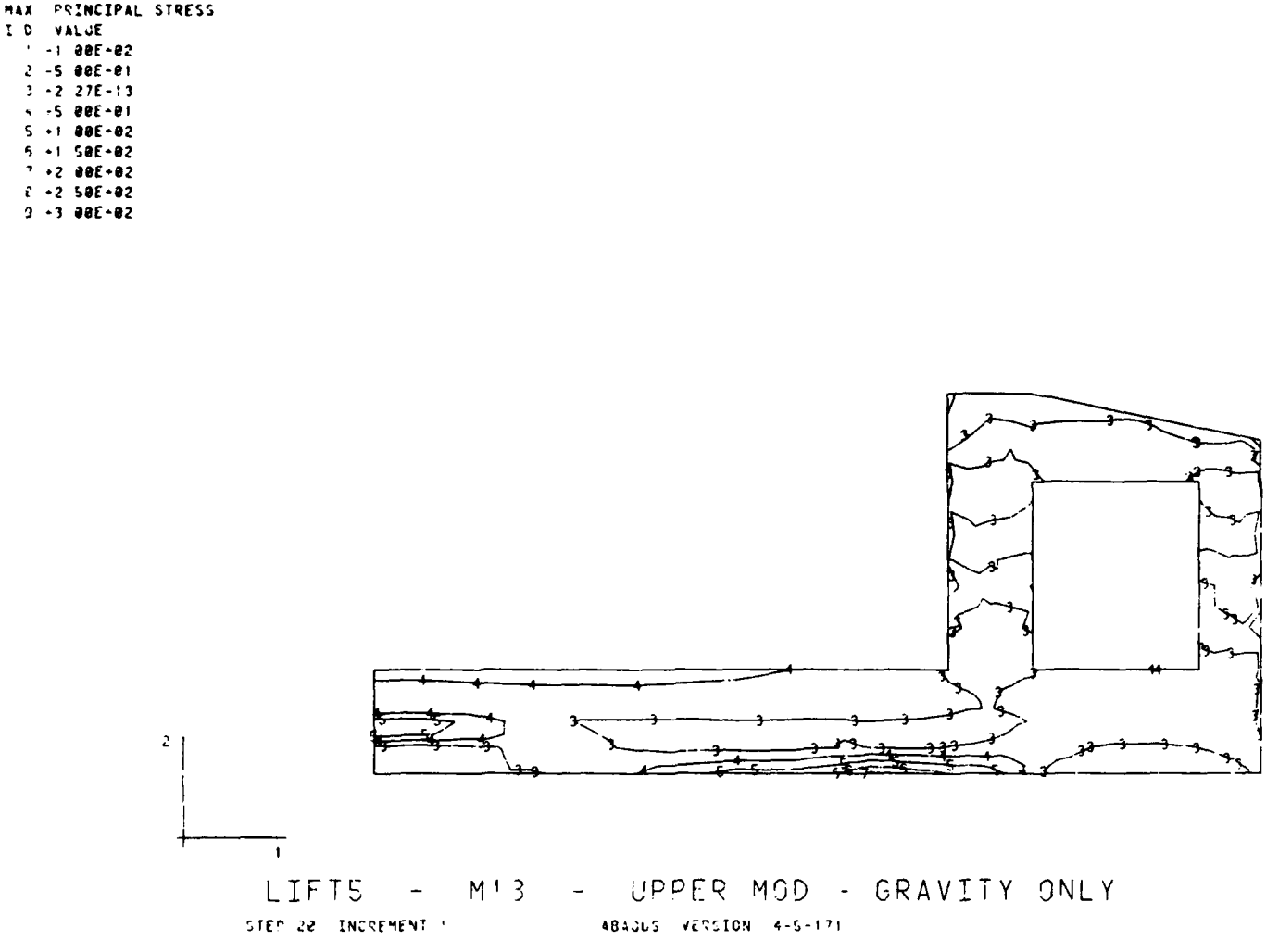

Figure 12c - Max. Principal stress contours in L-13, 5 days after lift 5 is placed, Gravity loading only, No creep/shrinkage

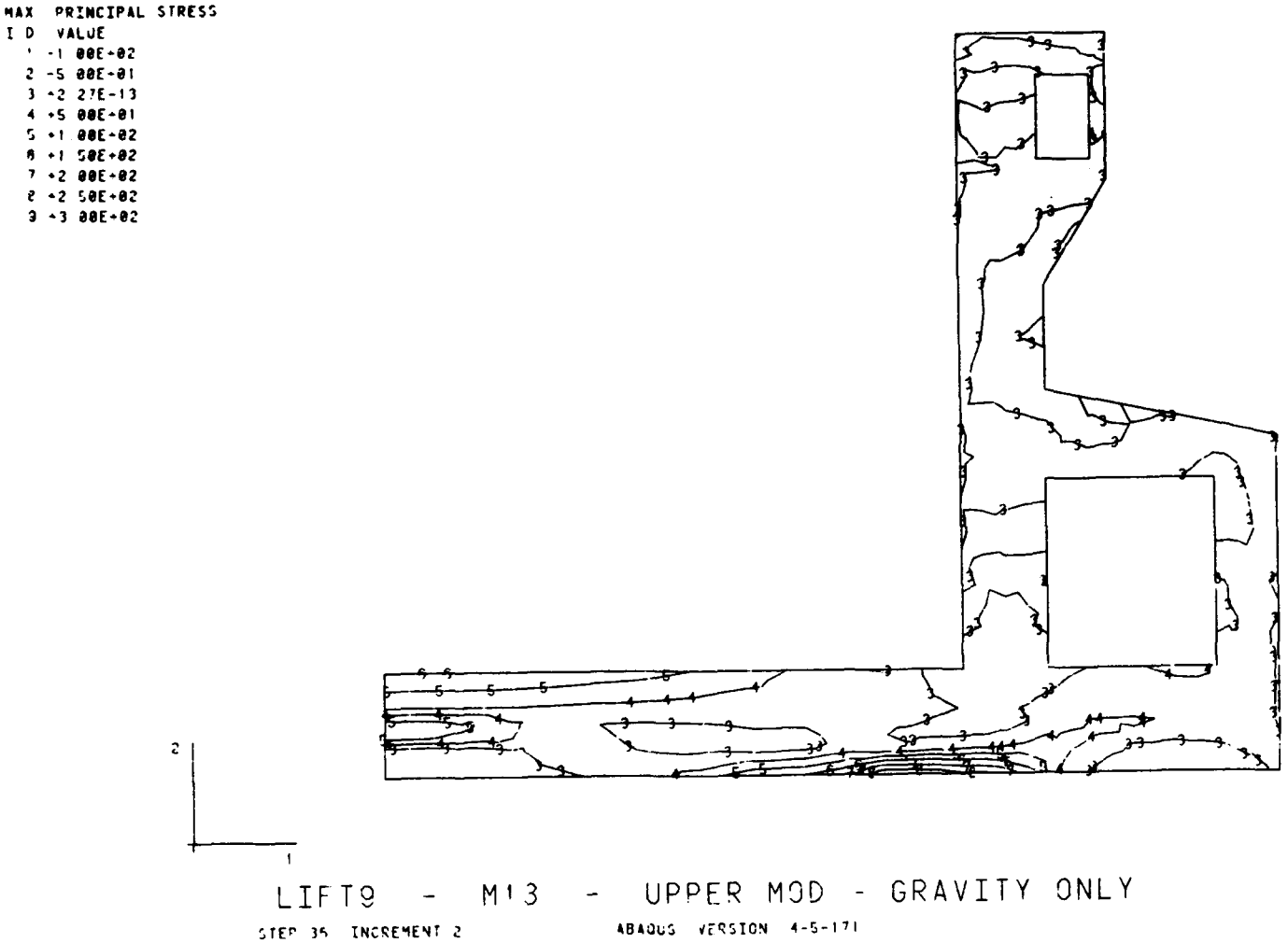

Figure 12d - Max. Principal stress contours in L-13, 7 days after lift 9 is placed, Gravity loading only, No creep/shrinkage

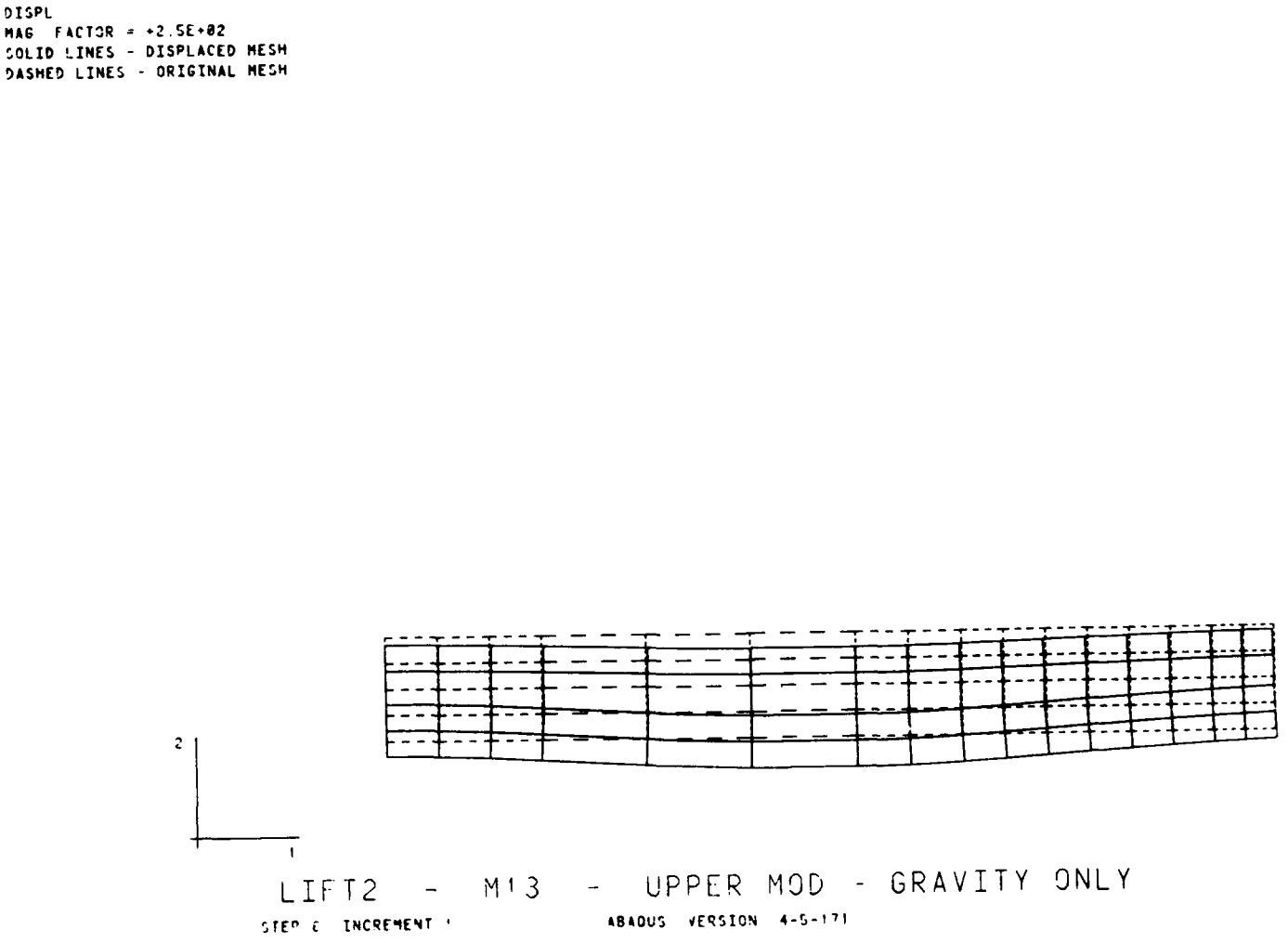

Figure 13a - Displaced shape of L-13, 5 days after lift 2 is placed, Gravity loading only, No creep/shrinkage

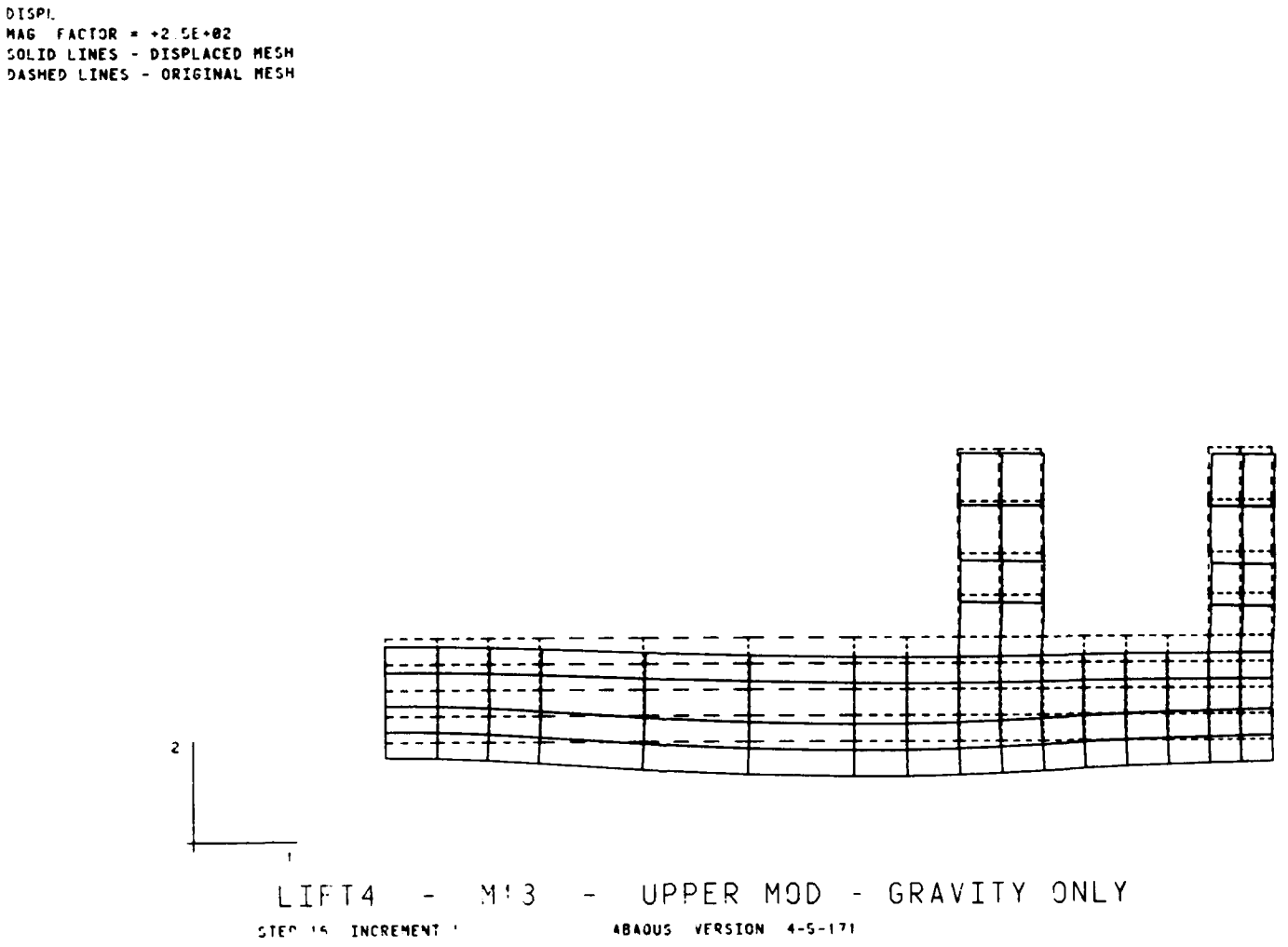

Figure 13b - Displaced shape of L-13, 5 days after lift 4 is placed, Gravity loading only, No creep/shrinkage

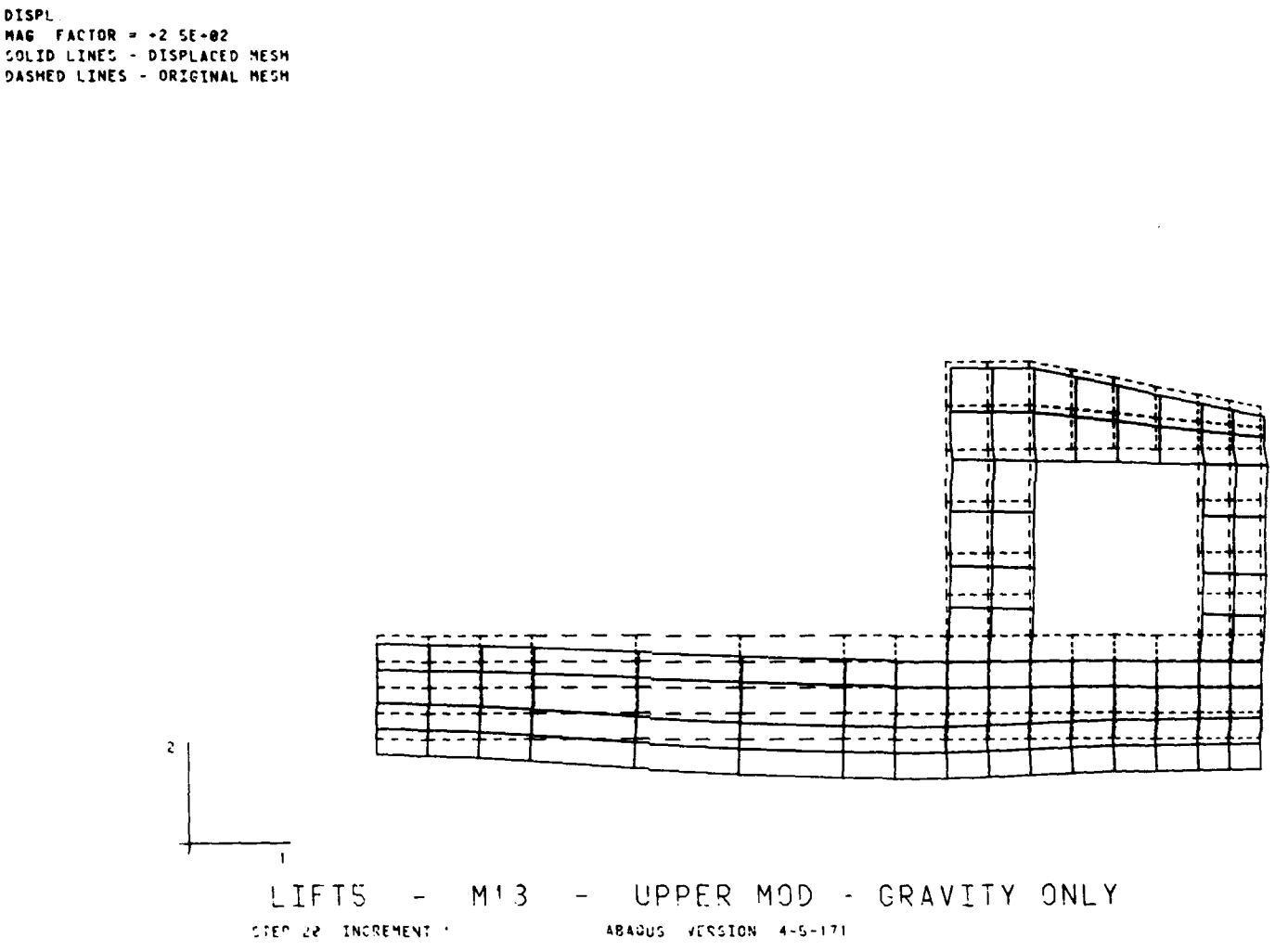

Figure 13c - Displaced shape of L-13, 5 days after lift 5 is placed, Gravity loading only, No creep/shrinkage

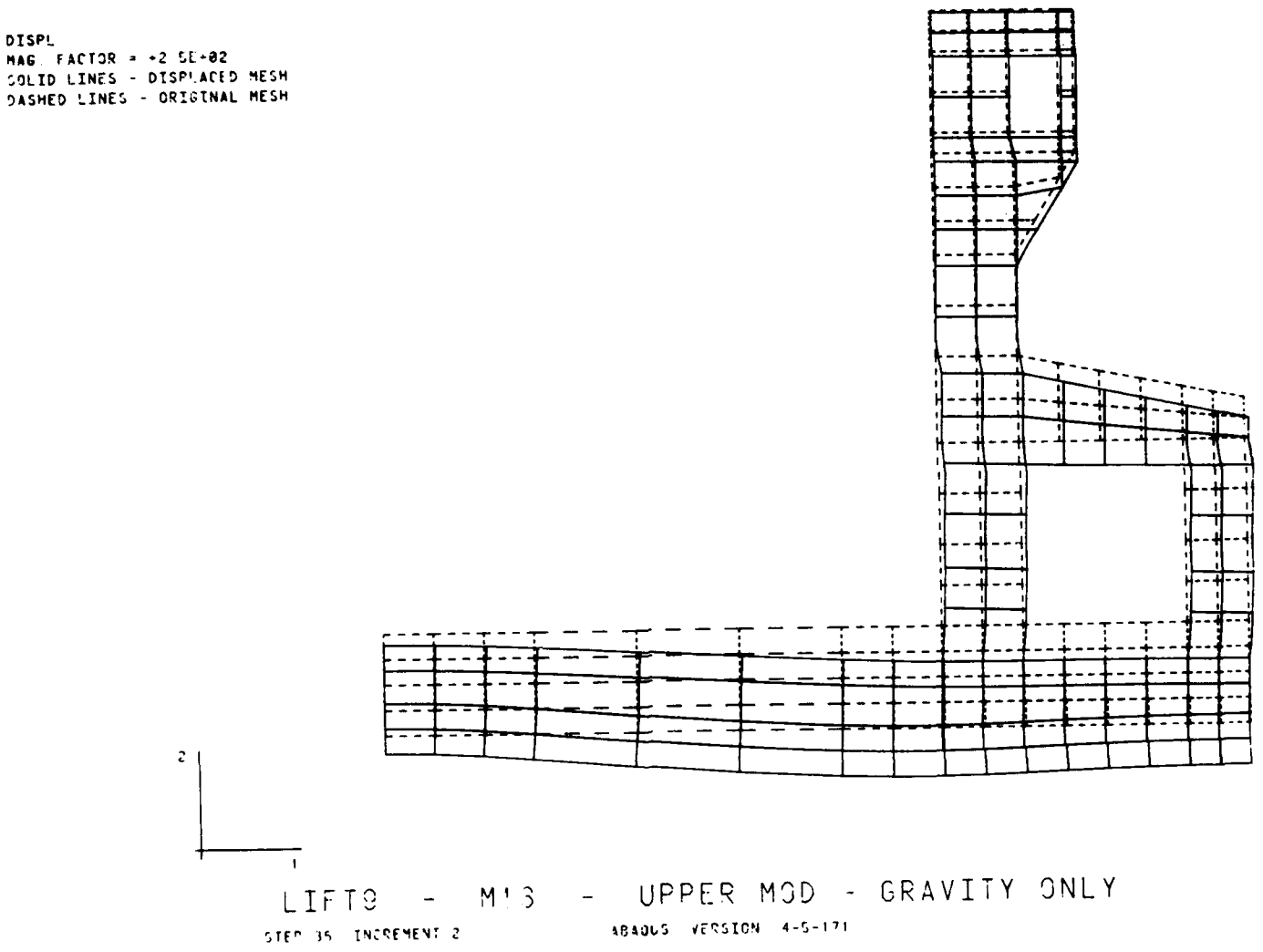

Figure 13d - Displaced shape of L-13, 7 days after lift 9 is placed, Gravity loading only, No creep/shrinkage

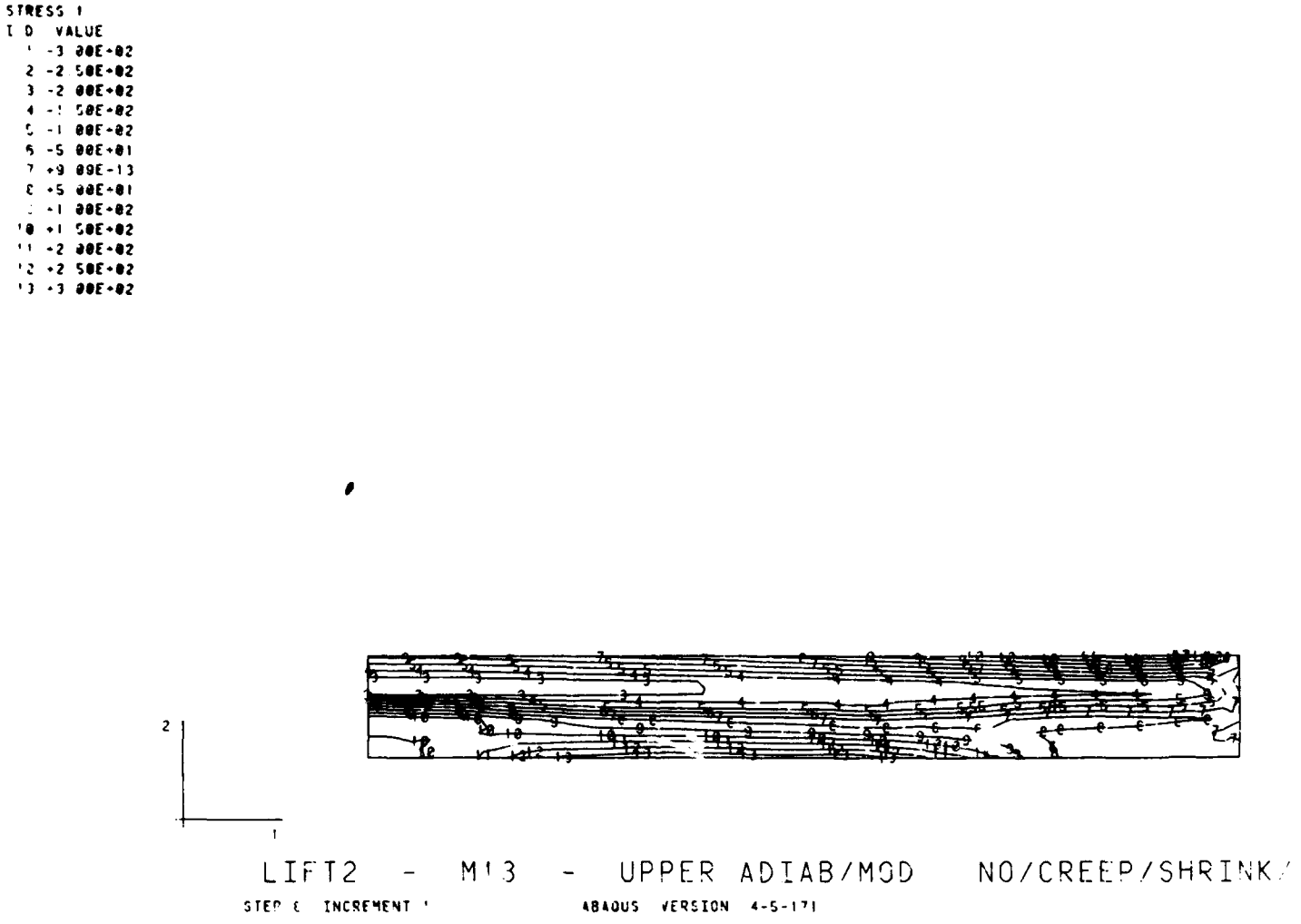

Figure 14a - Horizontal stress contours in L-13, 5 days after lift 2 is placed, Gravity & thermal loading, No creep/shrinkage

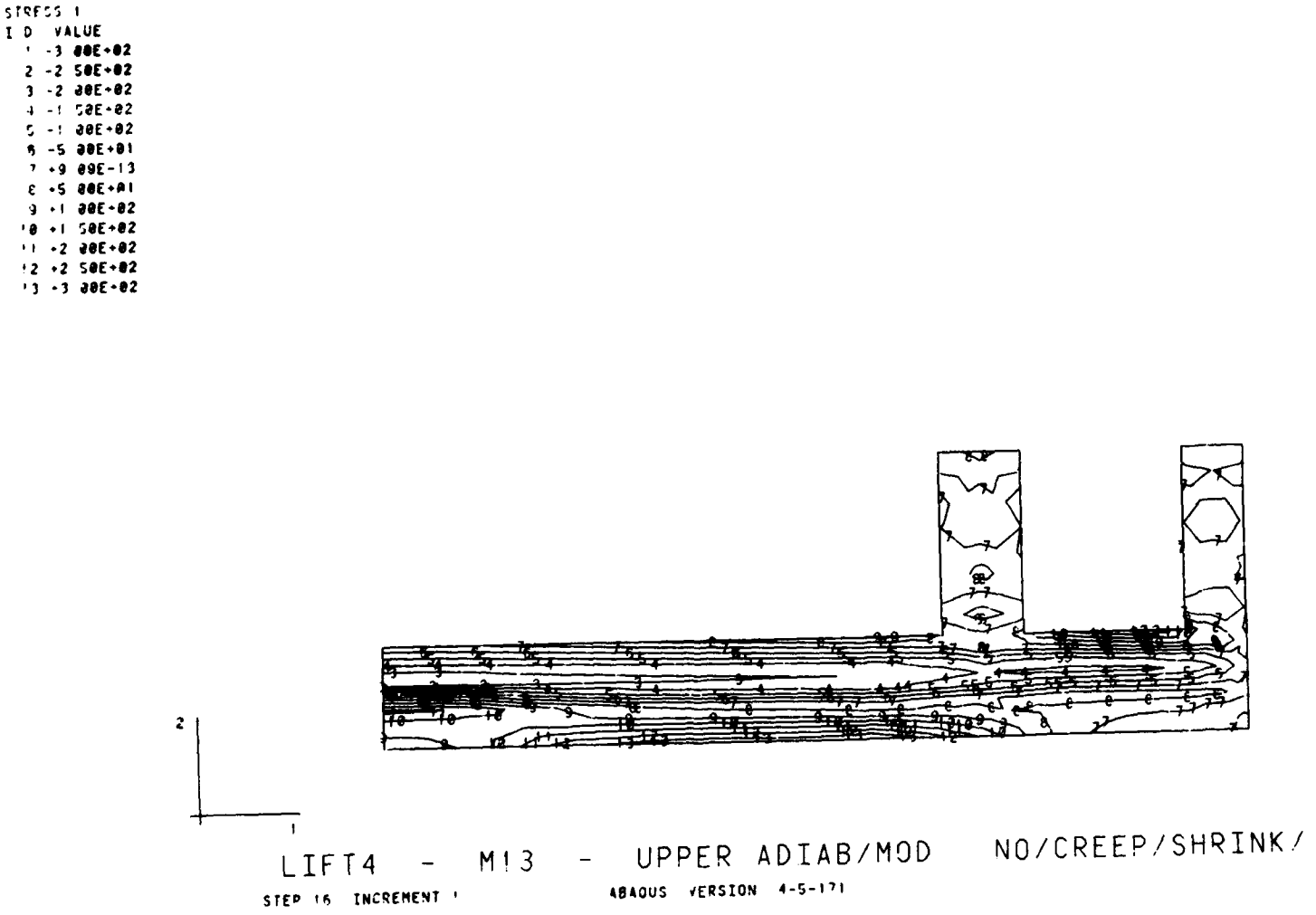

**Figure 14b - Horizontal stress contours in L-13,
5 days after lift 4 is placed,
Gravity & thermal loading, No creep/shrinkage**

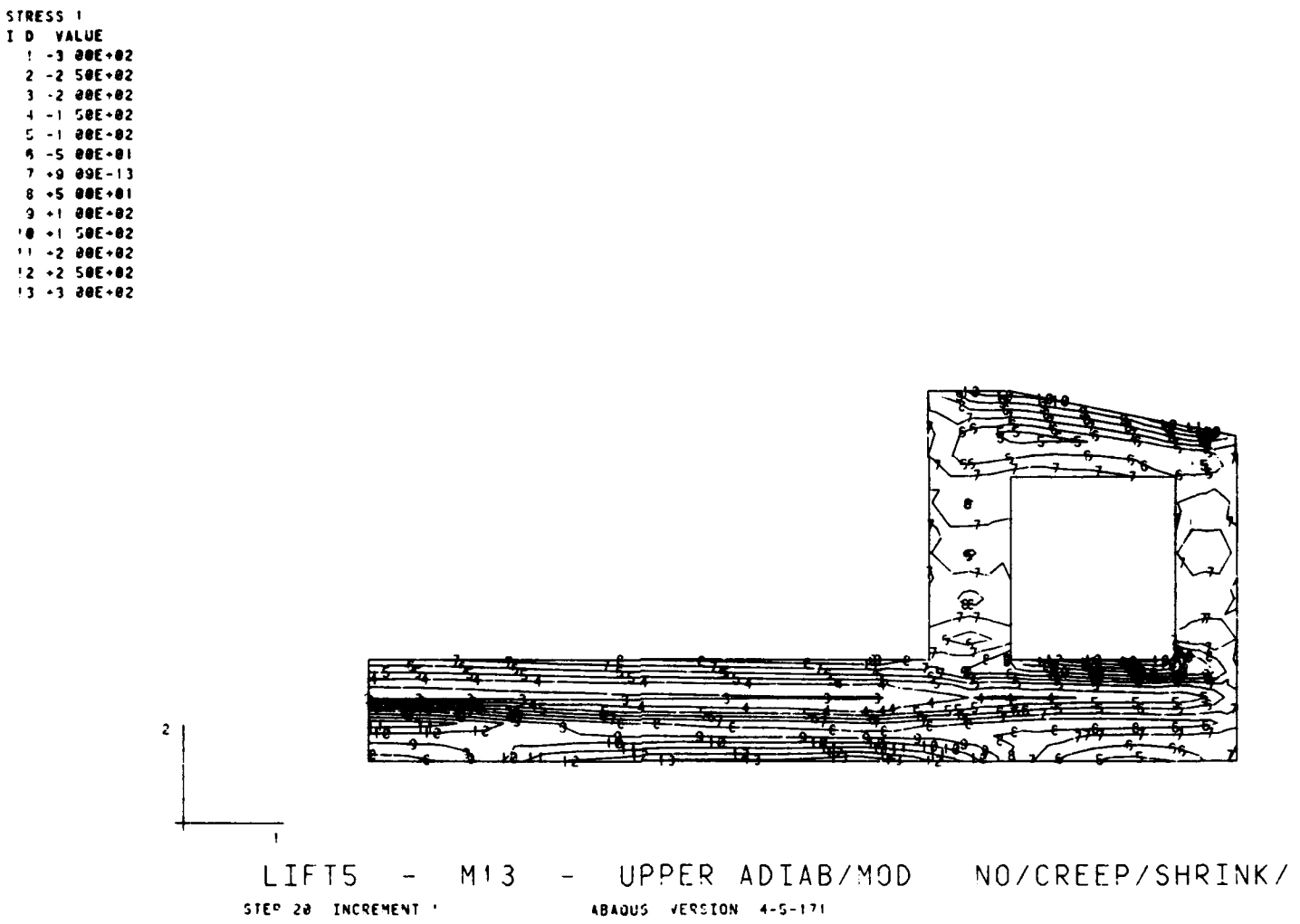

Figure 14c - Horizontal stress contours in L-13, 5 days after lift 5 is placed, Gravity & thermal loading, No creep/shrinkage

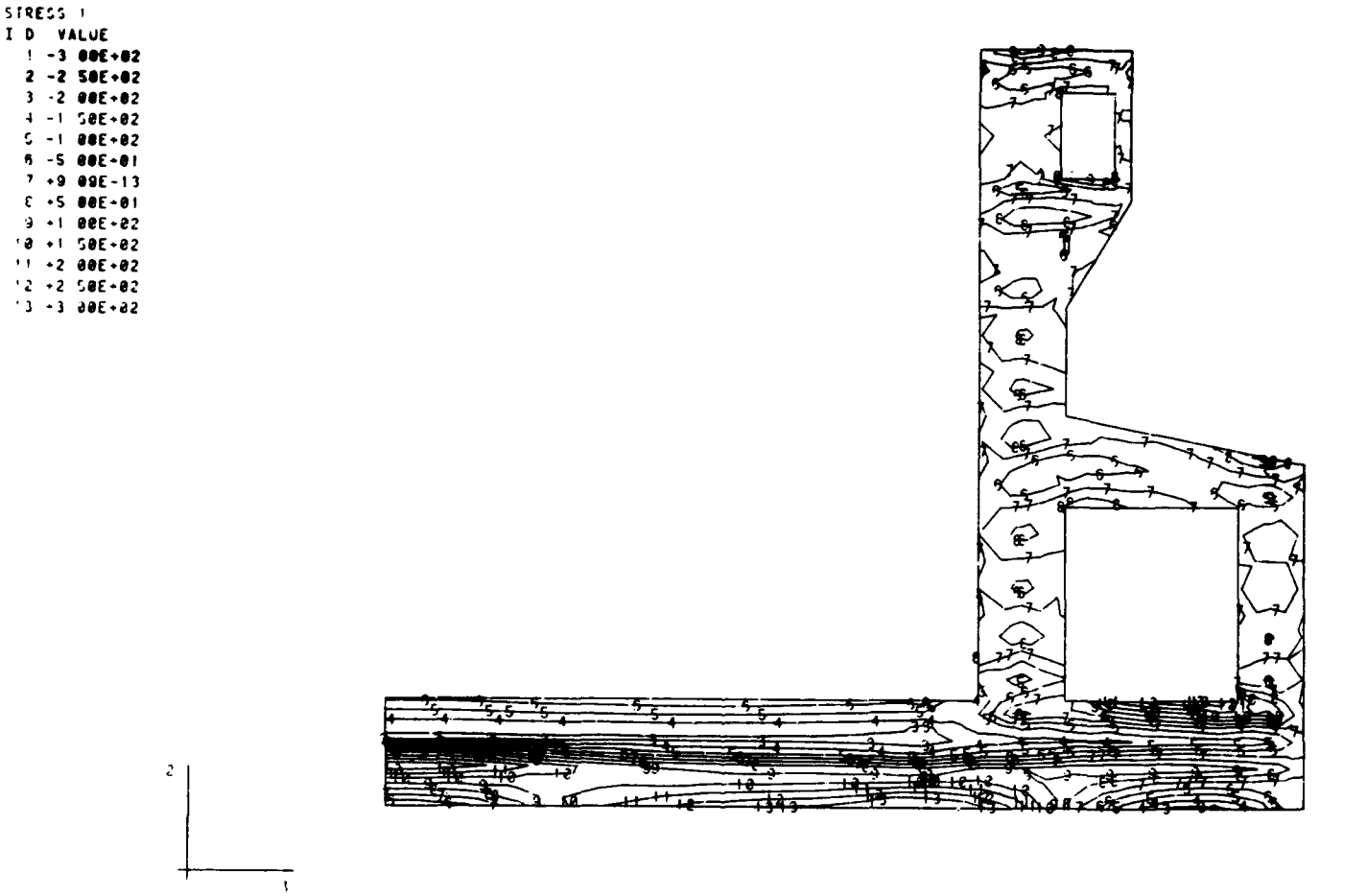

Figure 14d - Horizontal stress contours in L-13, 7 days after lift 9 is placed, Gravity & thermal loading, No creep/shrinkage

STRESS 2

I D	VALUE
1	-3 00E+02
2	-2 50E+02
3	-2 00E+02
4	-1 50E+02
5	-1 00E+02
6	-5 00E+01
7	+9 09E-13
8	+5 00E+01
9	+1 00E+02
10	+1 50E+02
11	+2 00E+02
12	+2 50E+02
13	+3 00E+02

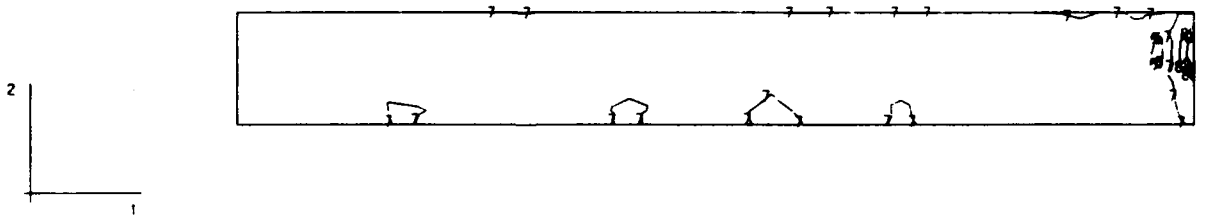

LIFT2 - M13 - UPPER ADIAB/MOD NO/CREEP/SHRINK/

STEP 6 INCREMENT 1 ABAQUS VERSION 4-5-171

Figure 15a - Vertical stress contours in L-13, 5 days after lift 2 is placed, Gravity & thermal loading, No creep/shrinkage

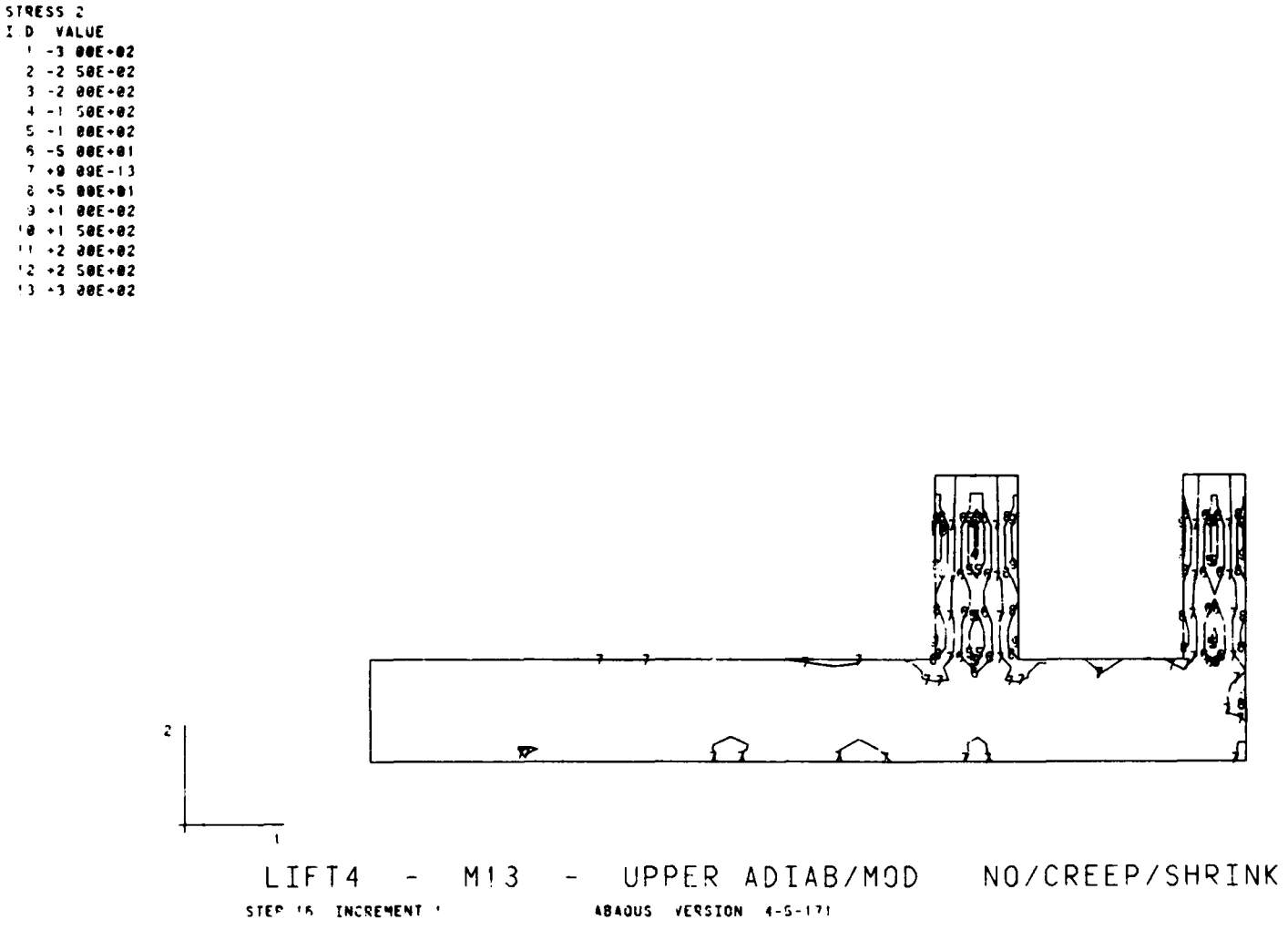

Figure 15b - Vertical stress contours in L-13, 5 days after lift 4 is placed, Gravity & thermal loading, No creep/shrinkage

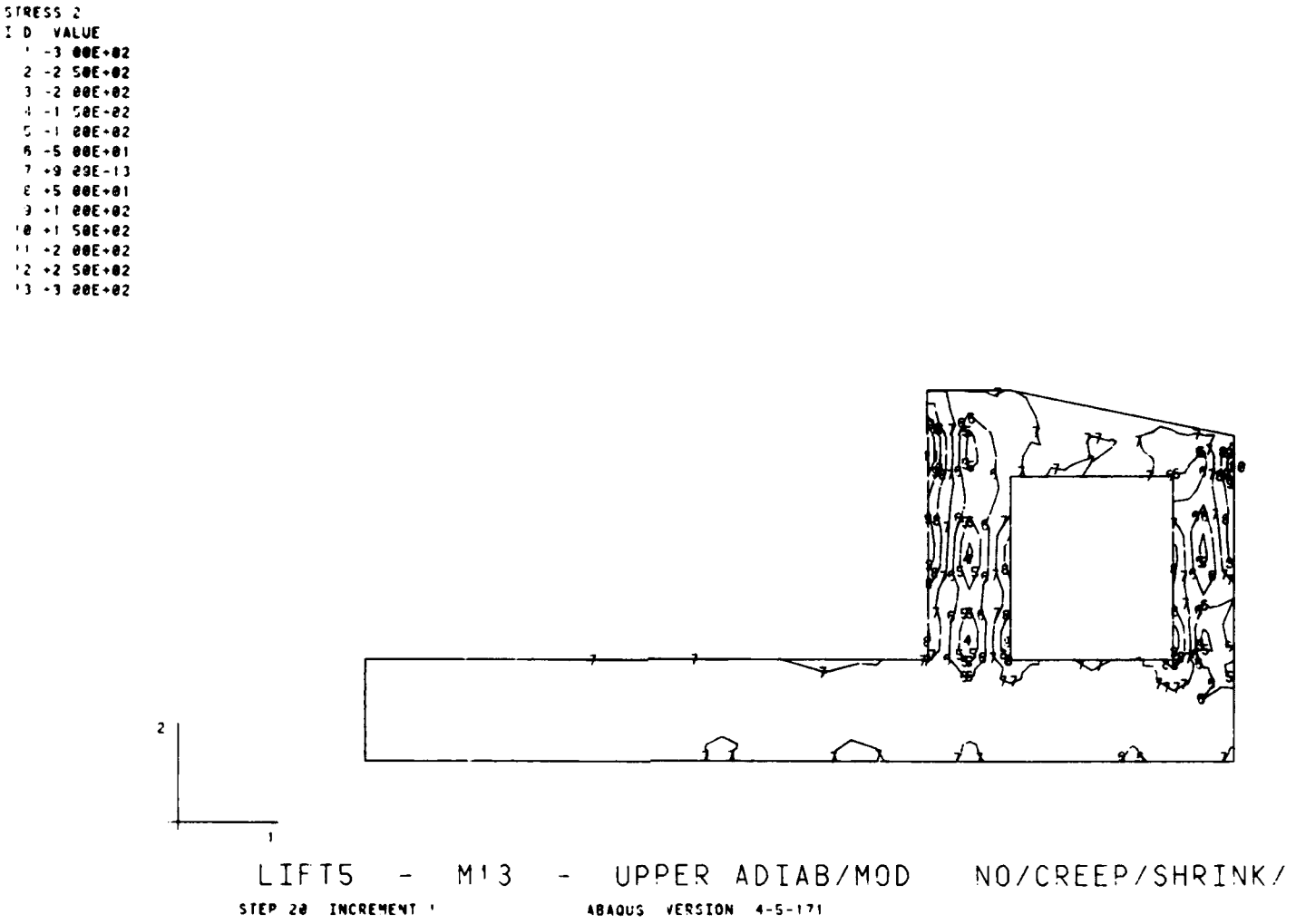

**Figure 15c - Vertical stress contours in L-13,
5 days after lift 5 is placed,
Gravity & thermal loading, No creep/shrinkage**

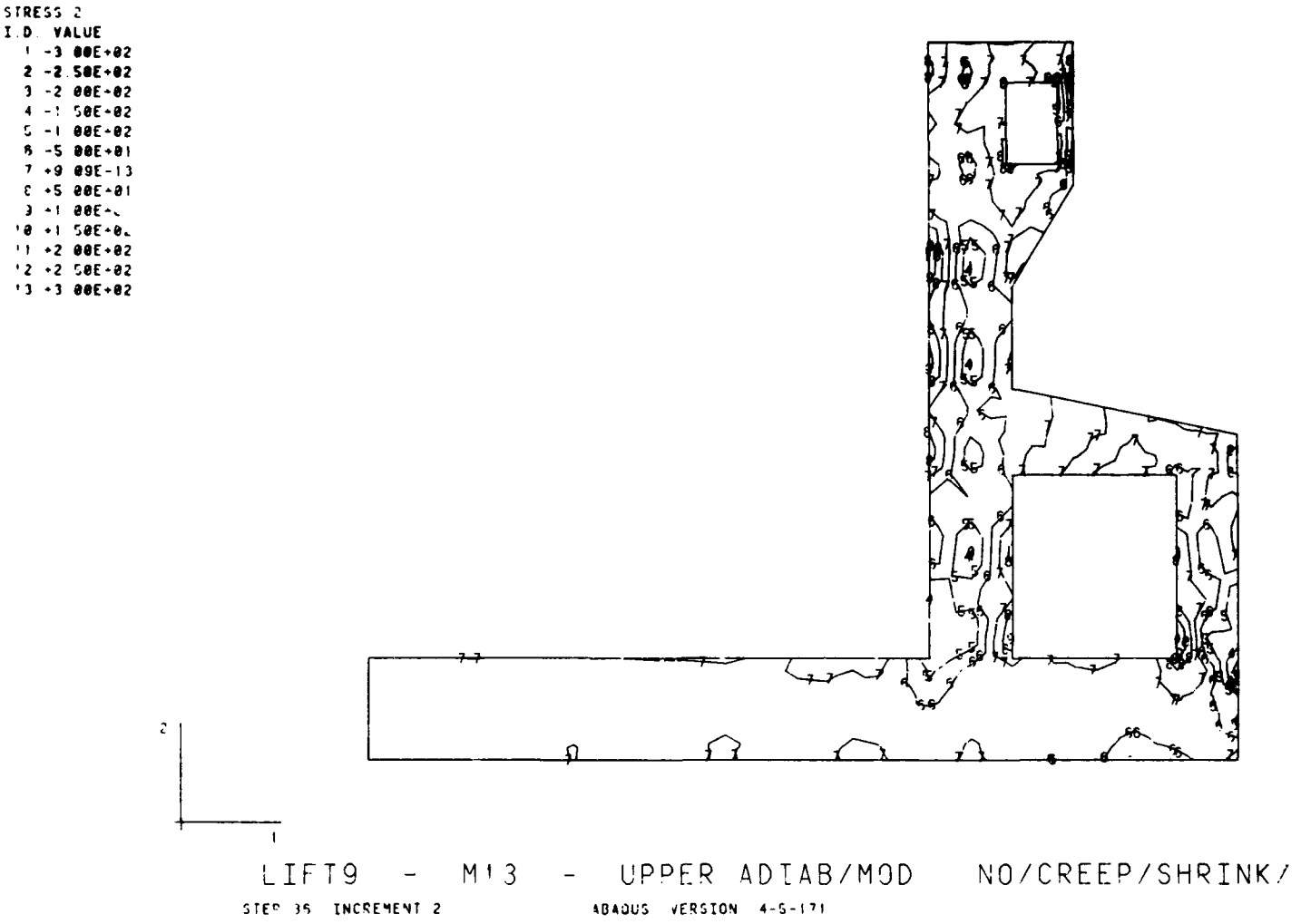

Figure 15d - Vertical stress contours in L-13, 7 days after lift 9 is placed, Gravity & thermal loading, No creep/shrinkage

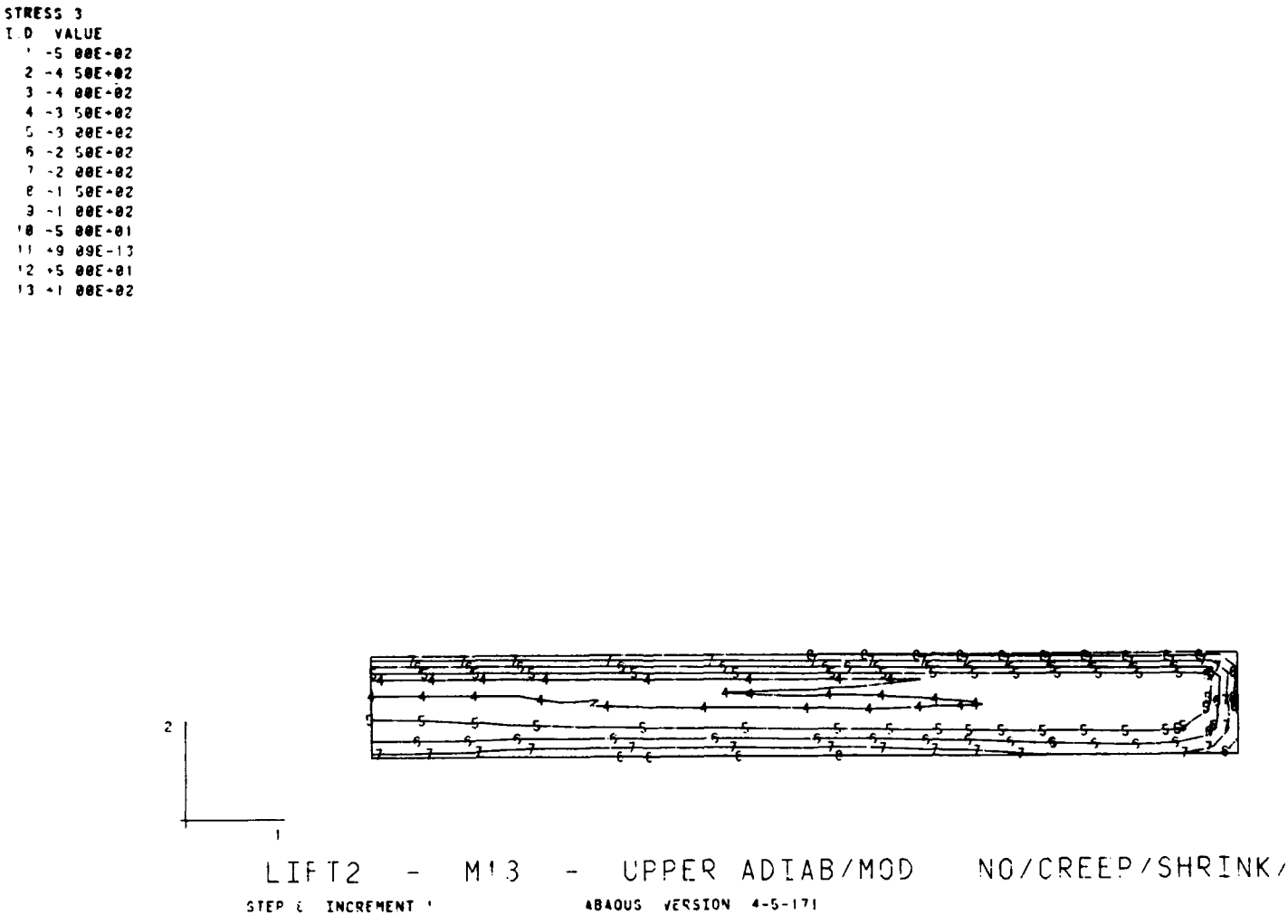

Figure 16a - Out-of-plane stress contours in L-13, 5 days after lift 2 is placed, Gravity & thermal loading, No creep/shrinkage

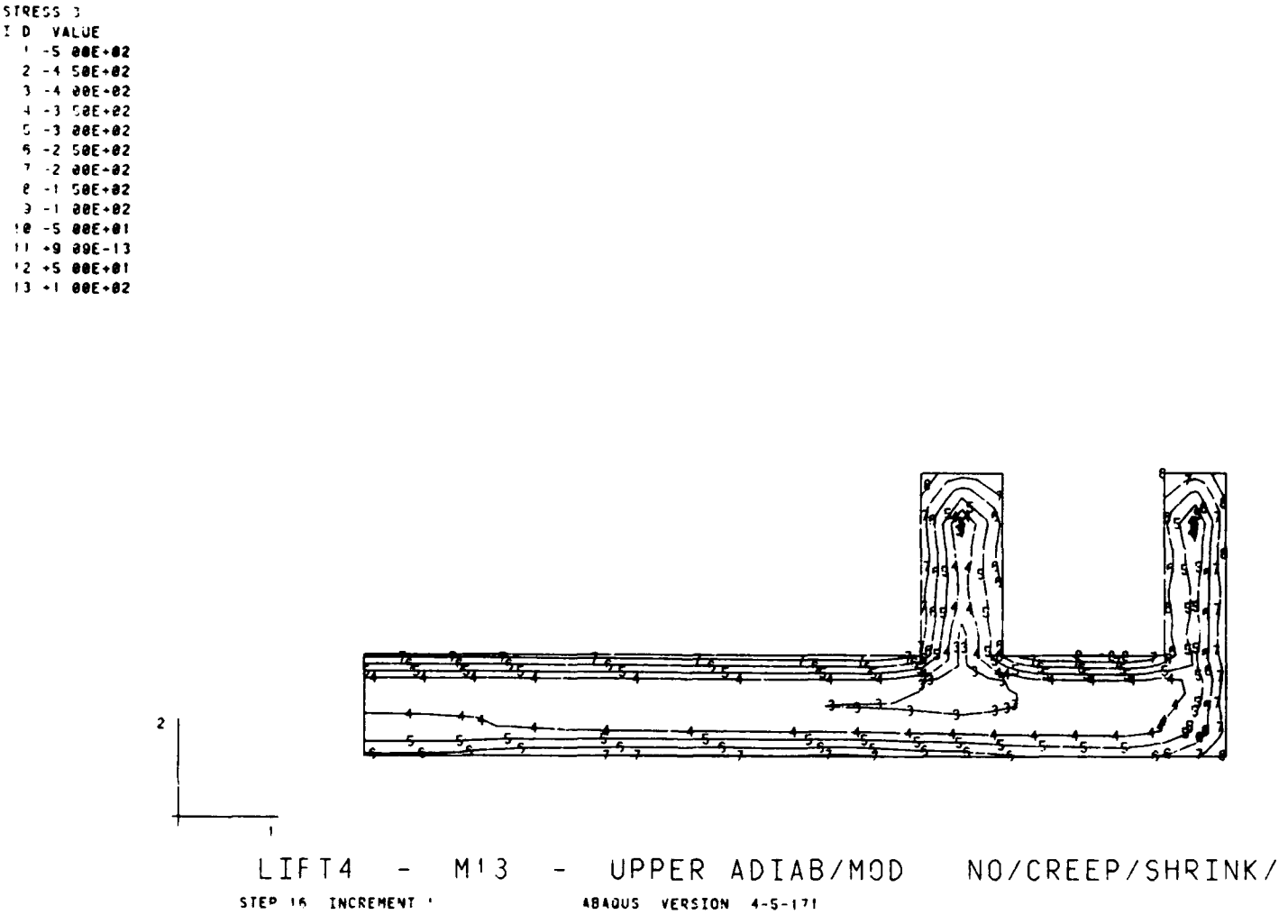

Figure 16b - Out-of-plane stress contours in L-13, 5 days after lift 4 is placed, Gravity & thermal loading, No creep/shrinkage

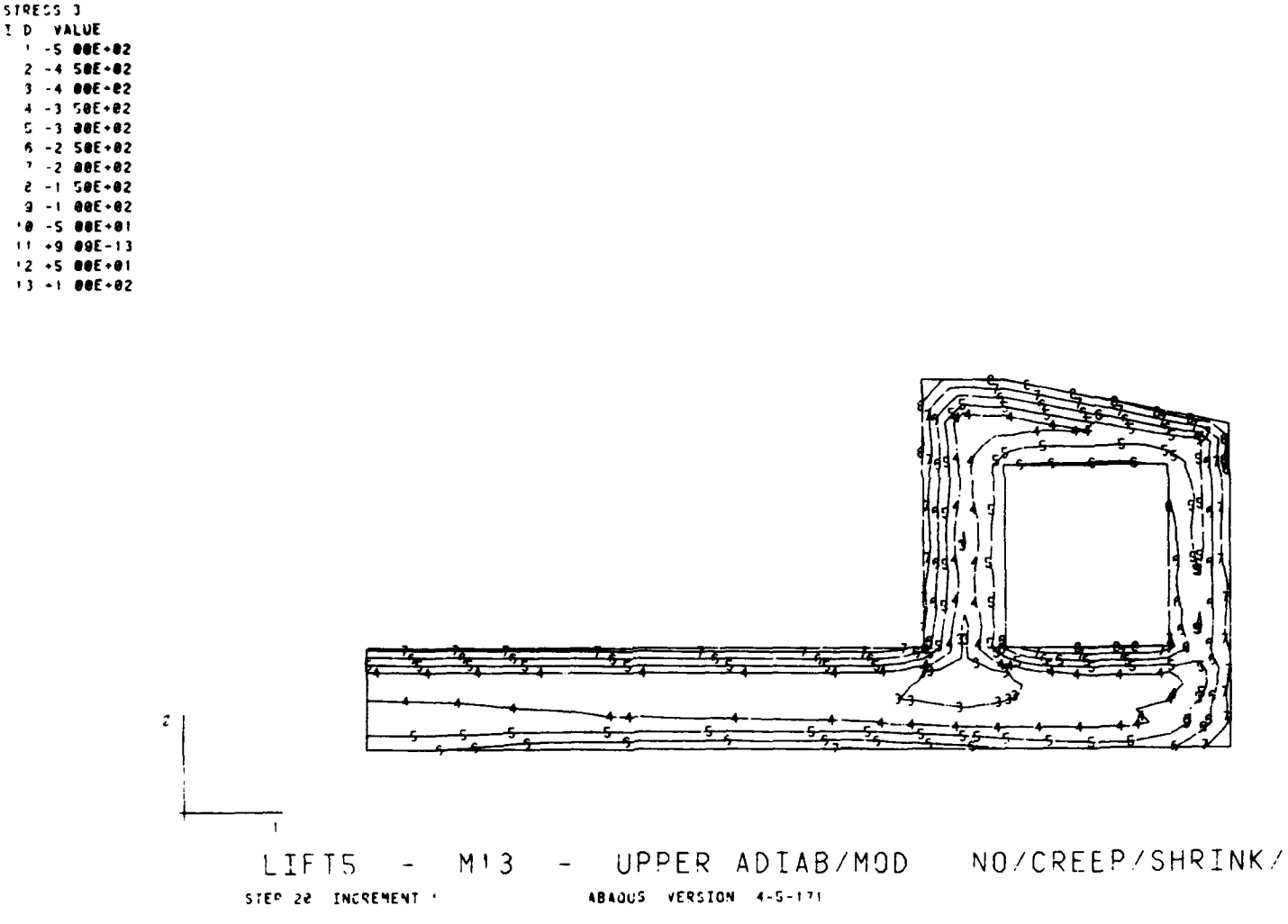

Figure 16c - Out-of-plane stress contours in L-13, 5 days after lift 5 is placed, Gravity & thermal loading, No creep/shrinkage

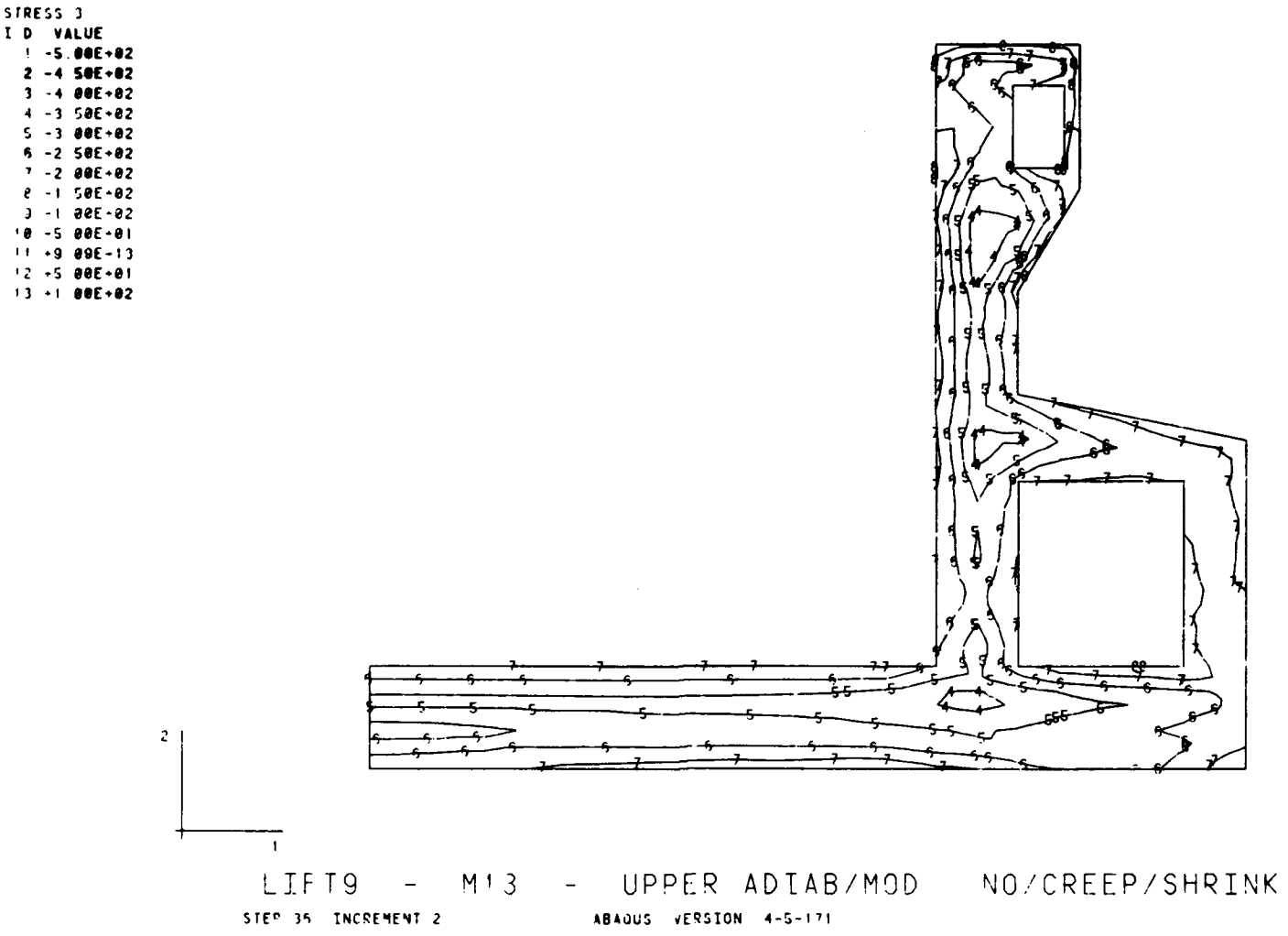

Figure 16d - Out-of-plane stress contours in L-13, 7 days after lift 9 is placed, Gravity & thermal loading, No creep/shrinkage

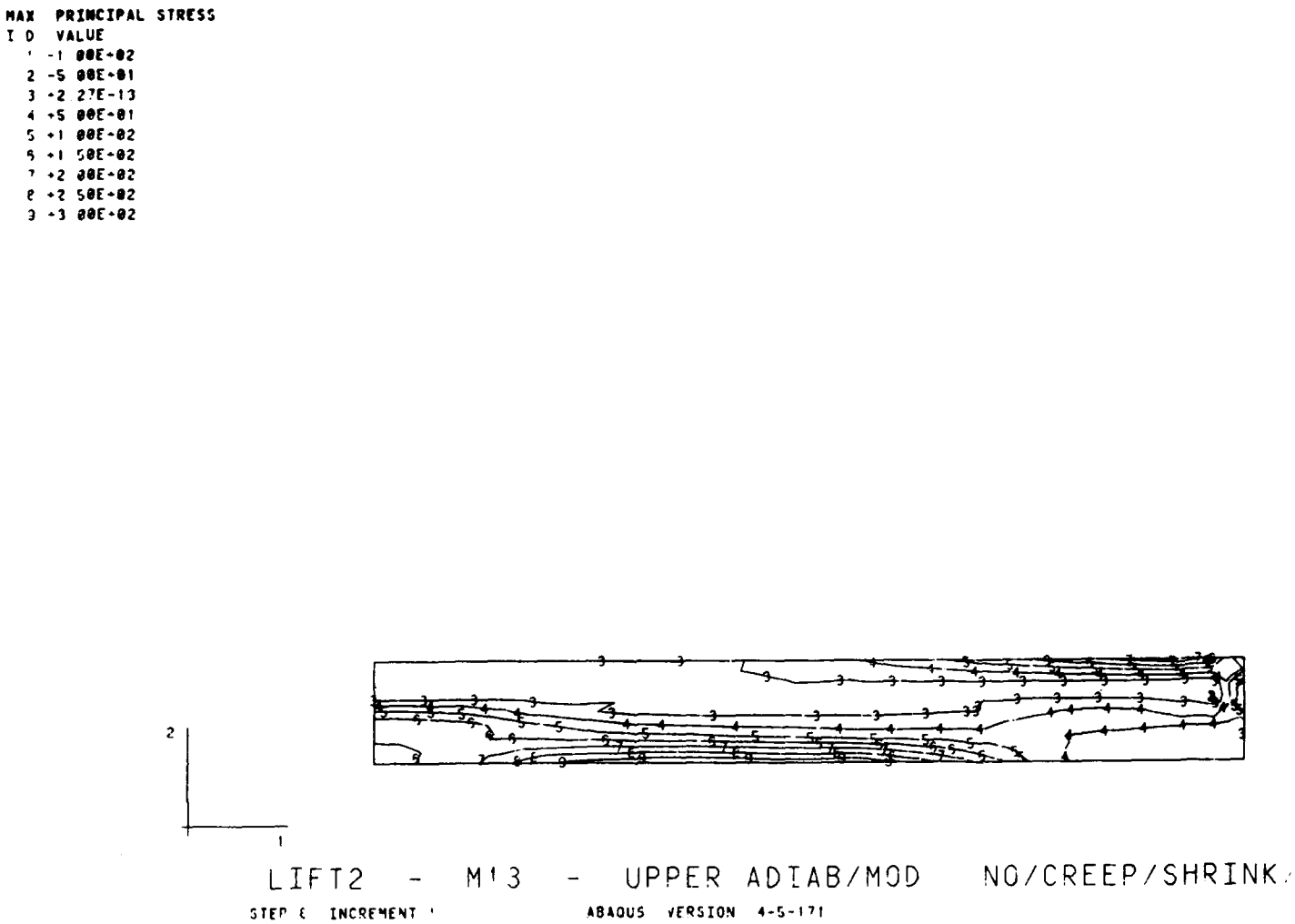

Figure 17a - Max. Principal stress contours in L-13,
5 days after lift 2 is placed,
Gravity & thermal loading, No creep/shrinkage

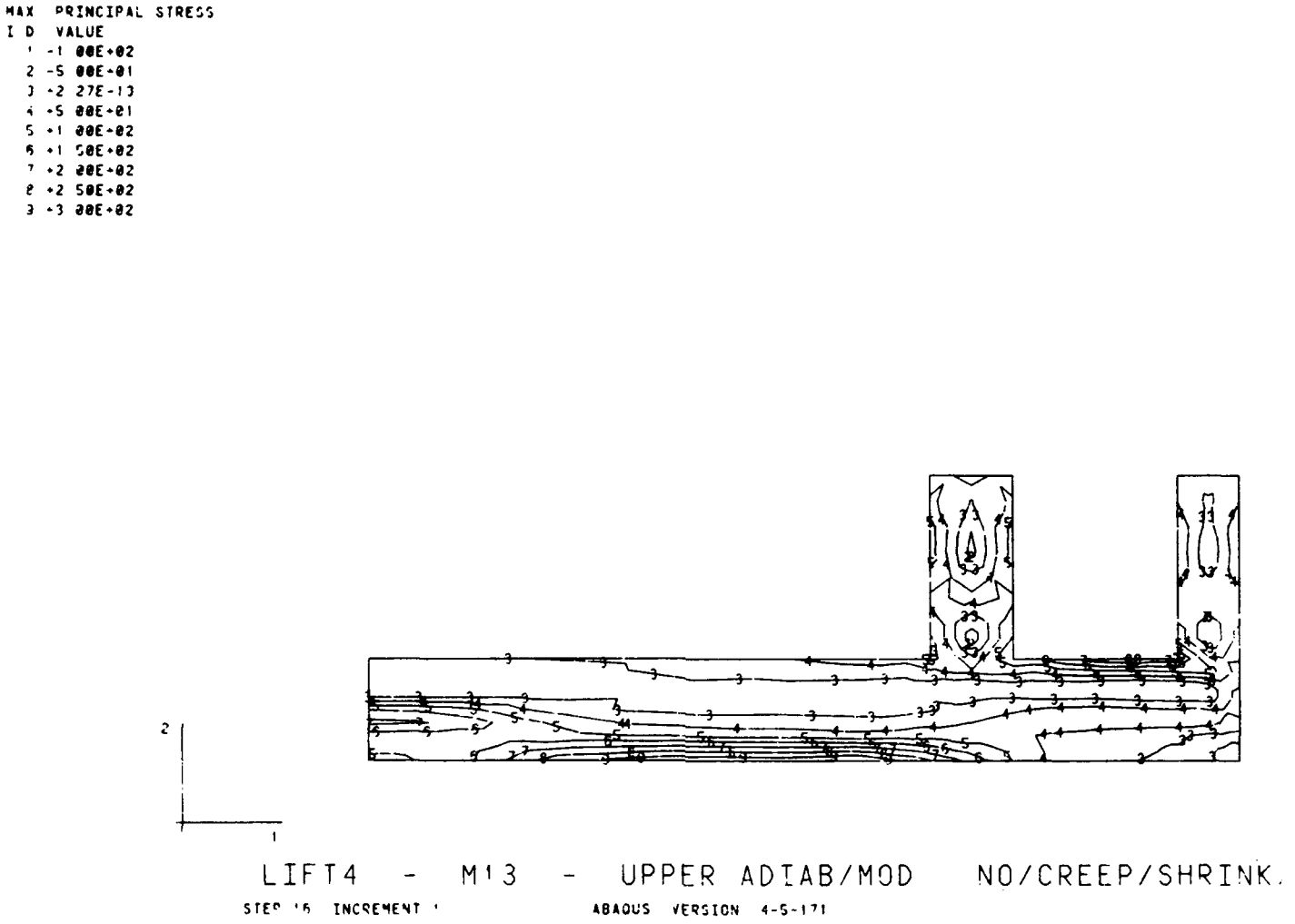

Figure 17b - Max. Principal stress contours in L-13, 5 days after lift 4 is placed, Gravity & thermal loading, No creep/shrinkage

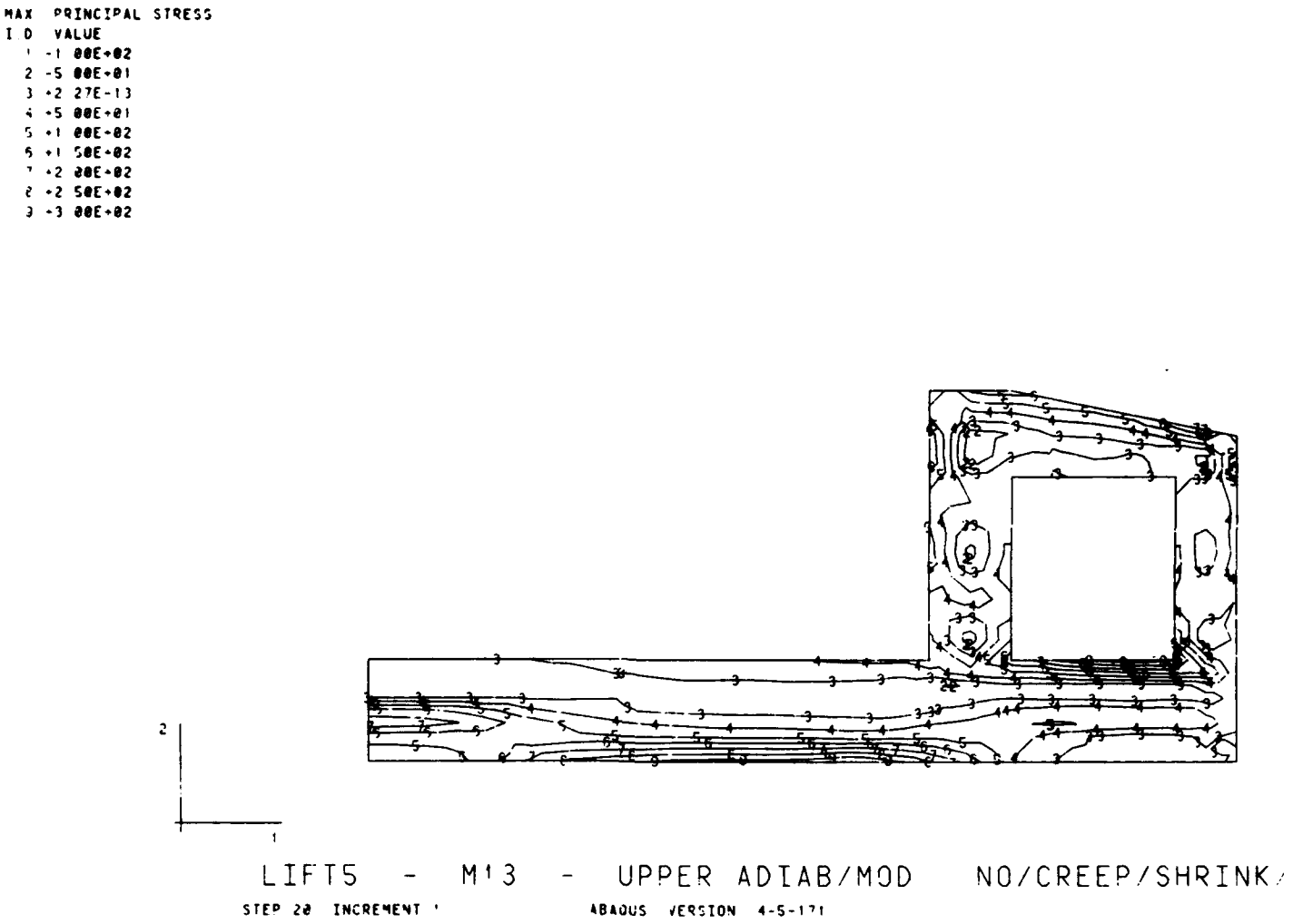

Figure 17c - Max. Principal stress contours in L-13, 5 days after lift 5 is placed, Gravity & thermal loading, No creep/shrinkage

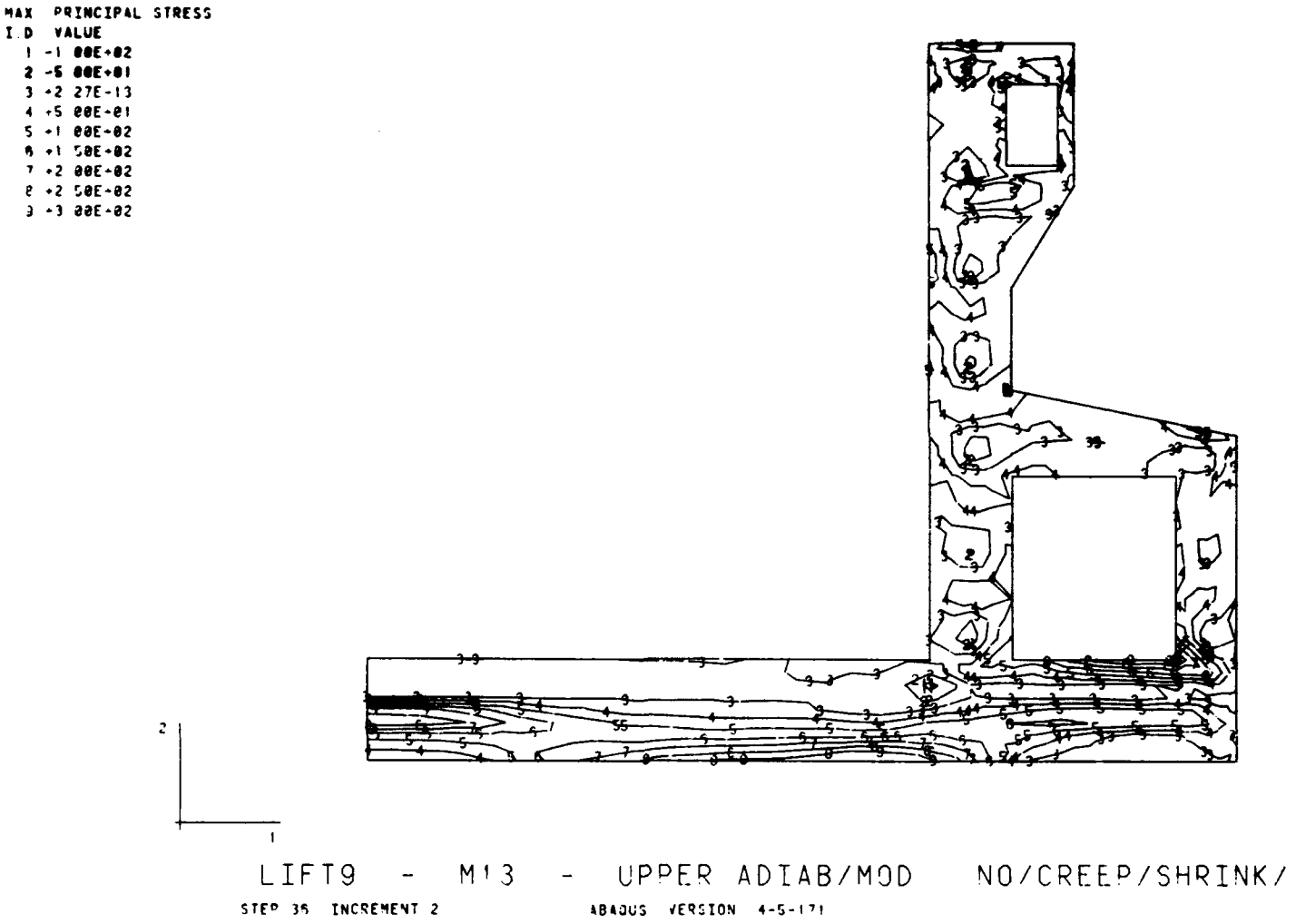

Figure 17d - Max. Principal stress contours in L-13, 7 days after lift 9 is placed, Gravity & thermal loading, No creep/shrinkage

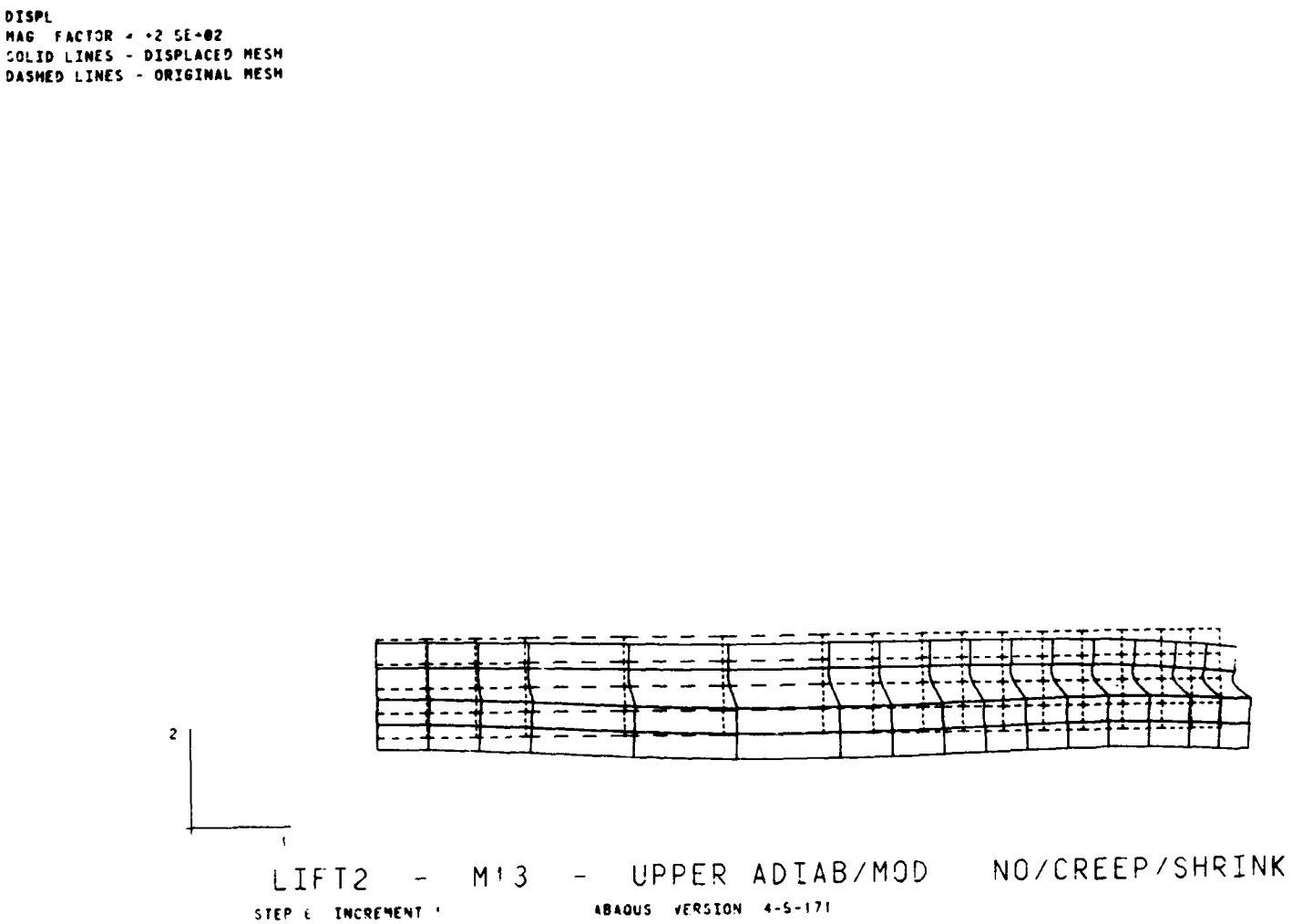

**Figure 18a - Displaced shape of L-13,
5 days after lift 2 is placed,
Gravity & thermal loading, No creep/shrinkage**

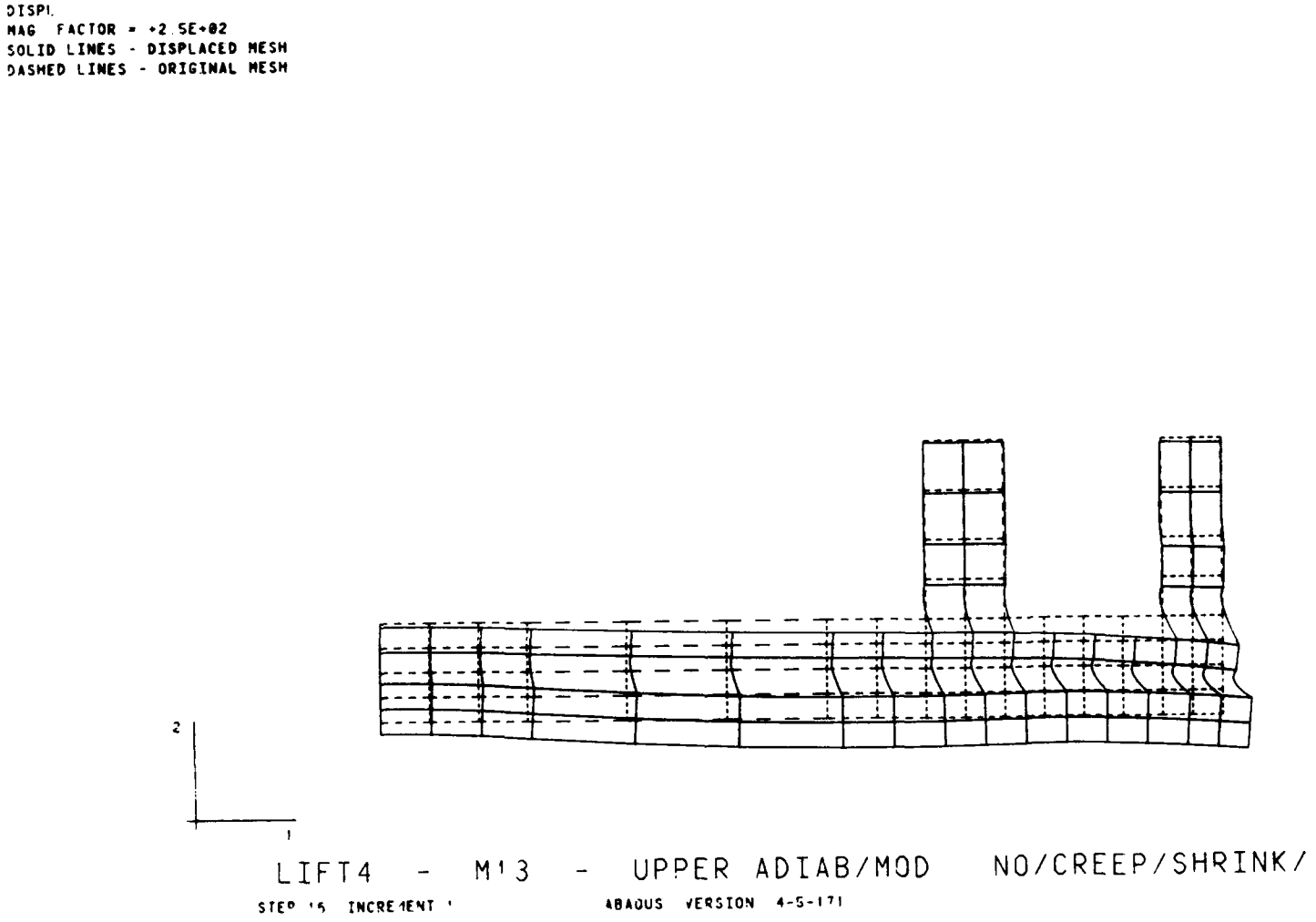

**Figure 18b - Displaced shape of L-13,
5 days after lift 4 is placed,
Gravity & thermal loading, No creep/shrinkage**

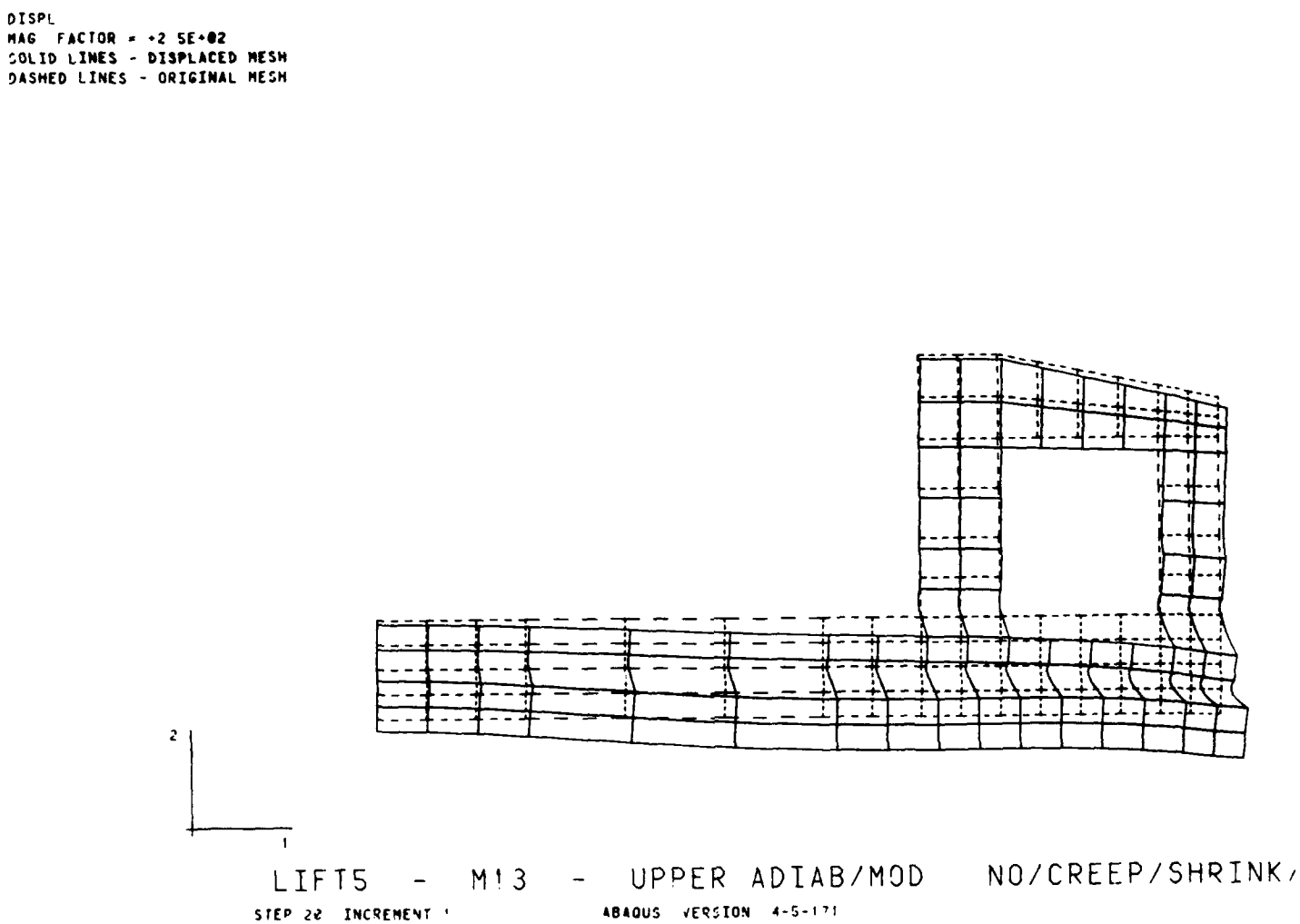

**Figure 18c - Displaced shape of L-13,
5 days after lift 5 is placed,
Gravity & thermal loading, No creep/shrinkage**

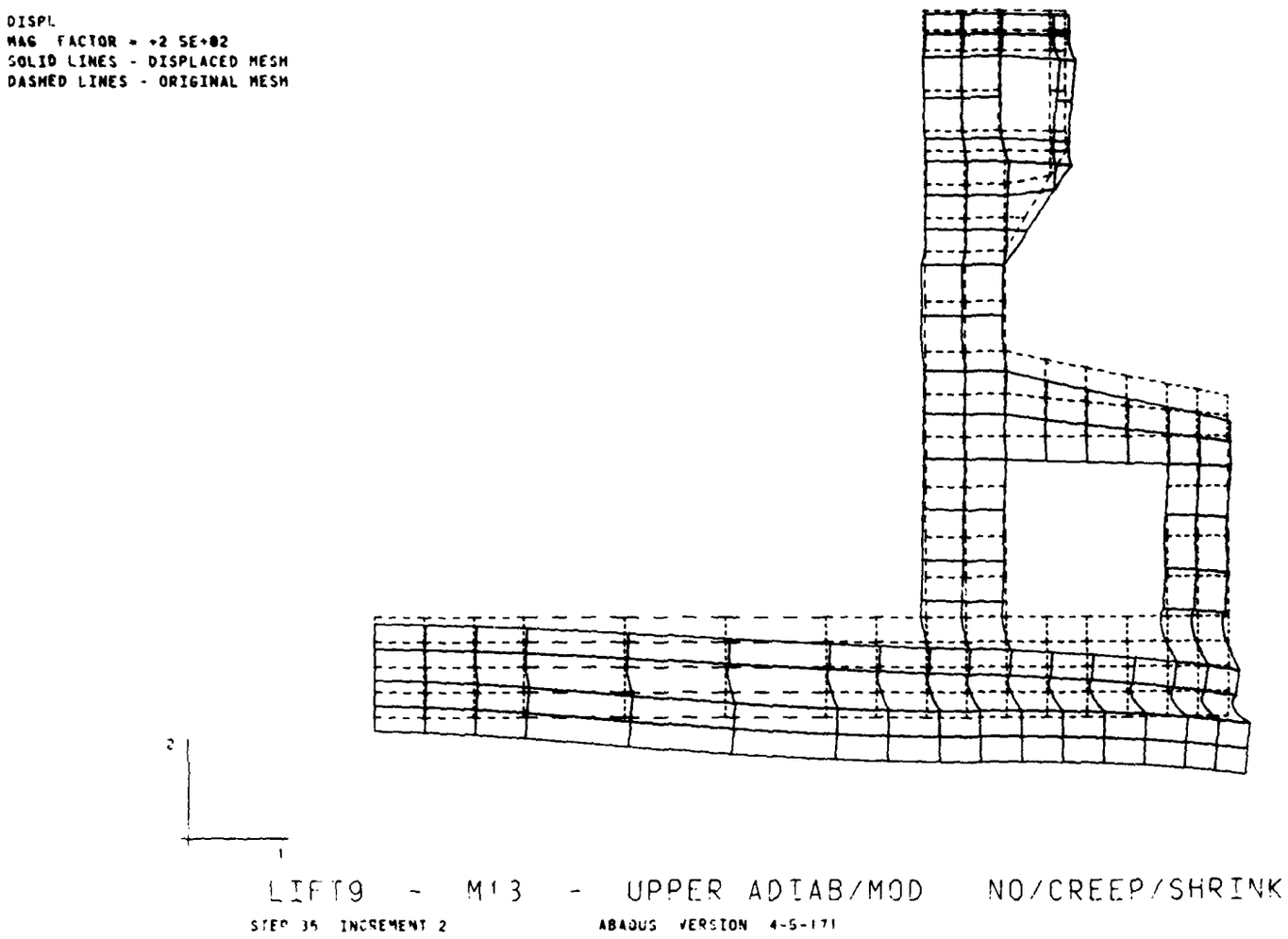

**Figure 18d - Displaced shape of L-13,
7 days after lift 9 is placed,
Gravity & thermal loading, No creep/shrinkage**

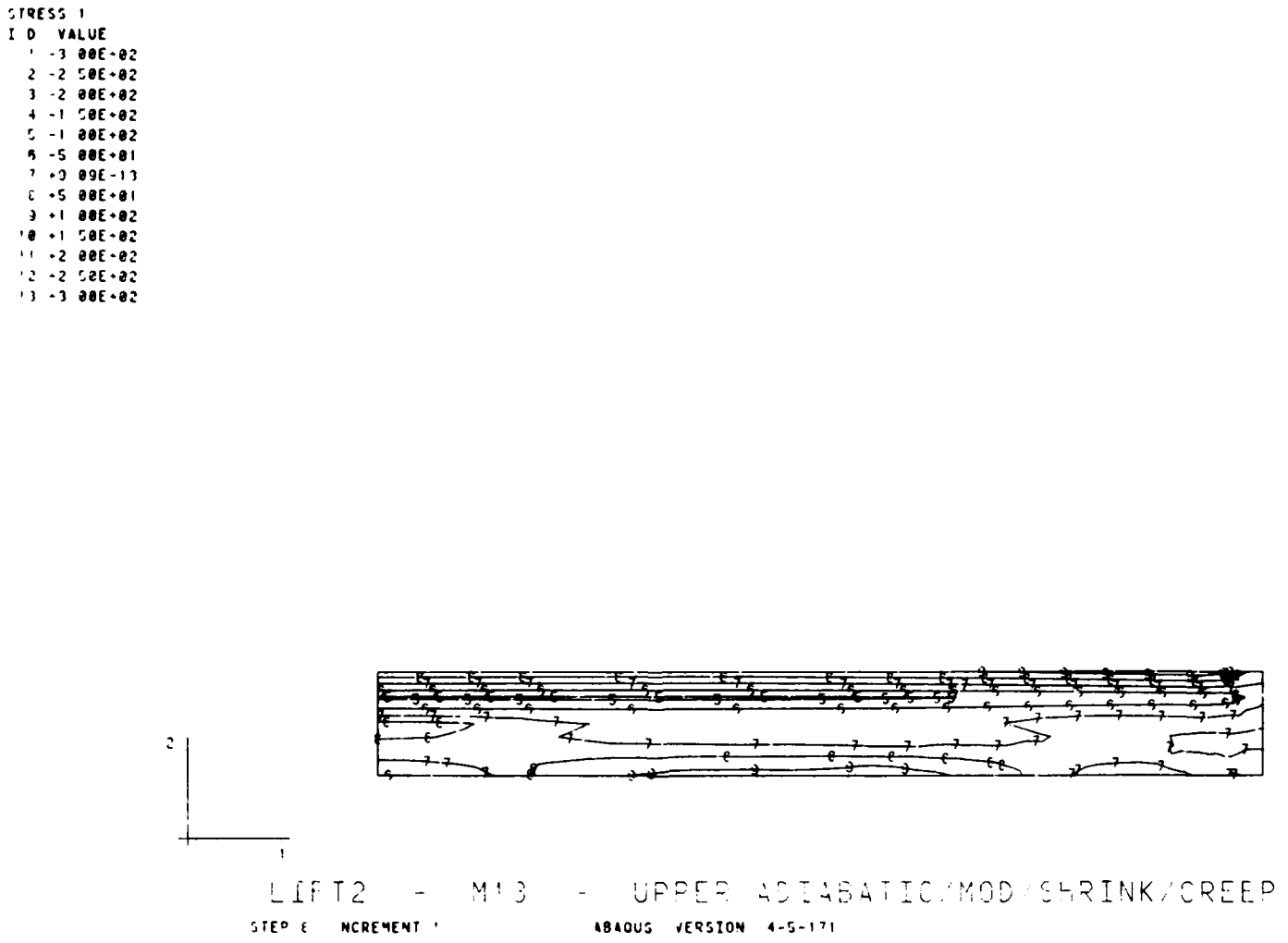

Figure 19a - Horizontal stress con ours in L-13,
5 days after lift 2 is placed,
Gravity & thermal loading, Upper creep/shrinkage

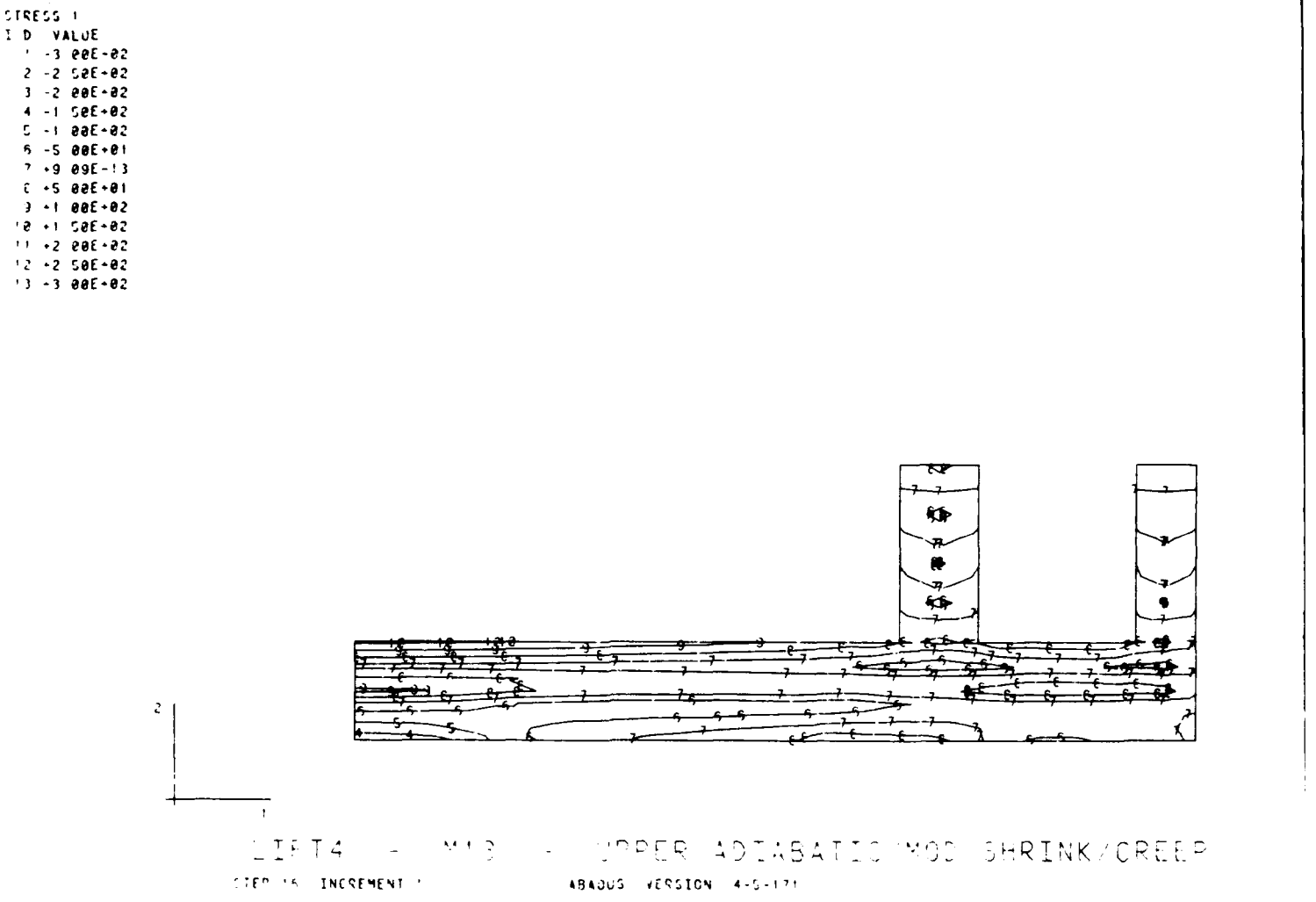

Figure 19b - Horizontal stress contours in L-13,
5 days after lift 4 is placed,
Gravity & thermal loading, Upper creep/shrinkage

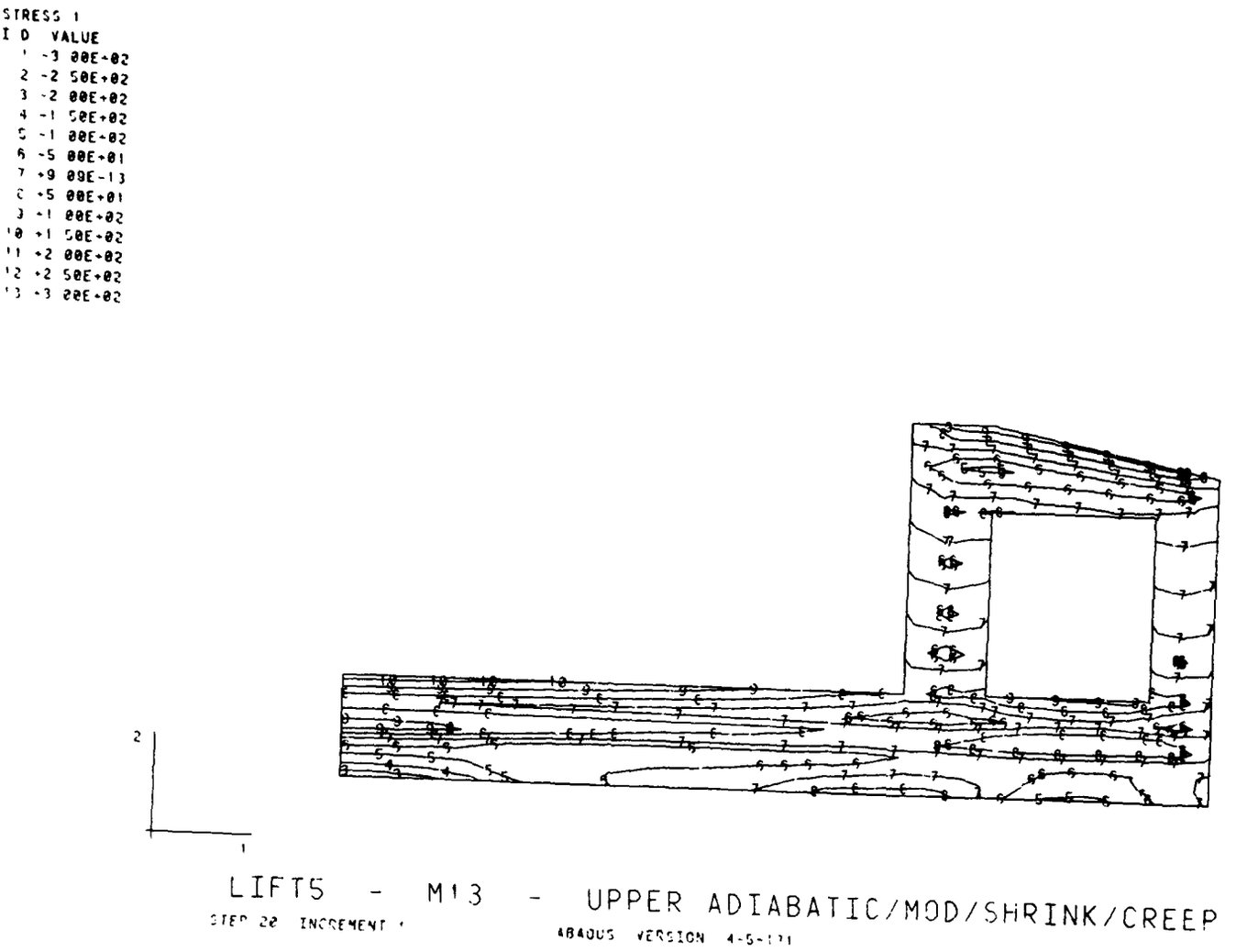

**Figure 19c - Horizontal stress contours in L-13,
5 days after lift 5 is placed,
Gravity & thermal loading, Upper creep/shrinkage**

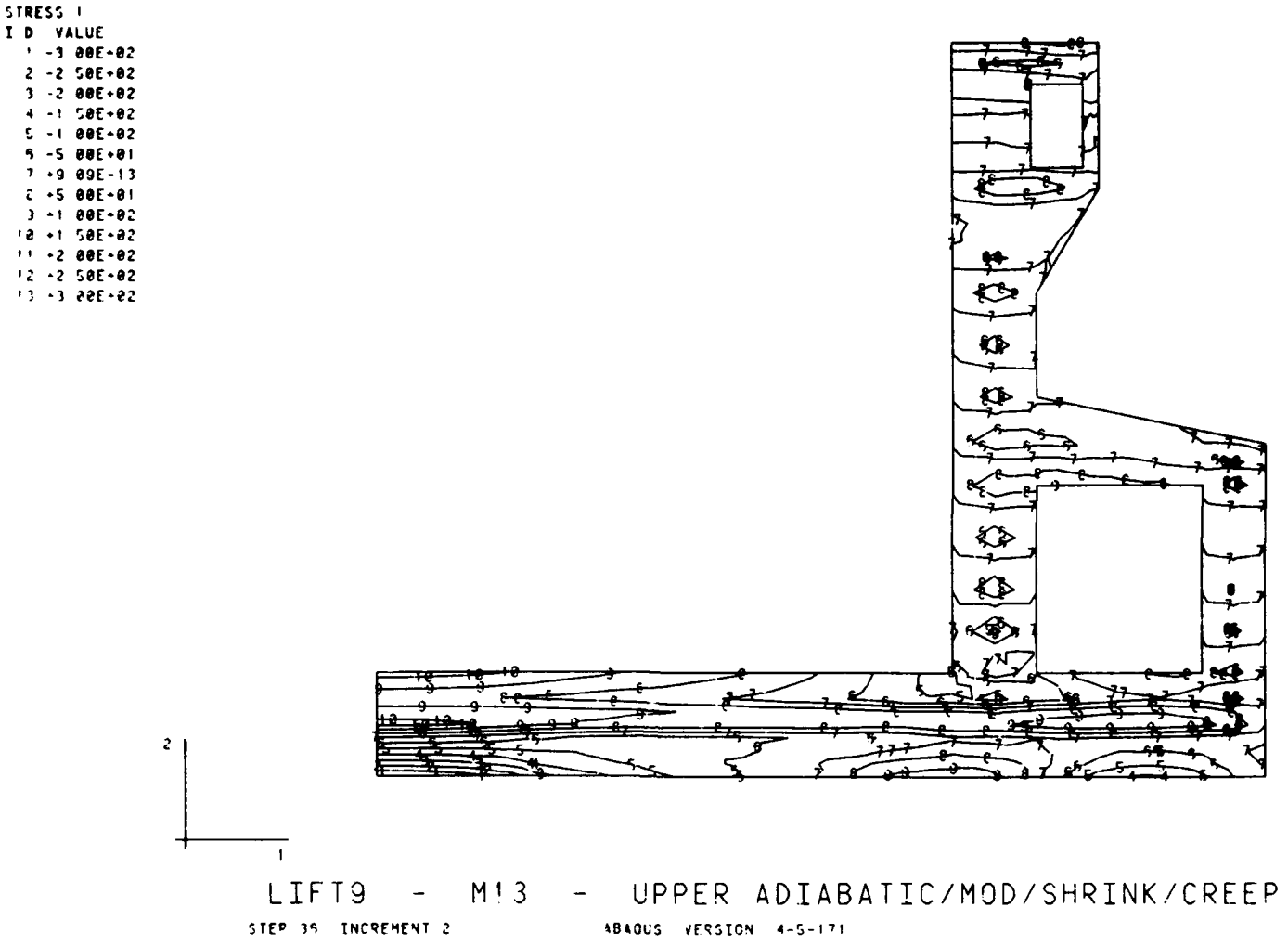

**Figure 19d - Horizontal stress contours in L-13,
7 days after lift 9 is placed,
Gravity & thermal loading, Upper creep/shrinkage**

STRESS 2

I D	VALUE
1	-3 00E+02
2	-2 50E+02
3	-2 00E+02
4	-1 50E+02
5	-1 00E+02
6	-5 00E+01
7	+9 09E-13
8	+5 00E+01
9	+1 00E+02
10	+1 50E+02
11	+2 00E+02
12	+2 50E+02
13	+3 00E+02

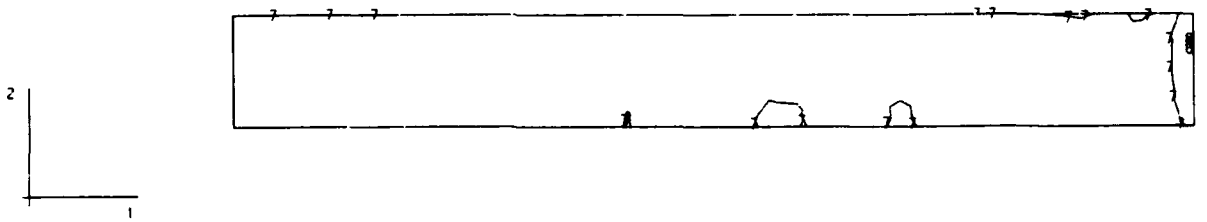

**Figure 20a - Vertical stress contours in L-13,
5 days after lift 2 is placed,
Gravity & thermal loading, Upper creep/shrinkage**

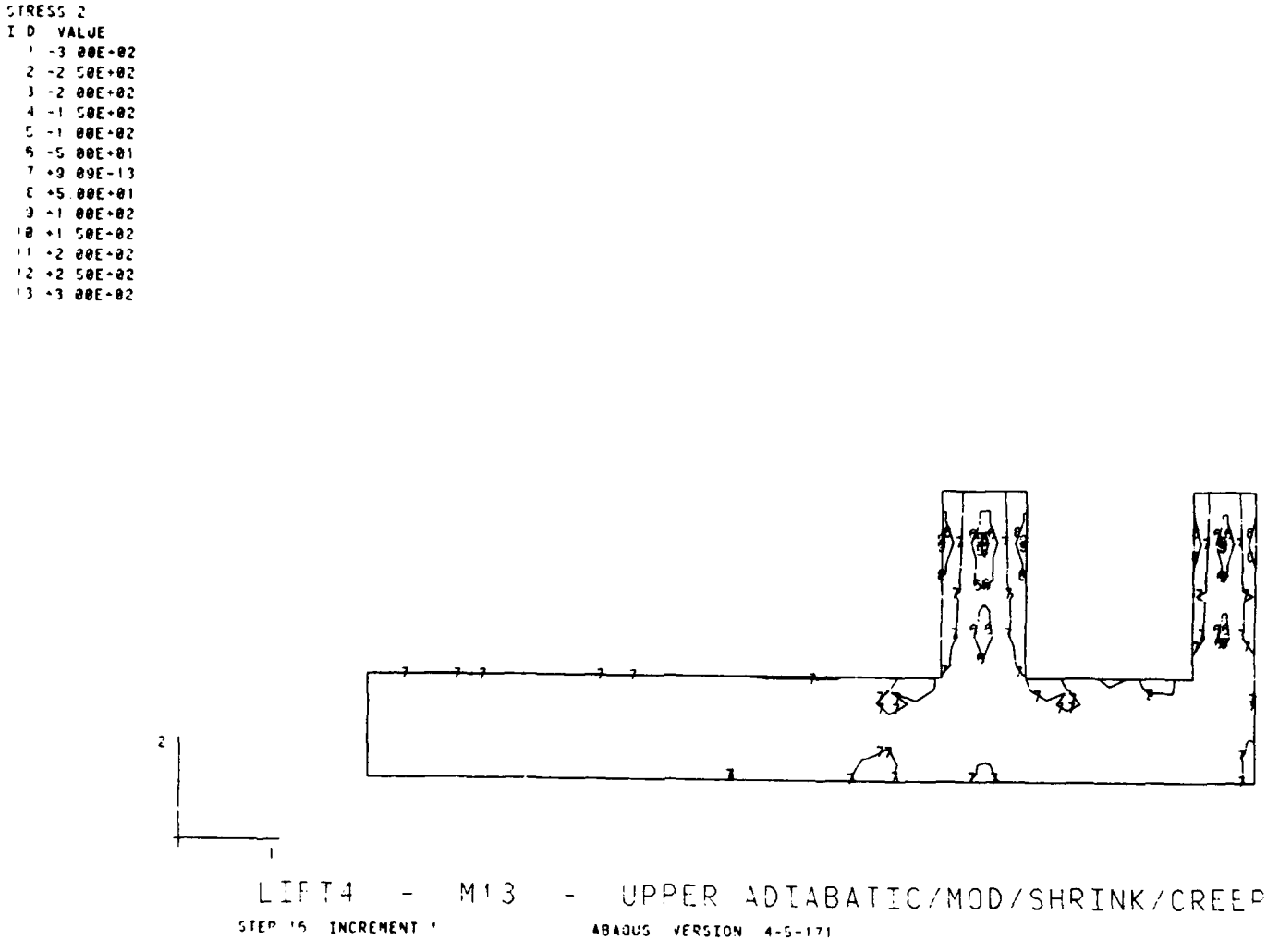

**Figure 20b - Vertical stress contours in L-13,
5 days after lift 4 is placed,
Gravity & thermal loading, Upper creep/shrinkage**

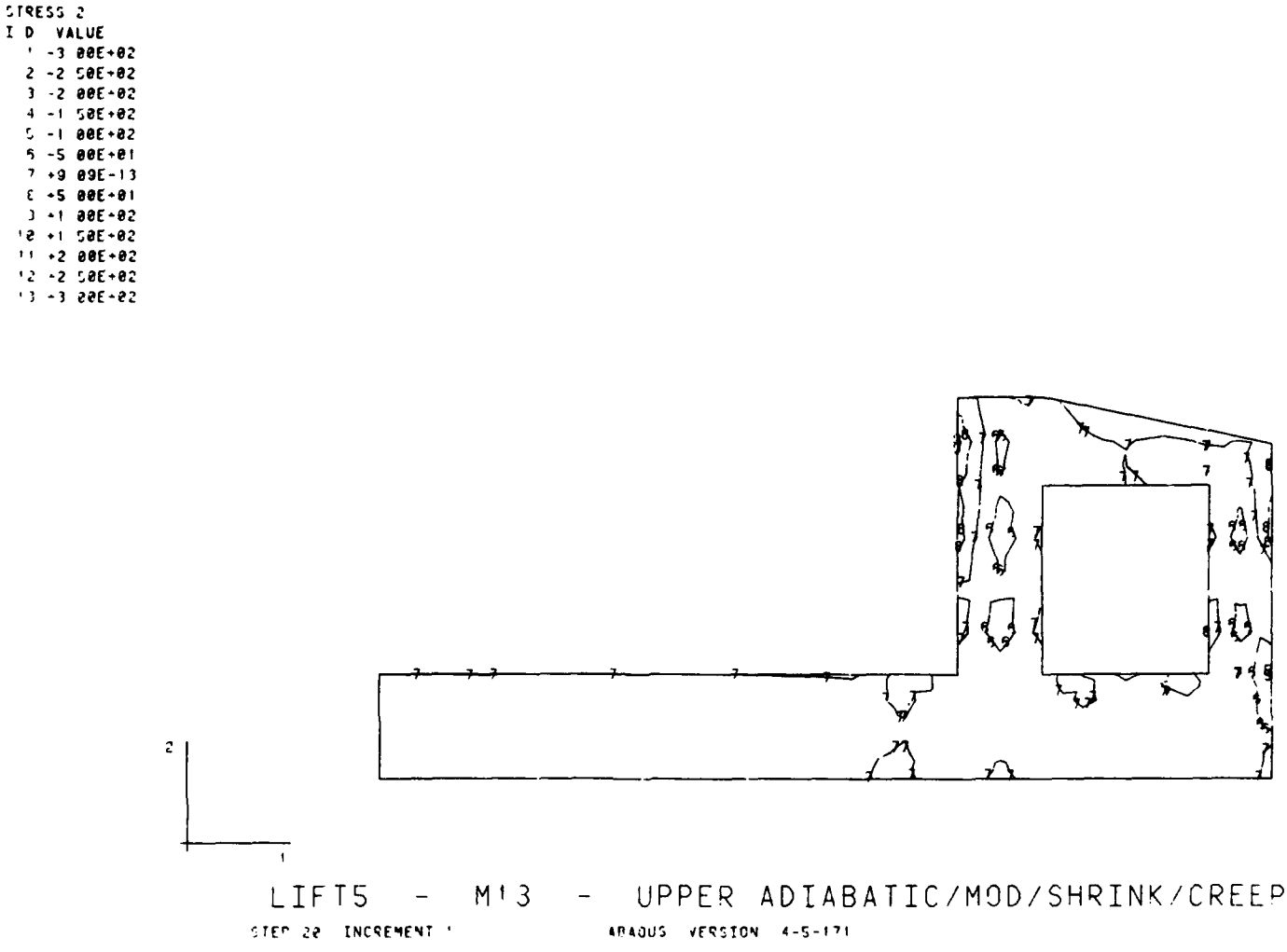

**Figure 20c - Vertical stress contours in L-13,
5 days after lift 5 is placed,
Gravity & thermal loading, Upper creep/shrinkage**

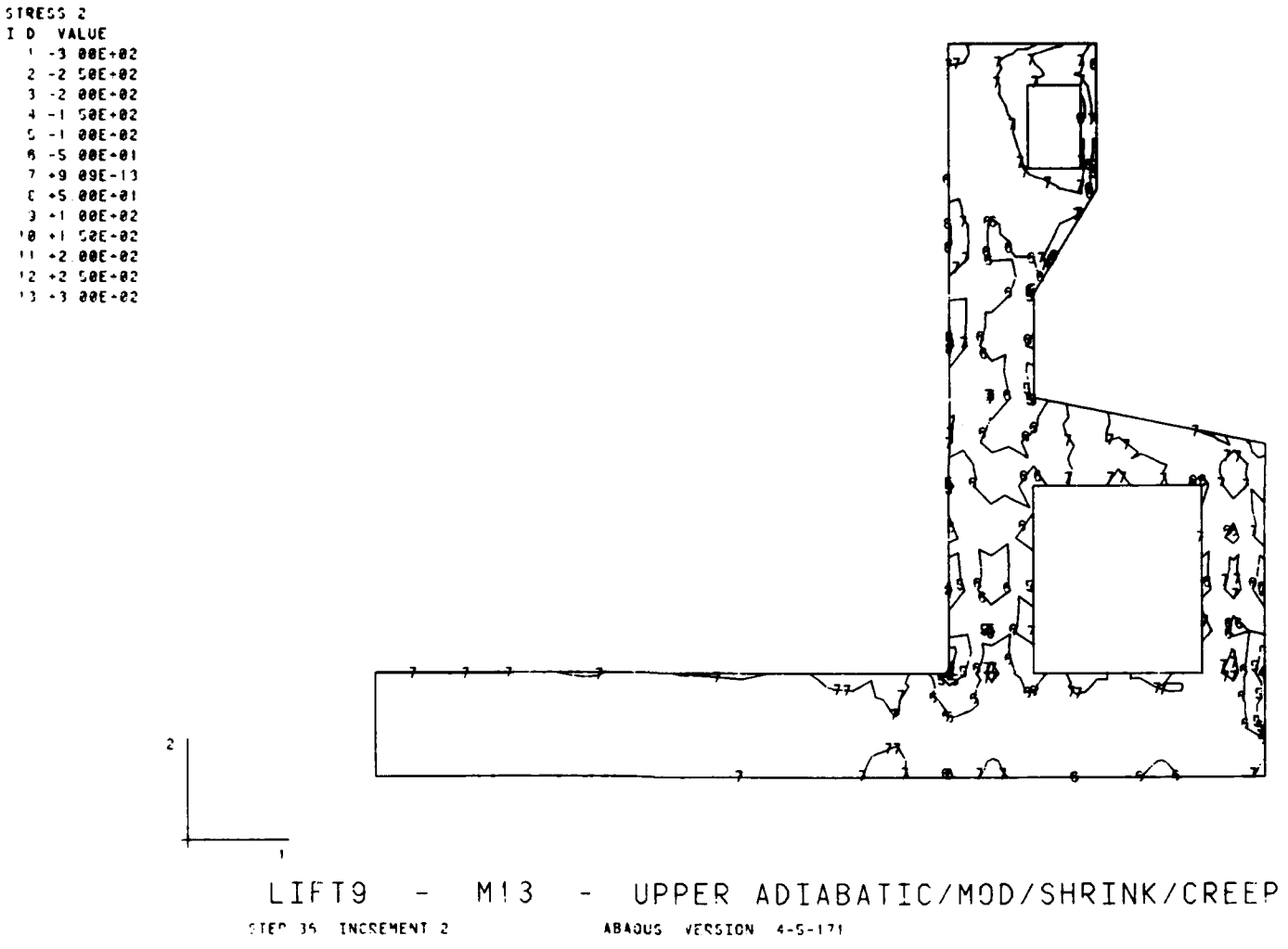

**Figure 20d - Vertical stress contours in L-13,
7 days after lift 9 is placed,
Gravity & thermal loading, Upper creep/shrinkage**

STRESS 3

I D	VALUE
1	-5 00E+02
2	-4 50E+02
3	-4 00E+02
4	-3 50E+02
5	-3 00E+02
6	-2 50E+02
7	-2 00E+02
8	-1 50E+02
9	-1 00E+02
10	-5 00E+01
11	+9 09E-13
12	+5 00E+01
13	+1 00E+02

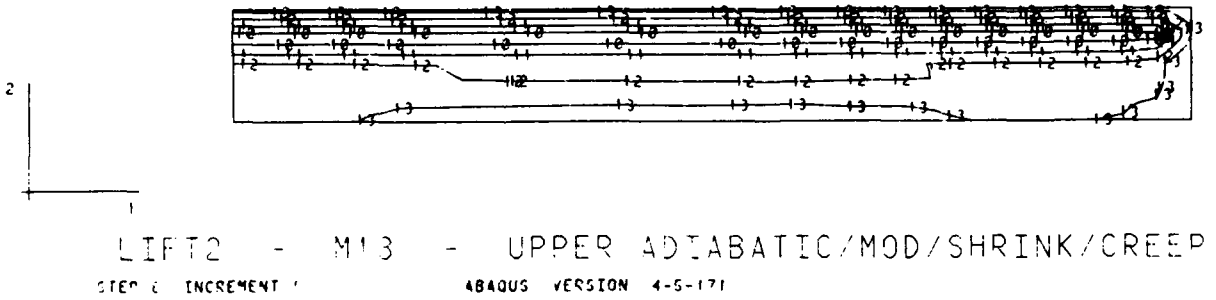

Figure 21a - Out-of-plane stress contours in L-13, 5 days after lift 2 is placed, Gravity & thermal loading, Upper creep/shrinkage

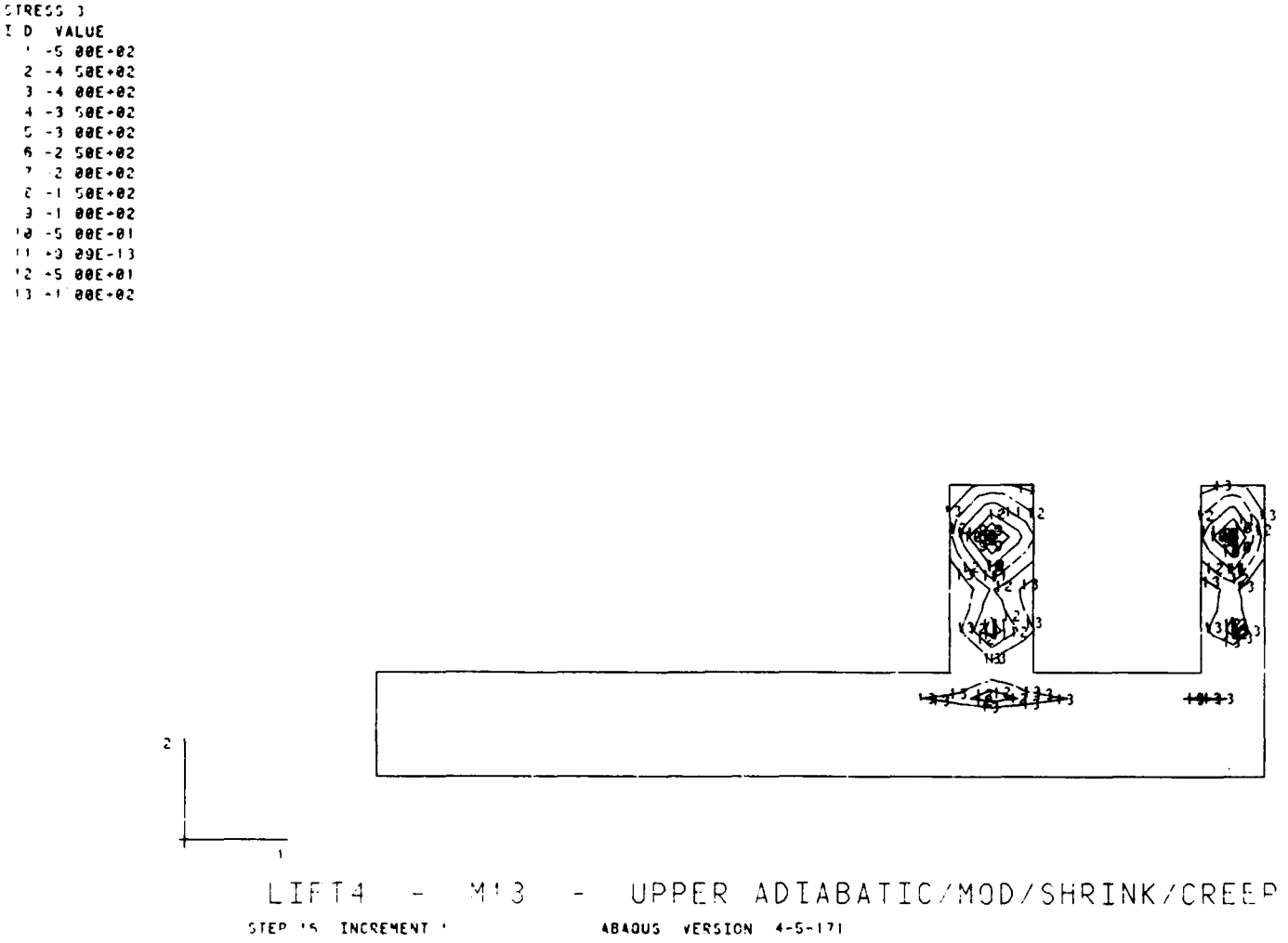

Figure 21b - Out-of-plane stress contours in L-13, 5 days after lift 4 is placed, Gravity & thermal loading, Upper creep/shrinkage

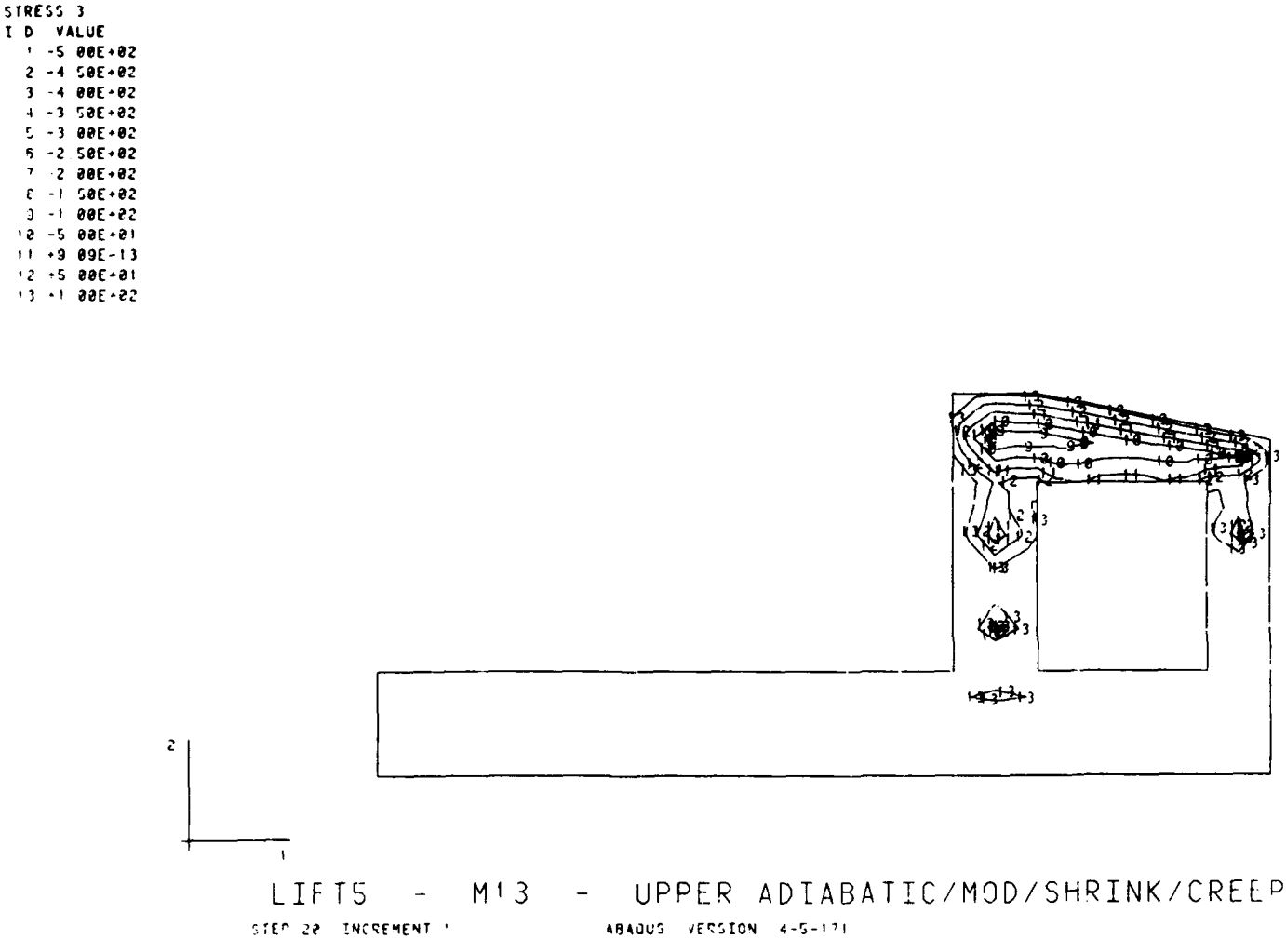

Figure 21c - Out-of-plane stress contours in L-13, 5 days after lift 5 is placed, Gravity & thermal loading, Upper creep/shrinkage

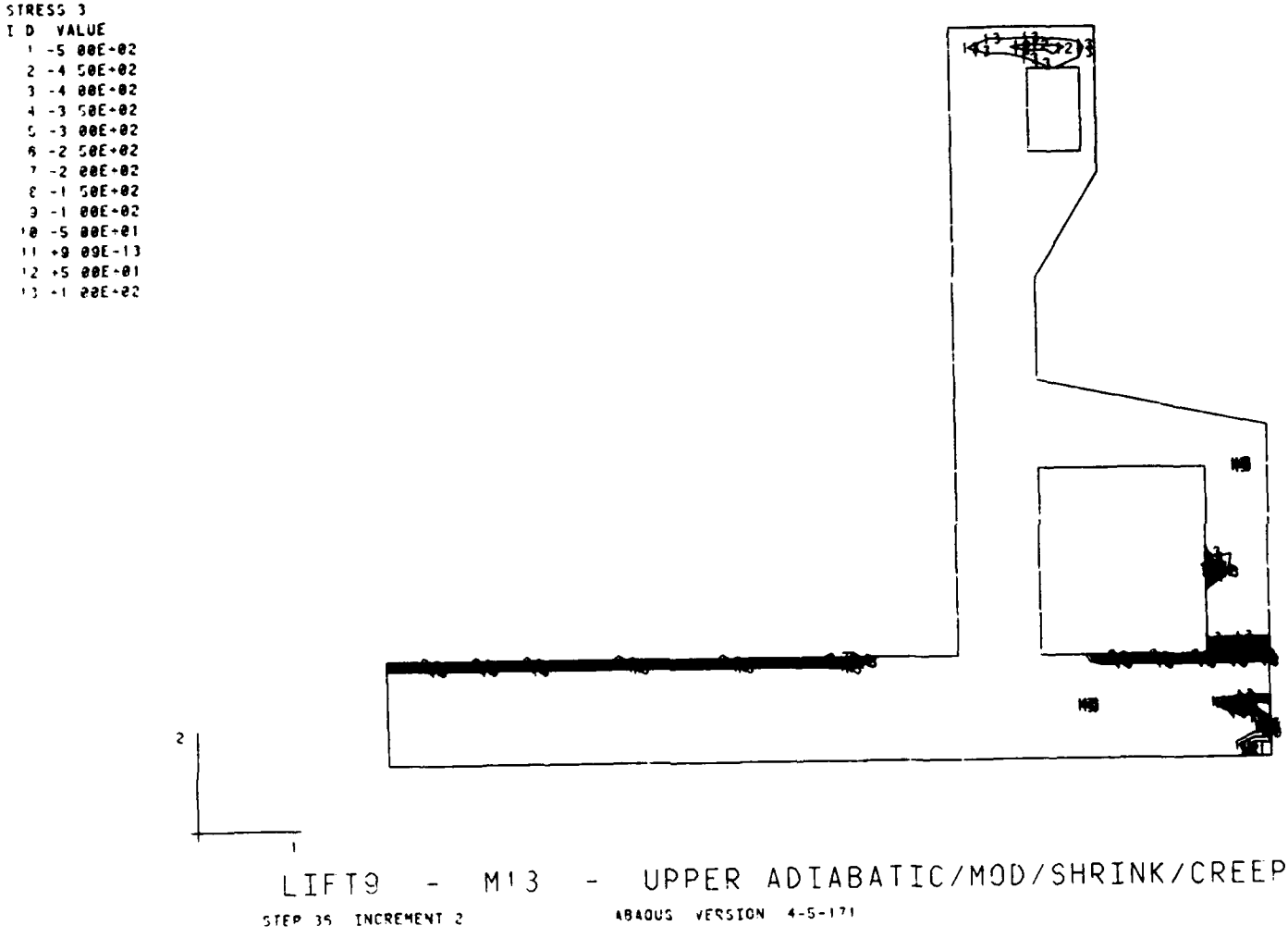

Figure 21d - Out-of-plane stress contours in L-13, 7 days after lift 9 is placed, Gravity & thermal loading, Upper creep/shrinkage

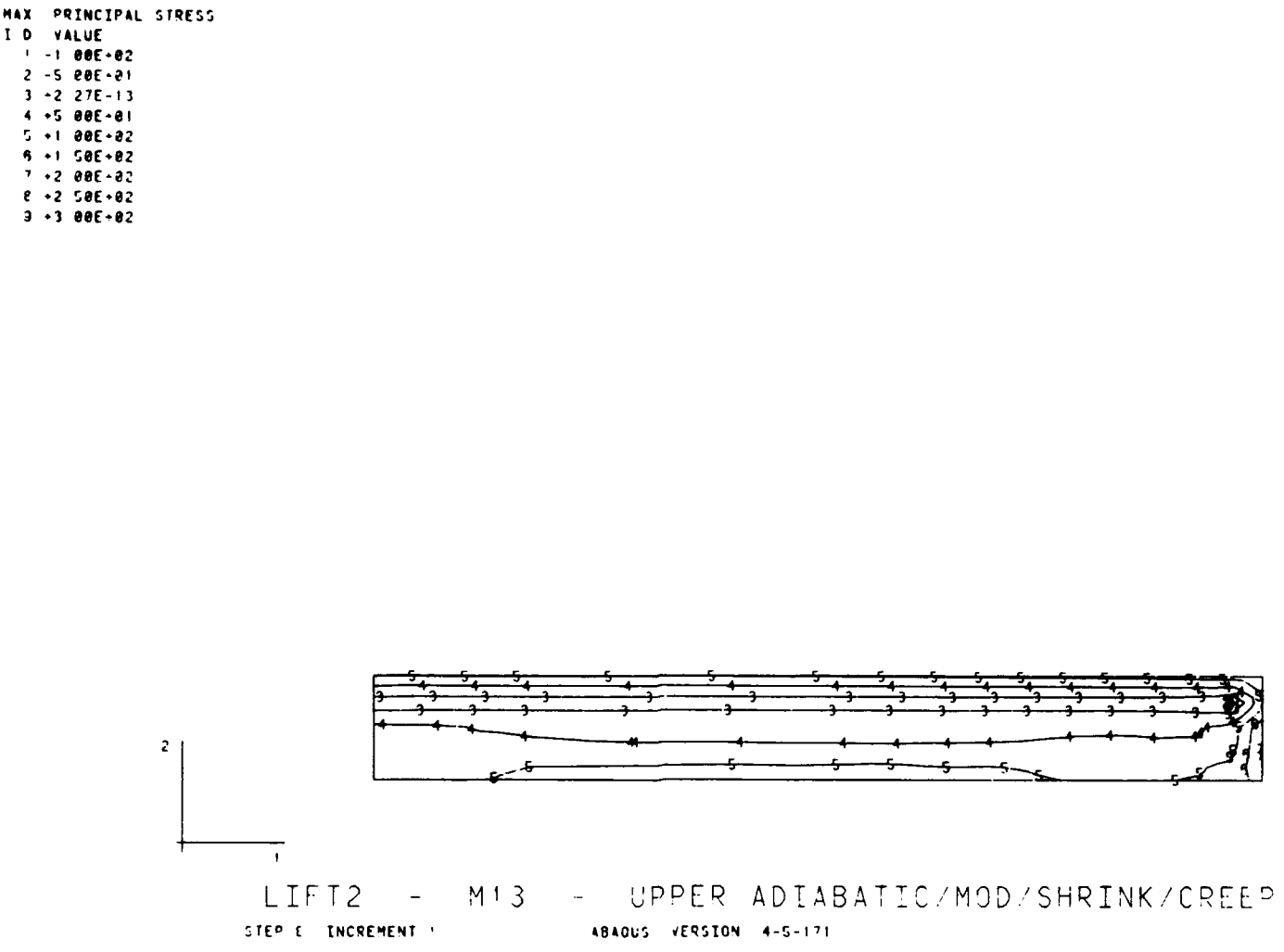

Figure 22a - Max. Principal stress contours in L-13, 5 days after lift 2 is placed, Gravity & thermal loading, Upper creep/shrinkage

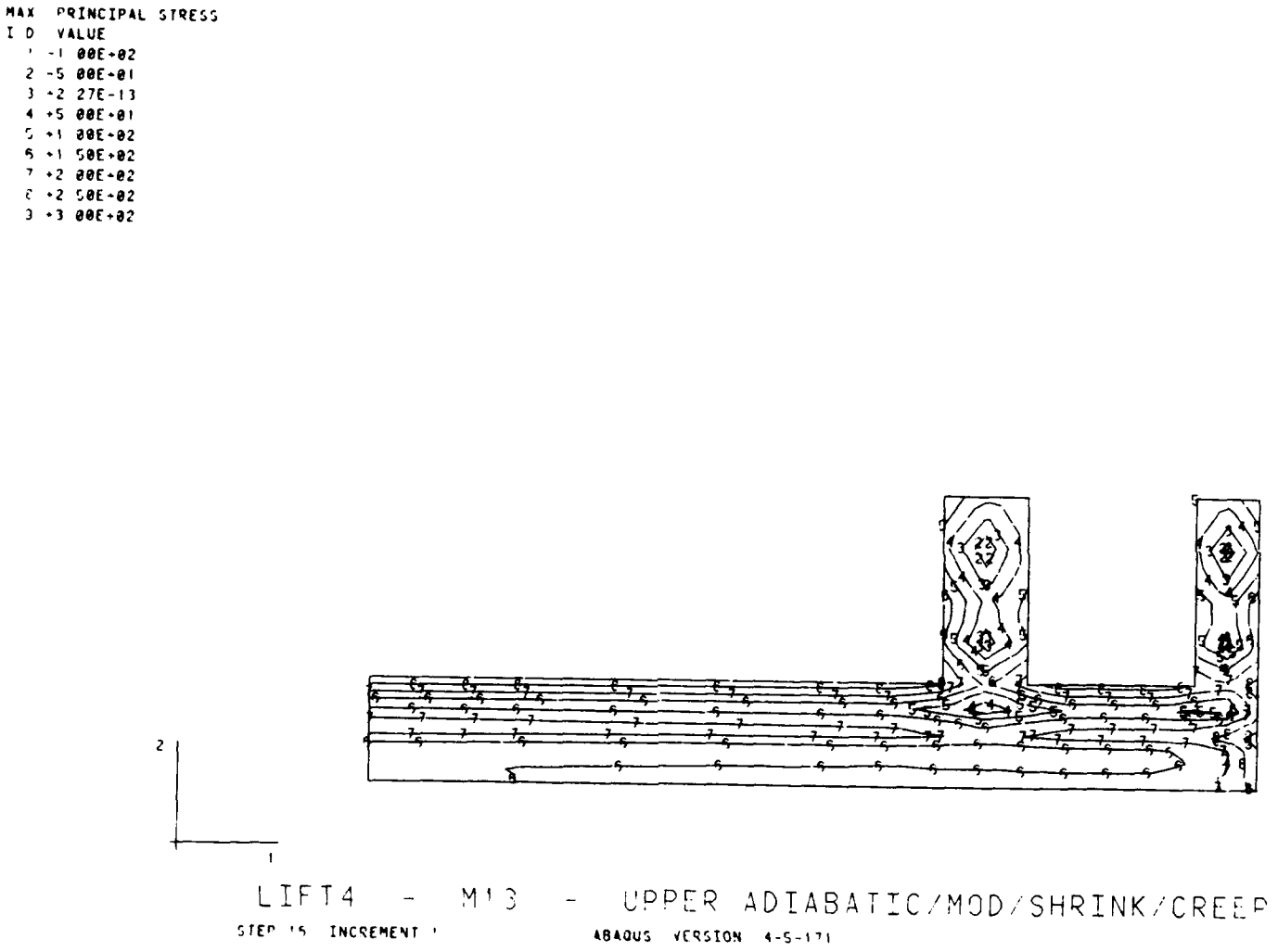

Figure 22b - Max. Principal stress contours in L-13, 5 days after lift 4 is placed, Gravity & thermal loading, Upper creep/shrinkage

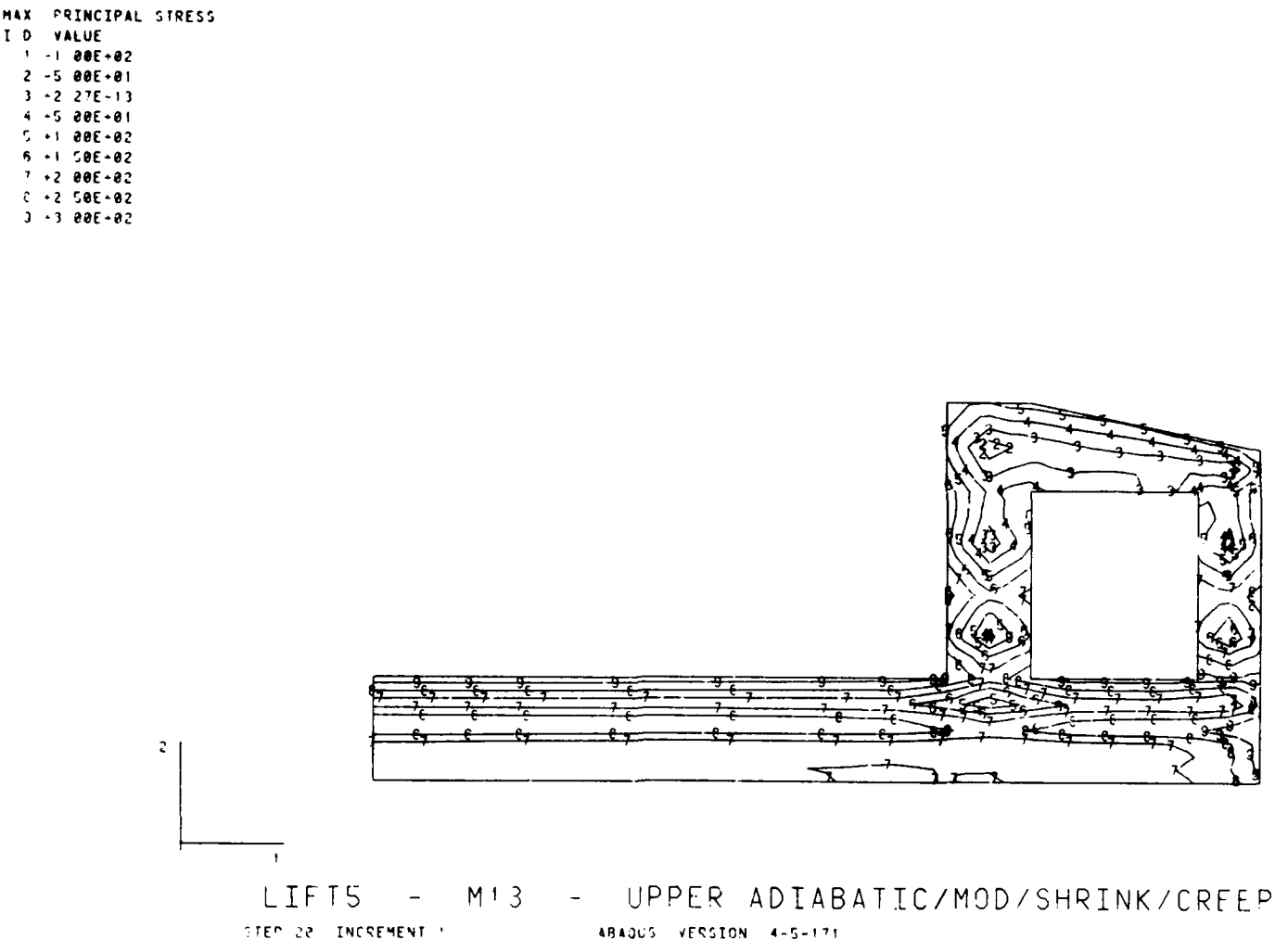

Figure 22c - Max. Principal stress contours in L-13, 5 days after lift 5 is placed, Gravity & thermal loading, Upper creep/shrinkage

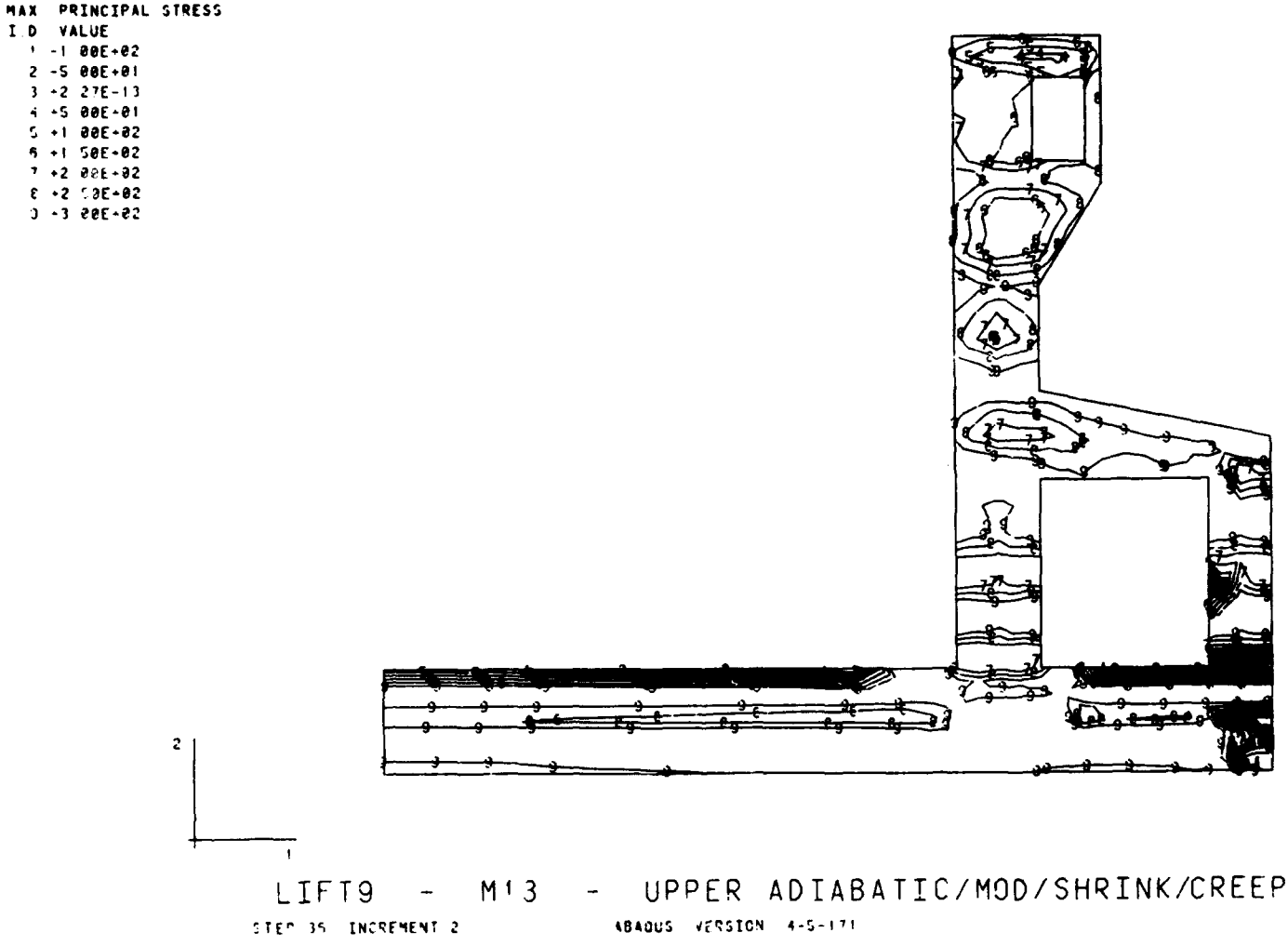

Figure 22d - Max. Principal stress contours in L-13, 7 days after lift 9 is placed, Gravity & thermal loading, Upper creep/shrinkage

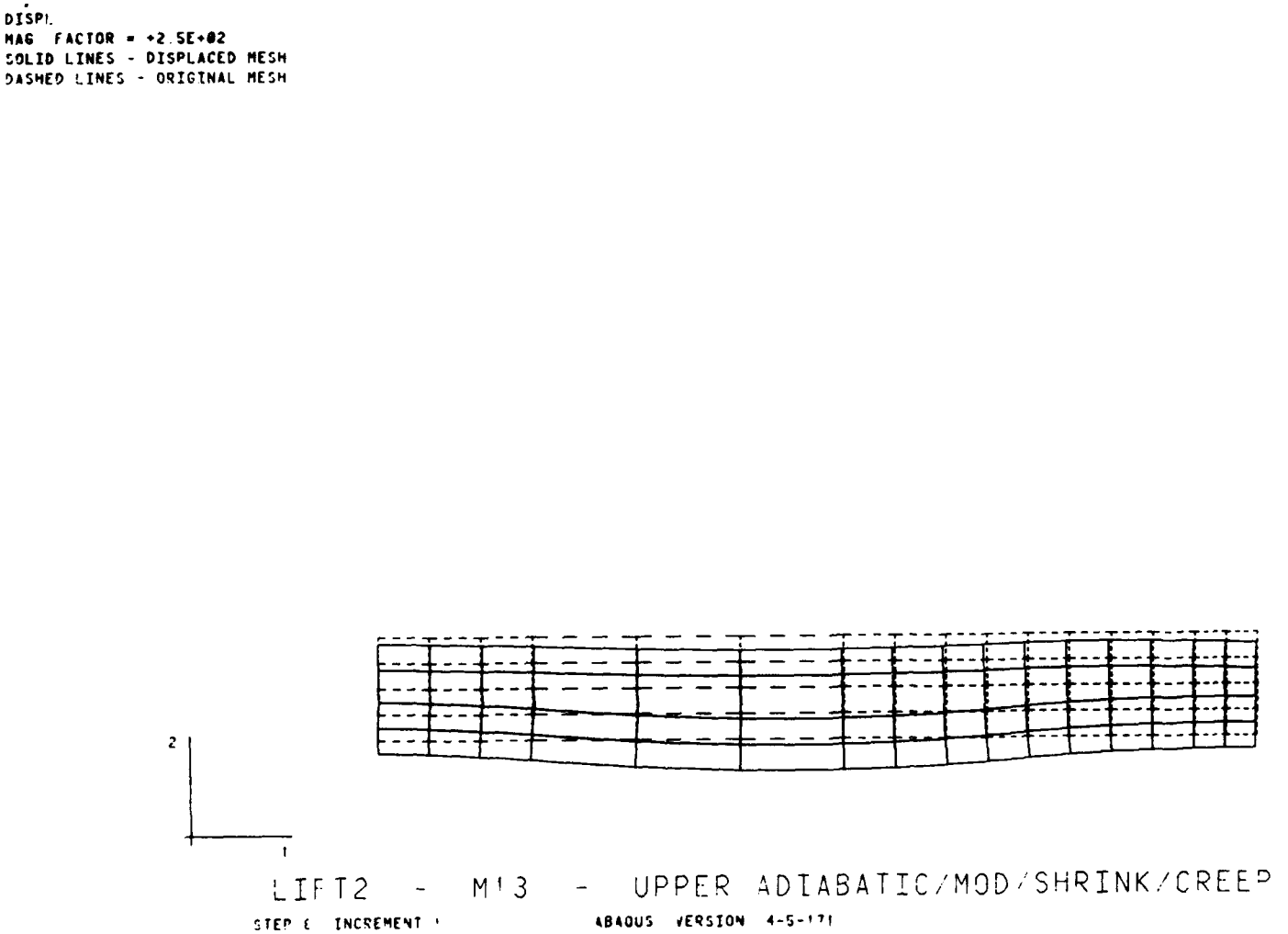

**Figure 23a - Displaced shape of L-13,
5 days after lift 2 is placed,
Gravity & thermal loading, Upper creep/shrinkage**

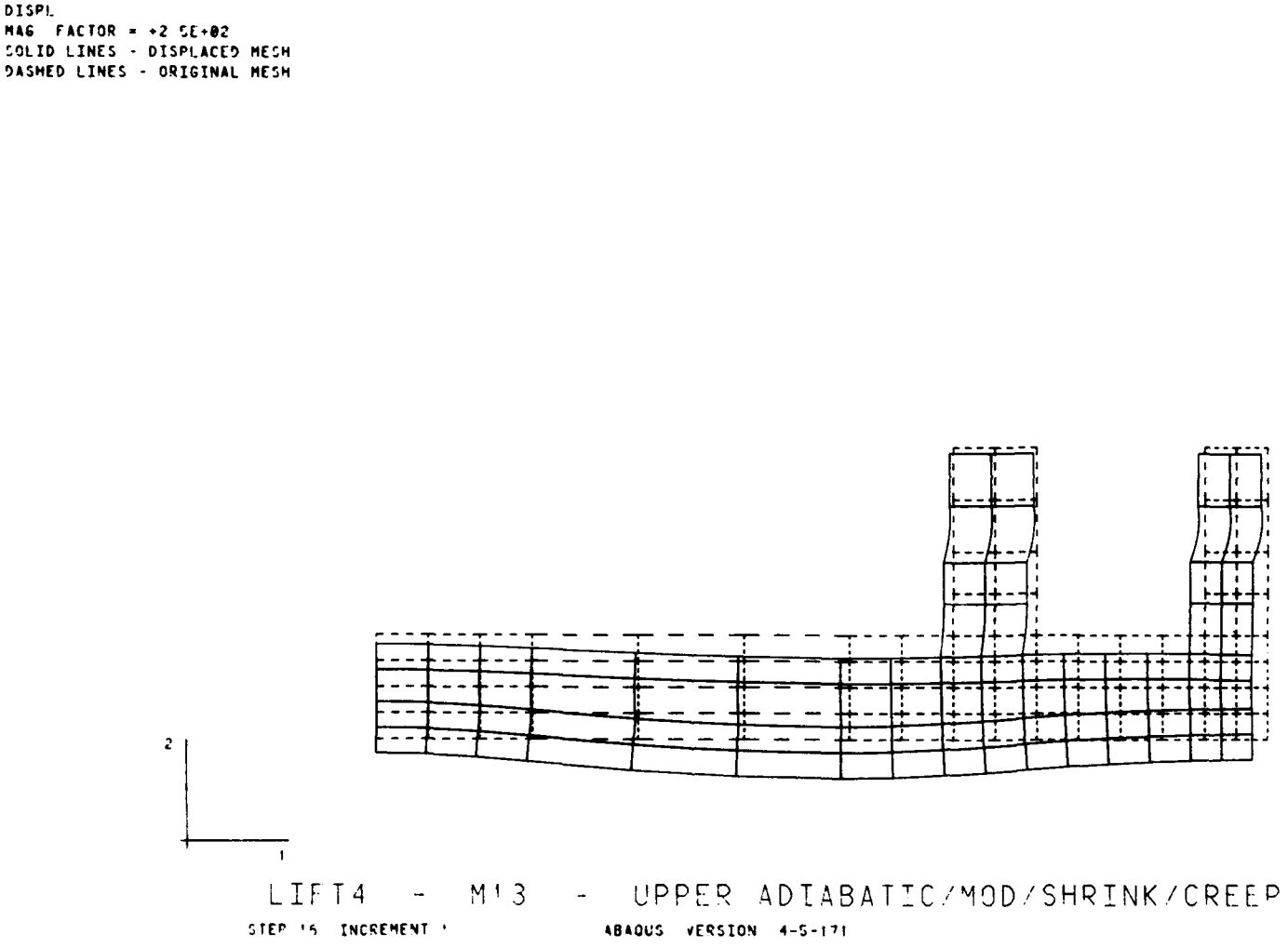

**Figure 23b - Displaced shape of L-13,
5 days after lift 4 is placed,
Gravity & thermal loading, Upper creep/shrinkage**

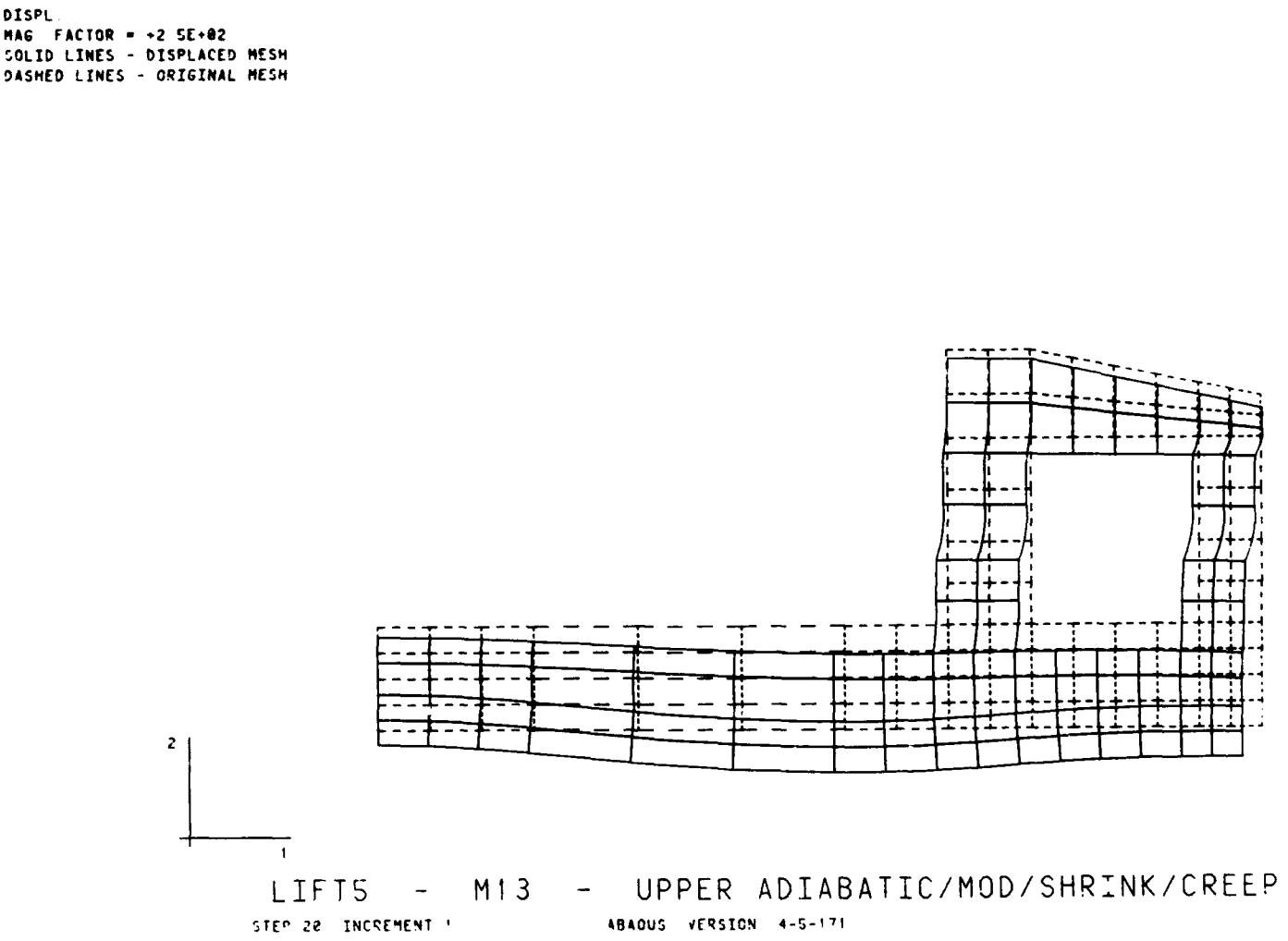

**Figure 23c - Displaced shape of L-13,
5 days after lift 5 is placed,
Gravity & thermal loading, Upper creep/shrinkage**

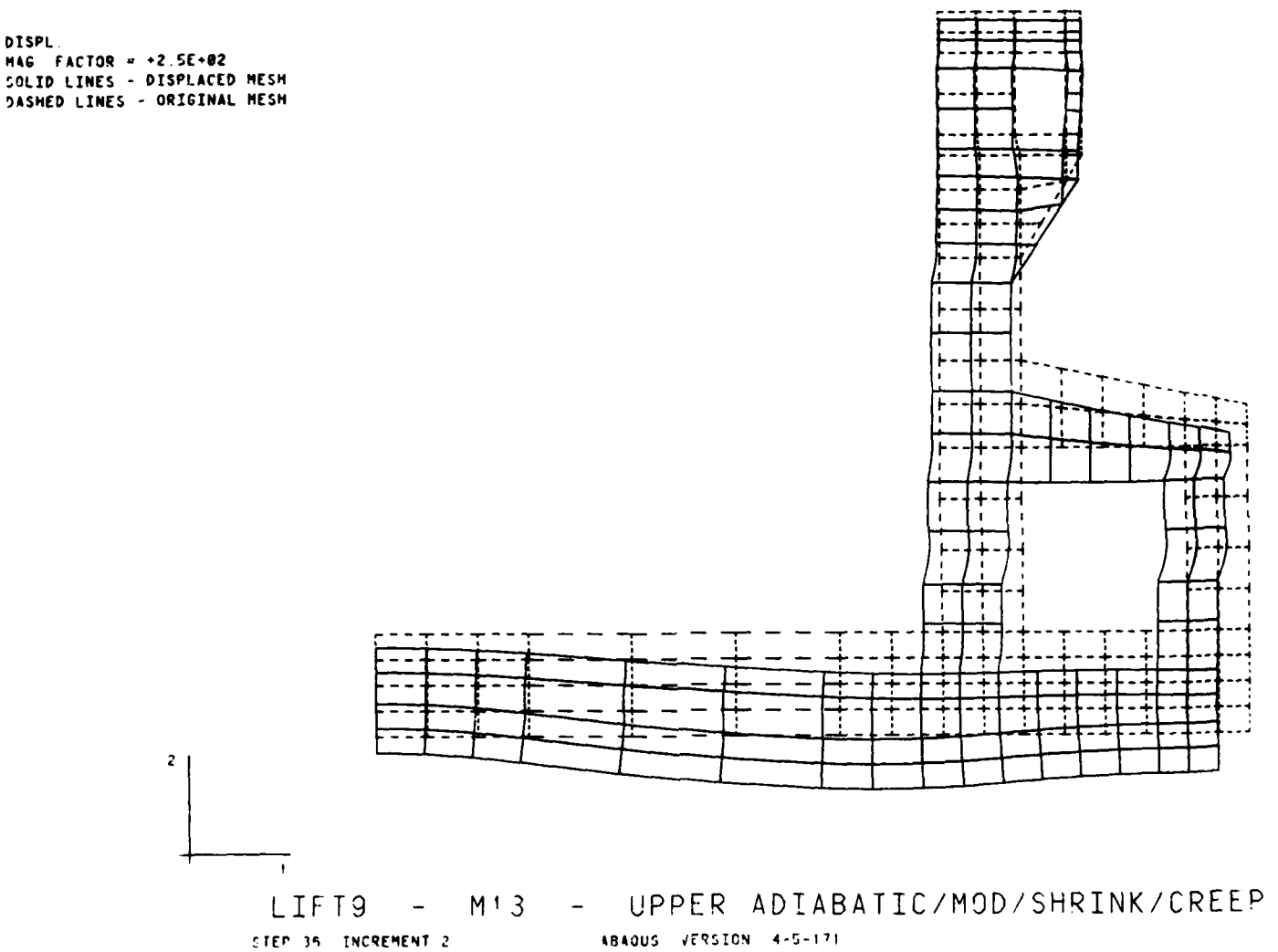

**Figure 23d - Displaced shape of L-13,
7 days after lift 9 is placed,
Gravity & thermal loading, Upper creep/shrinkage**

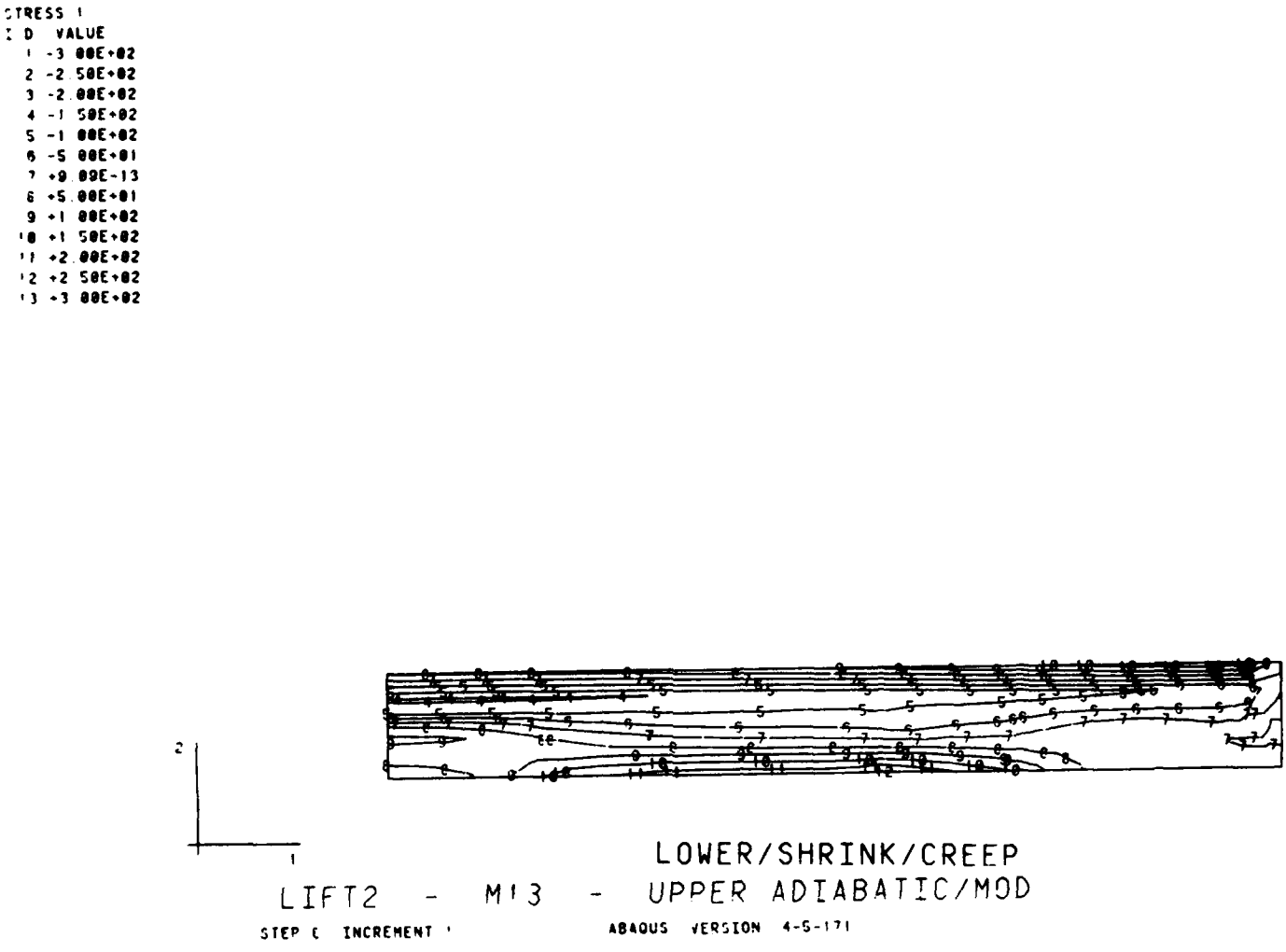

Figure 24a - Horizontal stress contours in L-13, 5 days after lift 2 is placed, Gravity & thermal loading, Lower creep/shrinkage

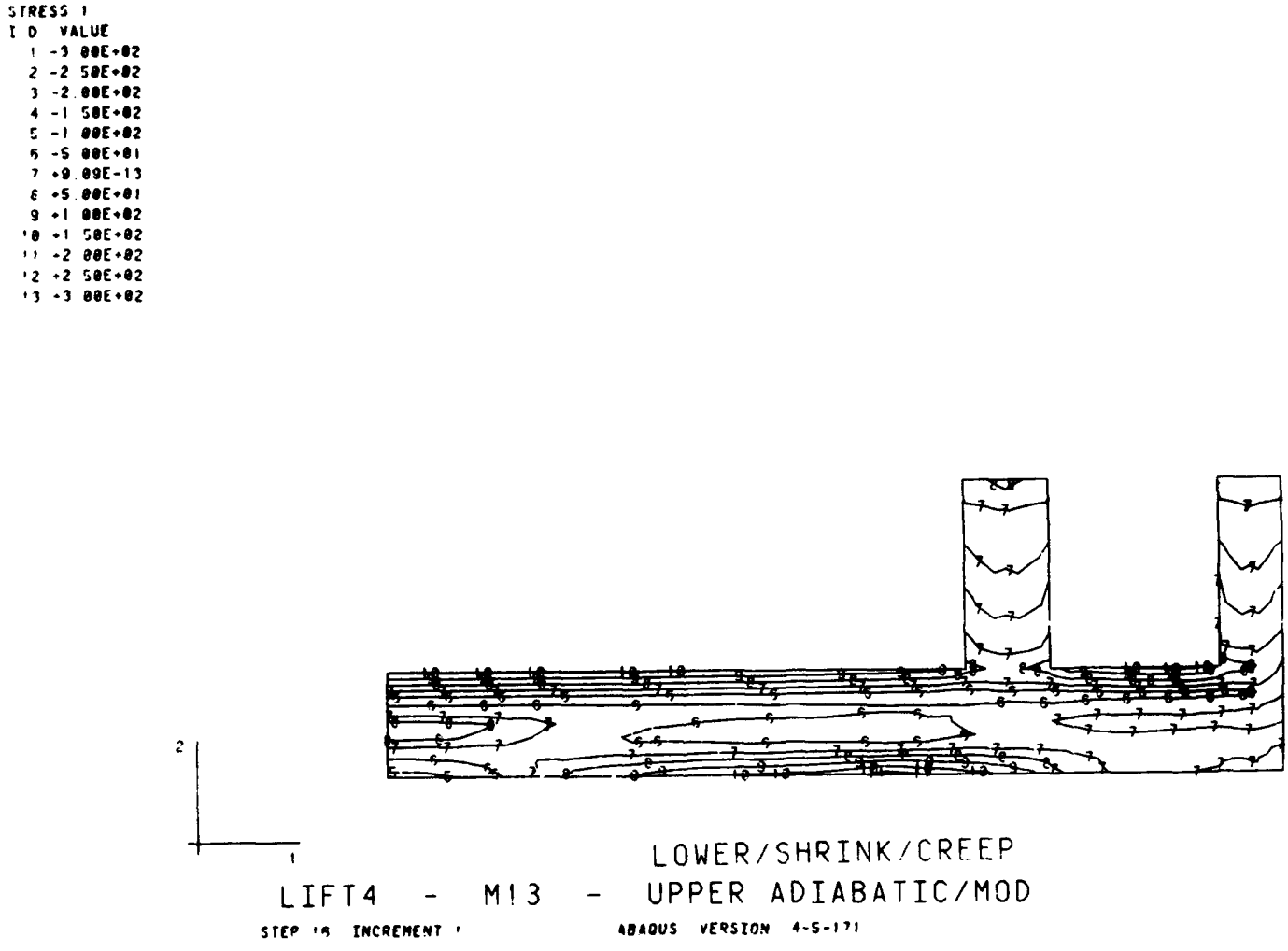

Figure 24b - Horizontal stress contours in L-13, 5 days after lift 4 is placed, Gravity & thermal loading, Lower creep/shrinkage

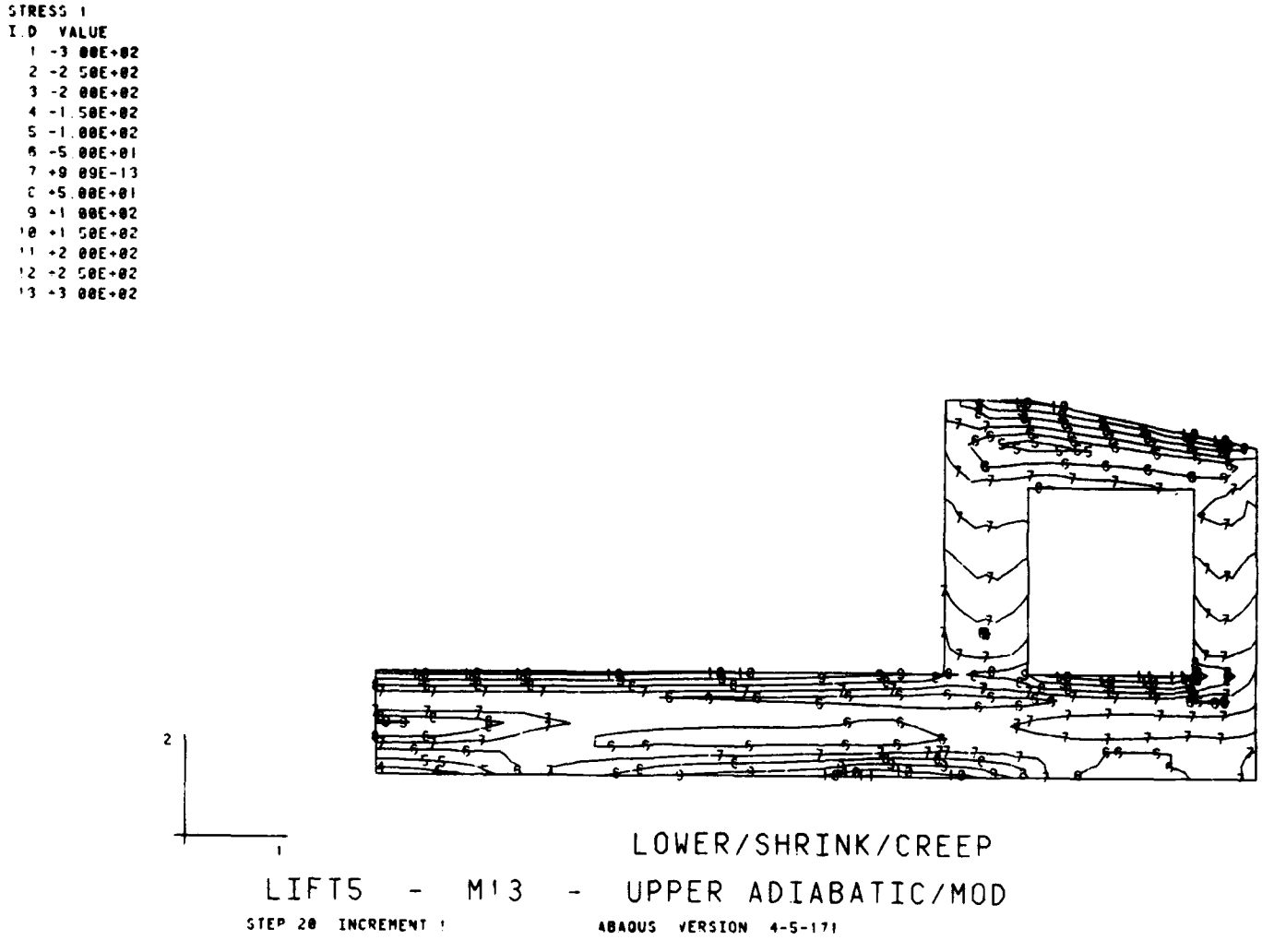

Figure 24c - Horizontal stress contours in L-13, 5 days after lift 5 is placed, Gravity & thermal loading, Lower creep/shrinkage

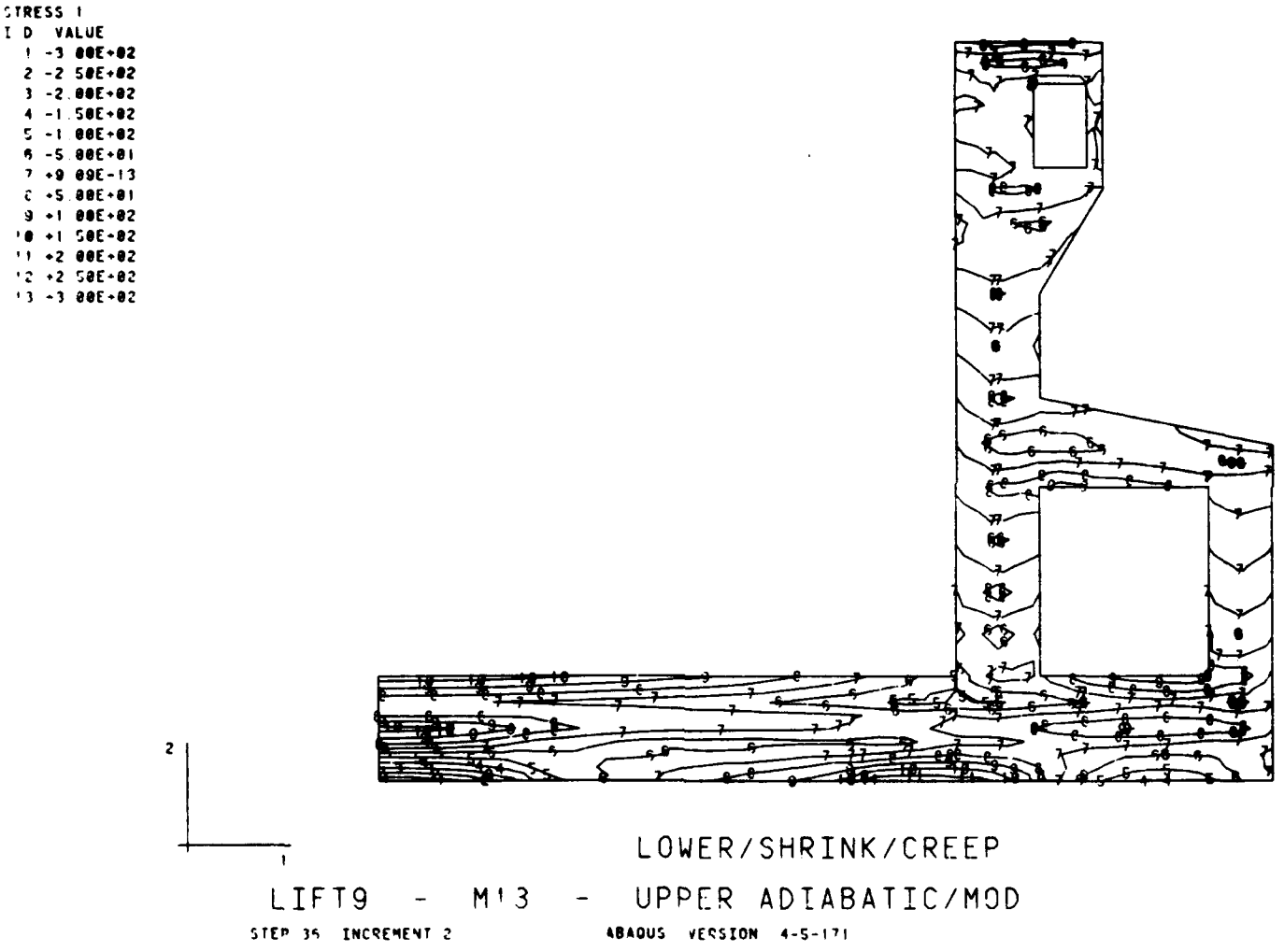

Figure 24d - Horizontal stress contours in L-13, 7 days after lift 9 is placed, Gravity & thermal loading, Lower creep/shrinkage

STRESS 2
I D VALUE
1 -3.00E+02
2 -2.50E+02
3 -2.00E+02
4 -1.50E+02
5 -1.00E+02
6 -5.00E+01
7 +0.00E-13
8 +5.00E+01
9 +1.00E+02
10 +1.50E+02
11 +2.00E+02
12 +2.50E+02
13 +3.00E+02

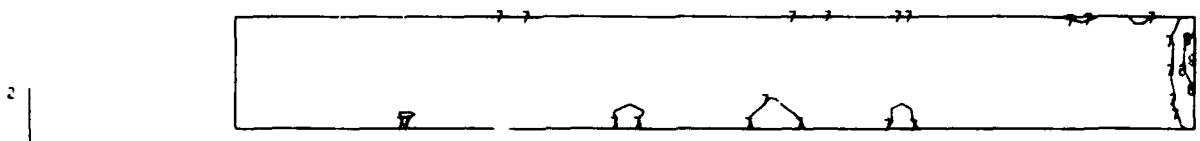

LOWER/SHRINK/CREEP

LIFT2 - M13 - UPPER ADIABATIC/MOD

STEP 6 INCREMENT 1 ABAQUS VERSION 4-5-171

Figure 25a - Vertical stress contours in L-13, 5 days after lift 2 is placed, Gravity & thermal loading, Lower creep/shrinkage

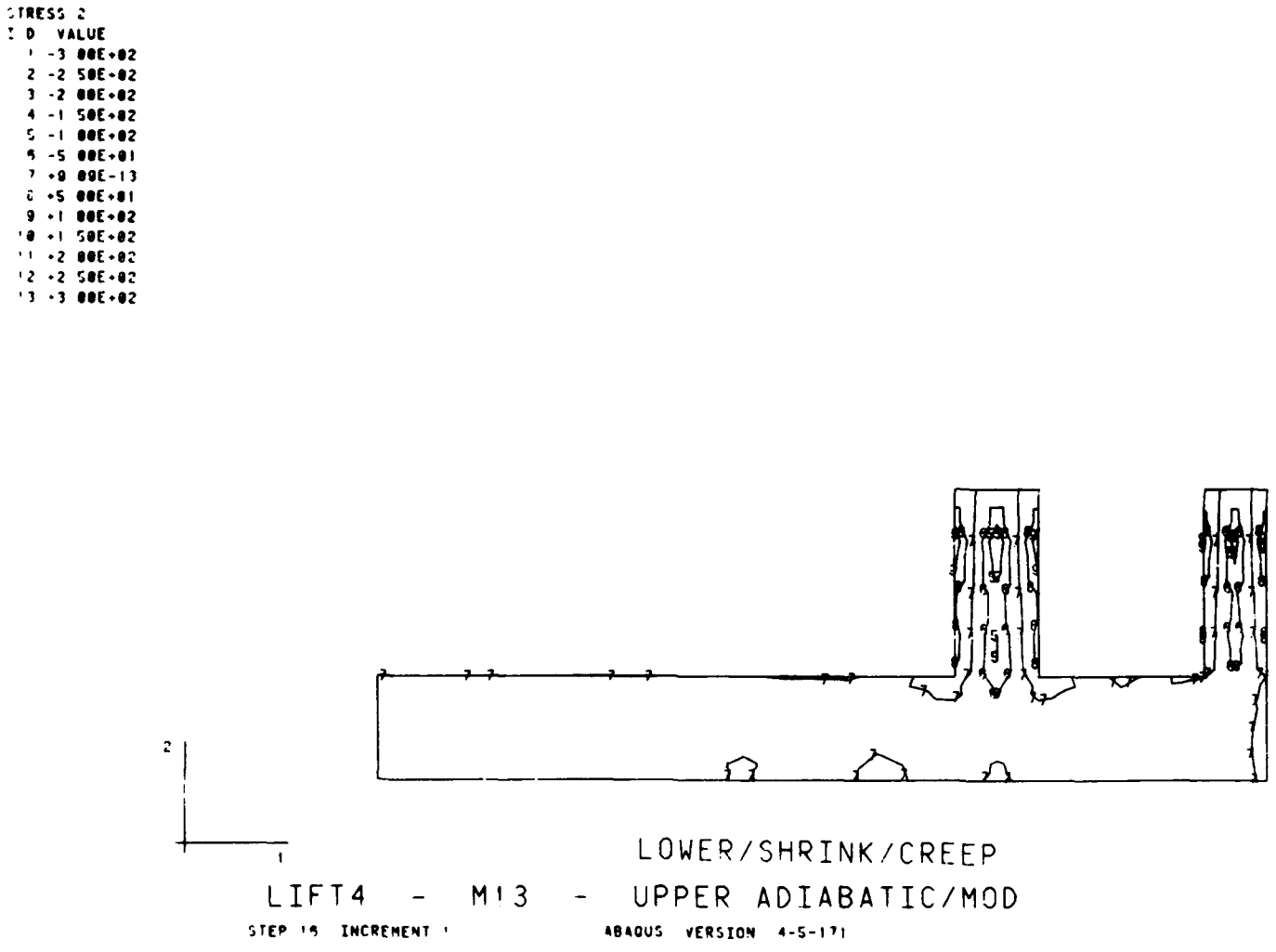

Figure 25b - Vertical stress contours in L-13, 5 days after lift 4 is placed, Gravity & thermal loading, Lower creep/shrinkage

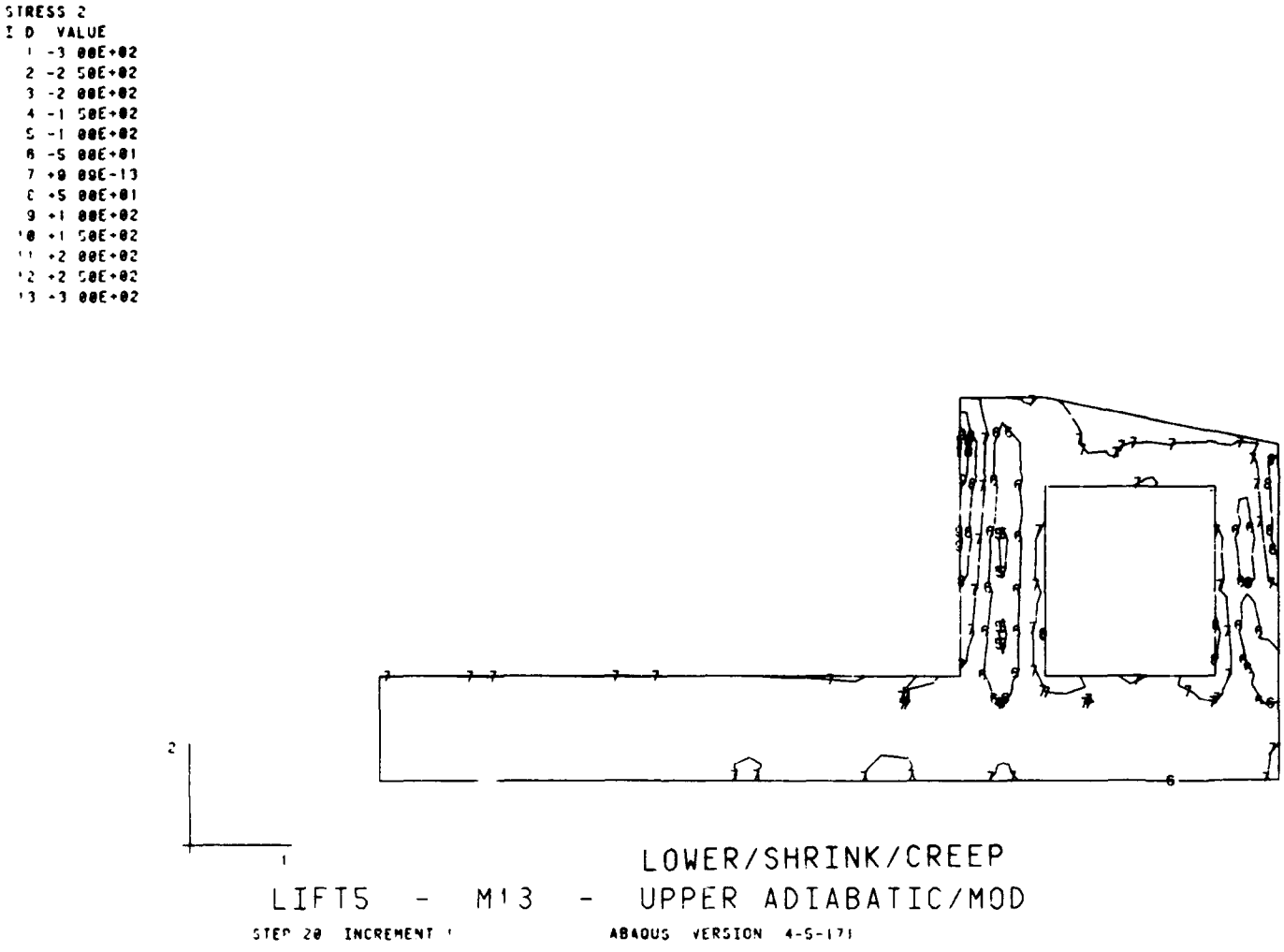

Figure 25c - Vertical stress contours in L-13,
5 days after lift 5 is placed,
Gravity & thermal loading, Lower creep/shrinkage

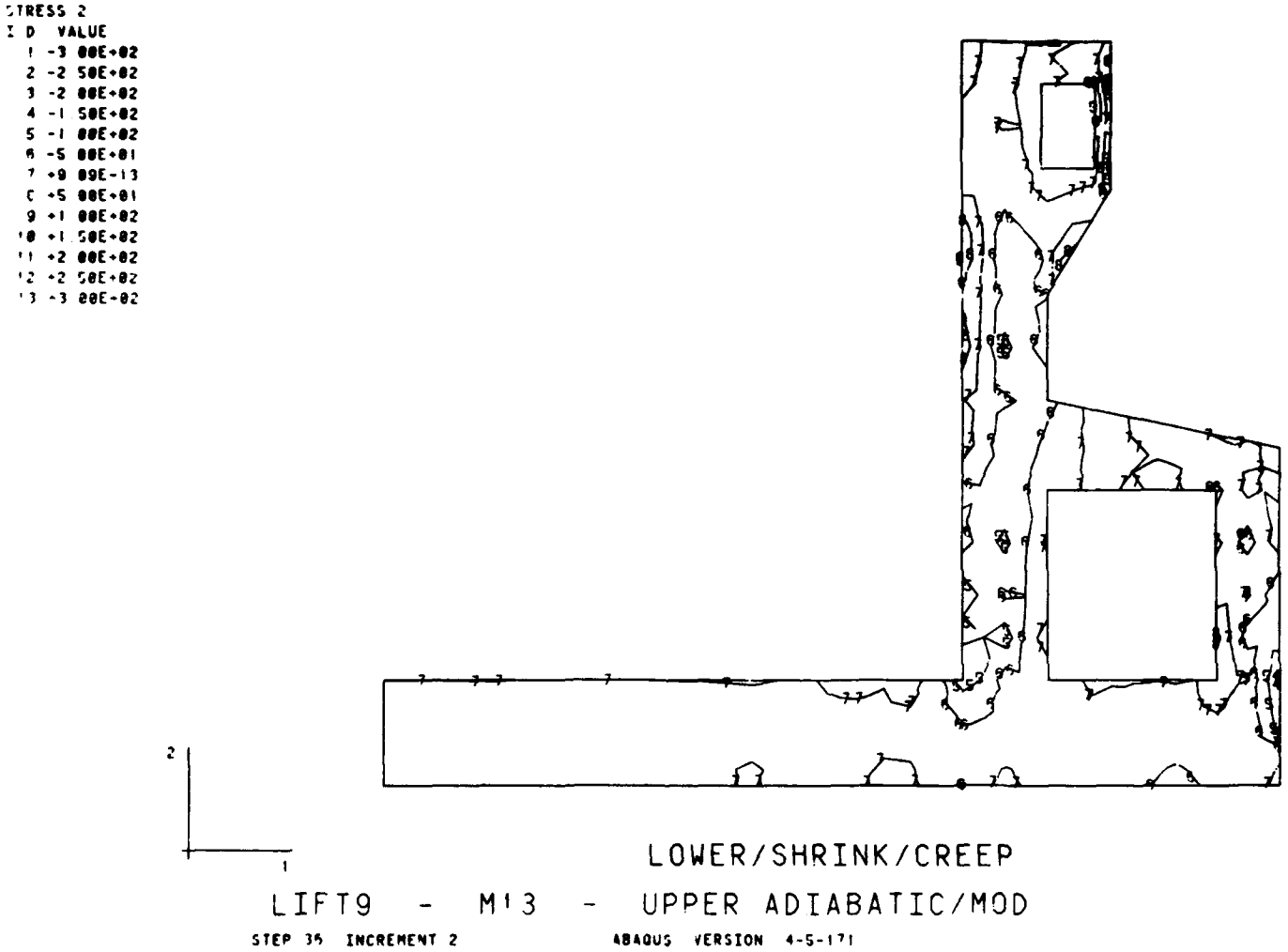

**Figure 25d - Vertical stress contours in L-13,
7 days after lift 9 is placed,
Gravity & thermal loading, Lower creep/shrinkage**

STRESS 3

I D	VALUE
1	-5 00E+02
2	-4 50E+02
3	-4 00E+02
4	-3 50E+02
5	-3 00E+02
6	-2 50E+02
7	-2 00E+02
8	-1 50E+02
9	-1 00E+02
10	-5 00E+01
11	+1 59E-12
12	+5 00E+01
13	+1 00E+02
14	+1 50E+02
15	+2 00E+02
16	+2 50E+02
17	+3 00E+02
18	+3 50E+02
19	+4 00E+02
20	+4 50E+02

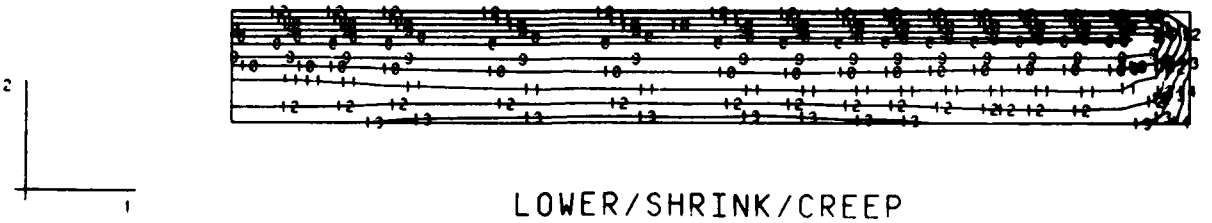

Figure 26a - Out-of-plane stress contours in L-13, 5 days after lift 2 is placed, Gravity & thermal loading, Lower creep/shrinkage

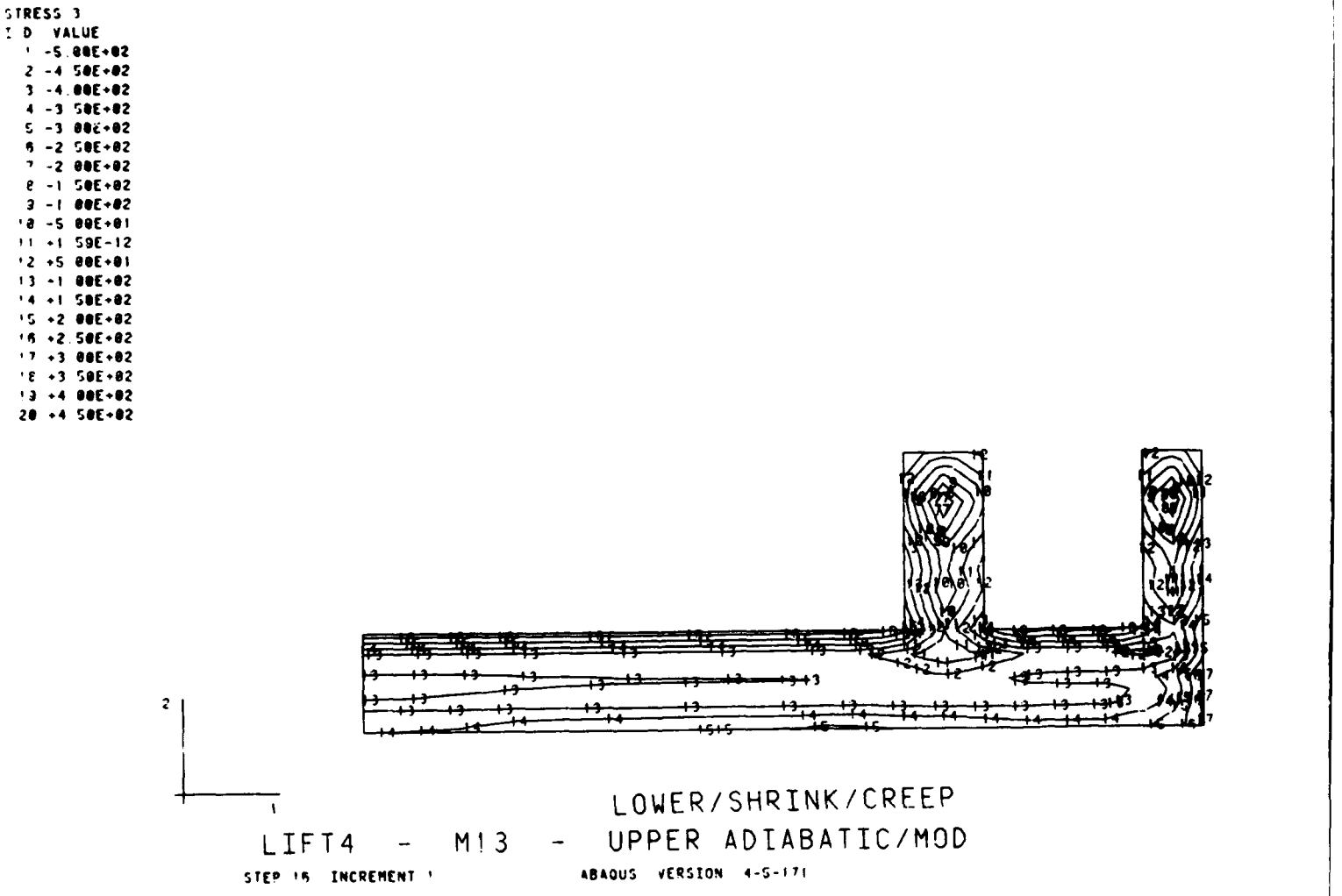

**Figure 26b - Out-of-plane stress contours in L-13,
5 days after lift 4 is placed,
Gravity & thermal loading, Lower creep/shrinkage**

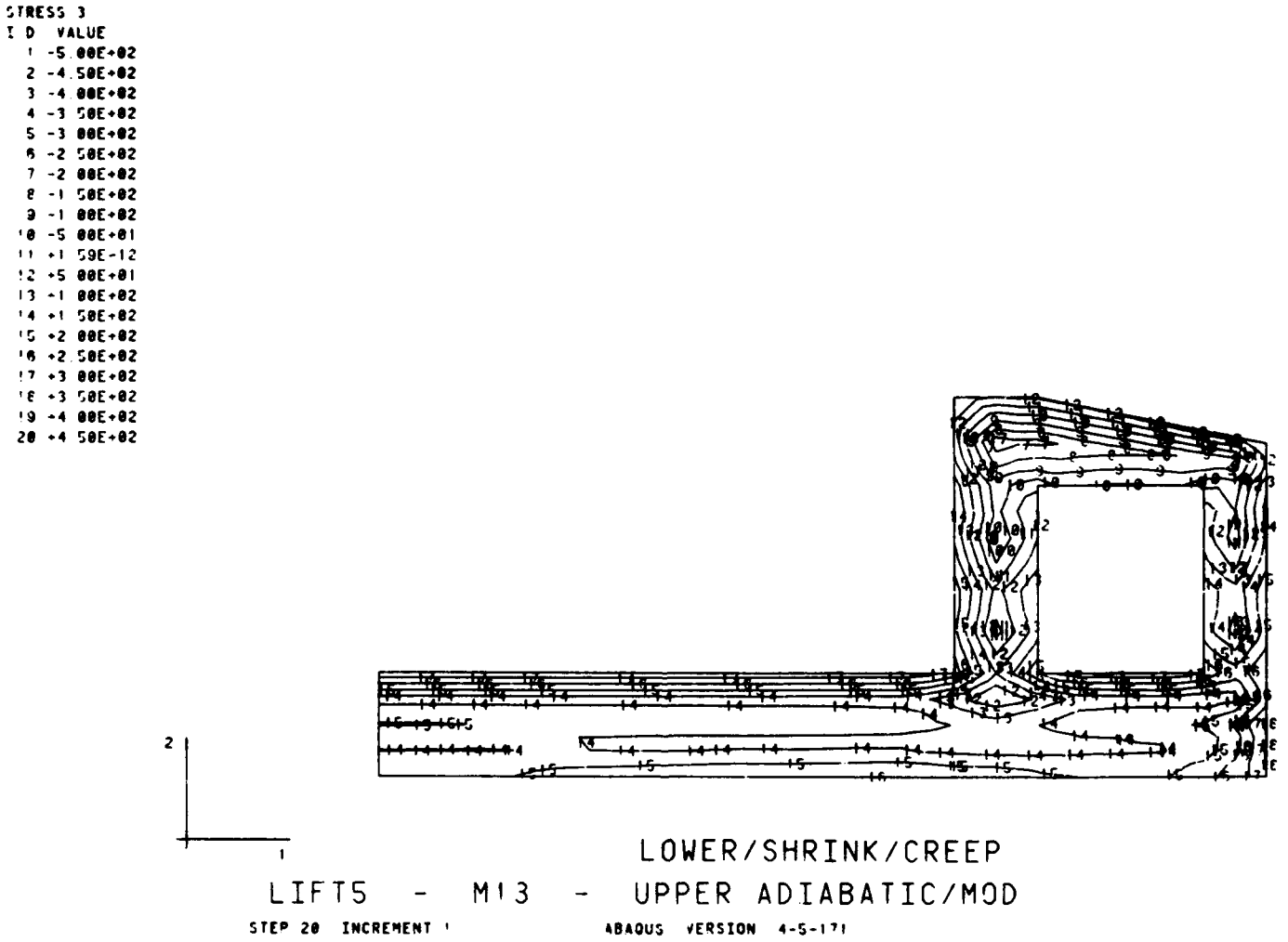

**Figure 26c - Out-of-plane stress contours in L-13,
5 days after lift 5 is placed,
Gravity & thermal loading, Lower creep/shrinkage**

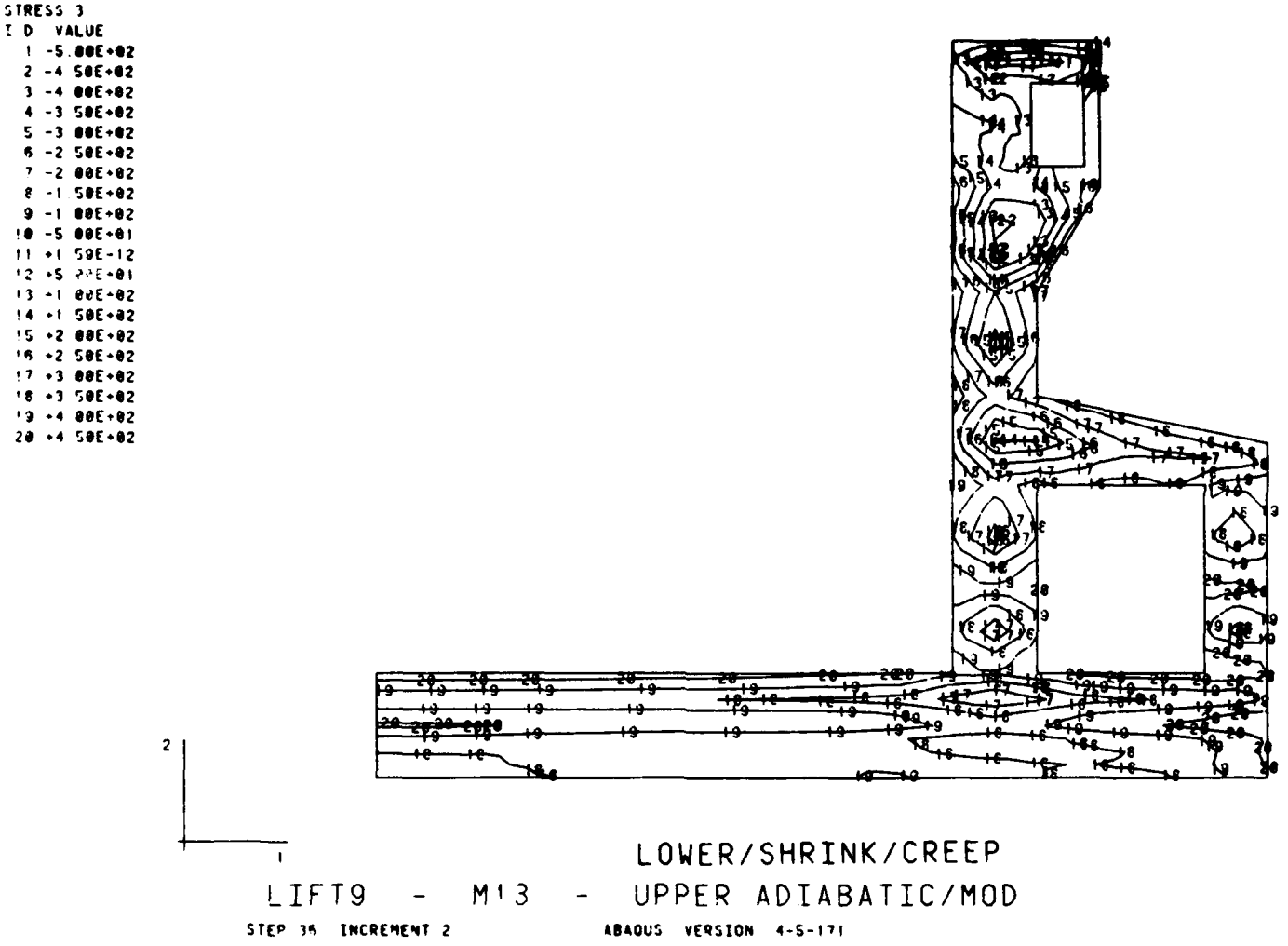

**Figure 26d - Out-of-plane stress contours in L-13,
7 days after lift 9 is placed,
Gravity & thermal loading, Lower creep/shrinkage**

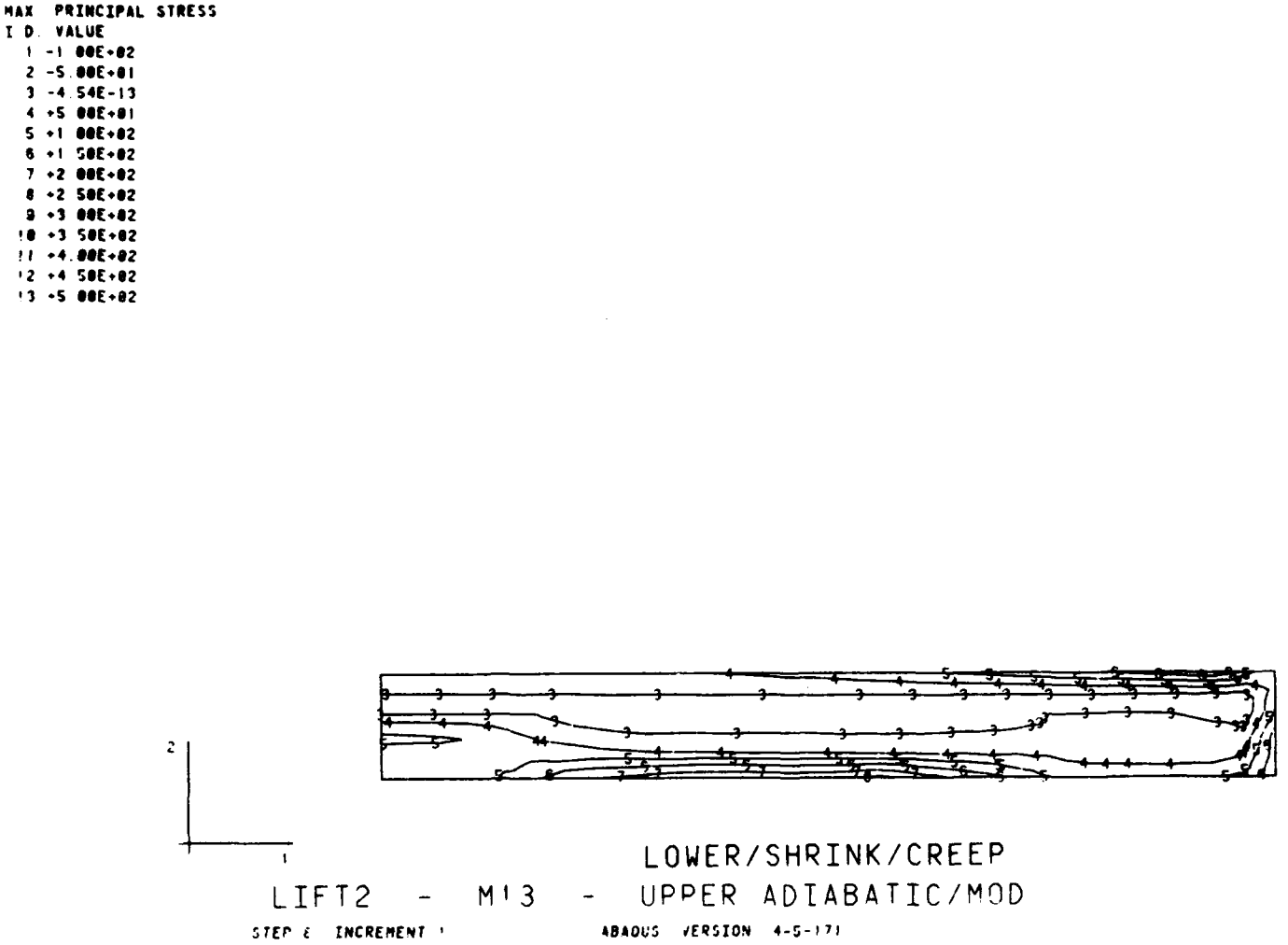

Figure 27a - Max. Principal stress contours in L-13, 5 days after lift 2 is placed, Gravity & thermal loading, Lower creep/shrinkage

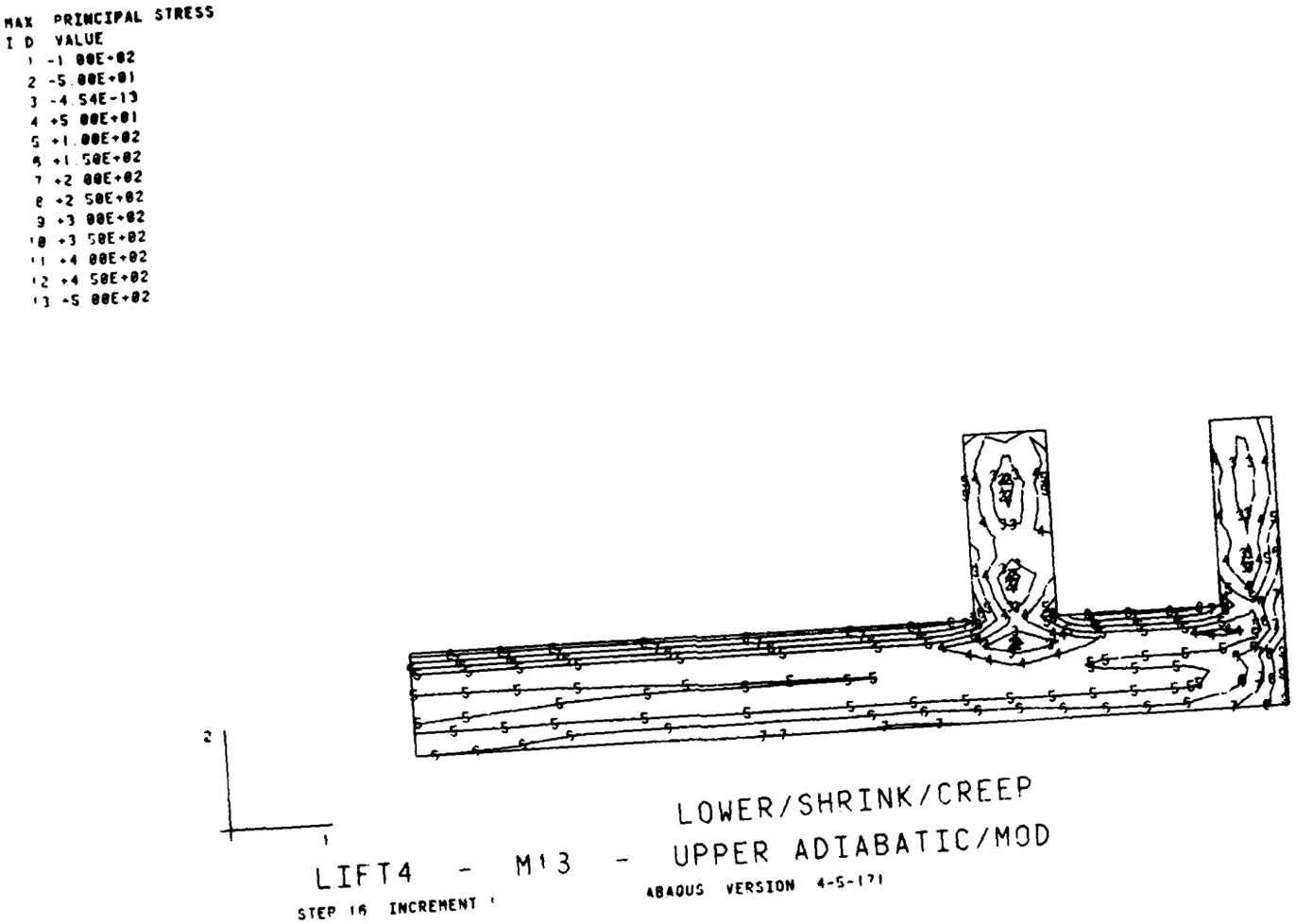

Figure 27b - Max. Principal stress contours in L-13, 5 days after lift 4 is placed, Gravity & thermal loading, Lower creep/shrinkage

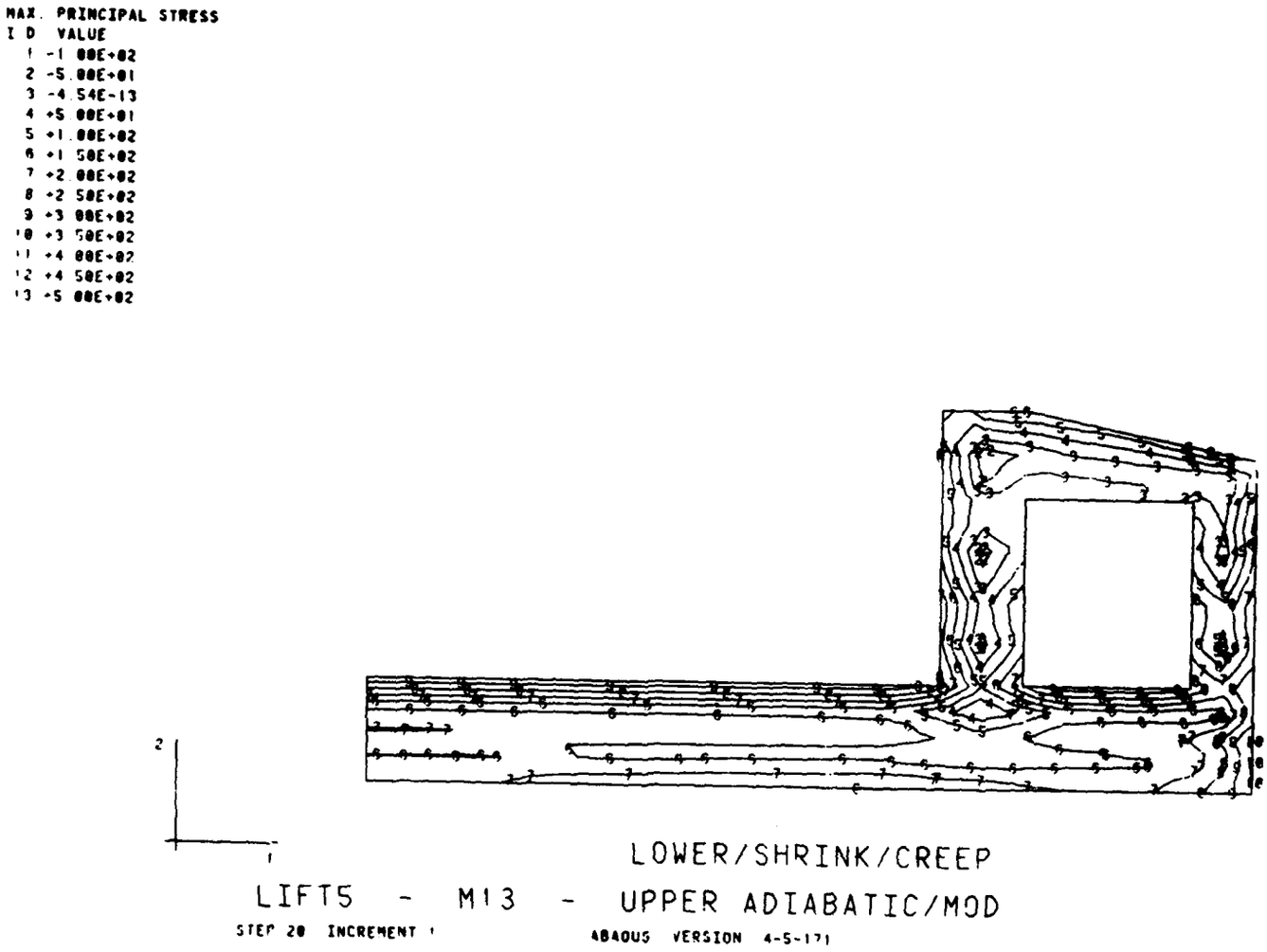

**Figure 27c - Max. Principal stress contours in L-13,
5 days after lift 5 is placed,
Gravity & thermal loading, Lower creep/shrinkage**

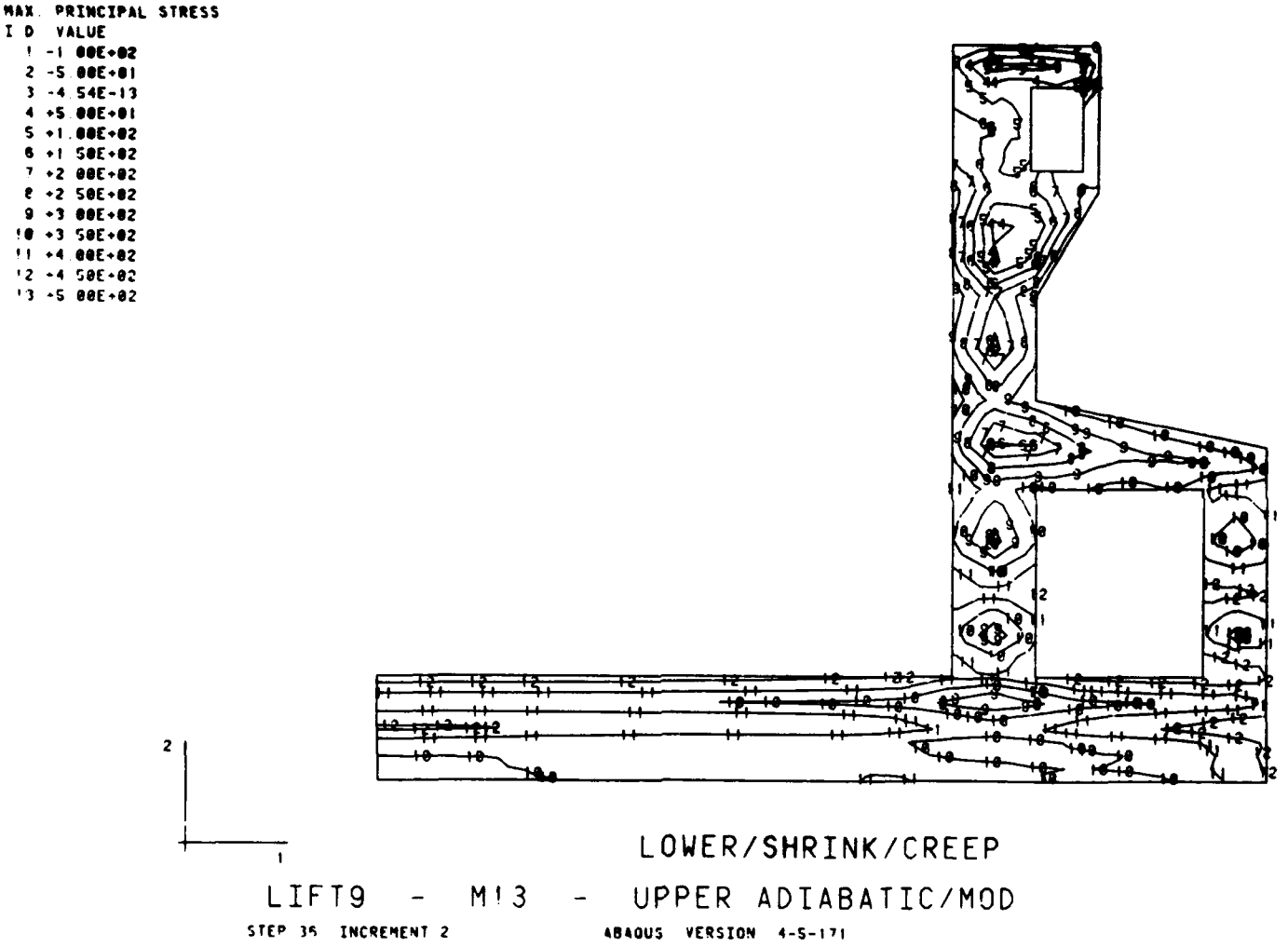

Figure 27d - Max. Principal stress contours in L-13, 7 days after lift 9 is placed, Gravity & thermal loading, Lower creep/shrinkage

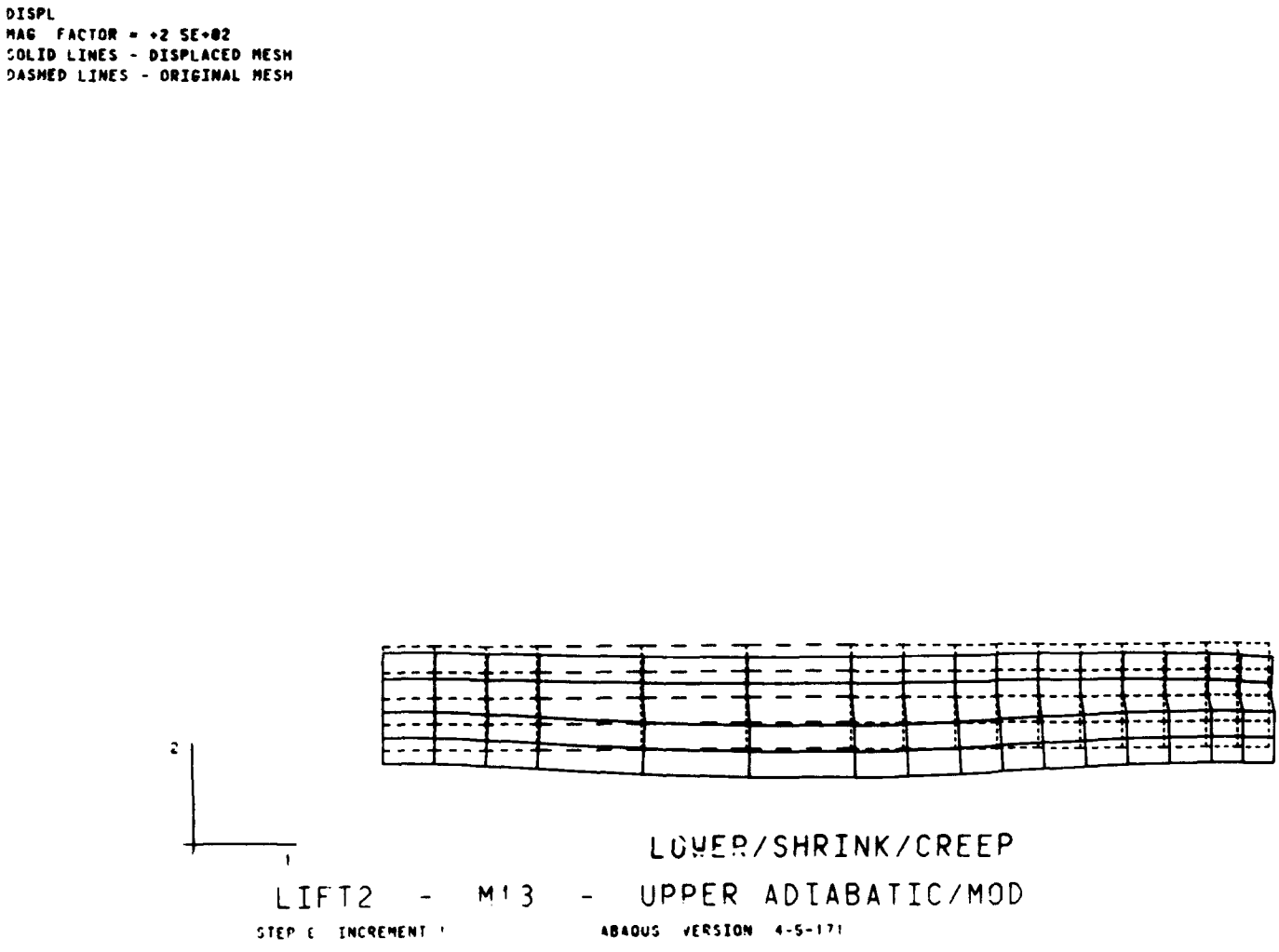

**Figure 28a - Displaced shape of L-13,
5 days after lift 2 is placed,
Gravity & thermal loading, Lower creep/shrinkage**

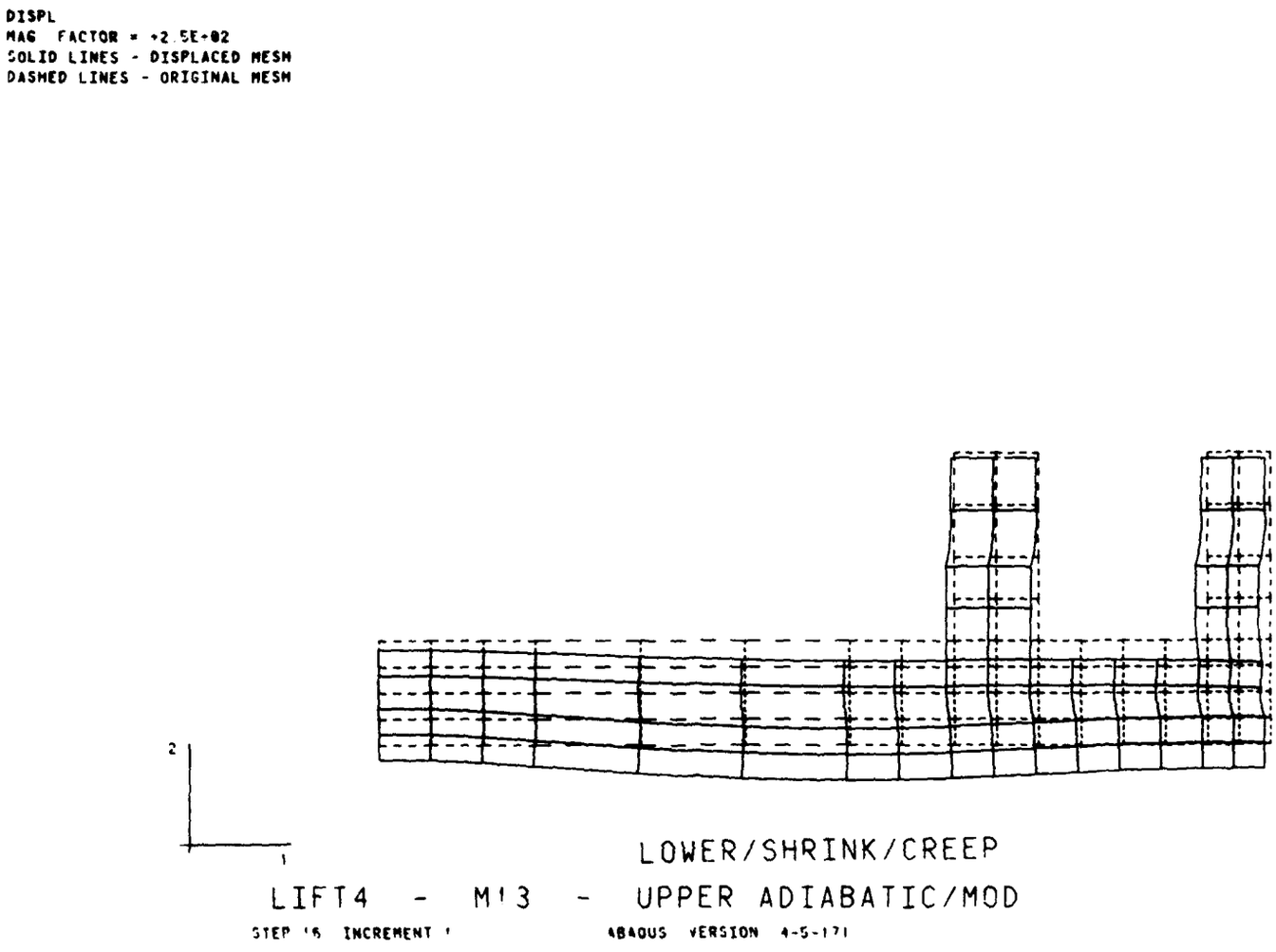

**Figure 28b - Displaced shape of L-13,
5 days after lift 4 is placed,
Gravity & thermal loading, Lower creep/shrinkage**

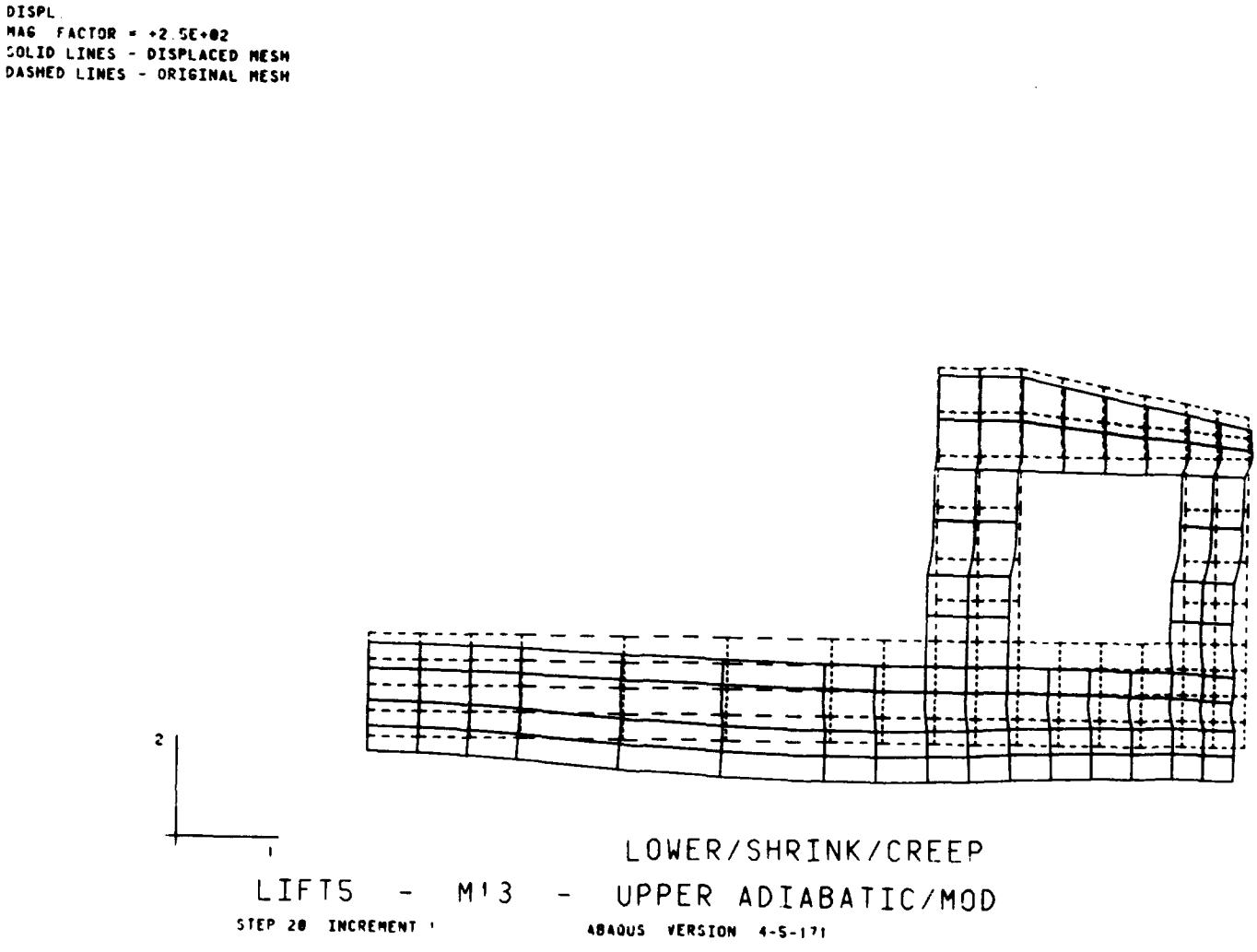

**Figure 28c - Displaced shape of L-13,
5 days after lift 5 is placed,
Gravity & thermal loading, Lower creep/shrinkage**

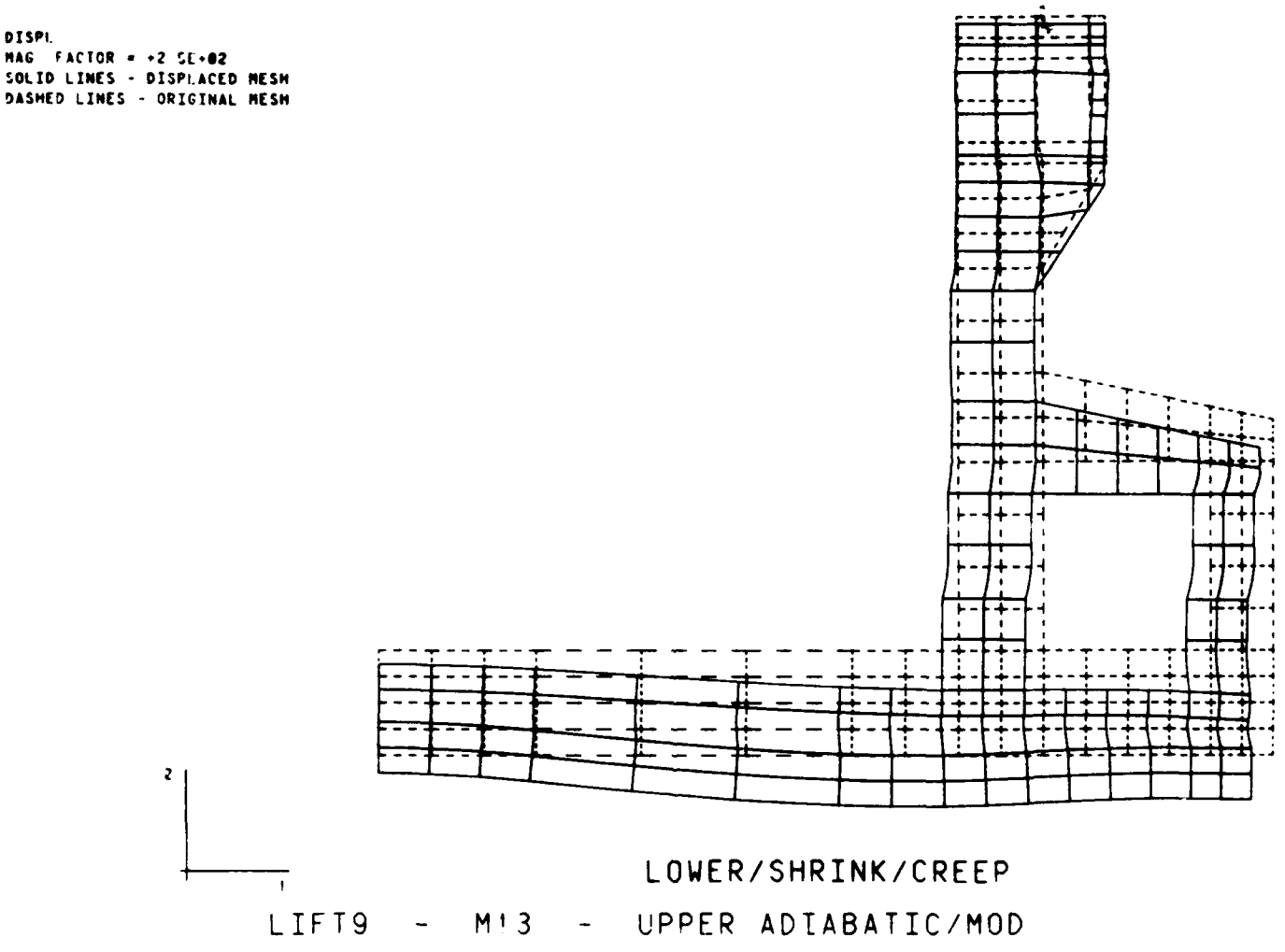

**Figure 28d - Displaced shape of L-13,
7 days after lift 9 is placed,
Gravity & thermal loading, Lower creep/shrinkage**

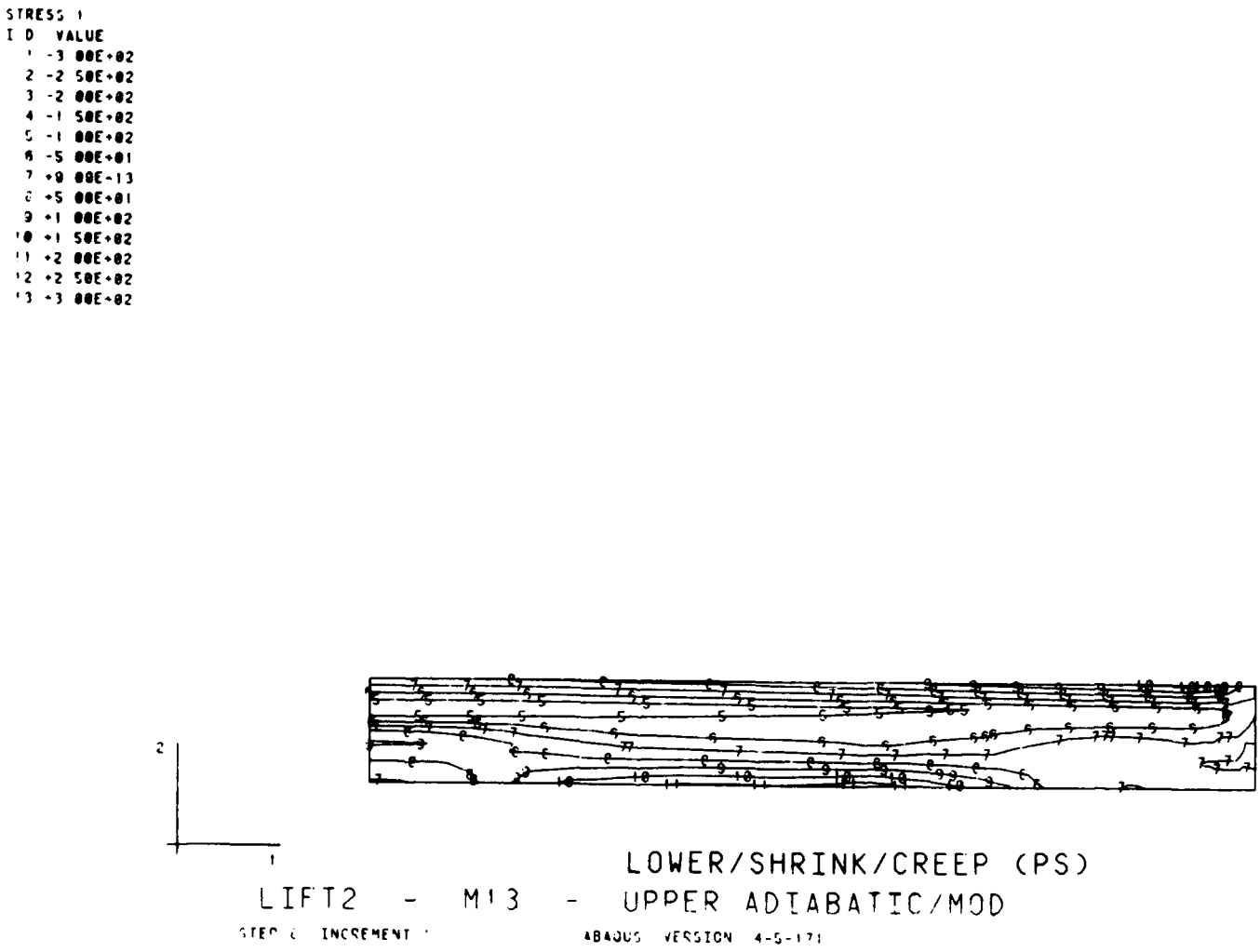

Figure 29a - Horizontal stress contours in L-13 (PS), 5 days after lift 2 is placed, Gravity & thermal loading, Lower creep/shrinkage

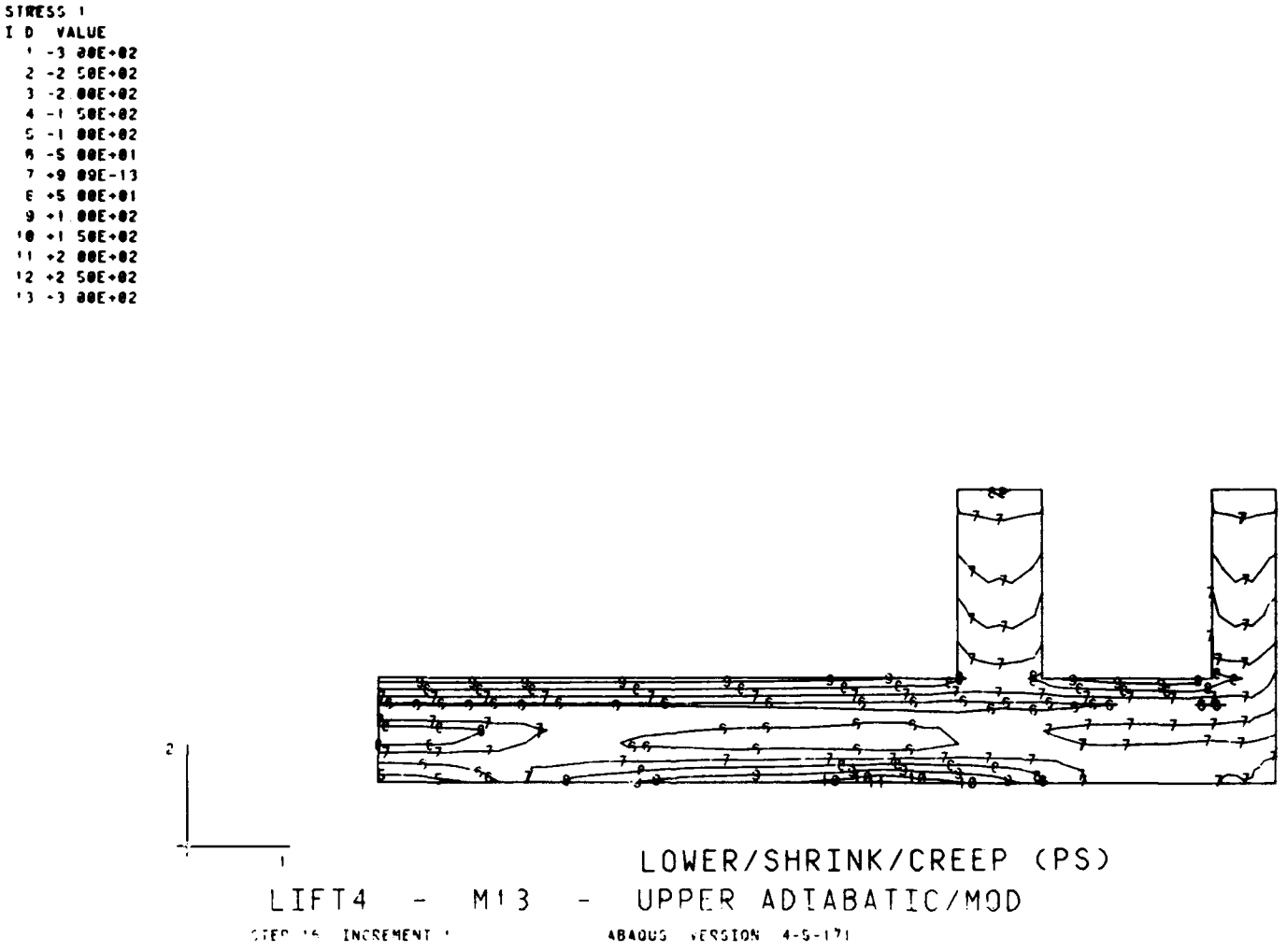

Figure 29b - Horizontal stress contours in L-13 (PS), 5 days after lift 4 is placed, Gravity & thermal loading, Lower creep/shrinkage

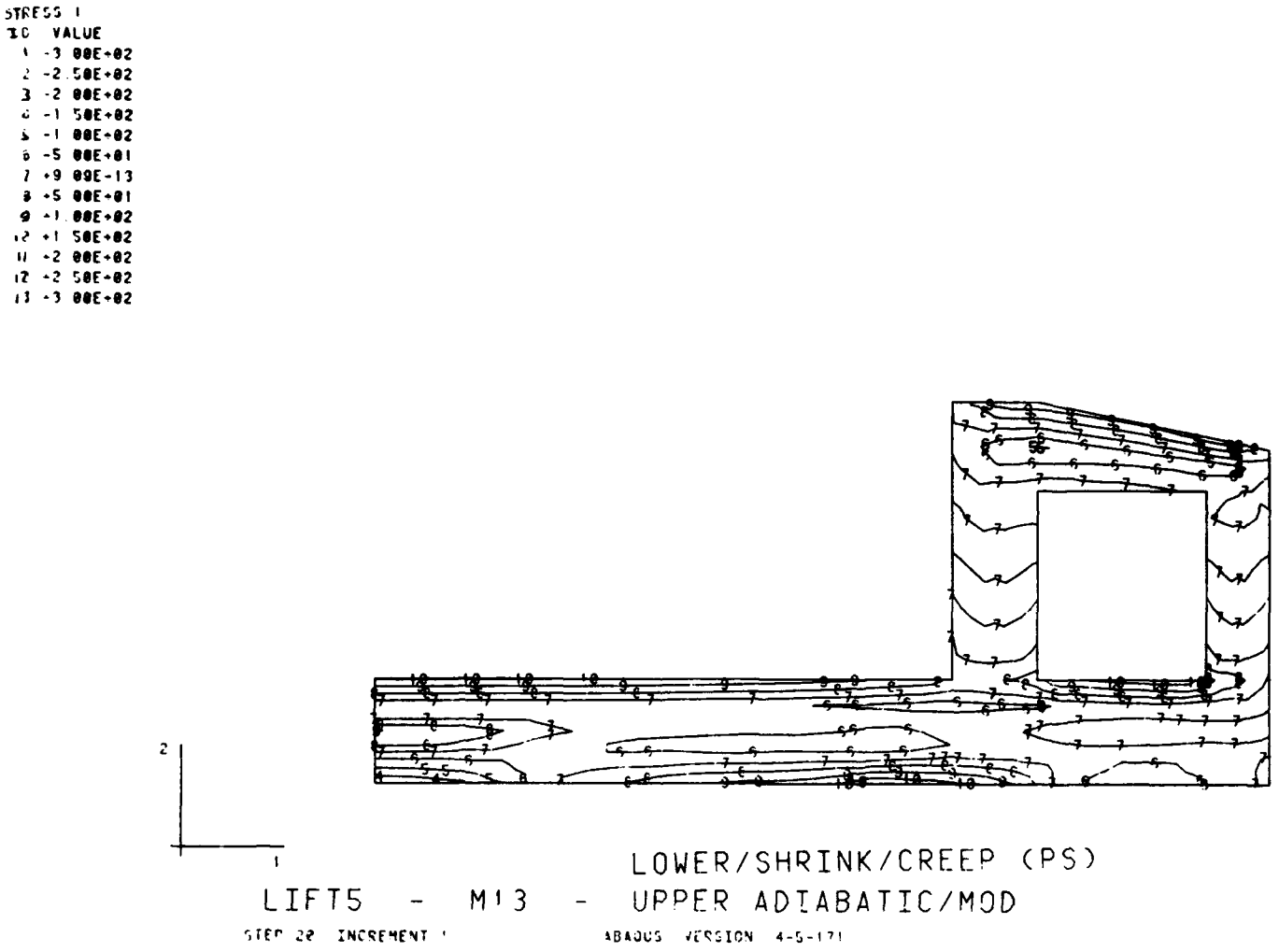

Figure 29c - Horizontal stress contours in L-13 (PS), 5 days after lift 5 is placed, Gravity & thermal loading, Lower creep/shrinkage

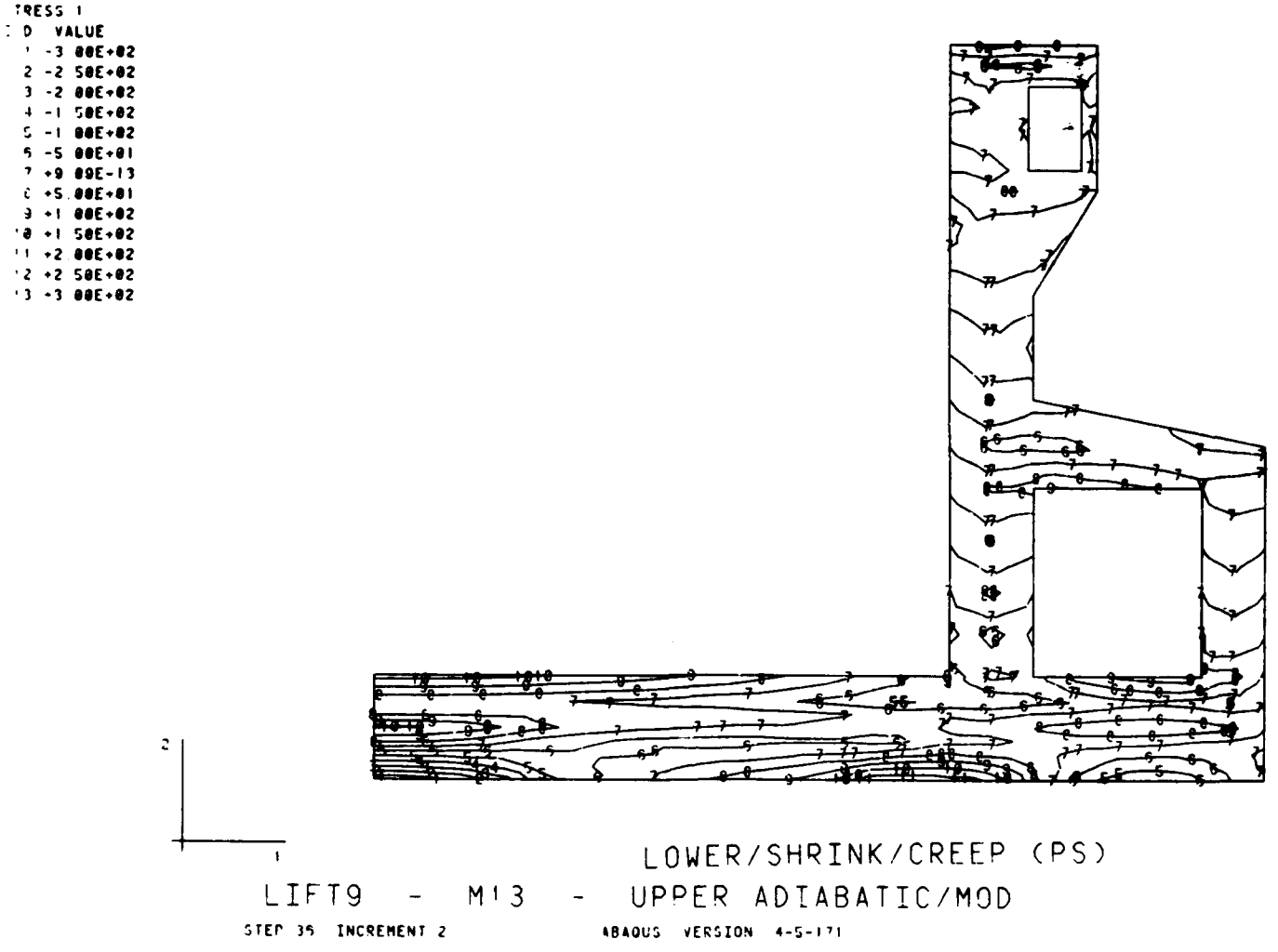

Figure 29d - Horizontal stress contours in L-13 (PS),
7 days after lift 9 is placed,
Gravity & thermal loading, Lower creep/shrinkage

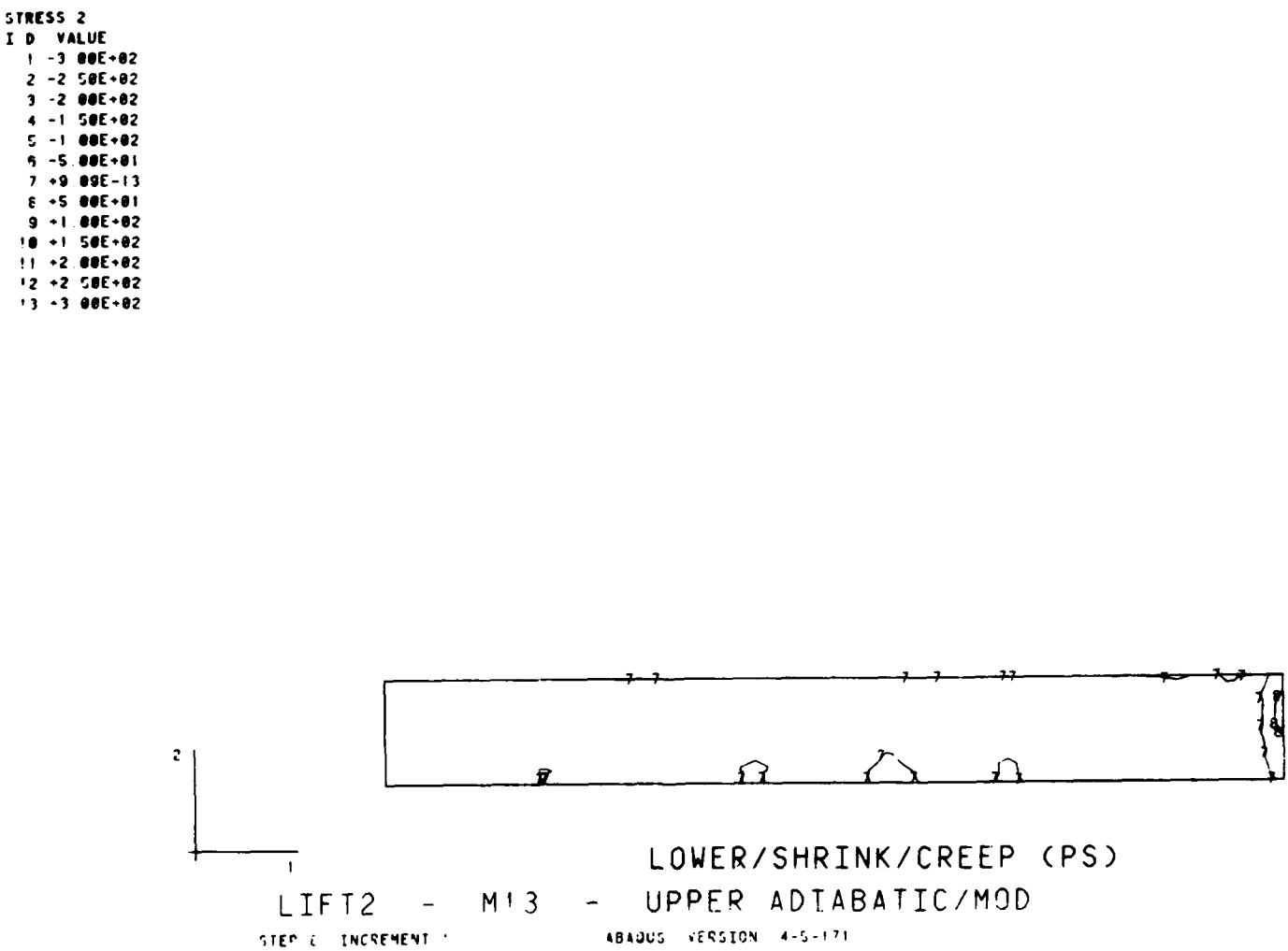

Figure 30a - Vertical stress contours in L-13 (PS), 5 days after lift 2 is placed, Gravity & thermal loading, Lower creep/shrinkage

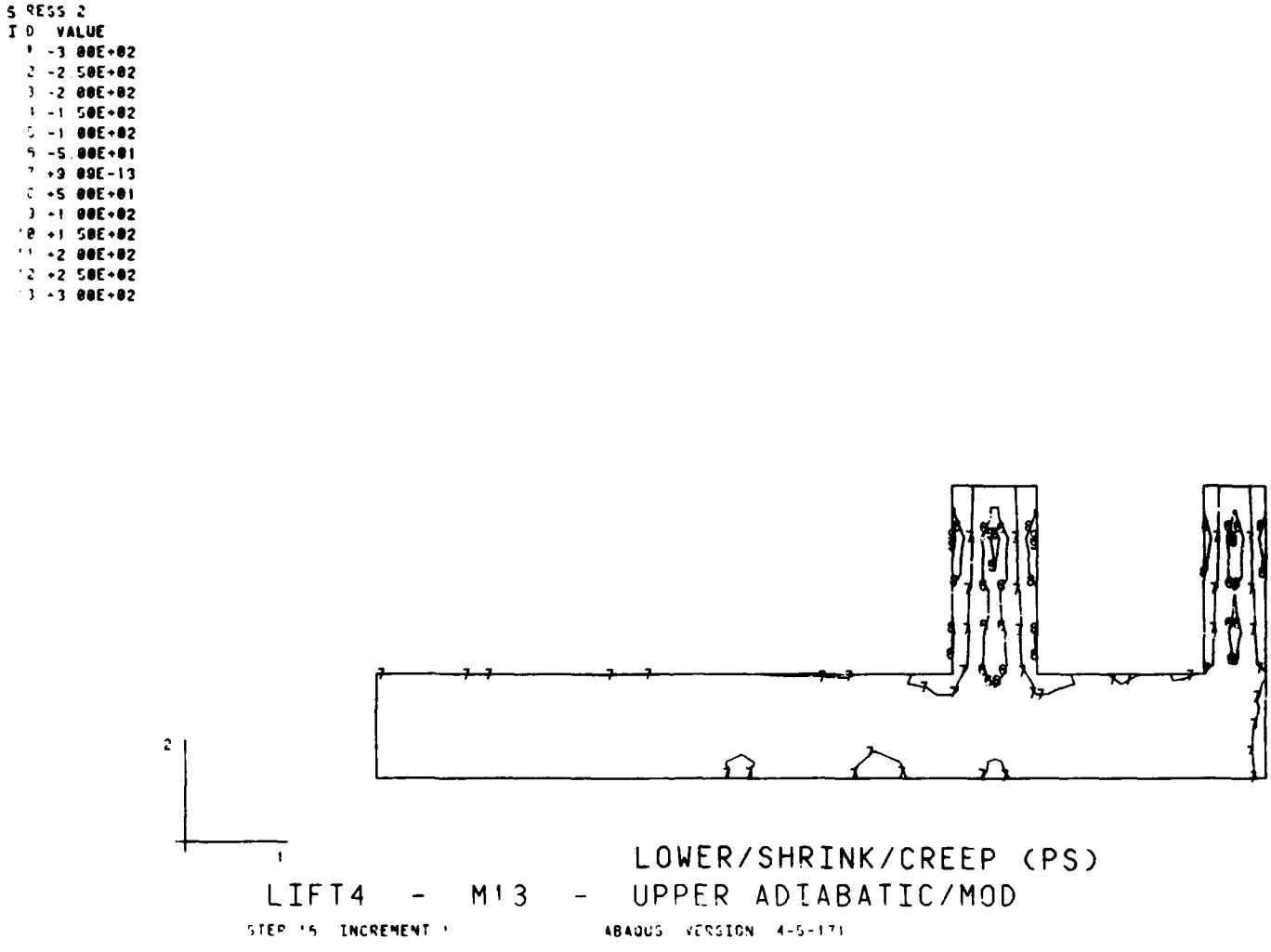

Figure 30b - Vertical stress contours in L-13 (PS), 5 days after lift 4 is placed, Gravity & thermal loading, Lower creep/shrinkage

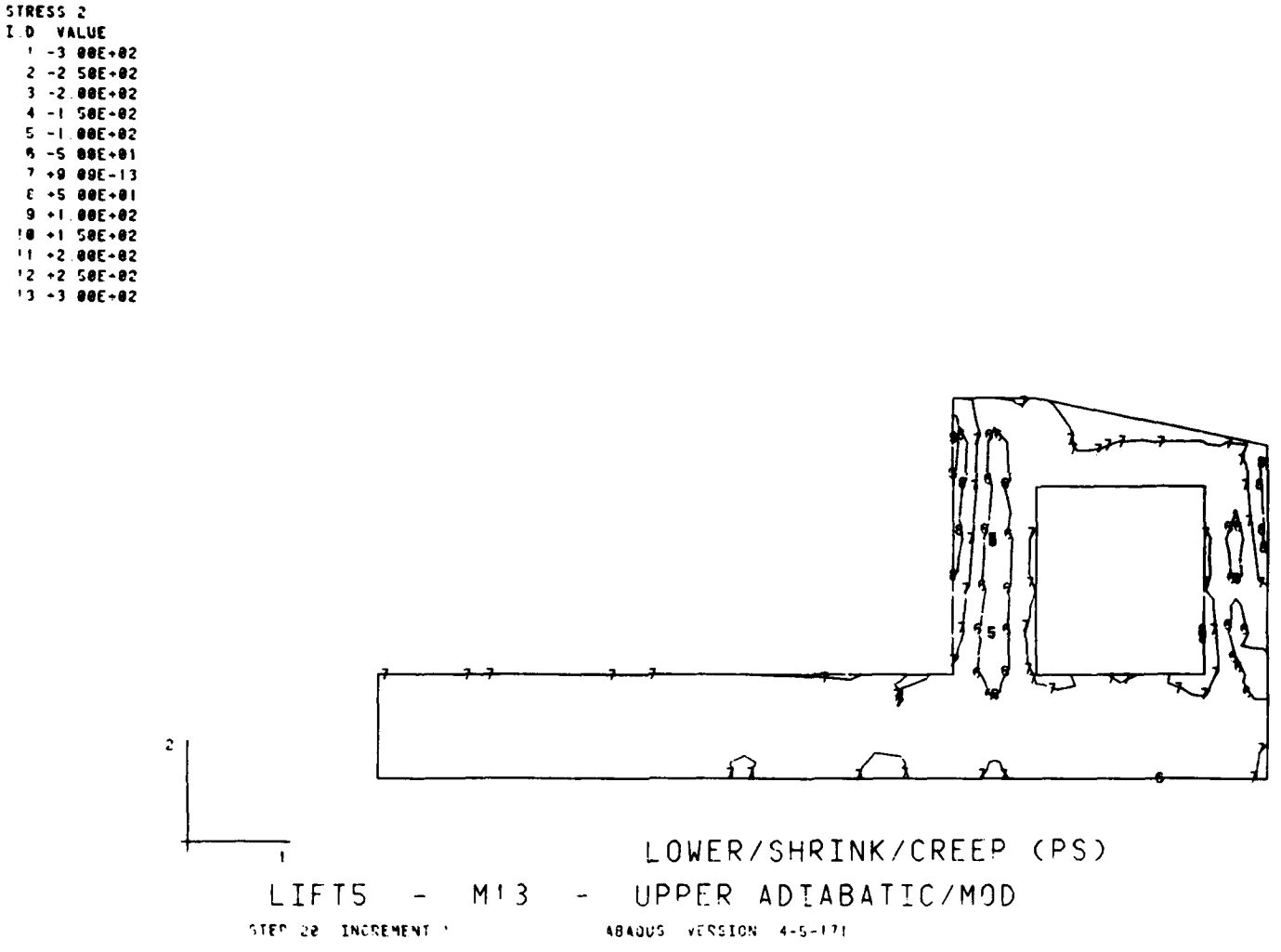

Figure 30c - Vertical stress contours in L-13 (PS), 5 days after lift 5 is placed, Gravity & thermal loading, Lower creep/shrinkage

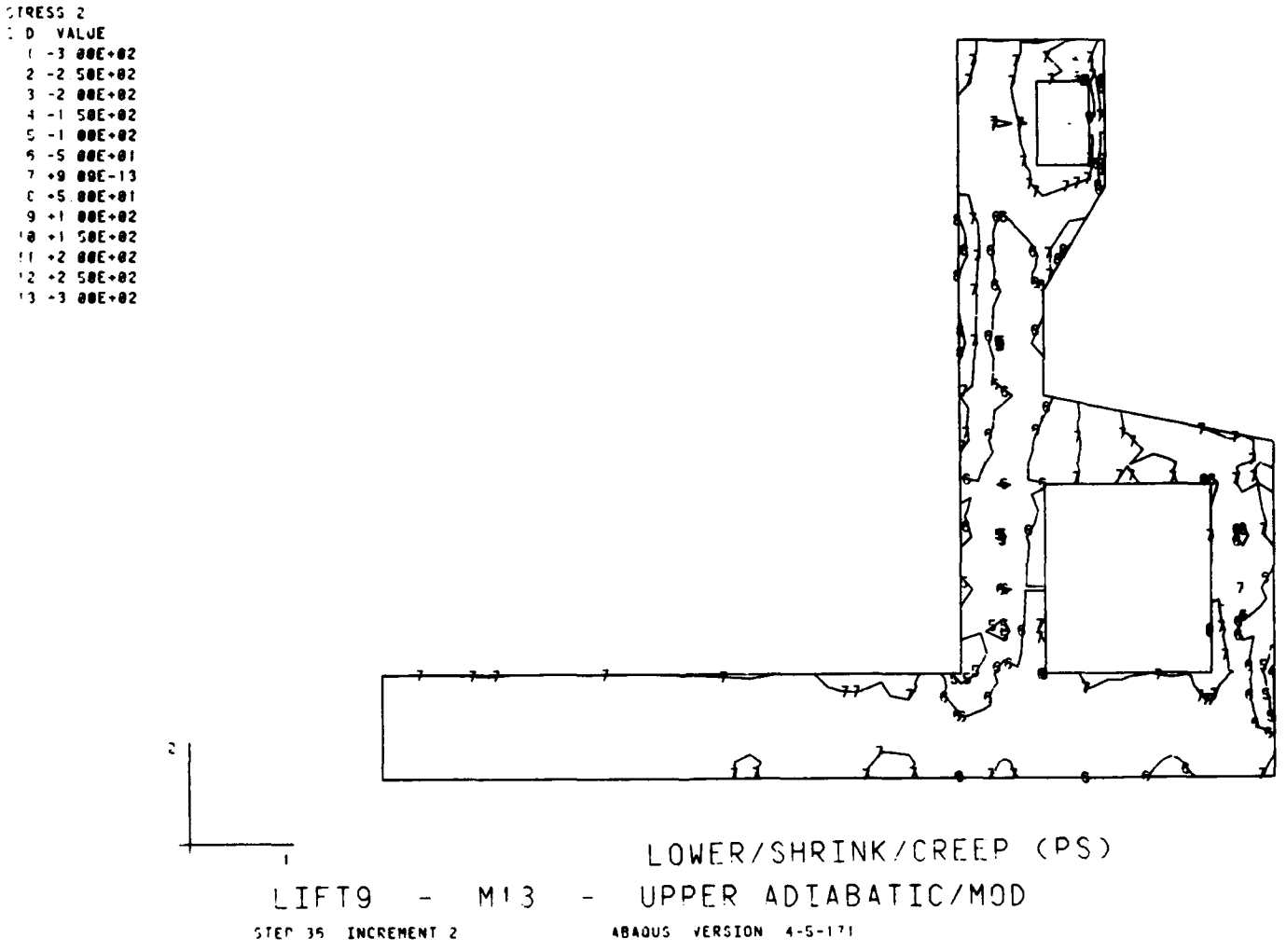

Figure 30d - Vertical stress contours in L-13 (PS), 7 days after lift 9 is placed, Gravity & thermal loading, Lower creep/shrinkage

STRESS 3

I D	VALUE
1	-5.00E+02
2	-4.50E+02
3	-4.00E+02
4	-3.50E+02
5	-3.00E+02
6	-2.50E+02
7	-2.00E+02
8	-1.50E+02
9	-1.00E+02
10	-5.00E+01
11	+0.00E-13
12	+5.00E+01
13	+1.00E+02

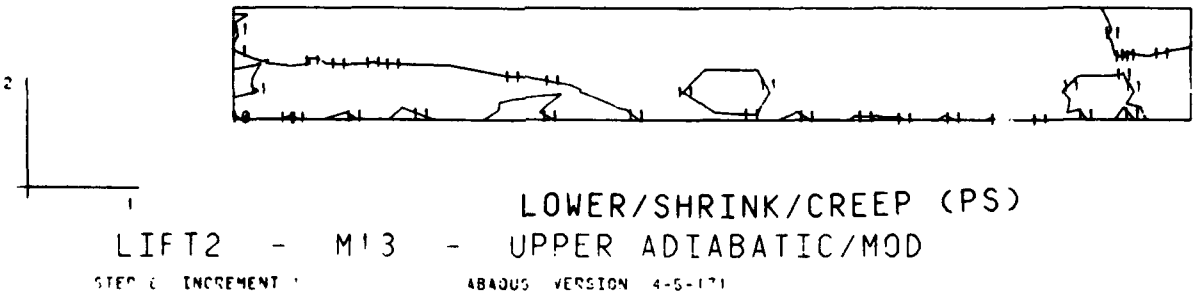

Figure 31a - Out-of-plane stress contours in L-13 (PS), 5 days after lift 2 is placed, Gravity & thermal loading, Lower creep/shrinkage

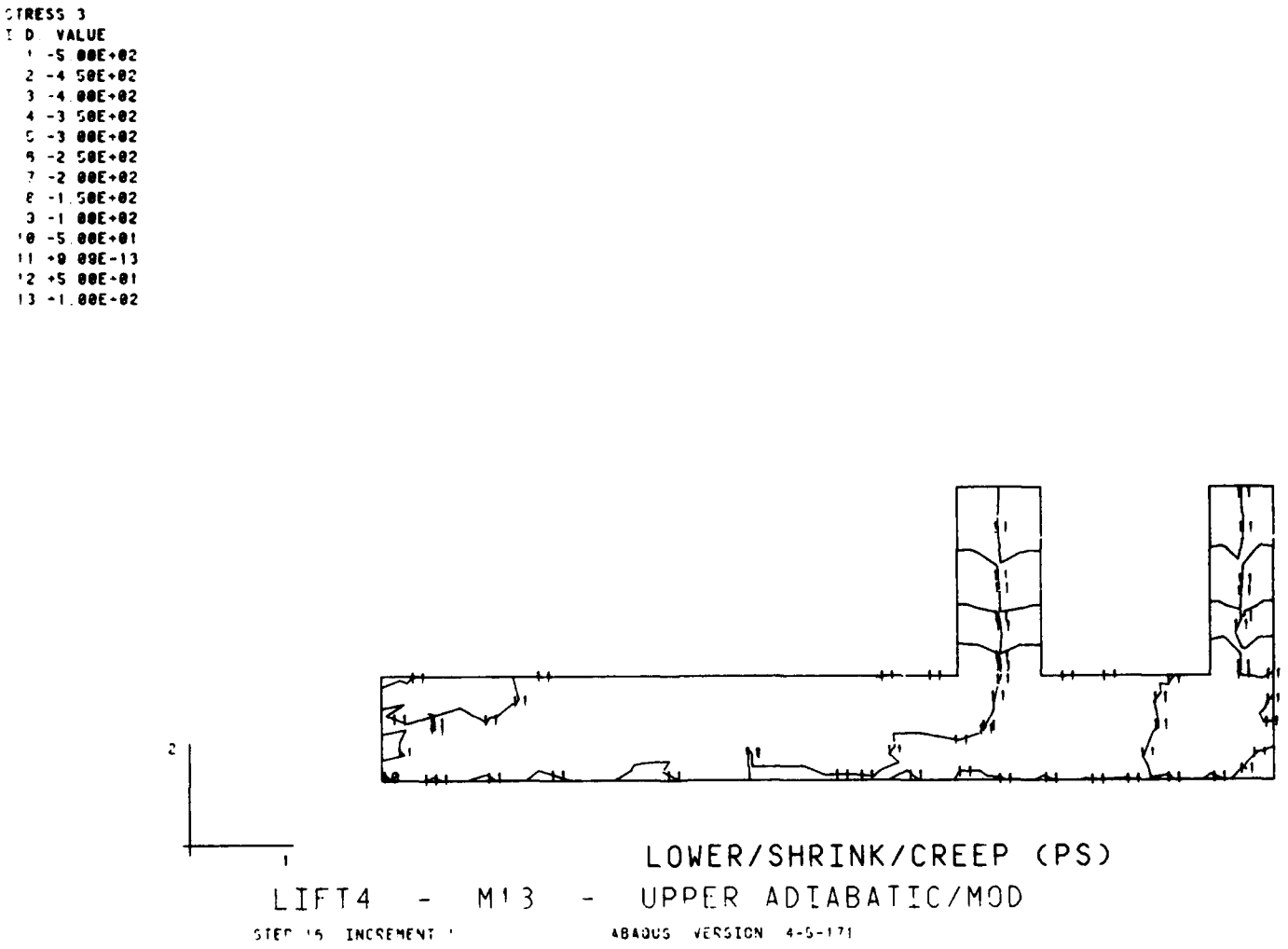

Figure 31b - Out-of-plane stress contours in L-13 (PS), 5 days after lift 4 is placed, Gravity & thermal loading, Lower creep/shrinkage

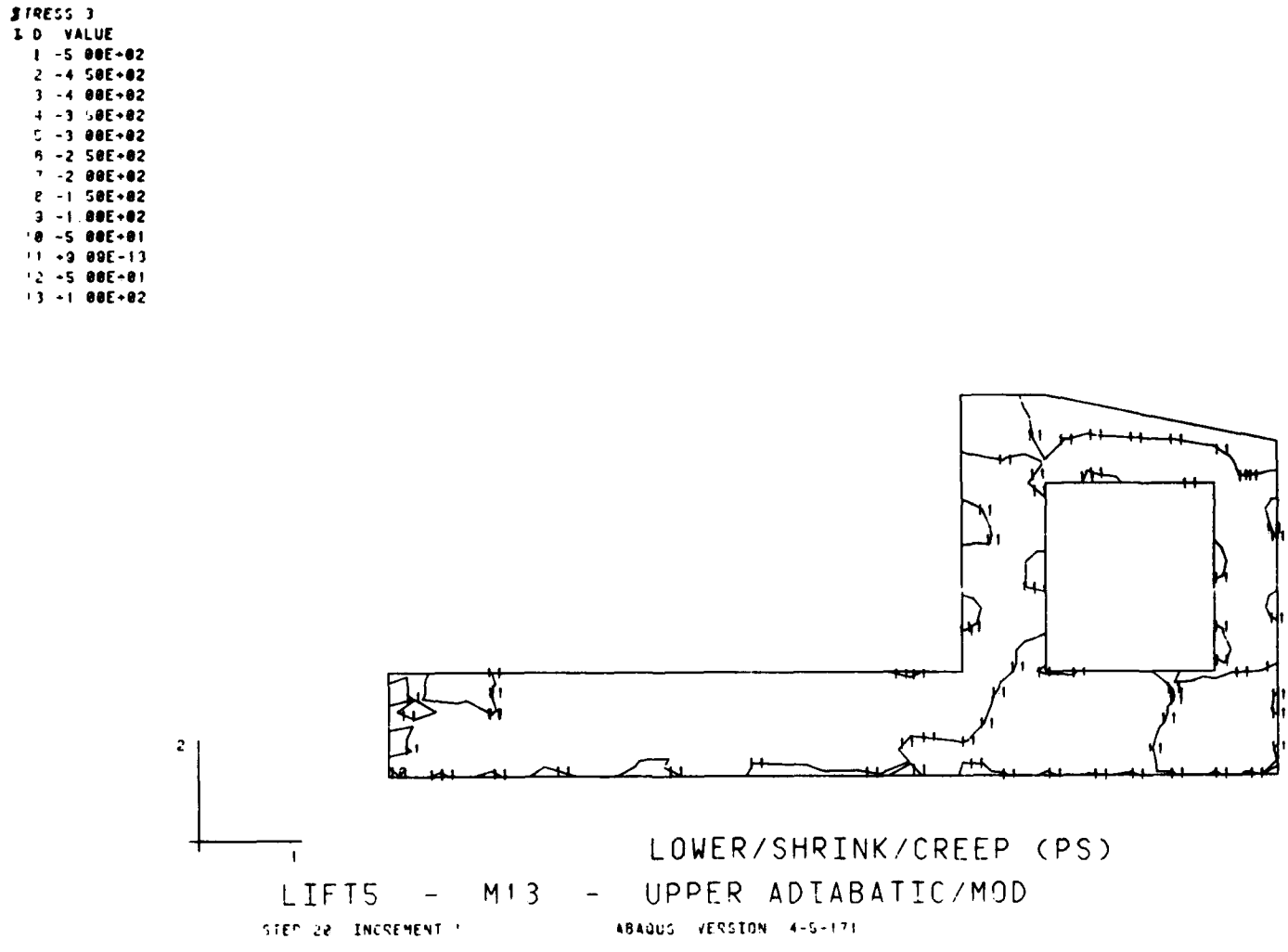

Figure 31c - Out-of-plane stress contours in L-13 (PS), 5 days after lift 5 is placed, Gravity & thermal loading, Lower creep/shrinkage

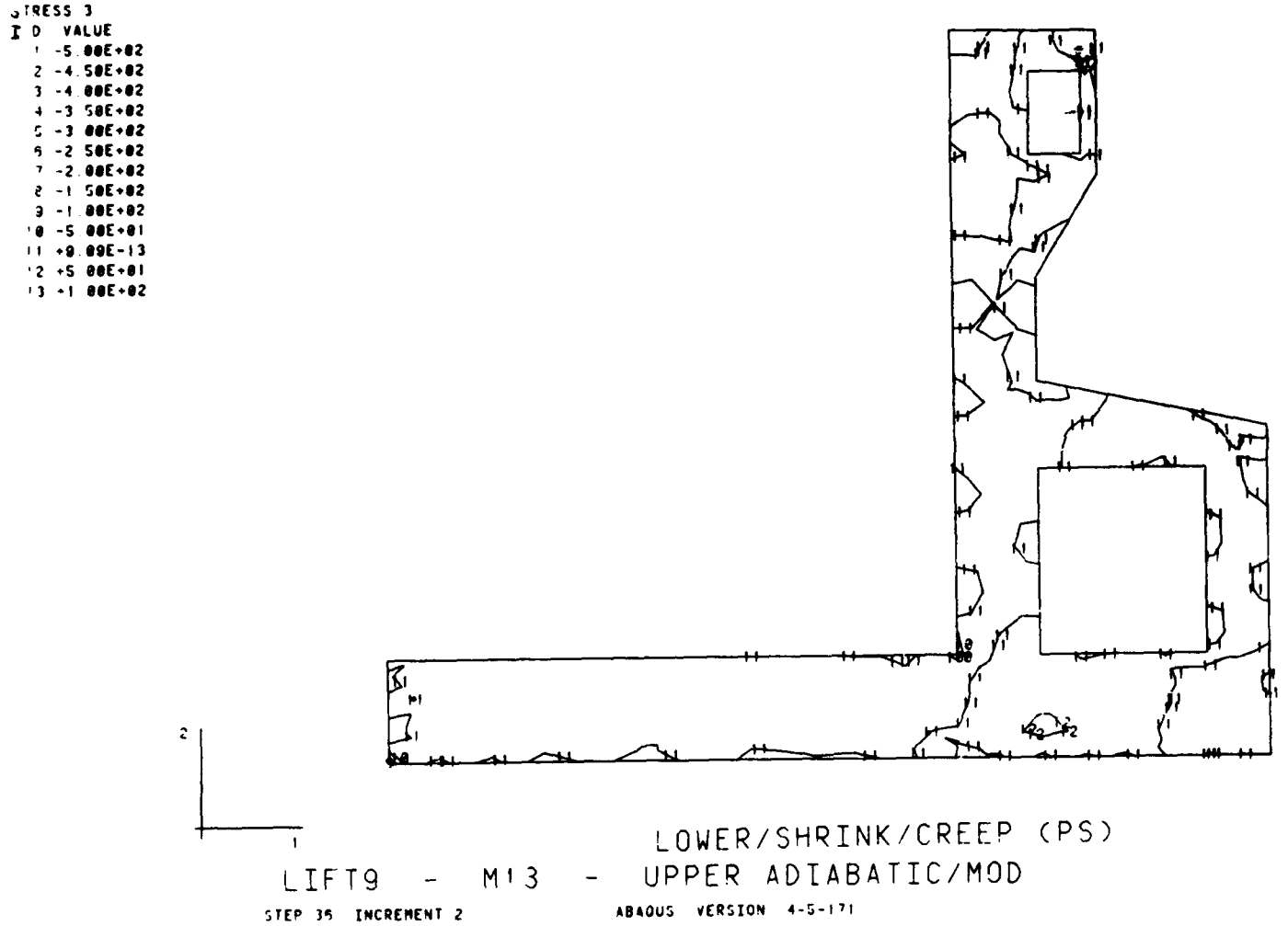

Figure 31d - Out-of-plane stress contours in L-13 (PS),
7 days after lift 9 is placed,
Gravity & thermal loading, Lower creep/shrinkage

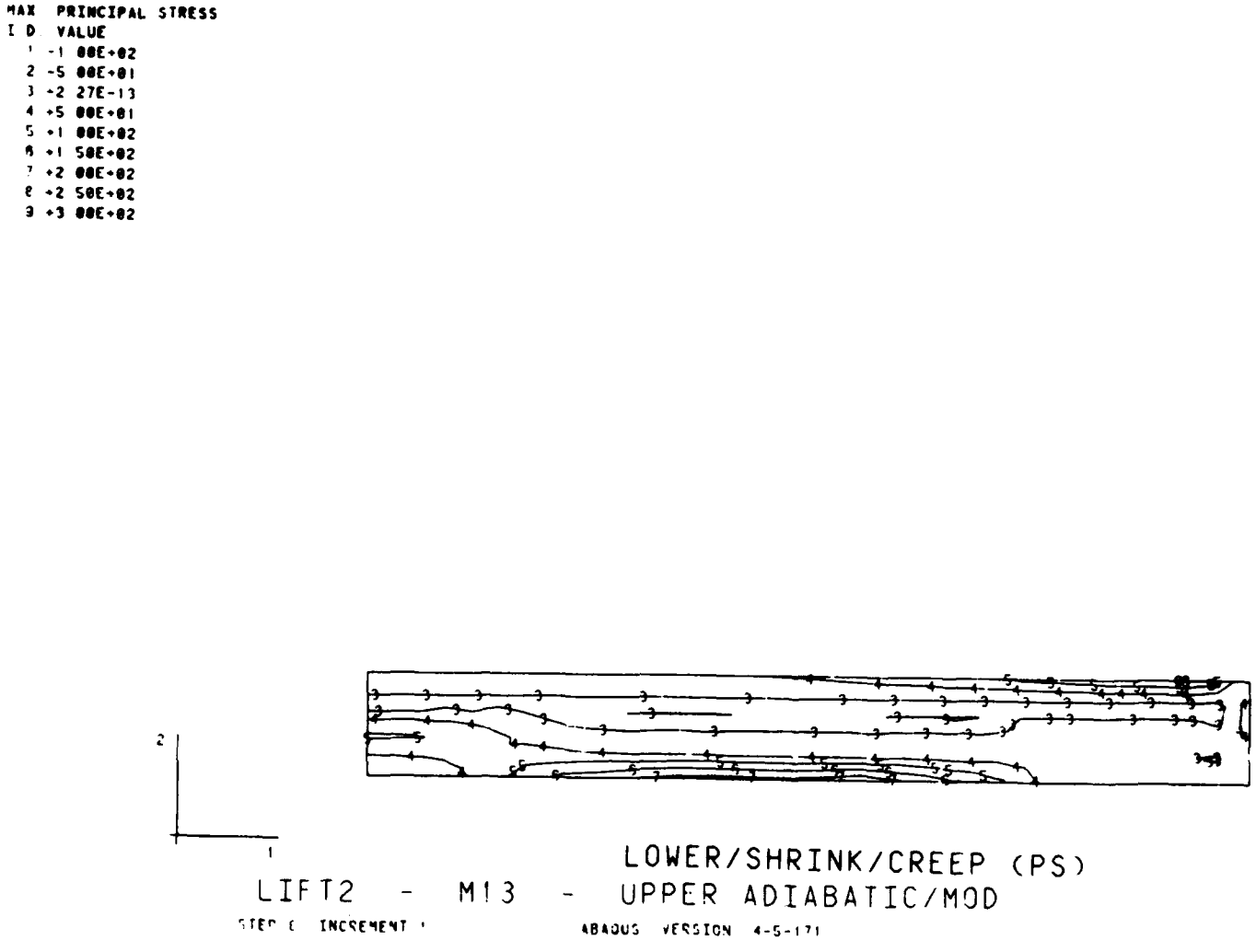

Figure 32a - Max. Principal stress contours in L-13 (PS), 5 days after lift 2 is placed, Gravity & thermal loading, Lower creep/shrinkage

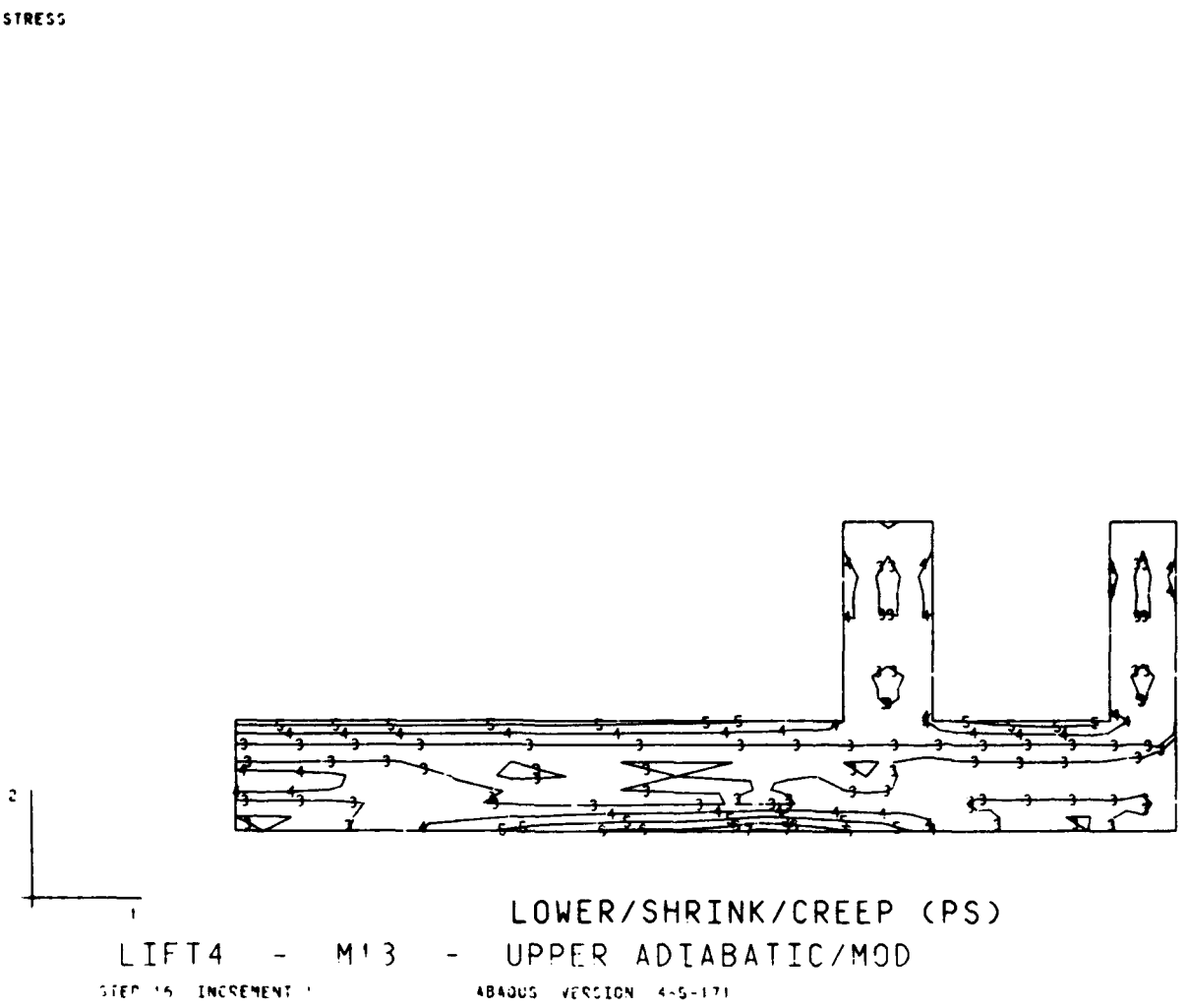

Figure 32b - Max. Principal stress contours in L-13 (PS), 5 days after lift 4 is placed, Gravity & thermal loading, Lower creep/shrinkage

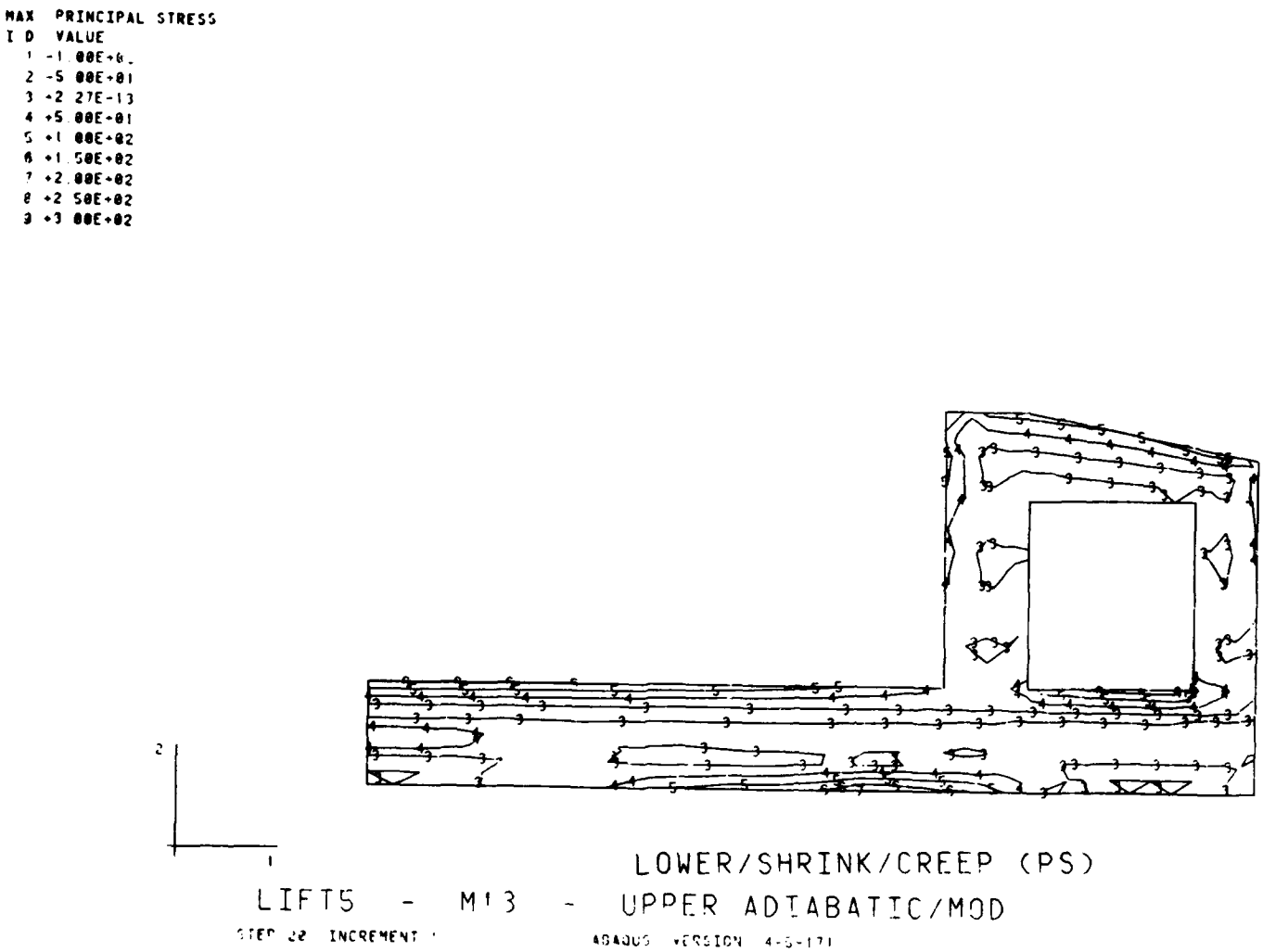

Figure 32c - Max. Principal stress contours in L-13 (PS), 5 days after lift 5 is placed, Gravity & thermal loading, Lower creep/shrinkage

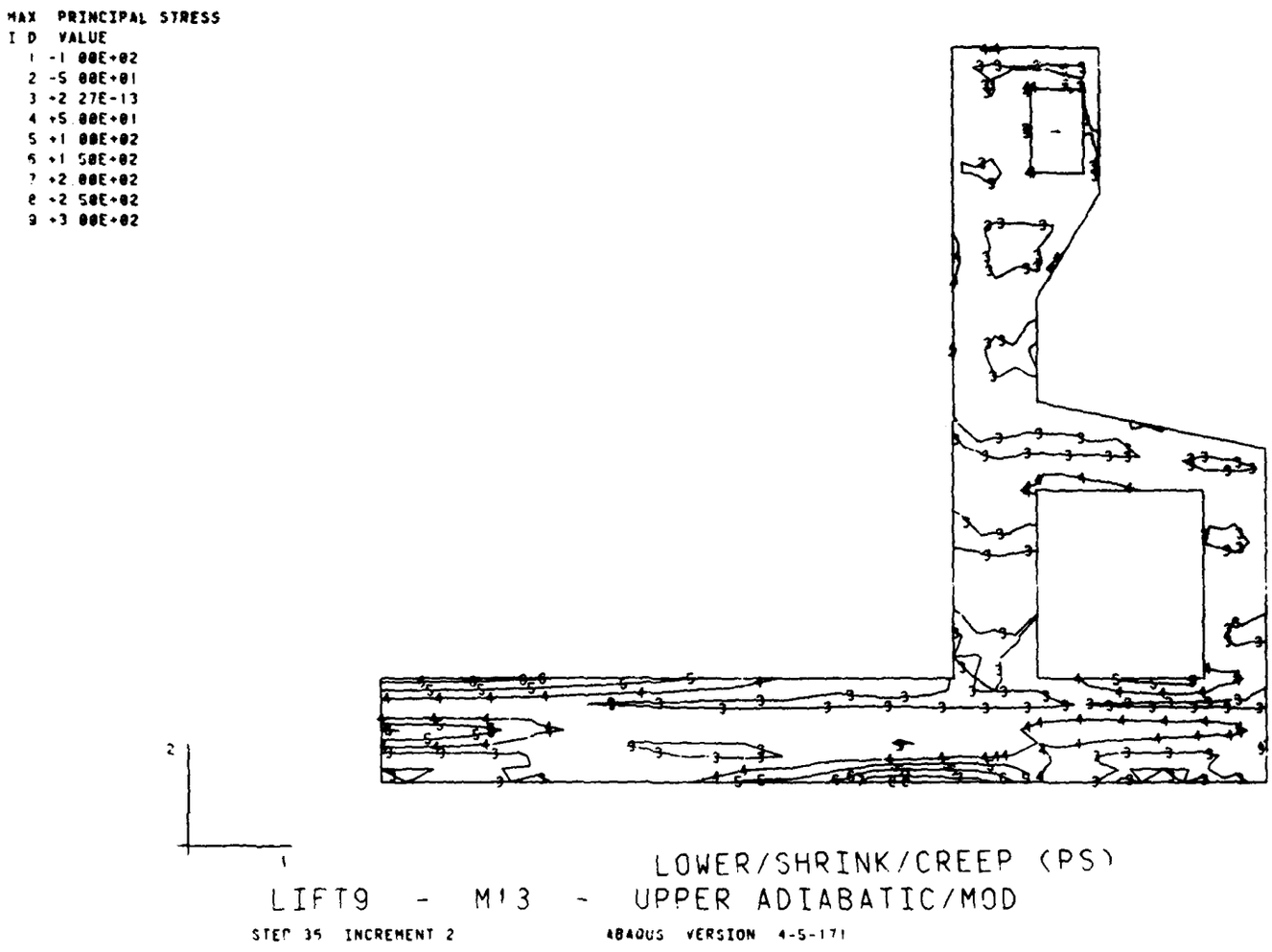

Figure 32d - Max. Principal stress contours in L-13 (PS), 7 days after lift 9 is placed, Gravity & thermal loading, Lower creep/shrinkage

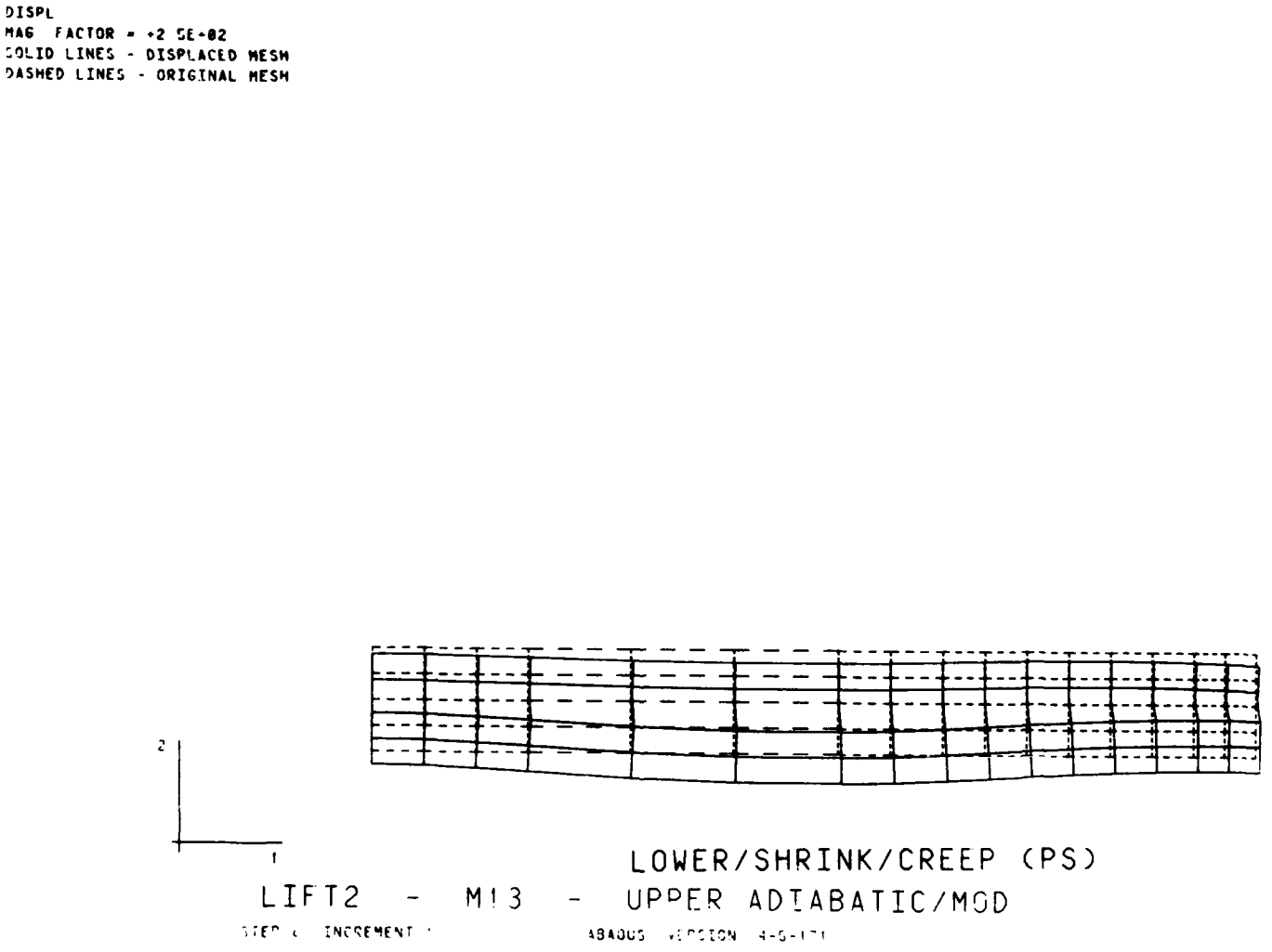

**Figure 33a - Displaced shape of L-13 (PS),
5 days after lift 2 is placed,
Gravity & thermal loading, Lower creep/shrinkage**

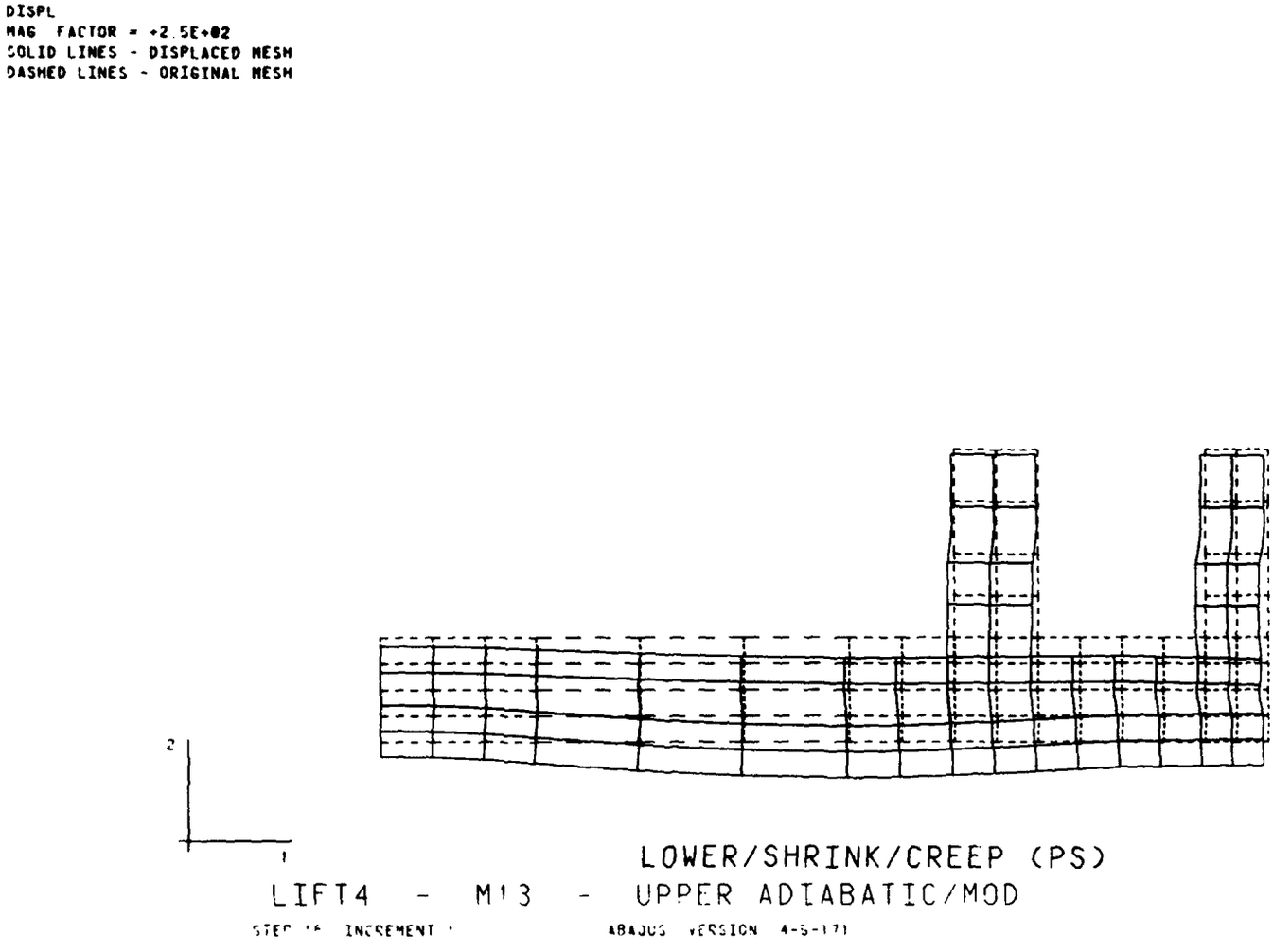

**Figure 33b - Displaced shape of L-13 (PS),
5 days after lift 4 is placed,
Gravity & thermal loading, Lower creep/shrinkage**

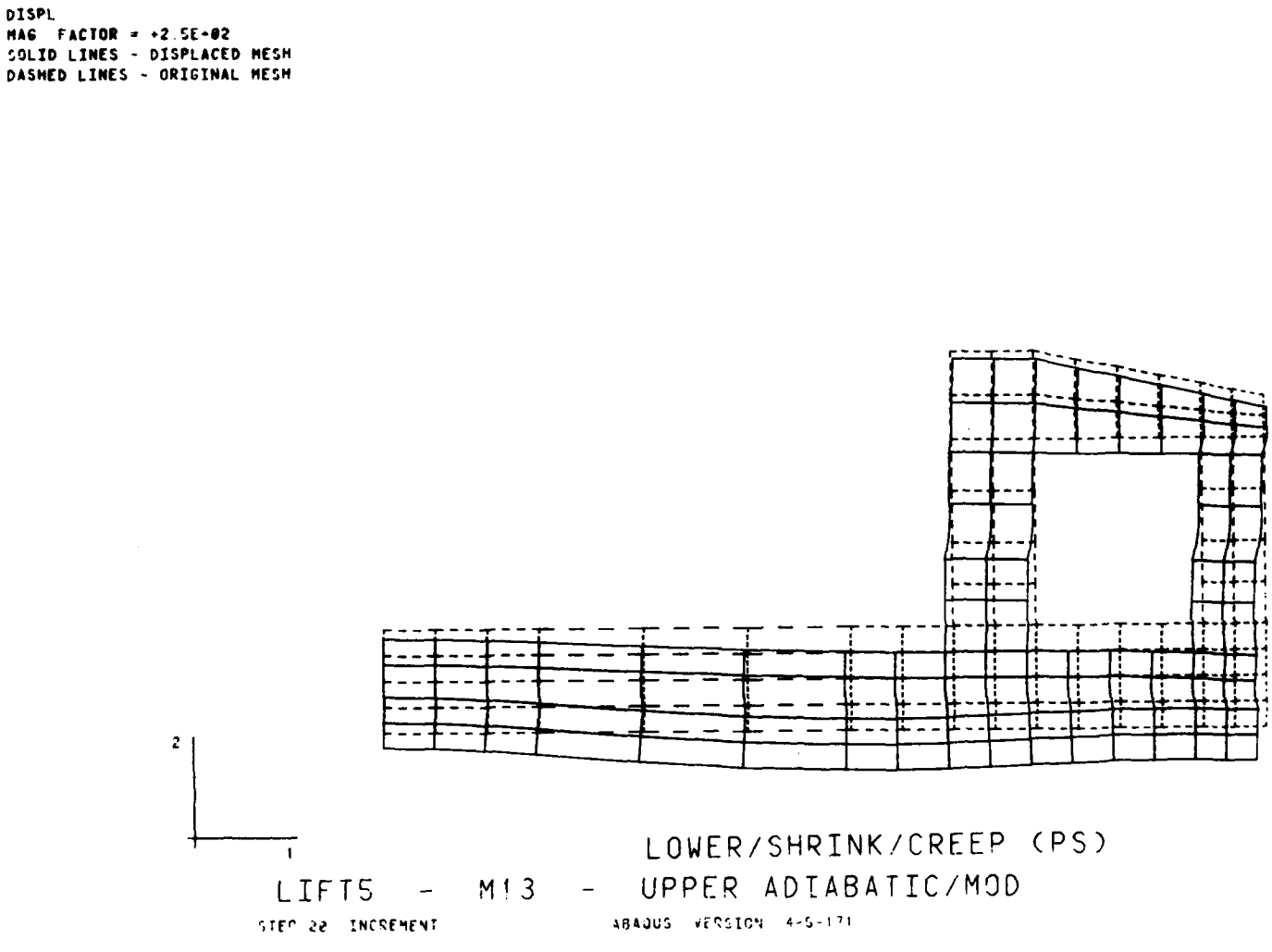

**Figure 33c - Displaced shape of L-13 (PS),
5 days after lift 5 is placed,
Gravity & thermal loading, Lower creep/shrinkage**

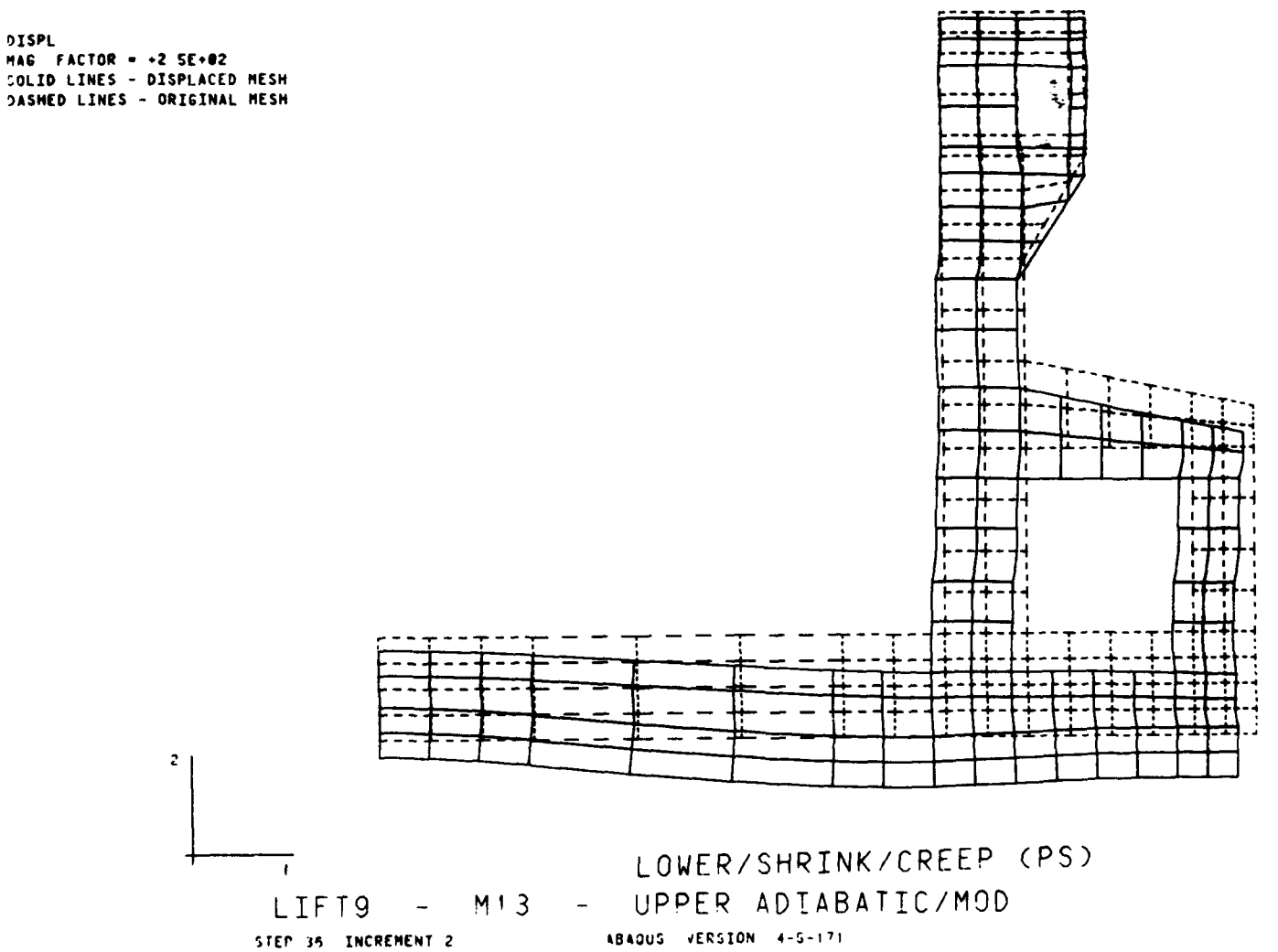

Figure 33d - Displaced shape of L-13 (PS), 7 days after lift 9 is placed, Gravity & thermal loading, Lower creep/shrinkage

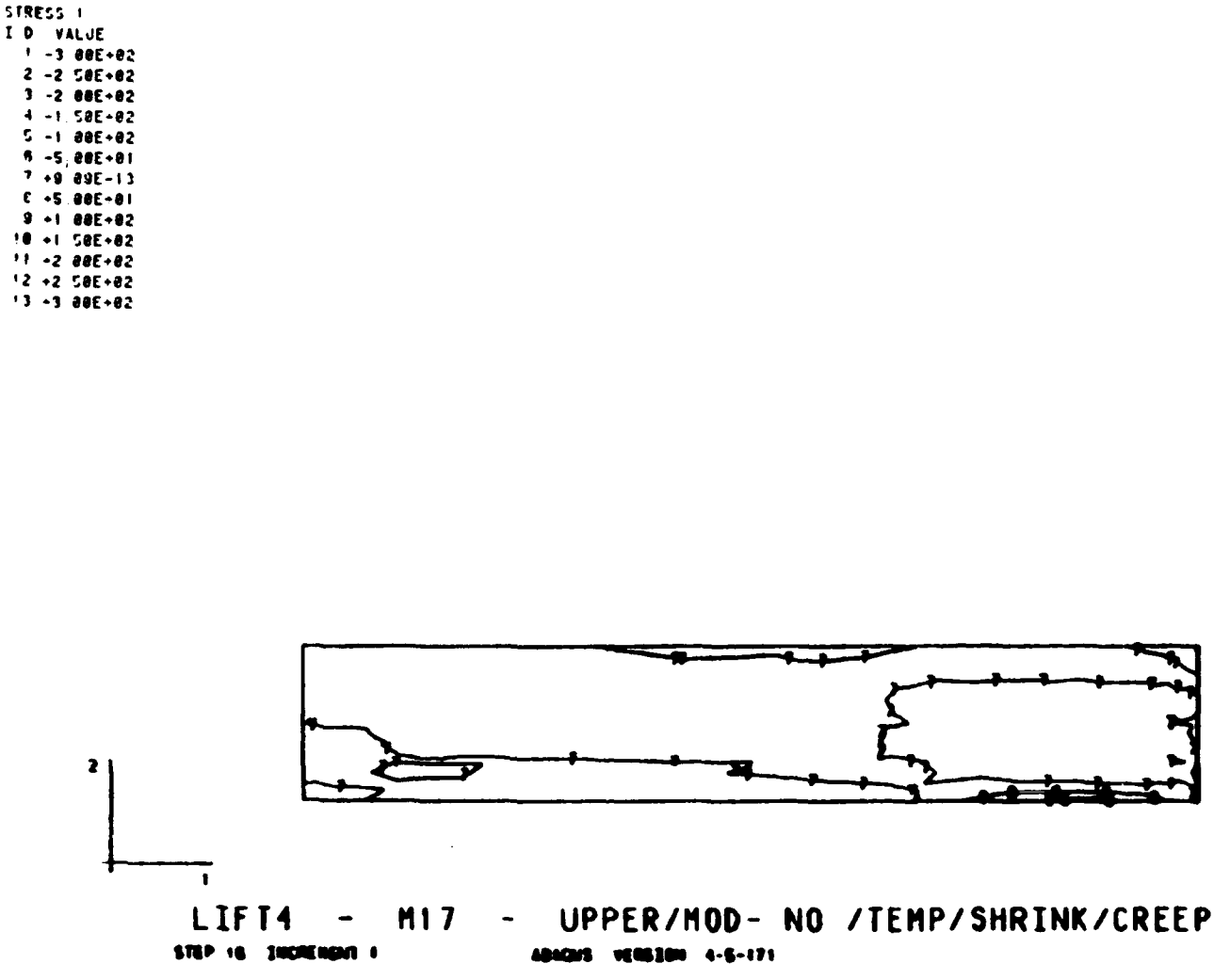

Figure 34a - Horizontal stress contours in L-17,
5 days after lift 4 is placed,
Gravity loading only, No creep/shrinkage

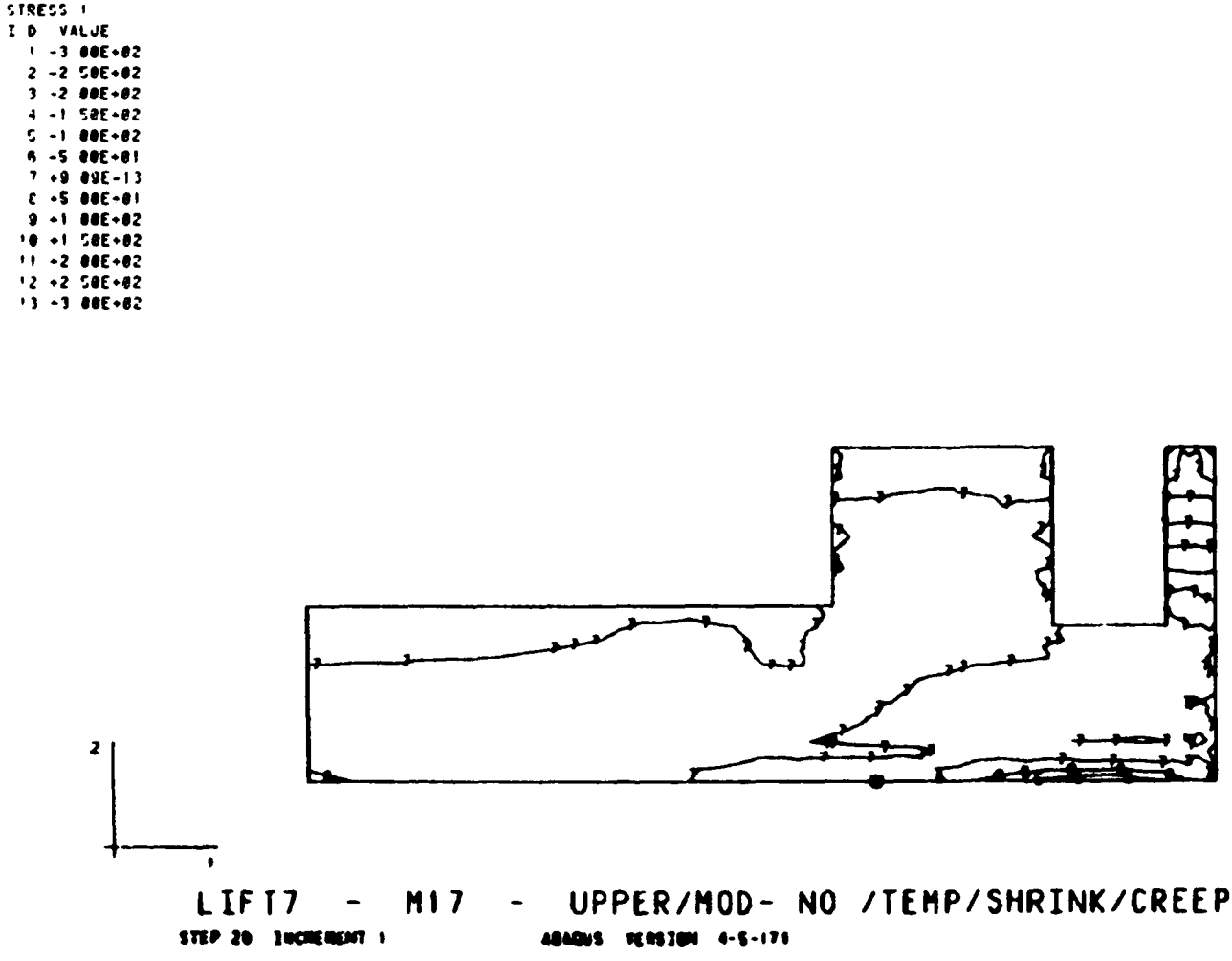

Figure 34b - Horizontal stress contours in L-17,
5 days after lift 7 is placed,
Gravity loading only, No creep/shrinkage

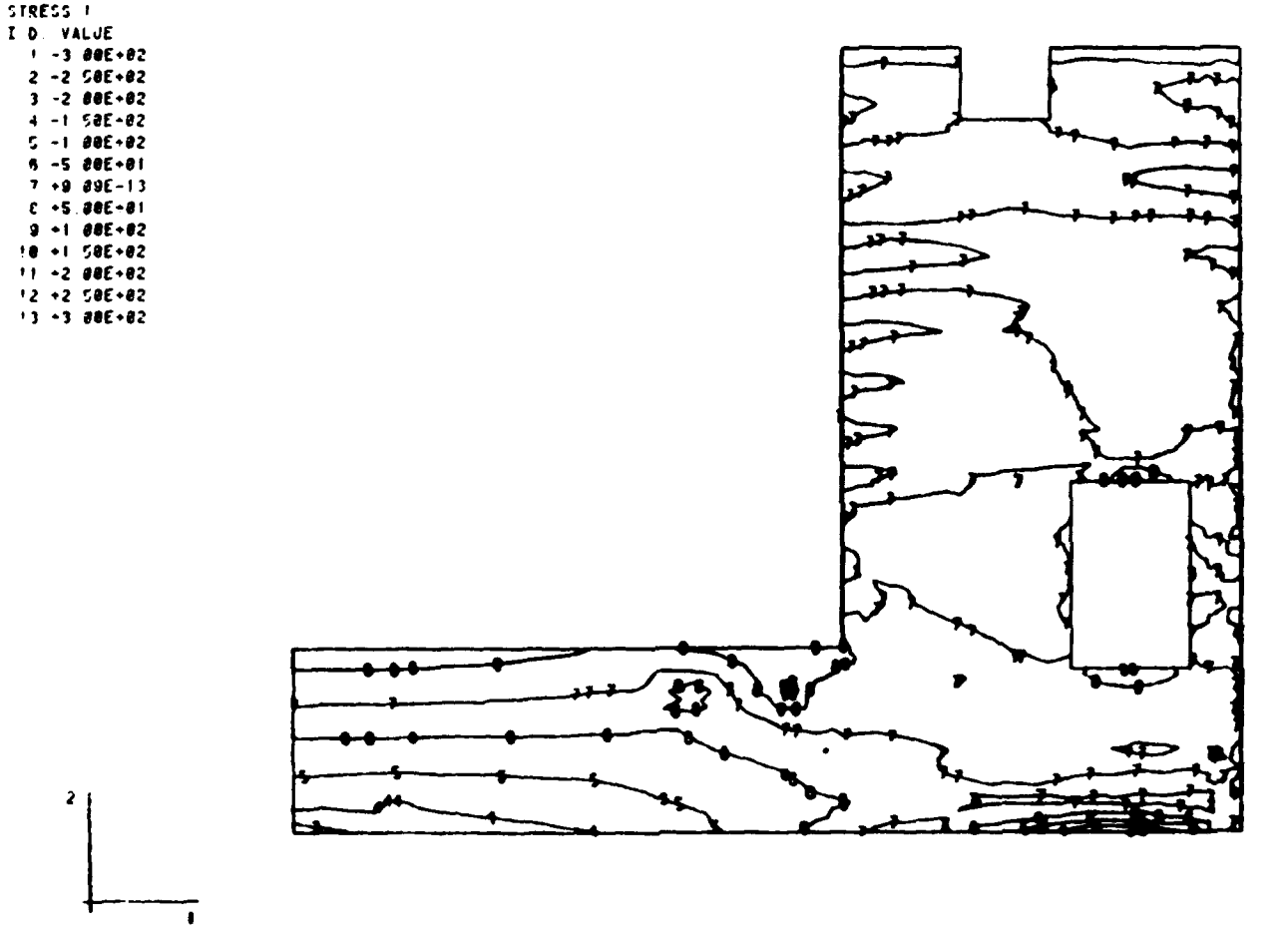

Figure 34c - Horizontal stress contours in L-17,
5 days after lift 16 is placed,
Gravity loading only, No creep/shrinkage

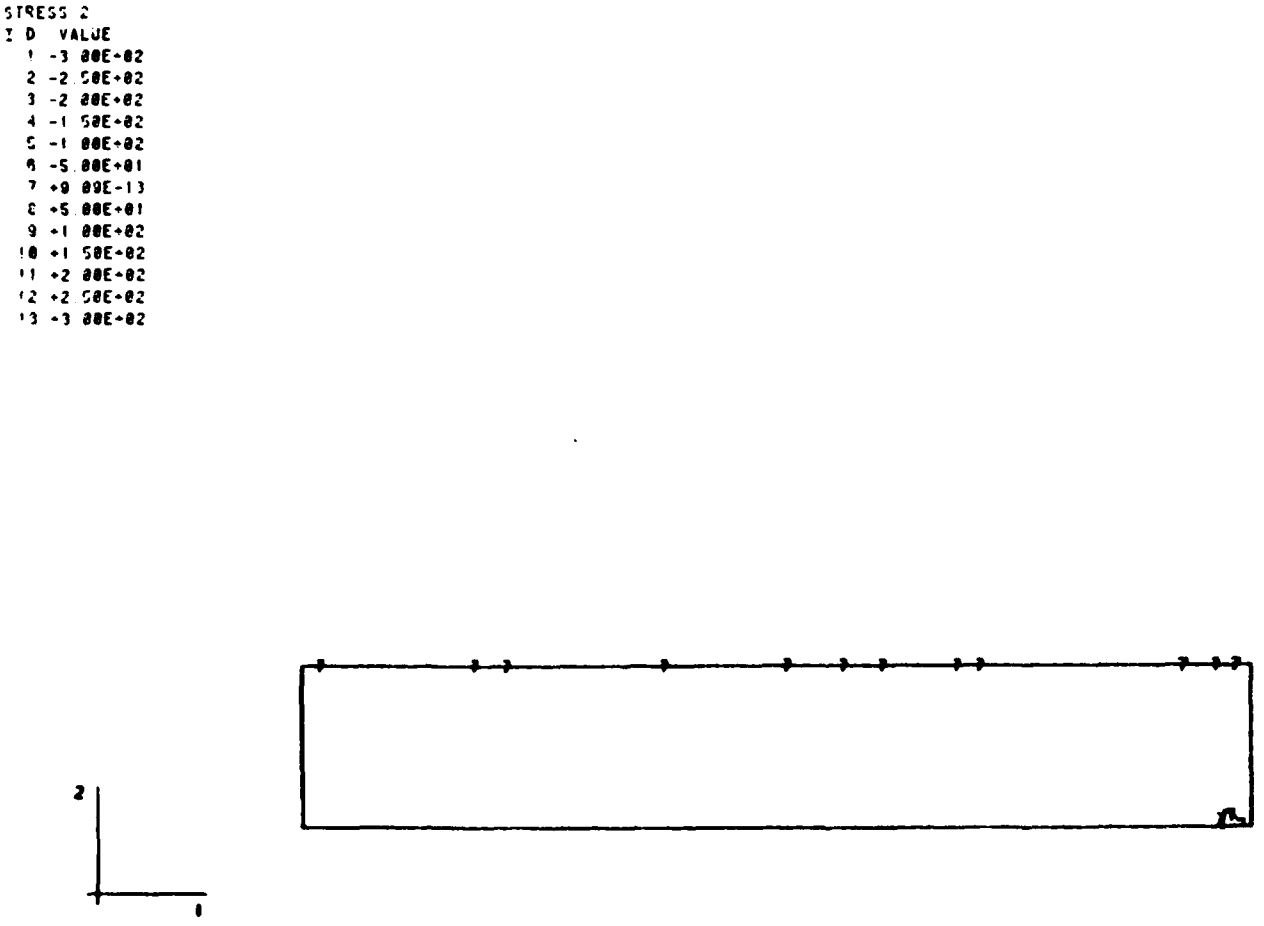

Figure 35a - Vertical stress contours in L-17,
5 days after lift 4 is placed,
Gravity loading only, No creep/shrinkage

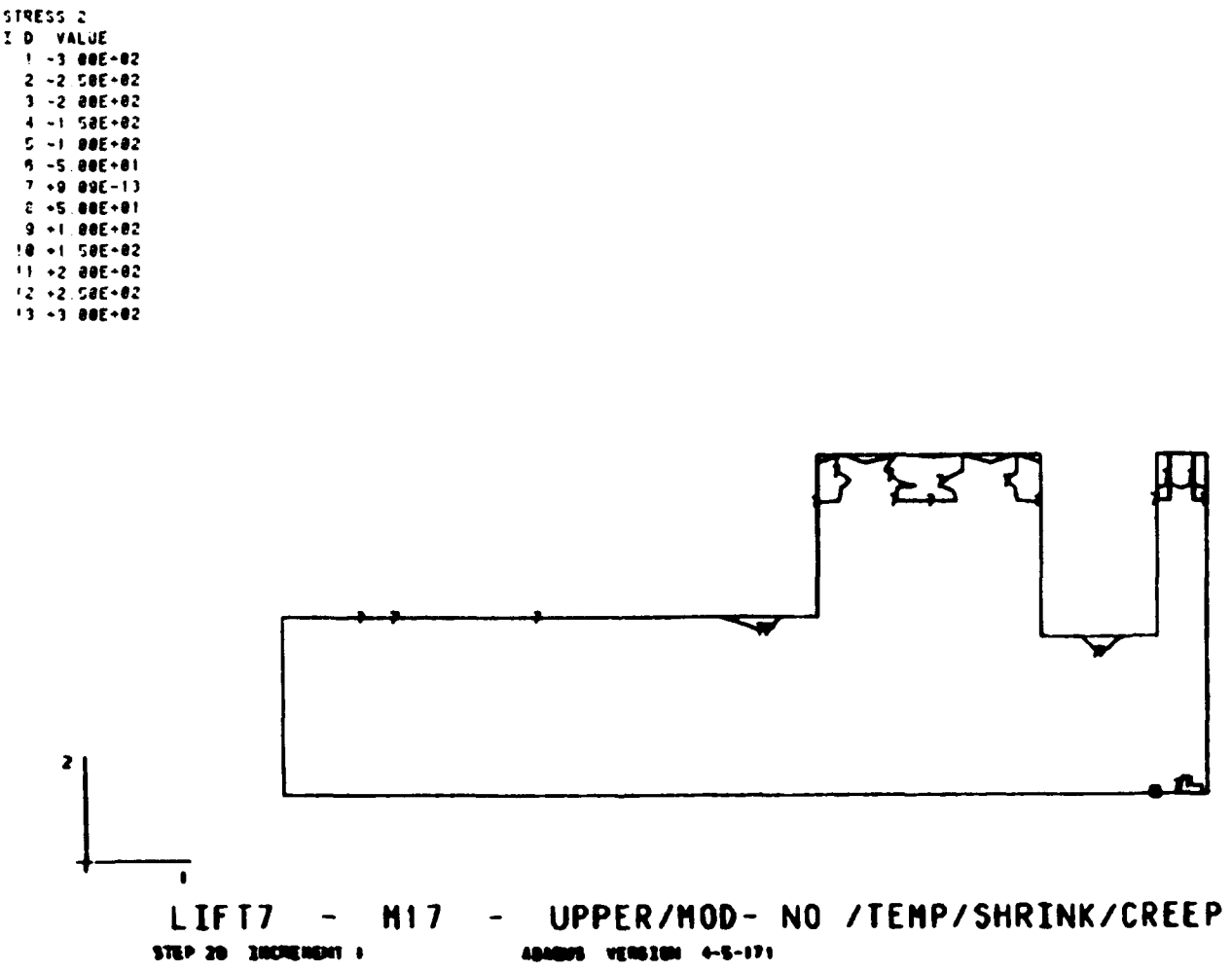

Figure 35b - Vertical stress contours in L-17,
5 days after lift 7 is placed,
Gravity loading only, No creep/shrinkage

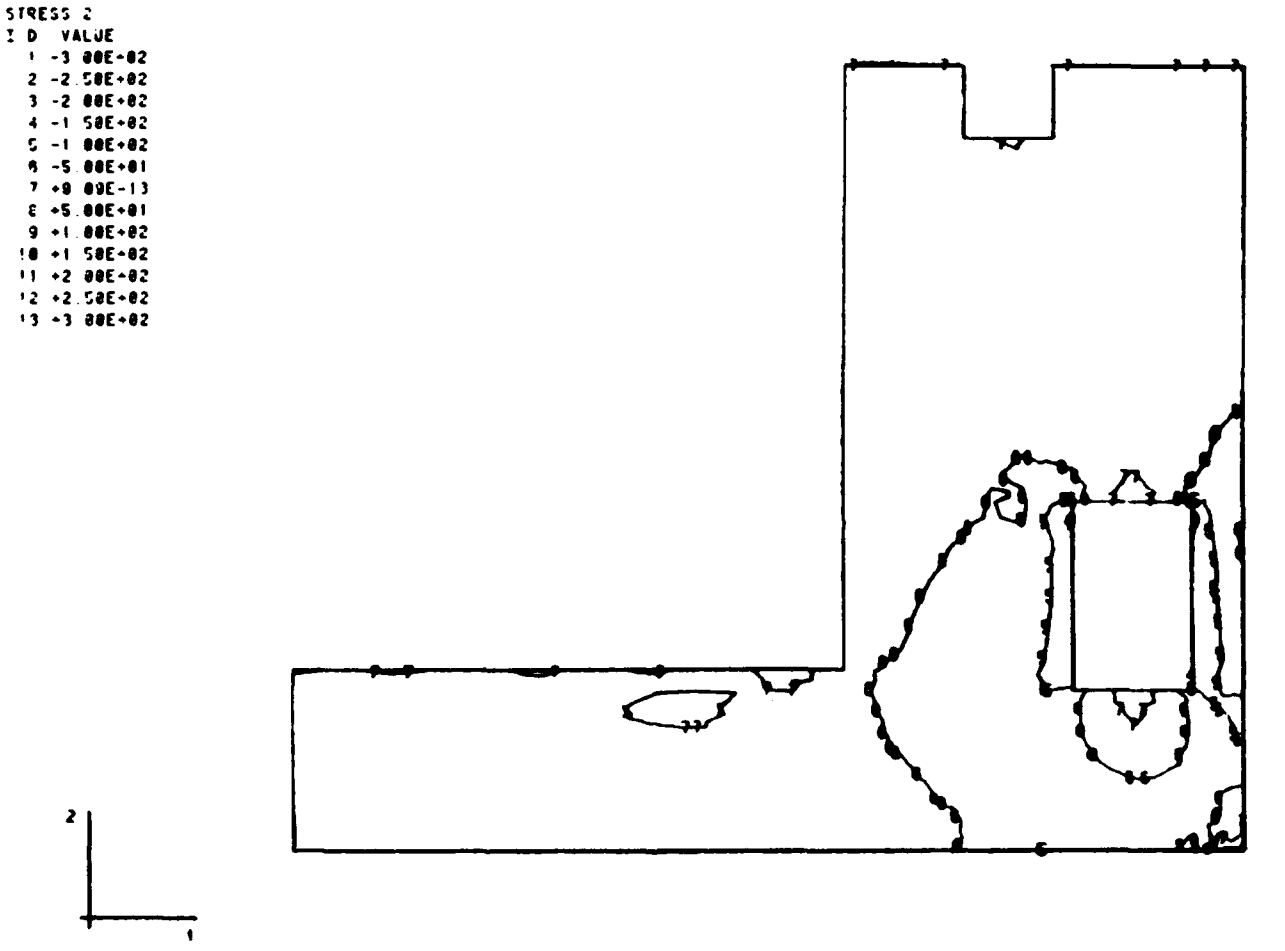

Figure 35c - Vertical stress contours in L-17,
5 days after lift 16 is placed,
Gravity loading only, No creep/shrinkage

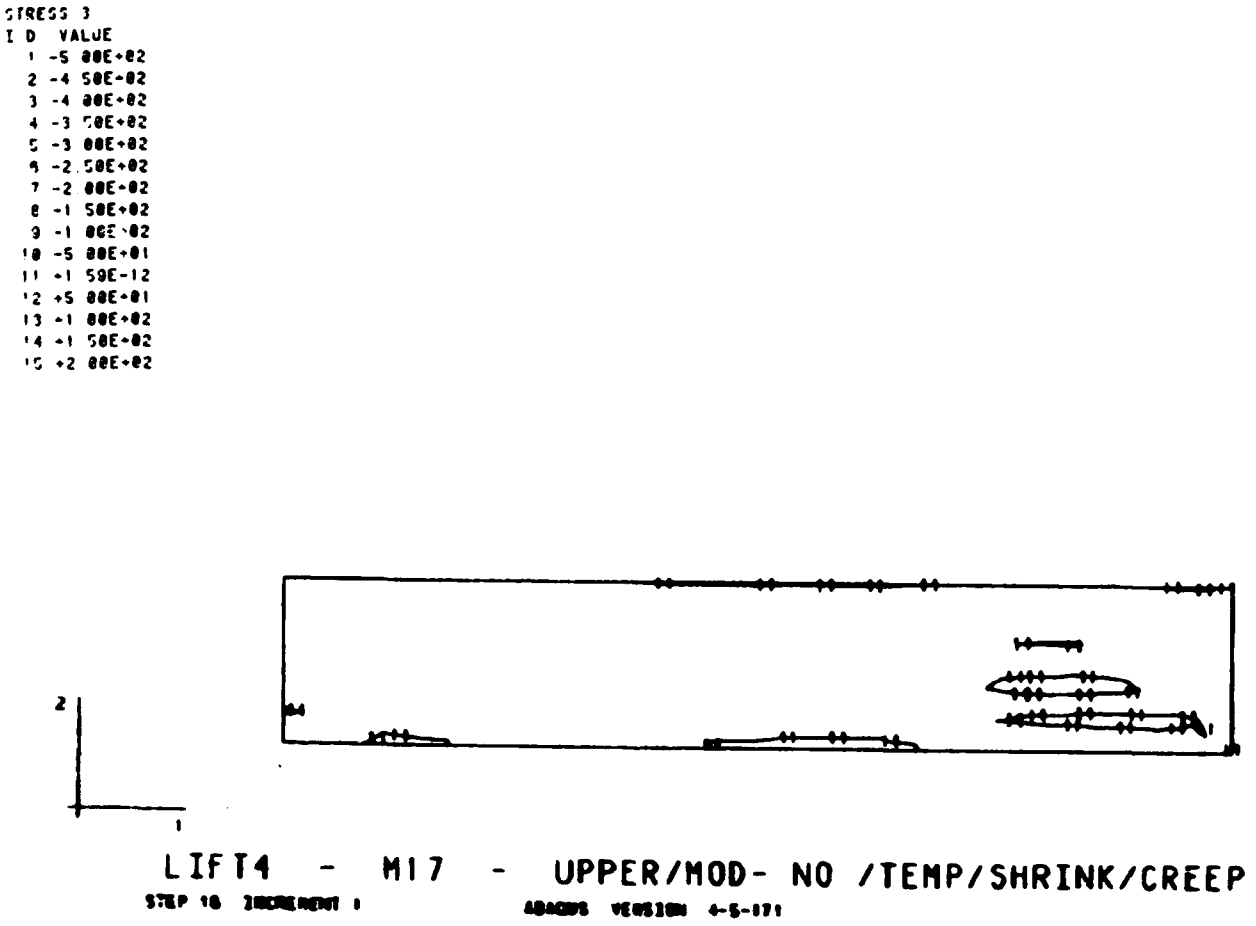

Figure 36a - Out-of-plane stress contours in L-17,
5 days after lift 4 is placed,
Gravity loading only, No creep/shrinkage

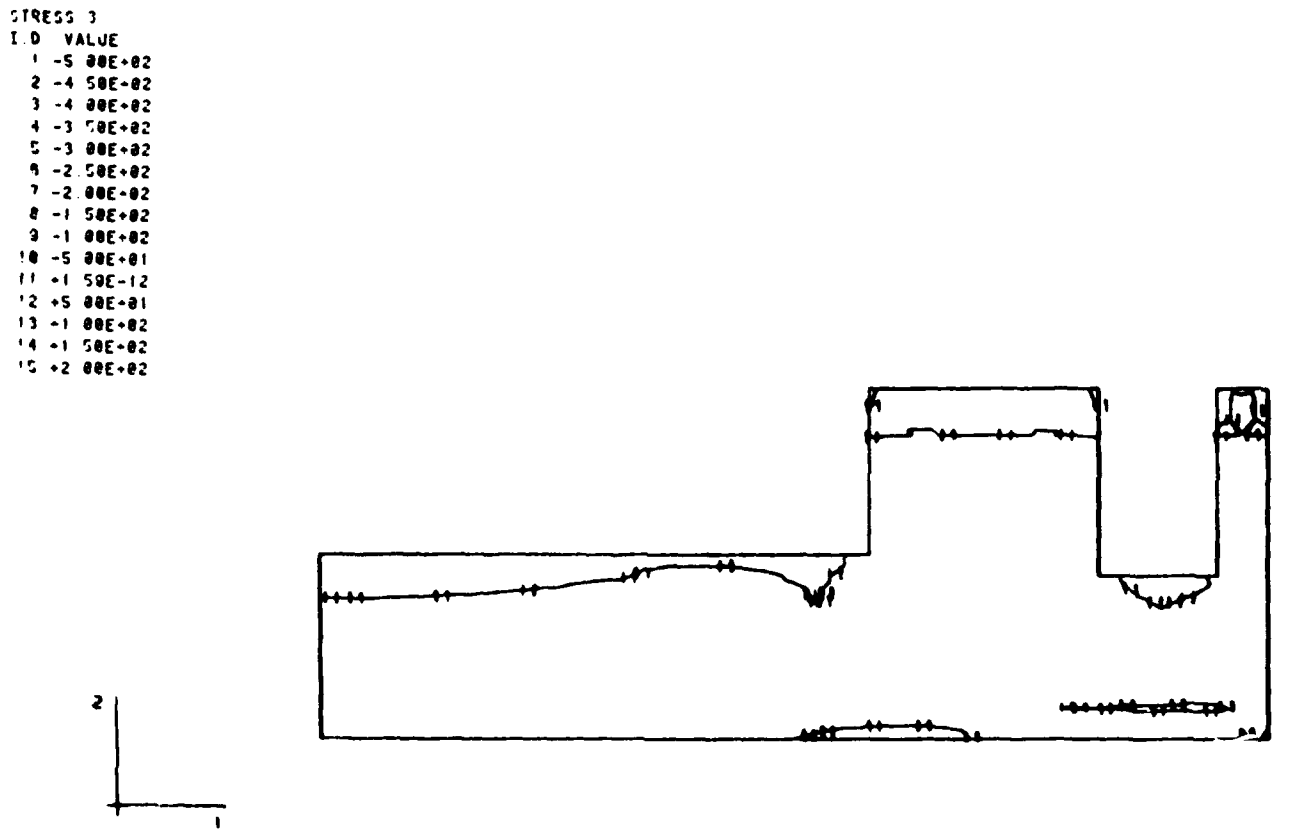

Figure 36b - Out-of-plane stress contours in L-17,
5 days after lift 7 is placed,
Gravity loading only, No creep/shrinkage

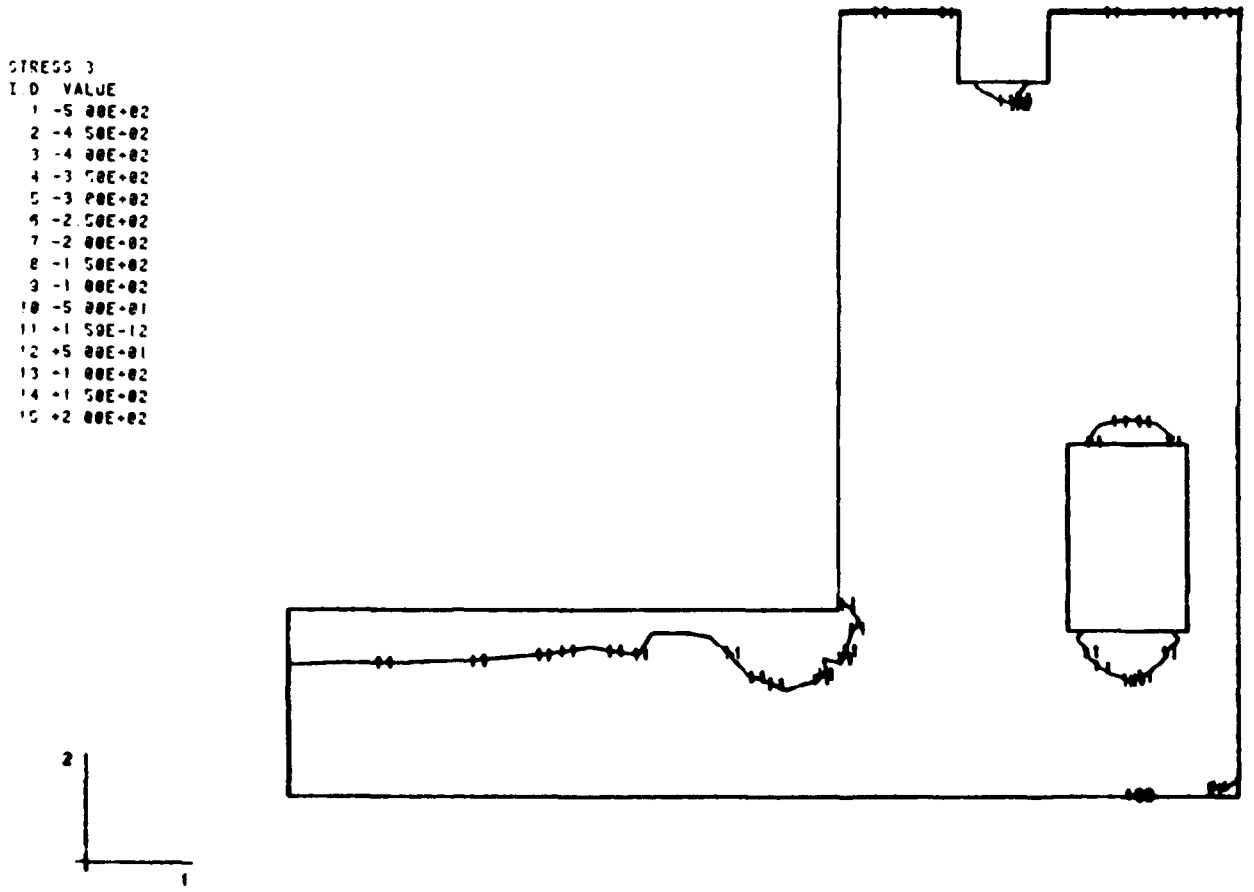

Figure 36c - Out-of-plane stress contours in L-17,
5 days after lift 16 is placed,
Gravity loading only, No creep/shrinkage

MAX PRINCIPAL STRESS I D	VALUE
1	-1.00E+02
2	-5.00E+01
3	-4.54E-13
4	+5.00E+01
5	+1.00E+02
6	+1.50E+02
7	+2.00E+02
8	+2.50E+02
9	+3.00E+02
10	+3.50E+02
11	+4.00E+02
12	+4.50E+02
13	+5.00E+02

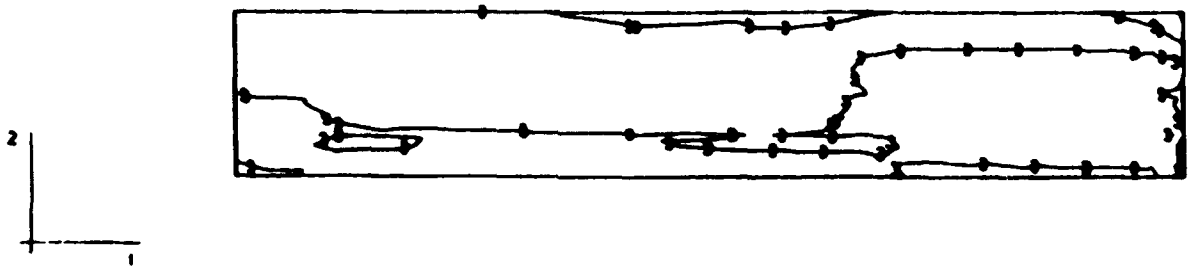

LIFT4 - M17 - UPPER/MOD- NO /TEMP/SHRINK/CREEP

STEP 18 INCREMENT 1 ABAQUS VERSION 4-5-179

Figure 37a - Max. Principal stress contours in L-17,
5 days after lift 4 is placed,
Gravity loading only, No creep/shrinkage

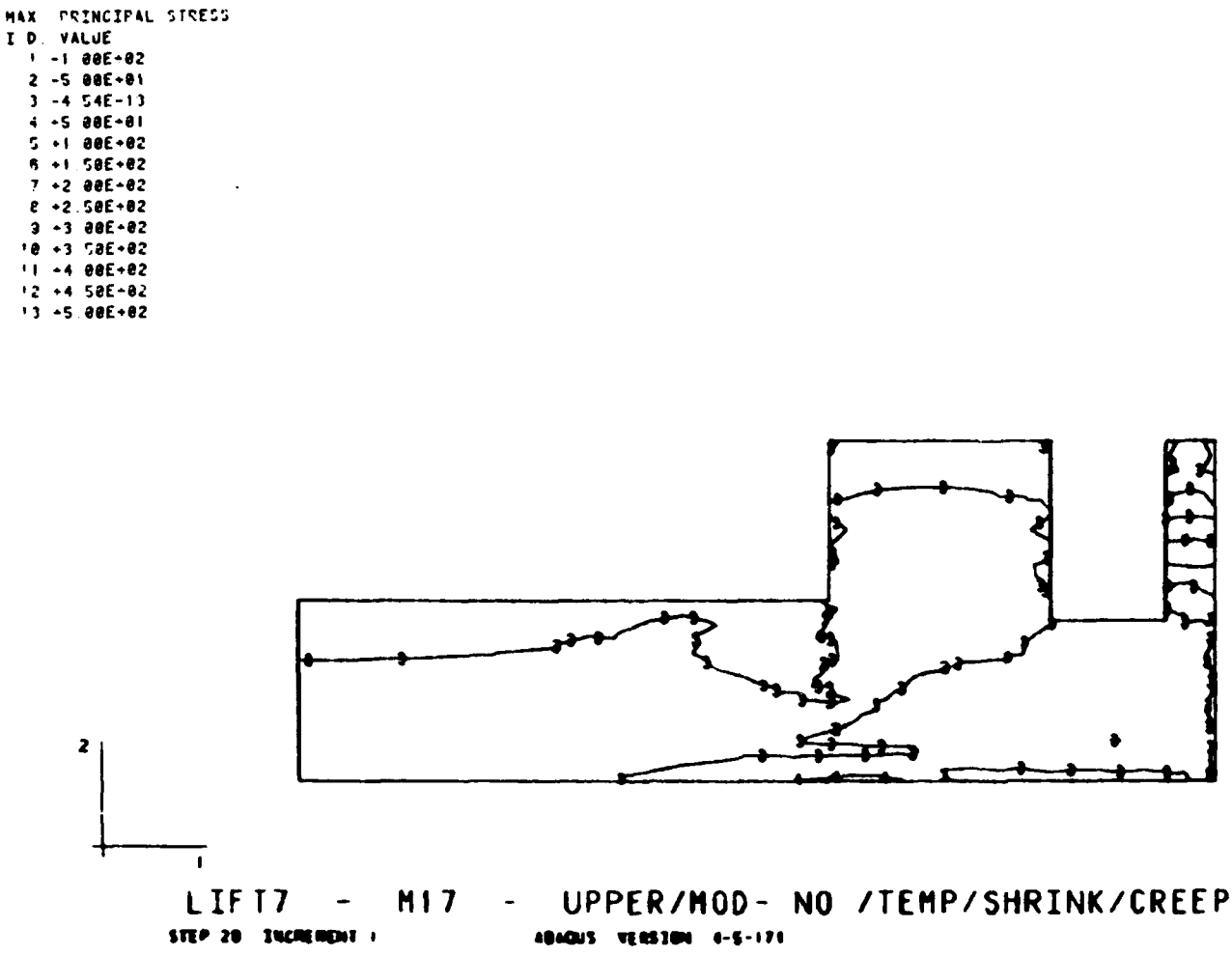

Figure 37b - Max. Principal stress contours in L-17,
5 days after lift 7 is placed,
Gravity loading only, No creep/shrinkage

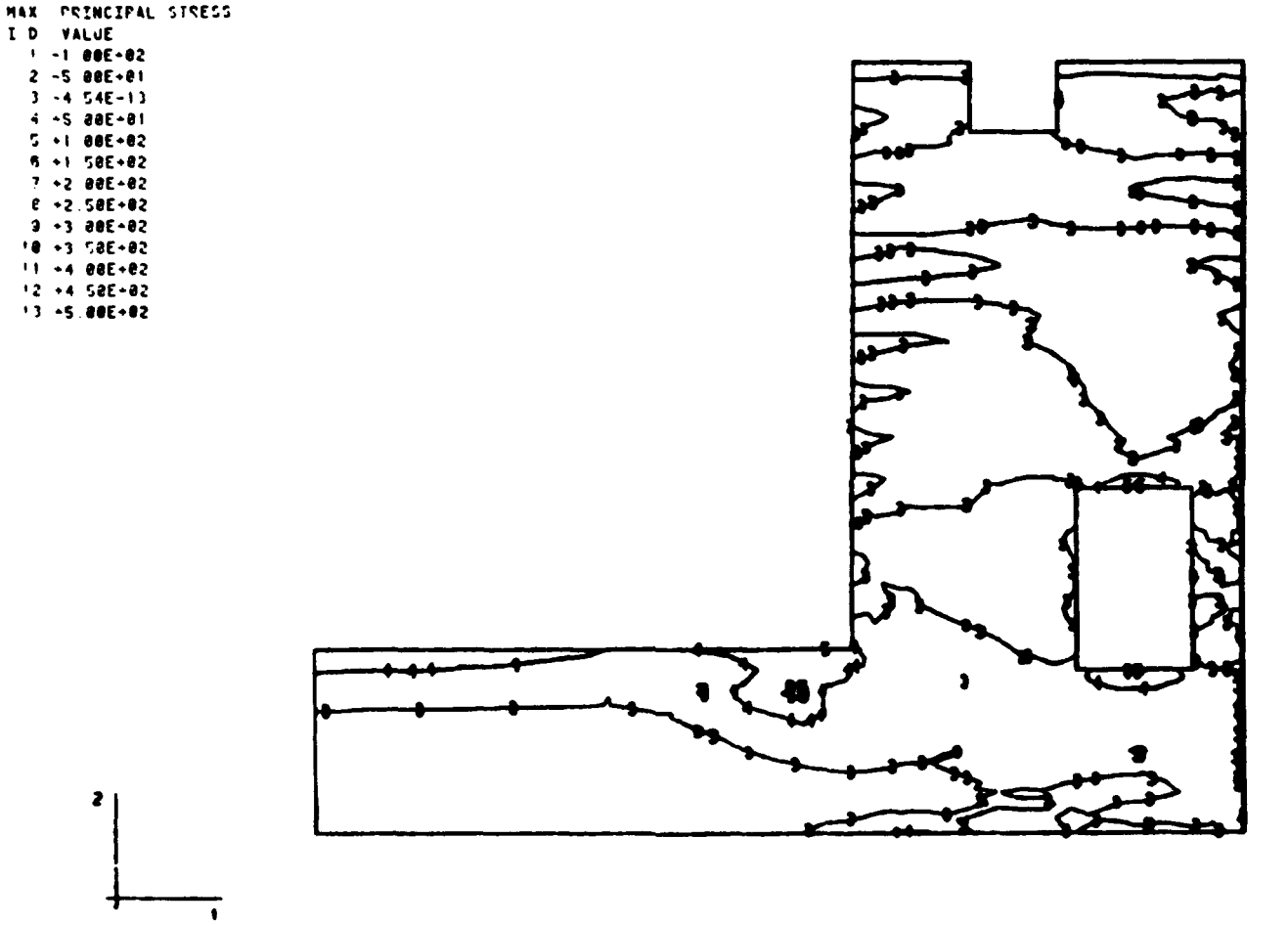

Figure 37c - Max. Principal stress contours in L-17,
5 days after lift 16 is placed,
Gravity loading only, No creep/shrinkage

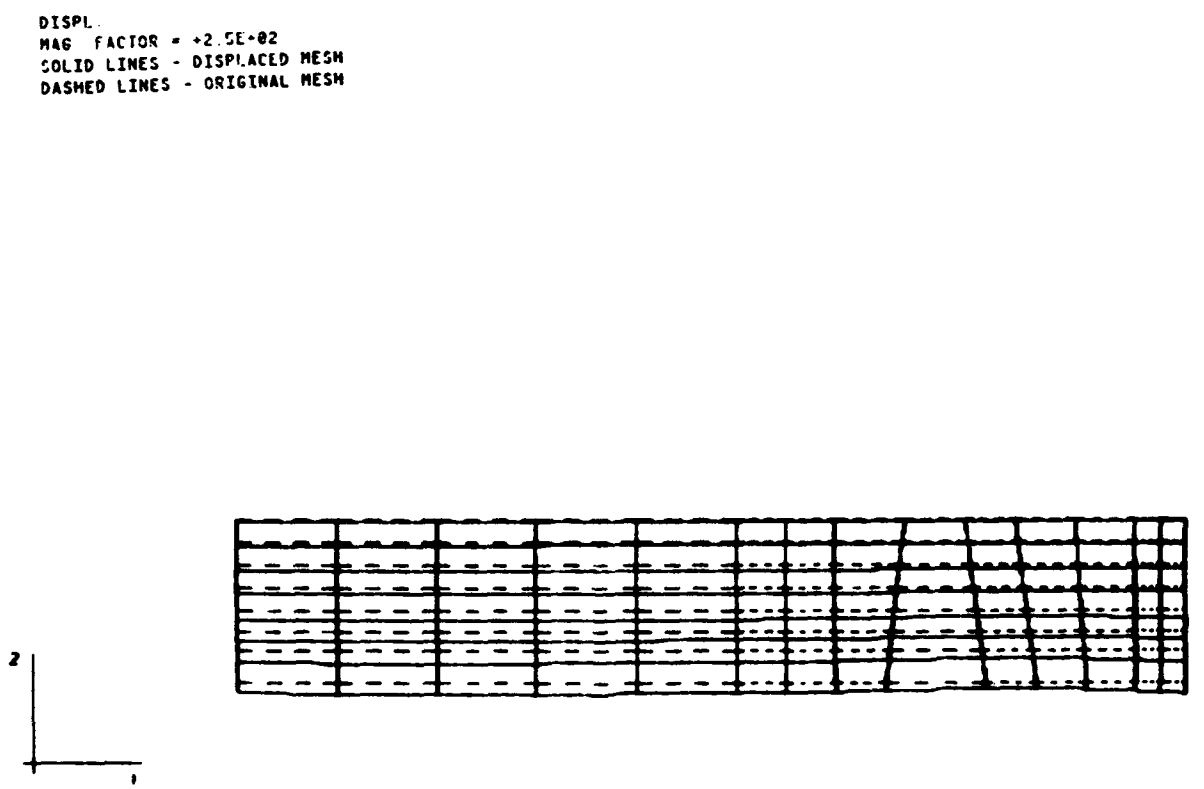

Figure 38a - Displaced shape of L-17, 5 days after lift 4 is placed, Gravity loading only, No creep/shrinkage

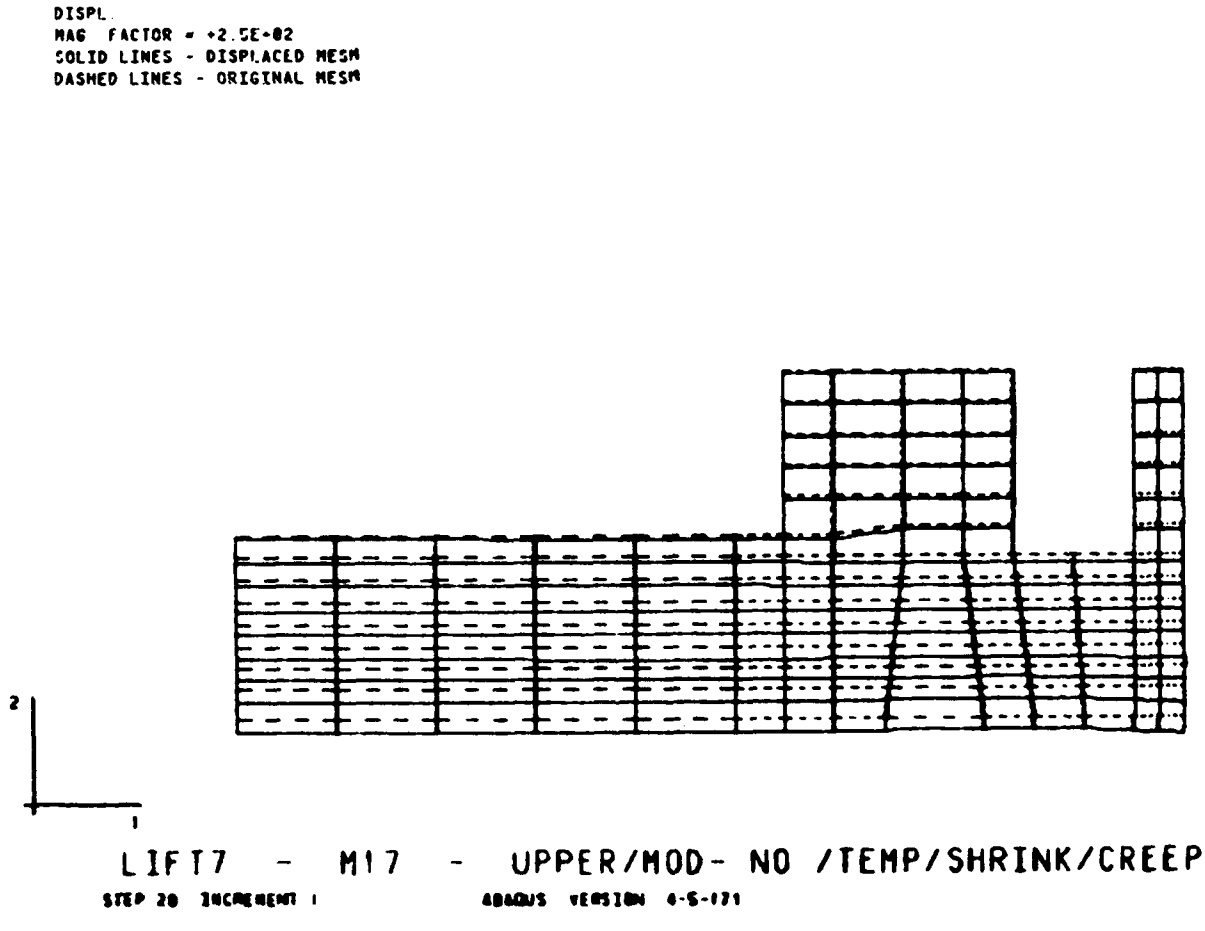

Figure 38b - Displaced shape of L-17, 5 days after lift 7 is placed, Gravity loading only, No creep/shrinkage

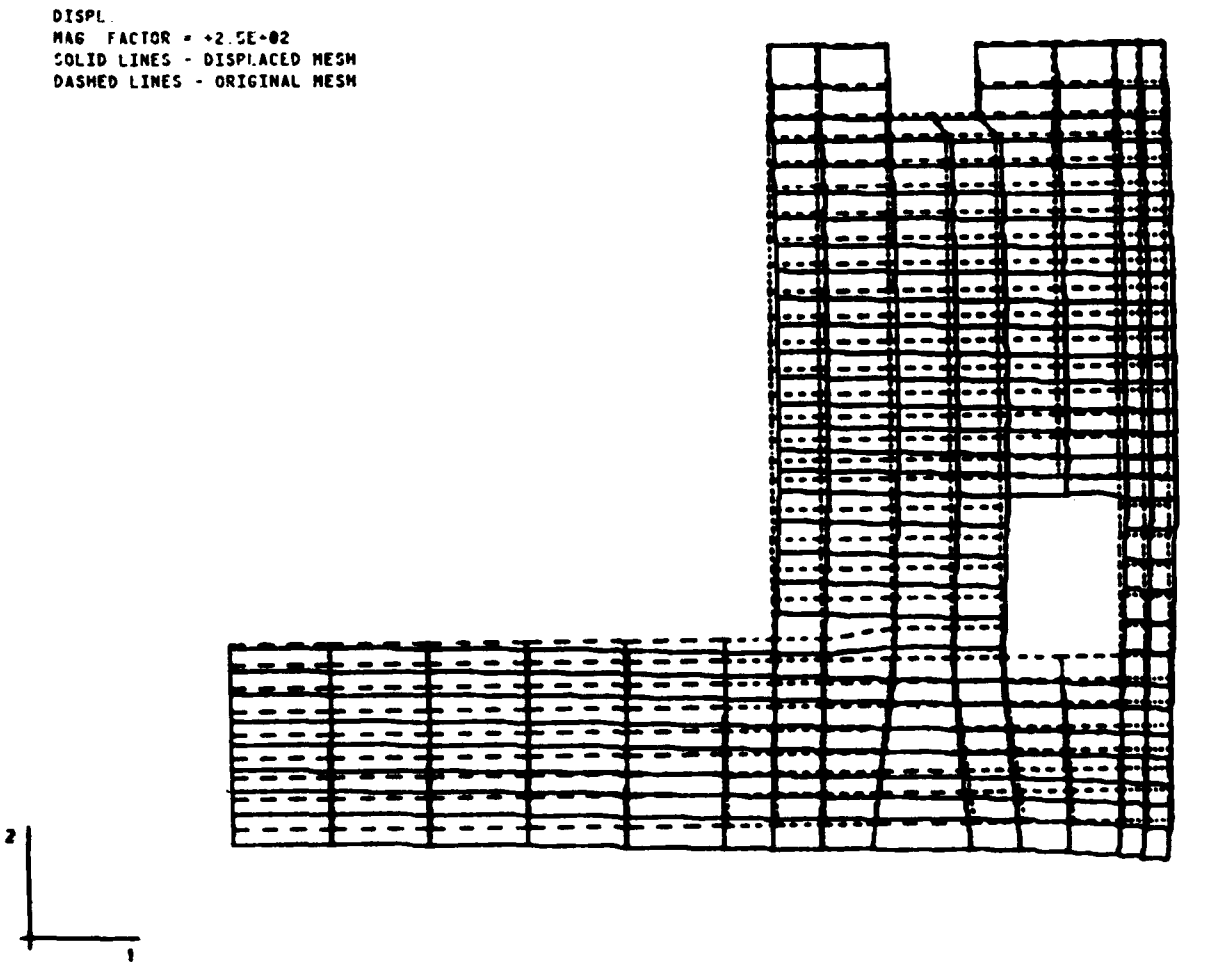

Figure 38c - Displaced shape of L-17, 5 days after lift 16 is placed, Gravity loading only, No creep/shrinkage

STRESS 1

I D	VALUE
1	-3 00E+02
2	-2 50E+02
3	-2 00E+02
4	-1 50E+02
5	-1 00E+02
6	-5 00E+01
7	+9 09E-13
8	+5 00E+01
9	+1 00E+02
10	+1 50E+02
11	+2 00E+02
12	+2 50E+02
13	+3 00E+02

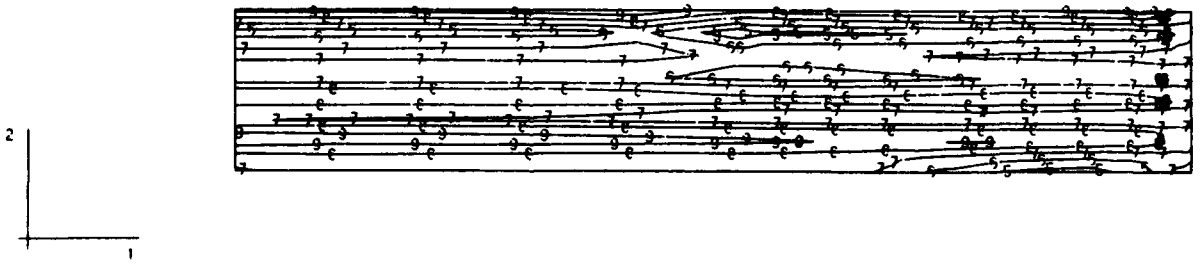

LIFT4 - M17 - UPPER/ADIABATIC/MOD/SHRINK/CREEP

STEP 16 INCREMENT 1 ABAQUS VERSION 4-5-171

Figure 39a - Horizontal stress contours in L-17, 5 days after lift 4 is placed, Gravity & thermal loadings, Upper creep/shrinkage

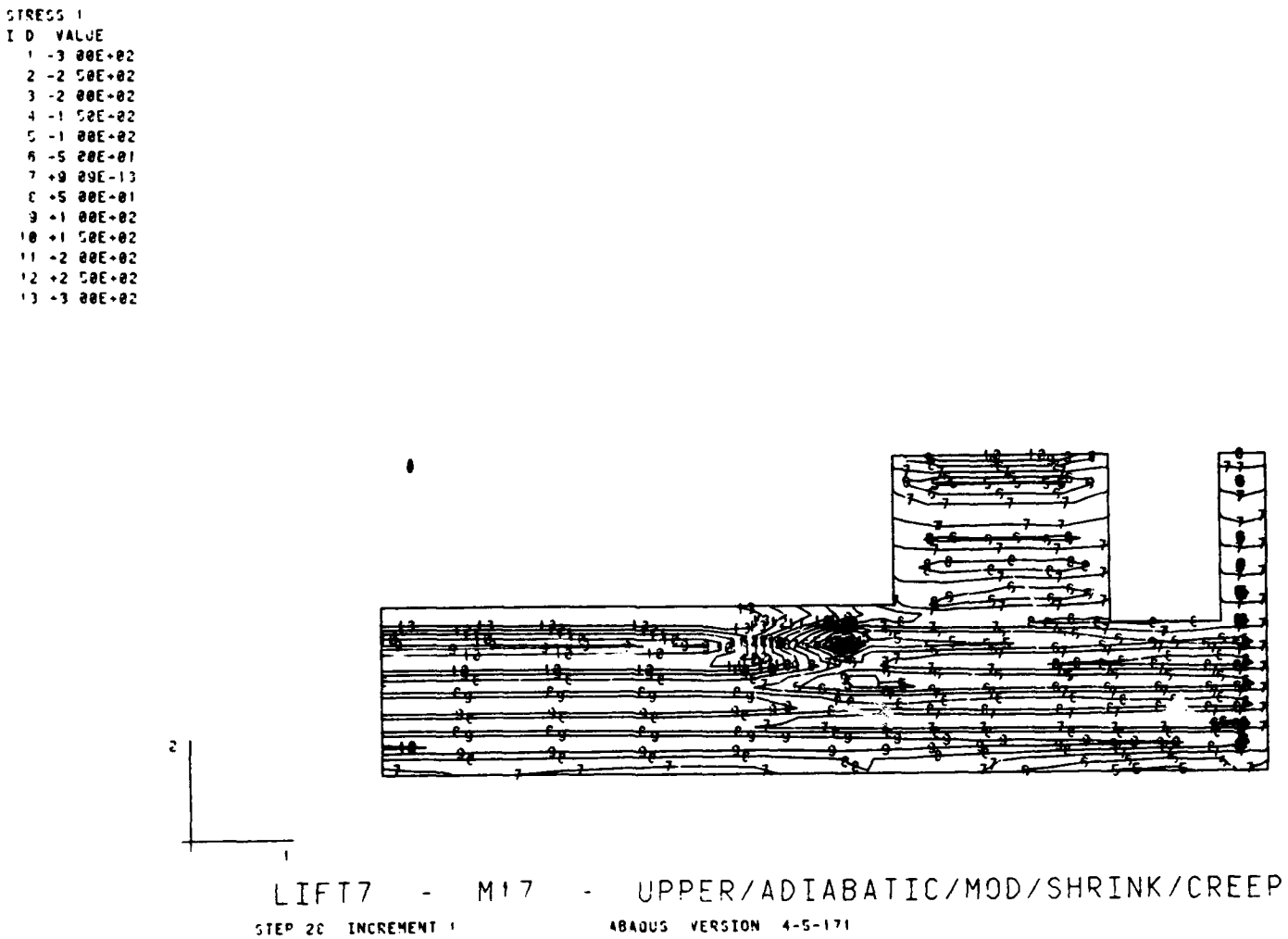

**Figure 39b - Horizontal stress contours in L-17,
5 days after lift 7 is placed,
Gravity & thermal loadings, Upper creep/shrinkage**

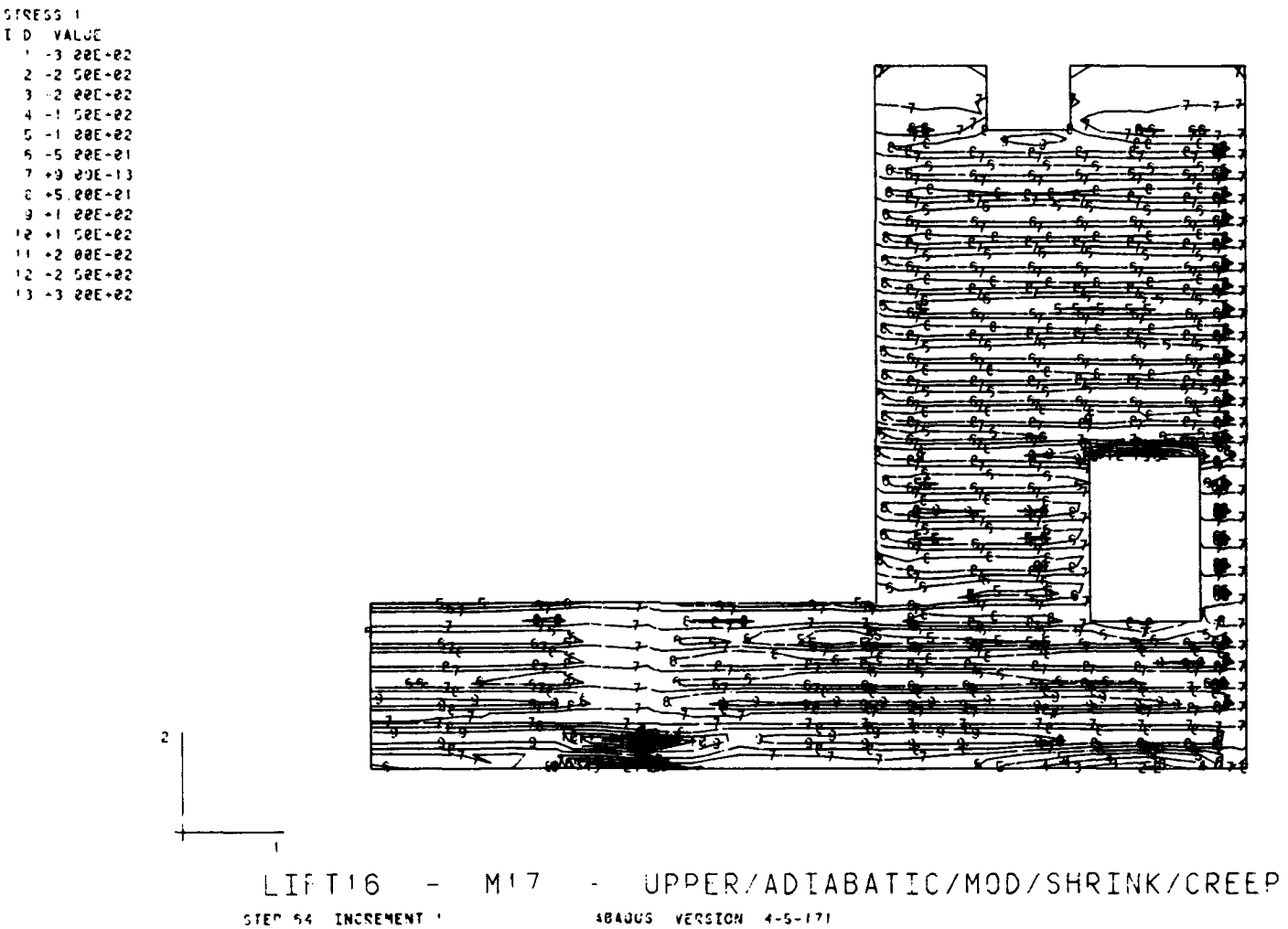

**Figure 39c - Horizontal stress contours in L-17,
5 days after lift 16 is placed,
Gravity & thermal loadings, Upper creep/shrinkage**

STRESS 2

I D	VALUE
1	-3 00E+02
2	-2 50E+02
3	-2 00E+02
4	-1 50E+02
5	-1 00E+02
6	-5 00E+01
7	+9 09E-13
8	+5 00E+01
9	+1 00E+02
10	+1 50E+02
11	+2 00E+02
12	+2 50E+02
13	+3 00E+02

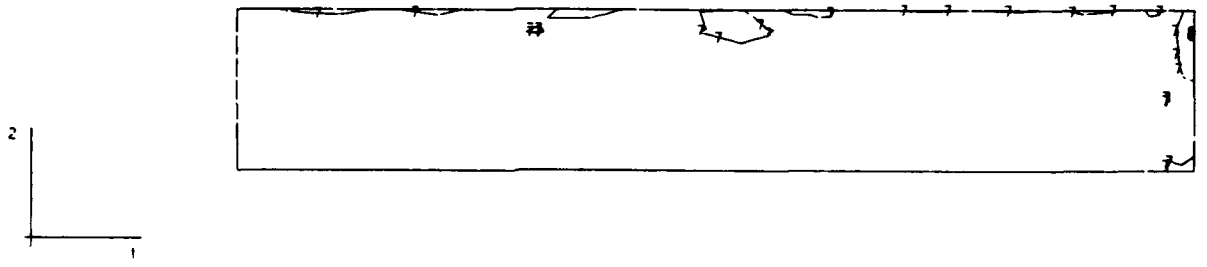

LIFT4 - M17 - UPPER/ADIABATIC/MOD/SHRINK/CREEP

STEP 15 INCREMENT 1 ABAQUS VERSION 4-5-171

Figure 40a - Vertical stress contours in L-17, 5 days after lift 4 is placed, Gravity & thermal loadings, Upper creep/shrinkage

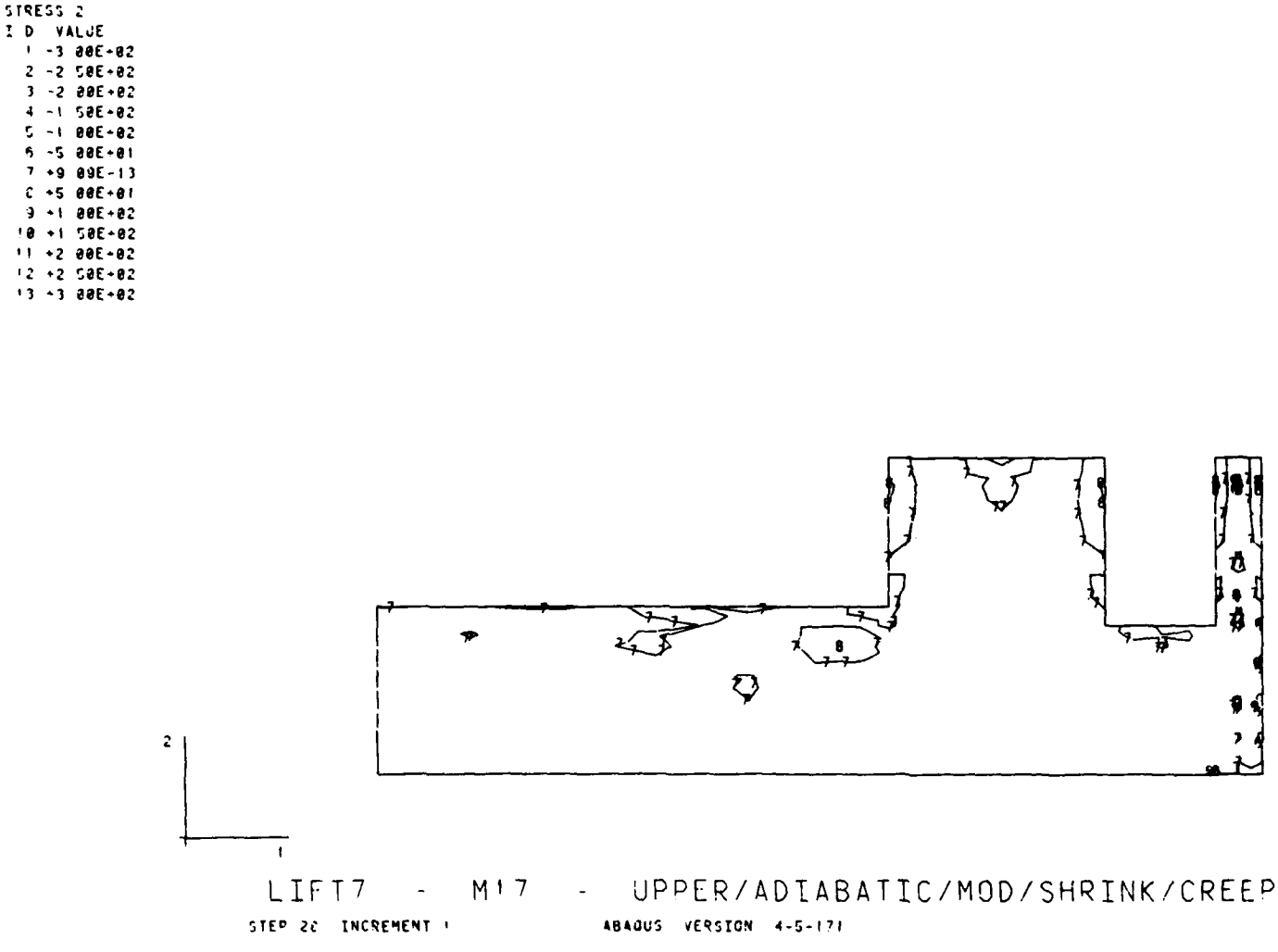

**Figure 40b - Vertical stress contours in L-17,
5 days after lift 7 is placed,
Gravity & thermal loadings, Upper creep/shrinkage**

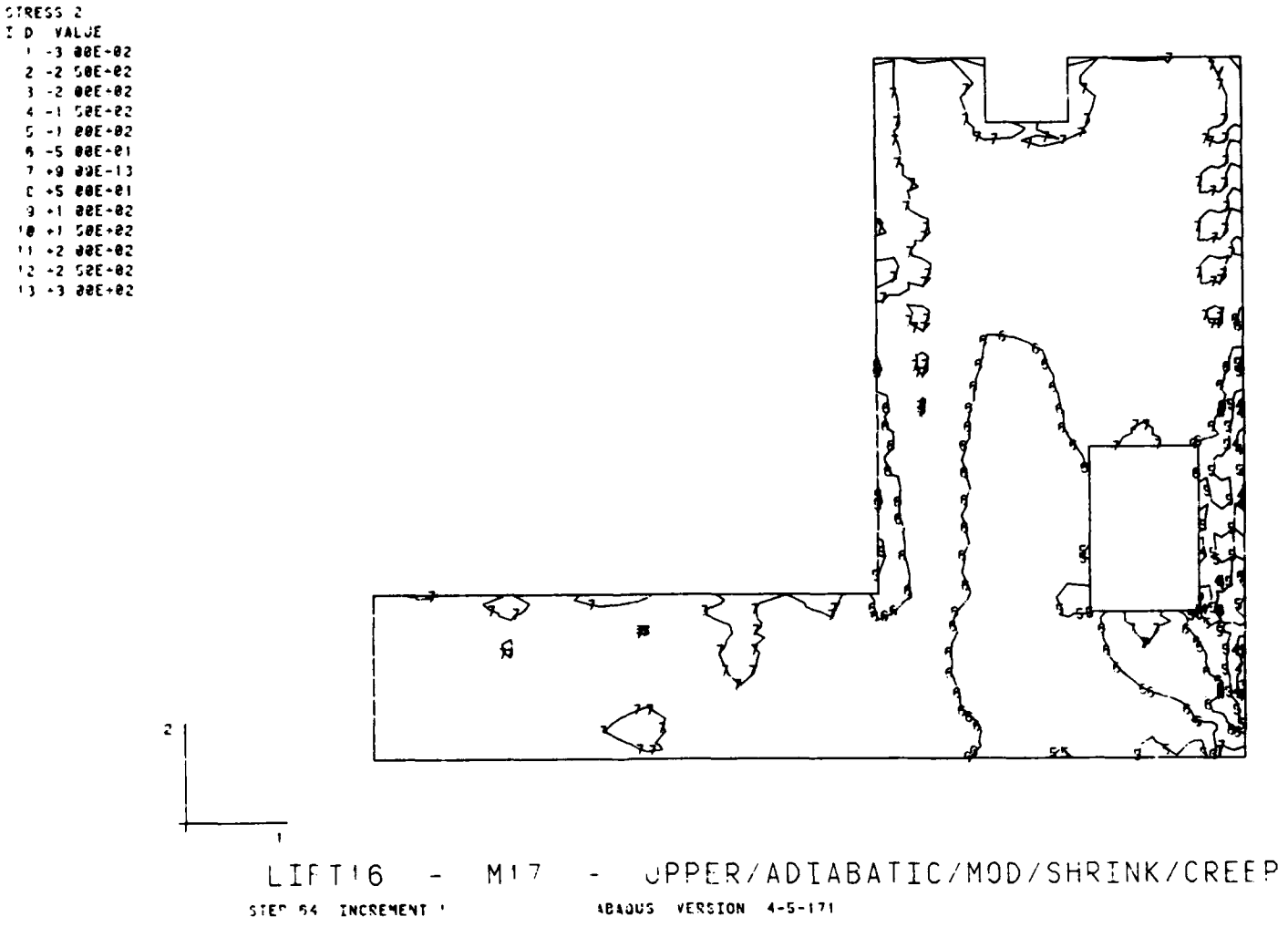

**Figure 40c - Vertical stress contours in L-17,
5 days after lift 16 is placed,
Gravity & thermal loadings, Upper creep/shrinkage**

STRESS 3

I D	VALUE
1	-5 00E+02
2	-4 50E+02
3	-4 00E+02
4	-3 50E+02
5	-3 00E+02
6	-2 50E+02
7	-2 00E+02
8	-1 50E+02
9	-1 00E+02
10	-5 00E+01
11	+1 59E-12
12	+5 00E+01
13	+1 00E+02
14	+1 50E+02
15	+2 00E+02
16	+2 50E+02
17	+3 00E+02
18	+3 50E+02
19	+4 00E+02
20	+4 50E+02

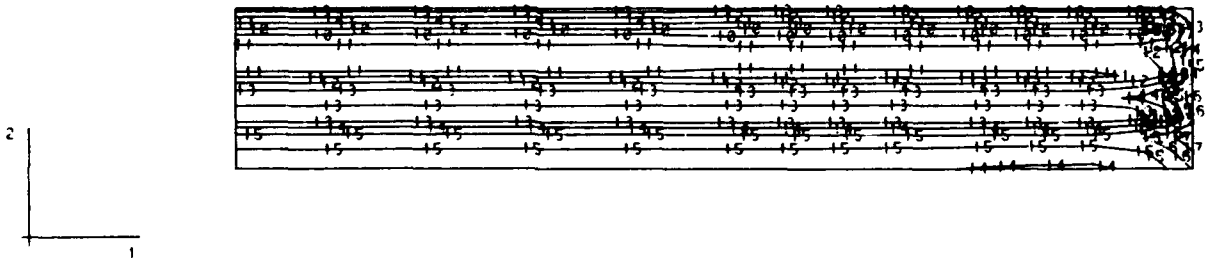

LIFT4 - M17 - UPPER/ADIABATIC/MOD/SHRINK/CREEP

STEP 15 INCREMENT 1 ABAQUS VERSION 4-5-171

Figure 41a - Out-of-plane stress contours in L-17, 5 days after lift 4 is placed, Gravity & thermal loadings, Upper creep/shrinkage

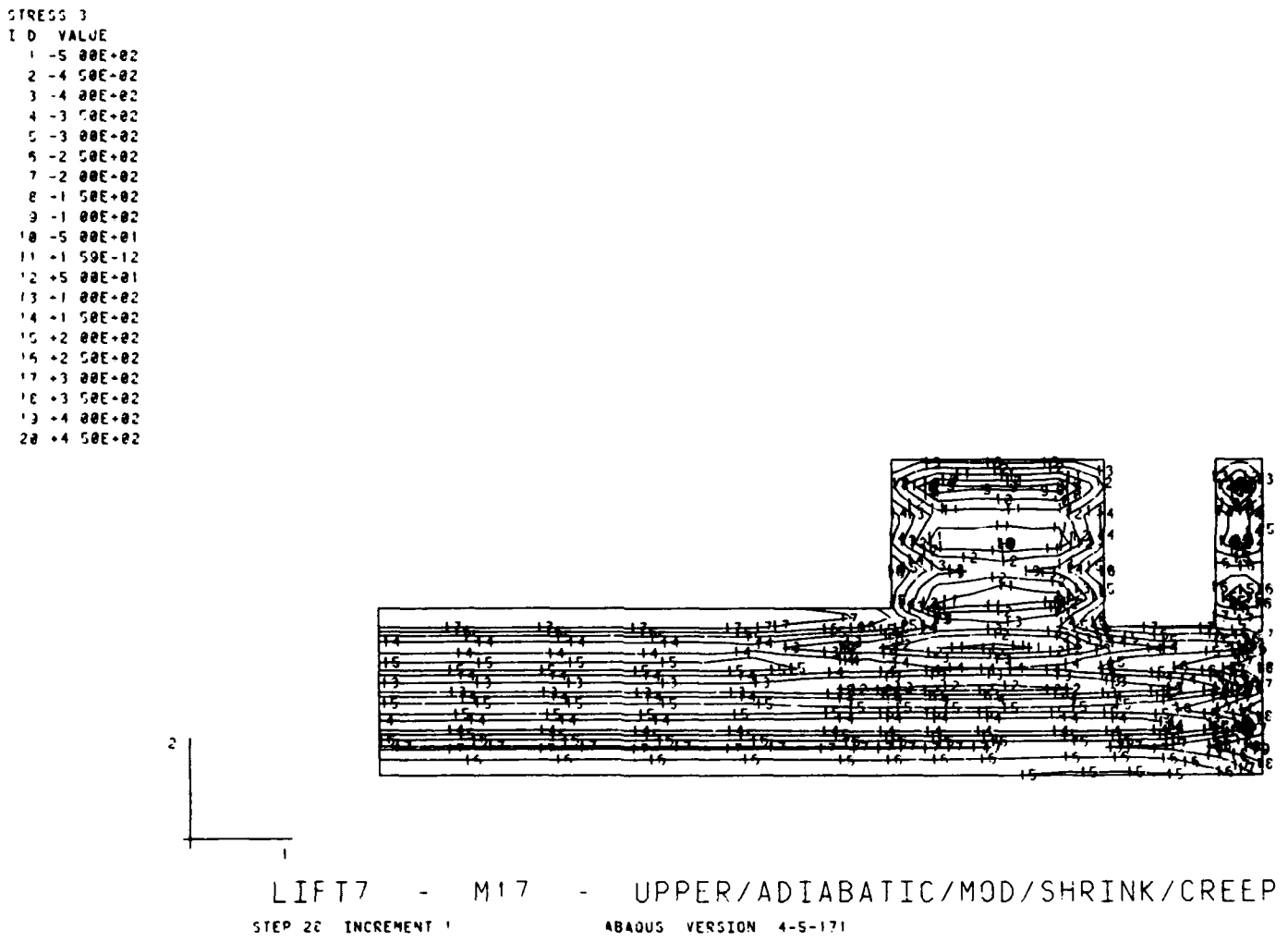

**Figure 41b - Out-of-plane stress contours in L-17,
5 days after lift 7 is placed,
Gravity & thermal loadings, Upper creep/shrinkage**

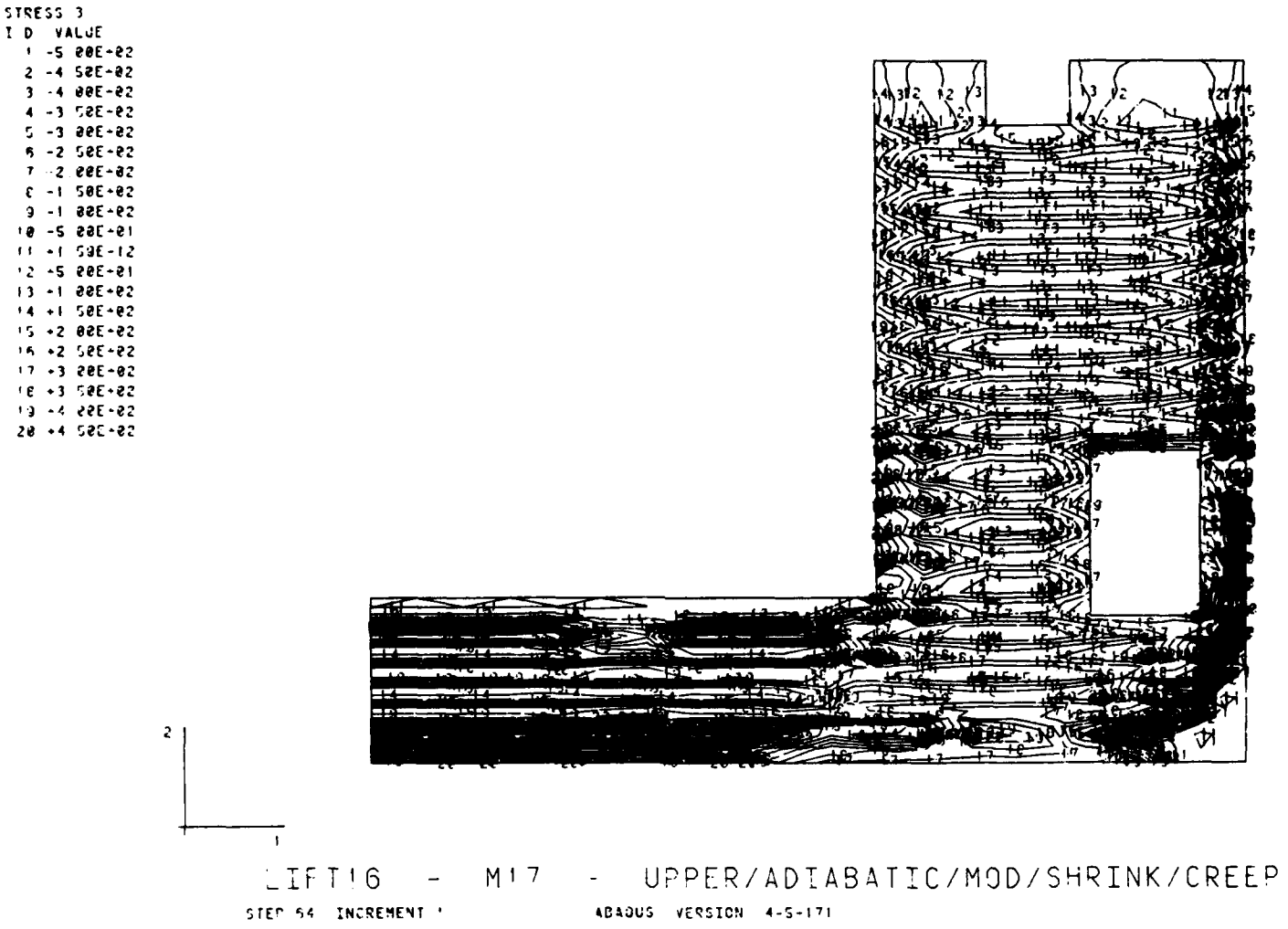

Figure 41c - Out-of-plane stress contours in L-17, 5 days after lift 16 is placed, Gravity & thermal loadings, Upper creep/shrinkage

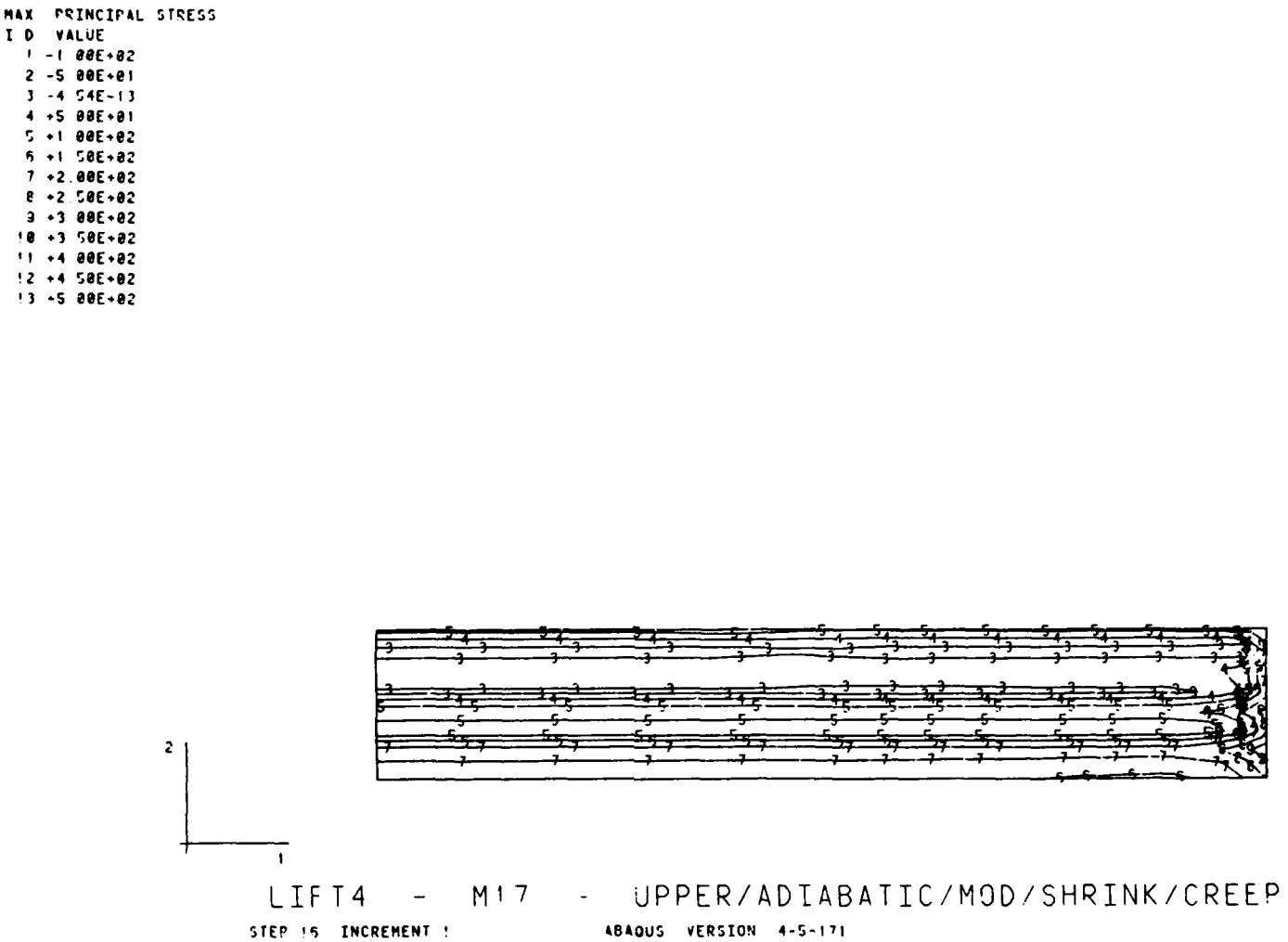

Figure 42a - Max. Principal stress contours in L-17, 5 days after lift 4 is placed, Gravity & thermal loadings, Upper creep/shrinkage

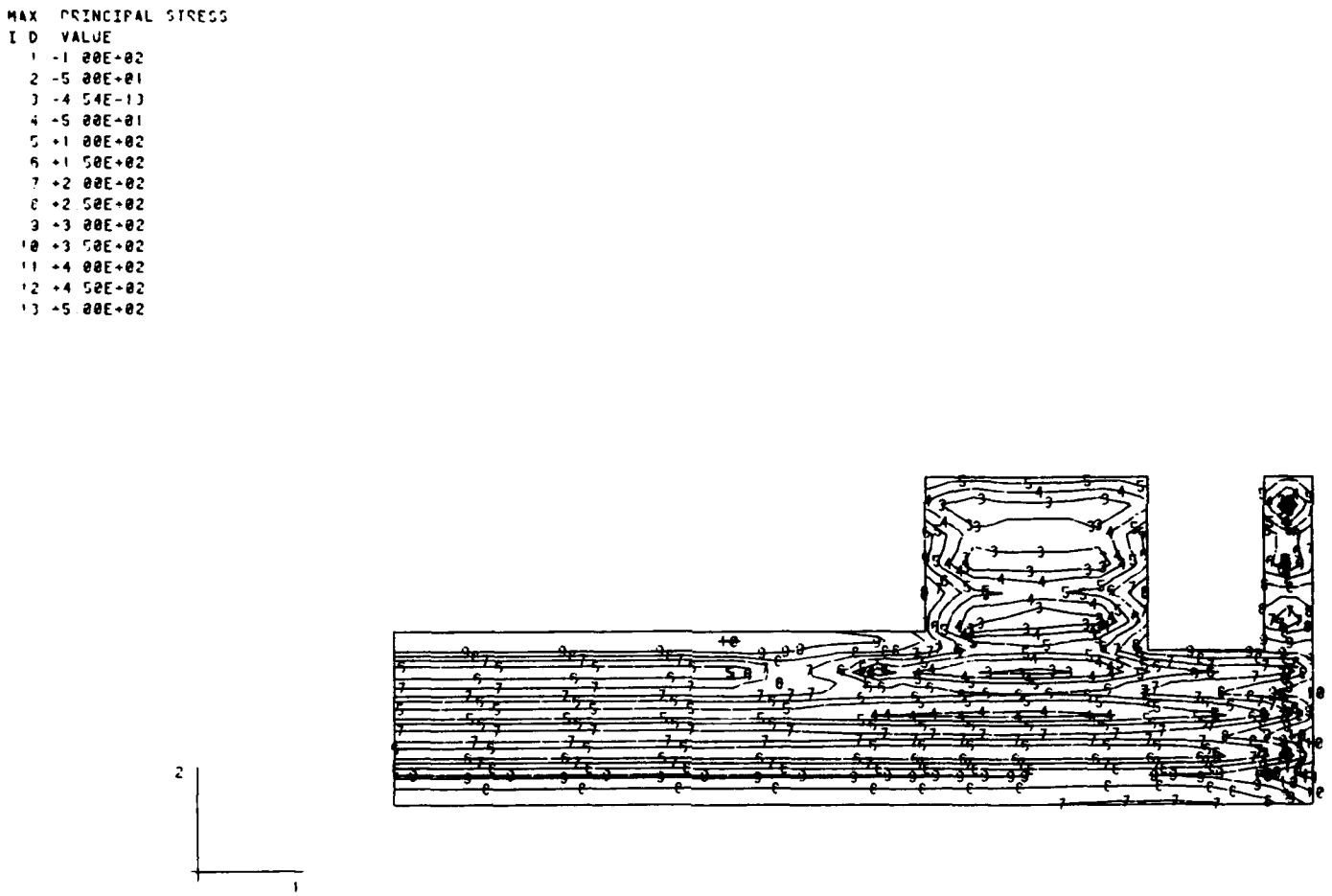

**Figure 42b - Max. Principal stress contours in L-17,
5 days after lift 7 is placed,
Gravity & thermal loadings, Upper creep/shrinkage**

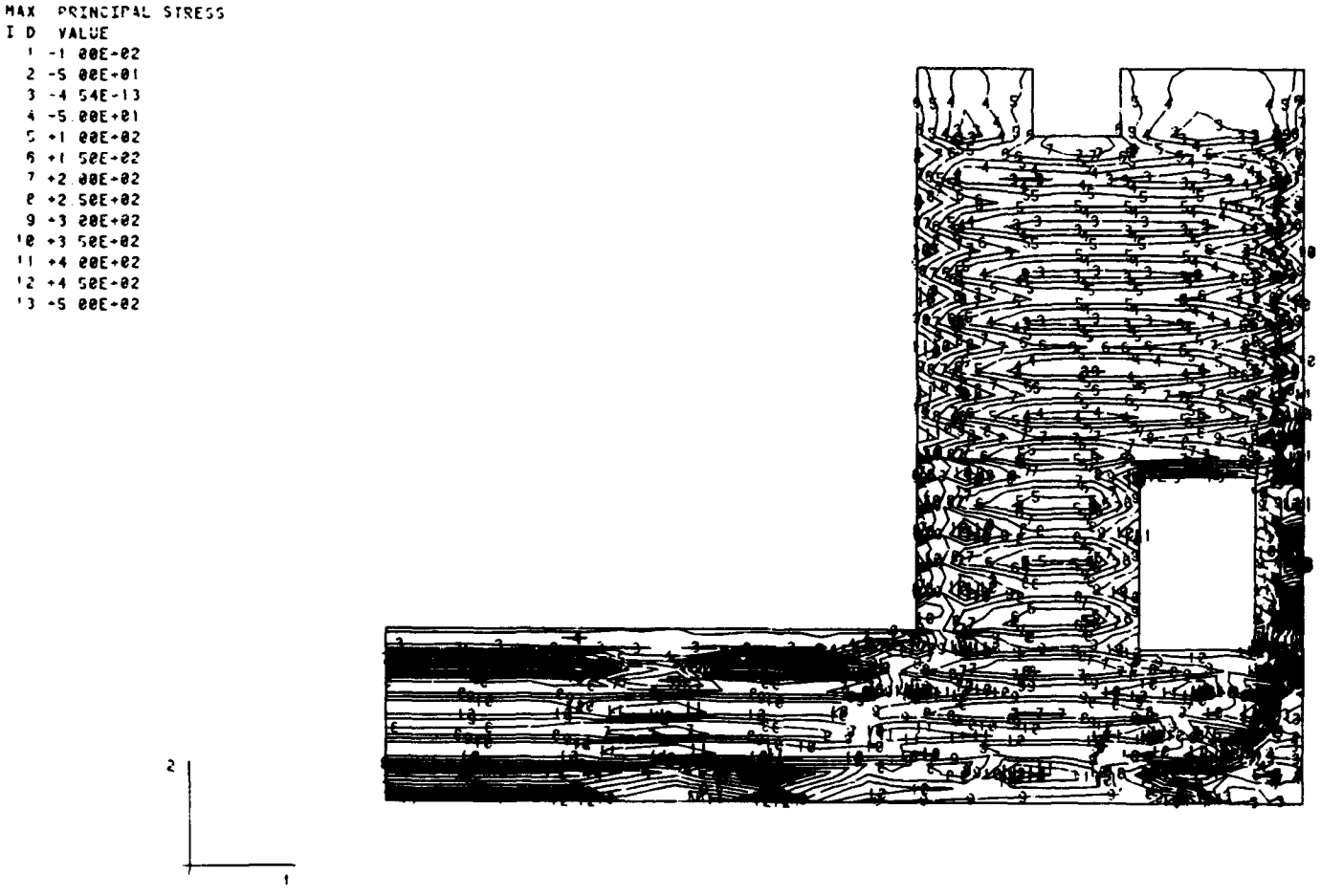

**Figure 42c - Max. Principal stress contours in L-17,
5 days after lift 16 is placed,
Gravity & thermal loadings, Upper creep/shrinkage**

DISPL
MAG FACTOR = +2.5E+02
SOLID LINES - DISPLACED MESH
DASHED LINES - ORIGINAL MESH

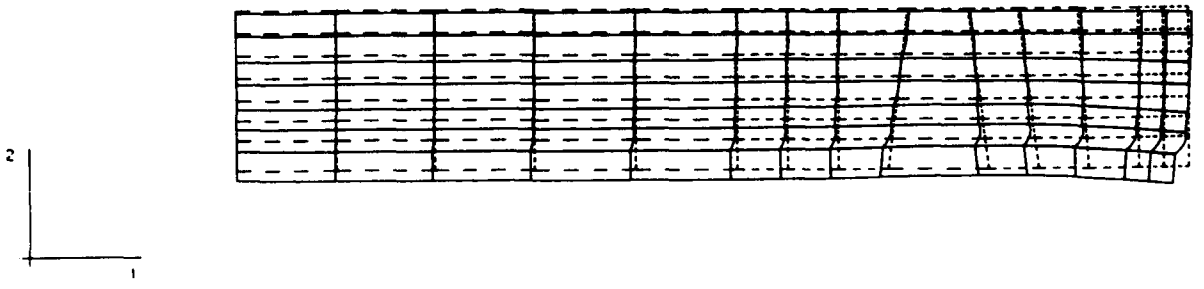

LIFT4 - M17 - UPPER/ADIABATIC/MOD/SHRINK/CREEP

STEP 16 INCREMENT 1 ABAQUS VERSION 4-5-171

**Figure 43a - Displaced shape of L-17,
5 days after lift 4 is placed,
Gravity & thermal loadings, Upper creep/shrinkage**

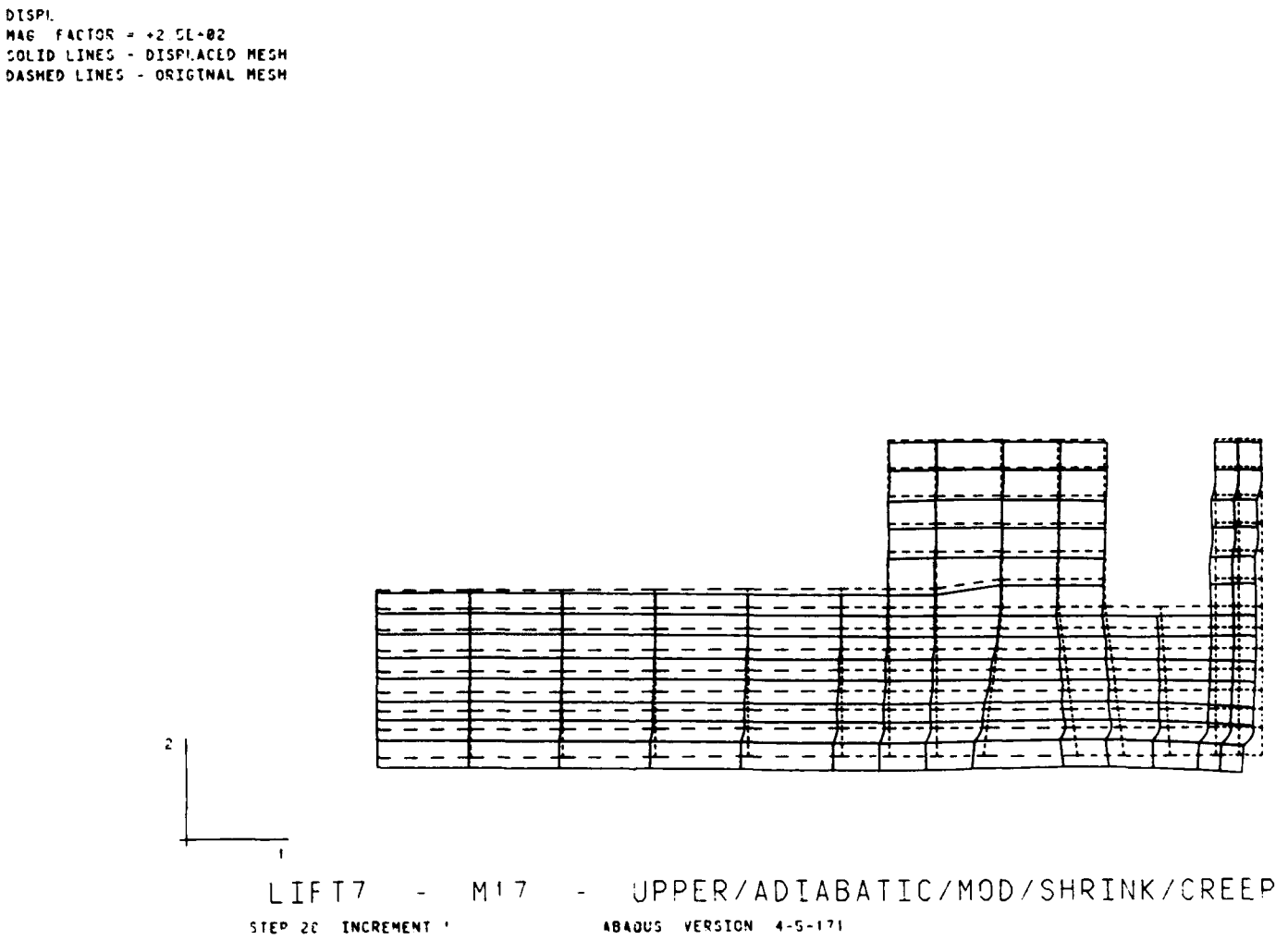

**Figure 43b - Displaced shape of L-17,
5 days after lift 7 is placed,
Gravity & thermal loadings, Upper creep/shrinkage**

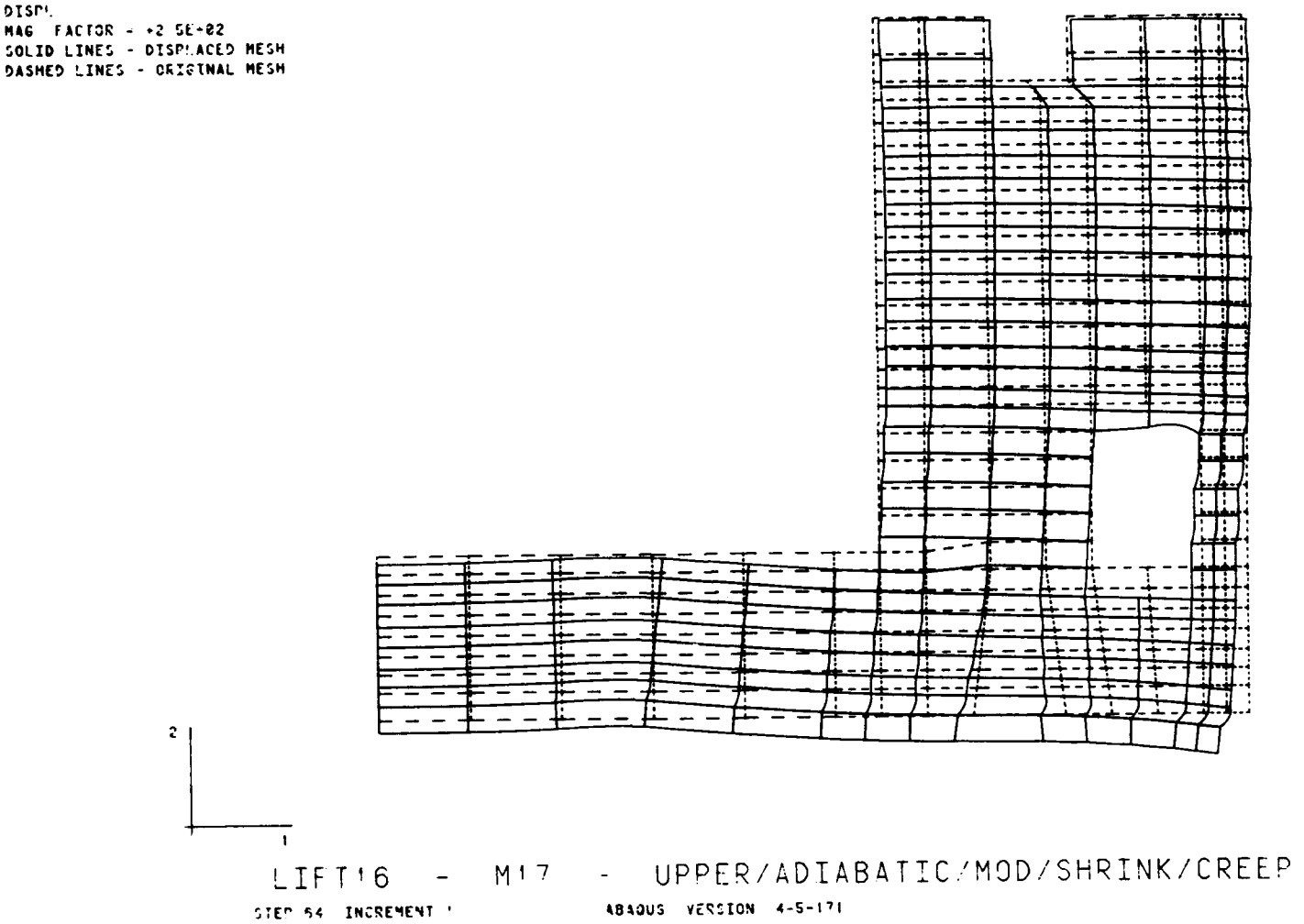

**Figure 43c - Displaced shape of L-17,
5 days after lift 16 is placed,
Gravity & thermal loadings, Upper creep/shrinkage**

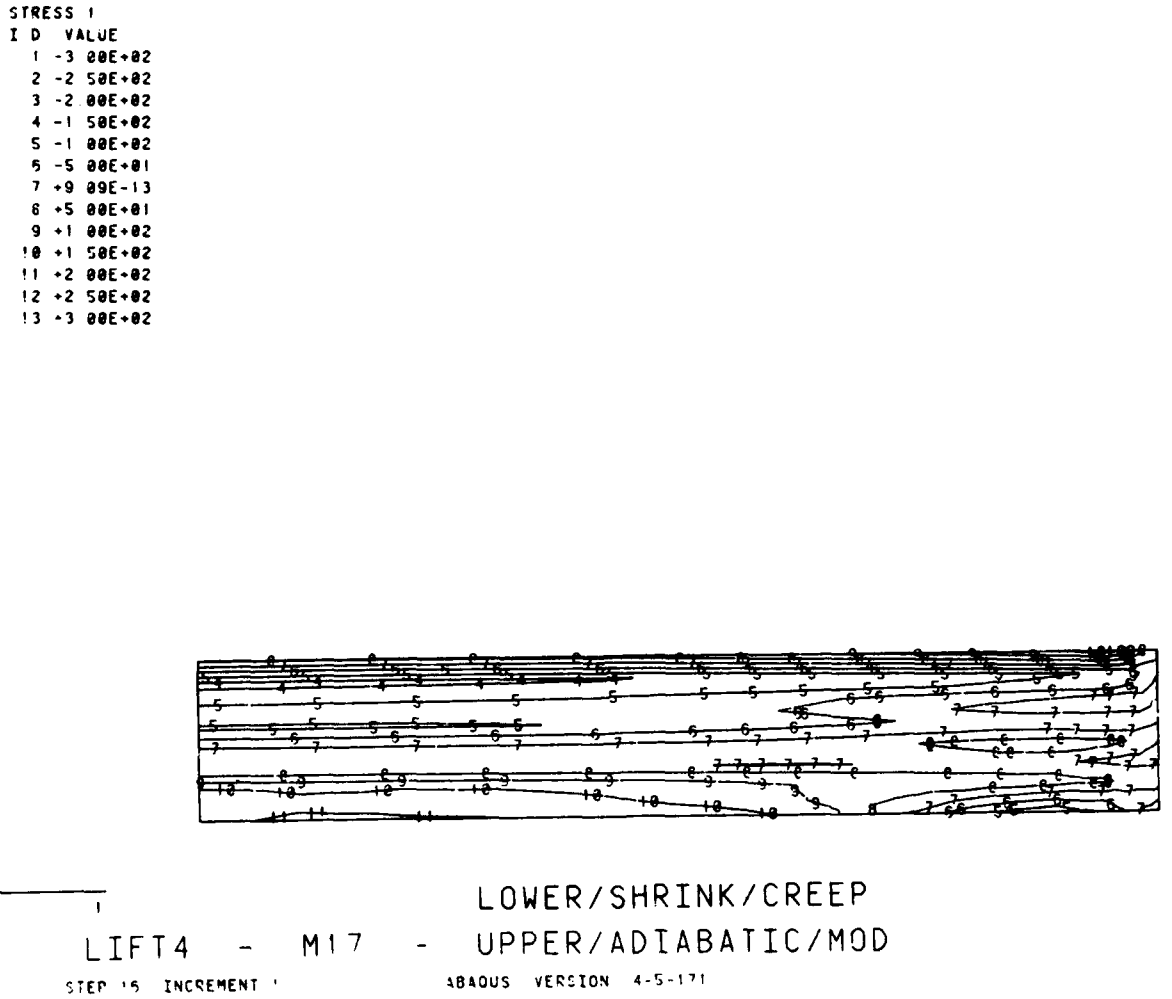

**Figure 44a - Horizontal stress contours in L-17,
5 days after lift 4 is placed,
Gravity & thermal loadings, Lower creep/shrinkage**

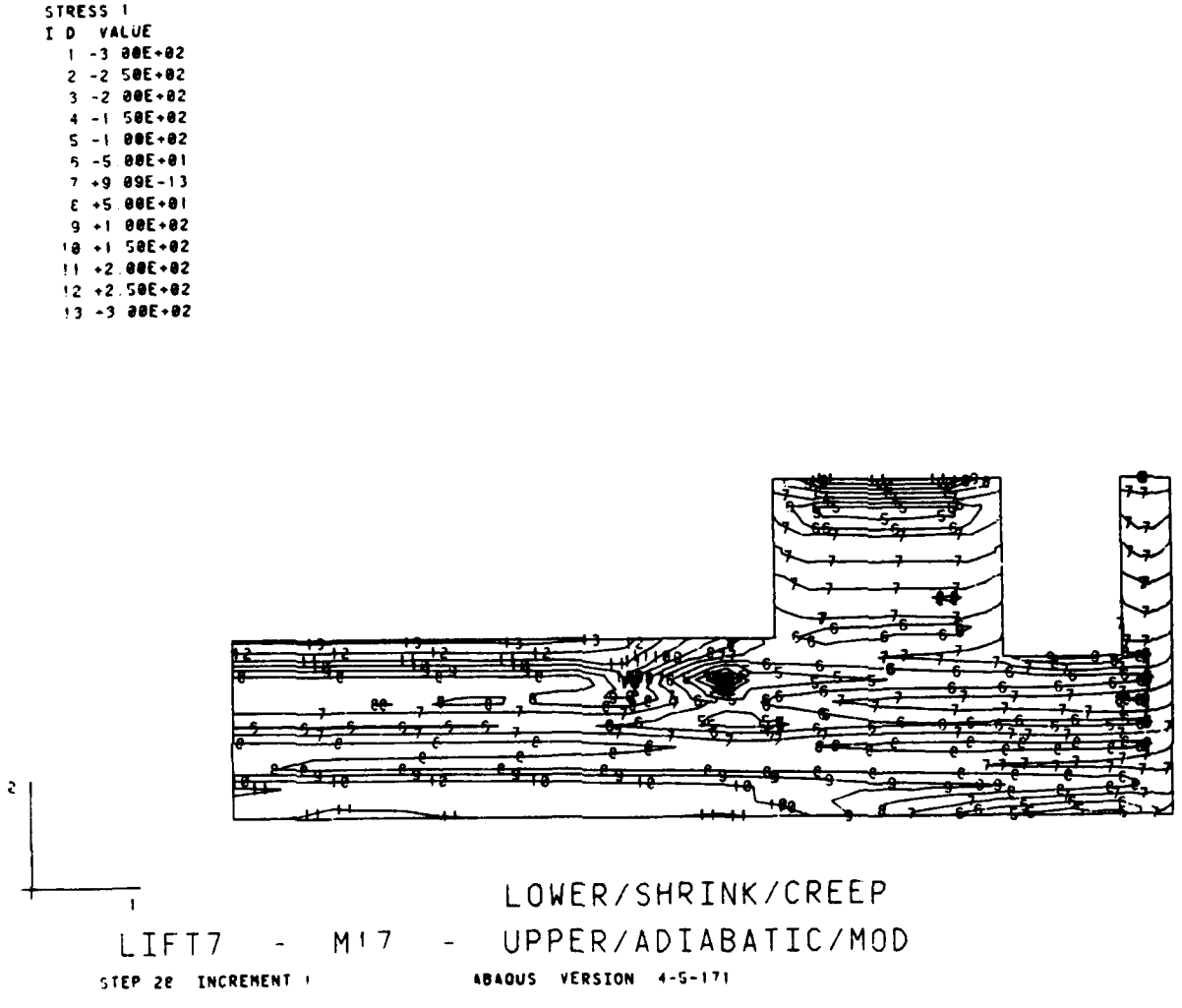

Figure 44b - Horizontal stress contours in L-17, 5 days after lift 7 is placed, Gravity & thermal loadings, Lower creep/shrinkage

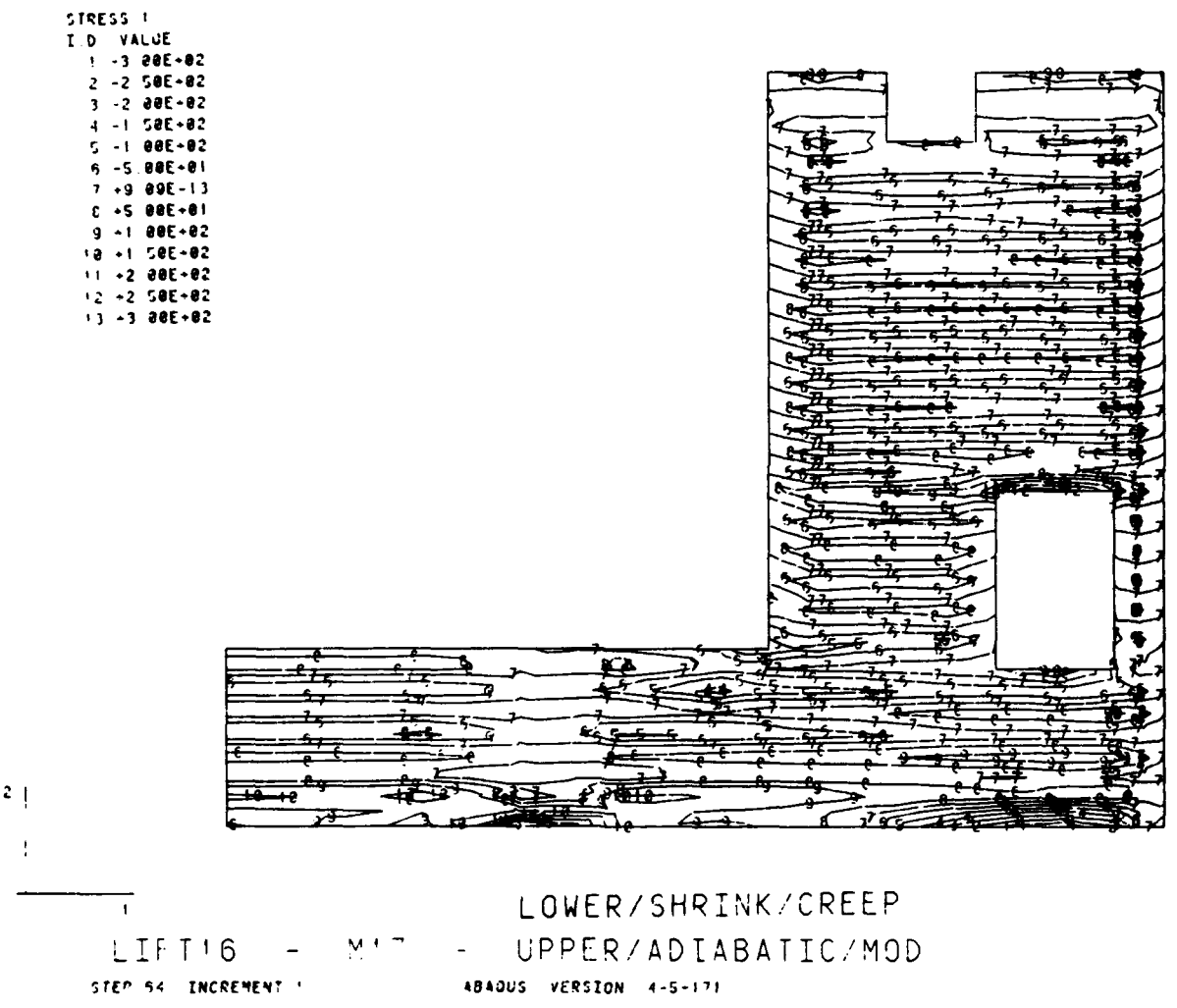

Figure 44c - Horizontal stress contours in L-17, 5 days after lift 16 is placed, Gravity & thermal loadings, Lower creep/shrinkage

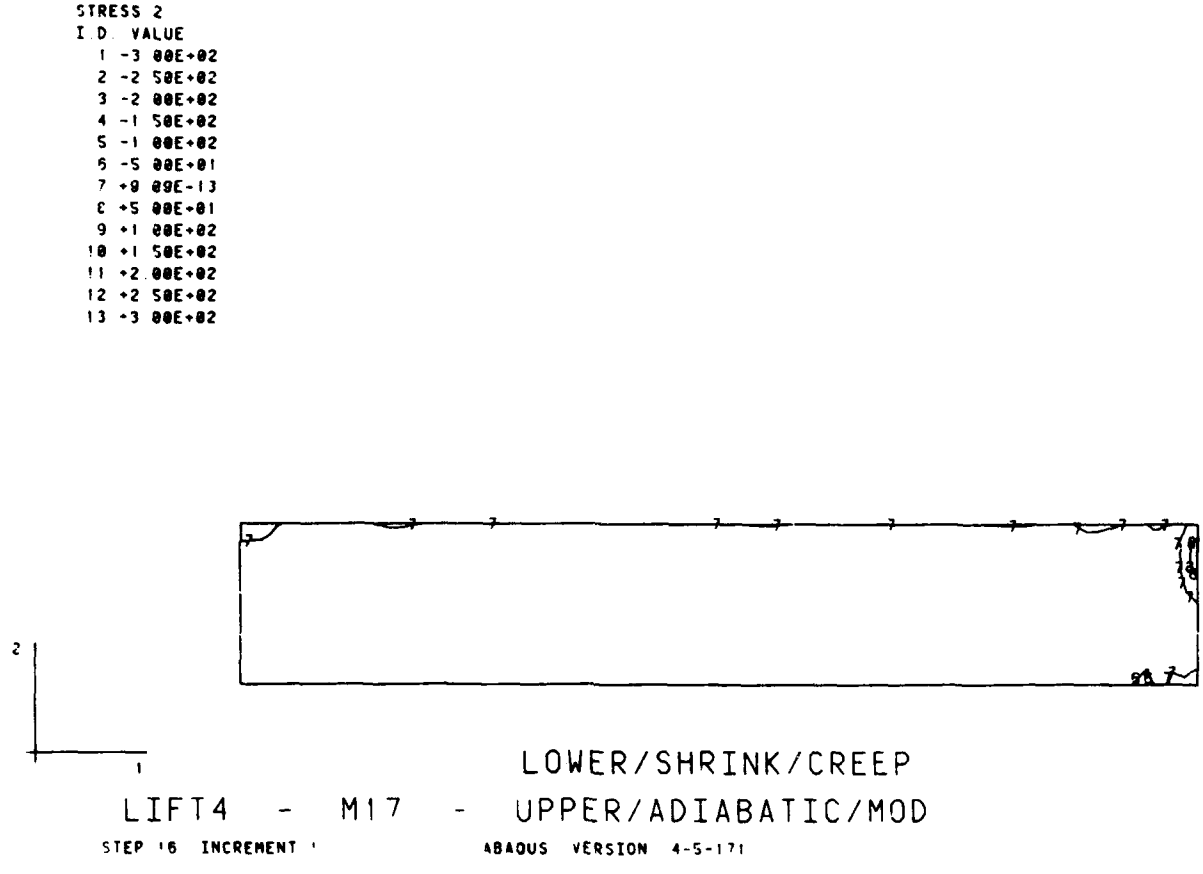

Figure 45a - Vertical stress contours in L-17, 5 days after lift 4 is placed, Gravity & thermal loadings, Lower creep/shrinkage

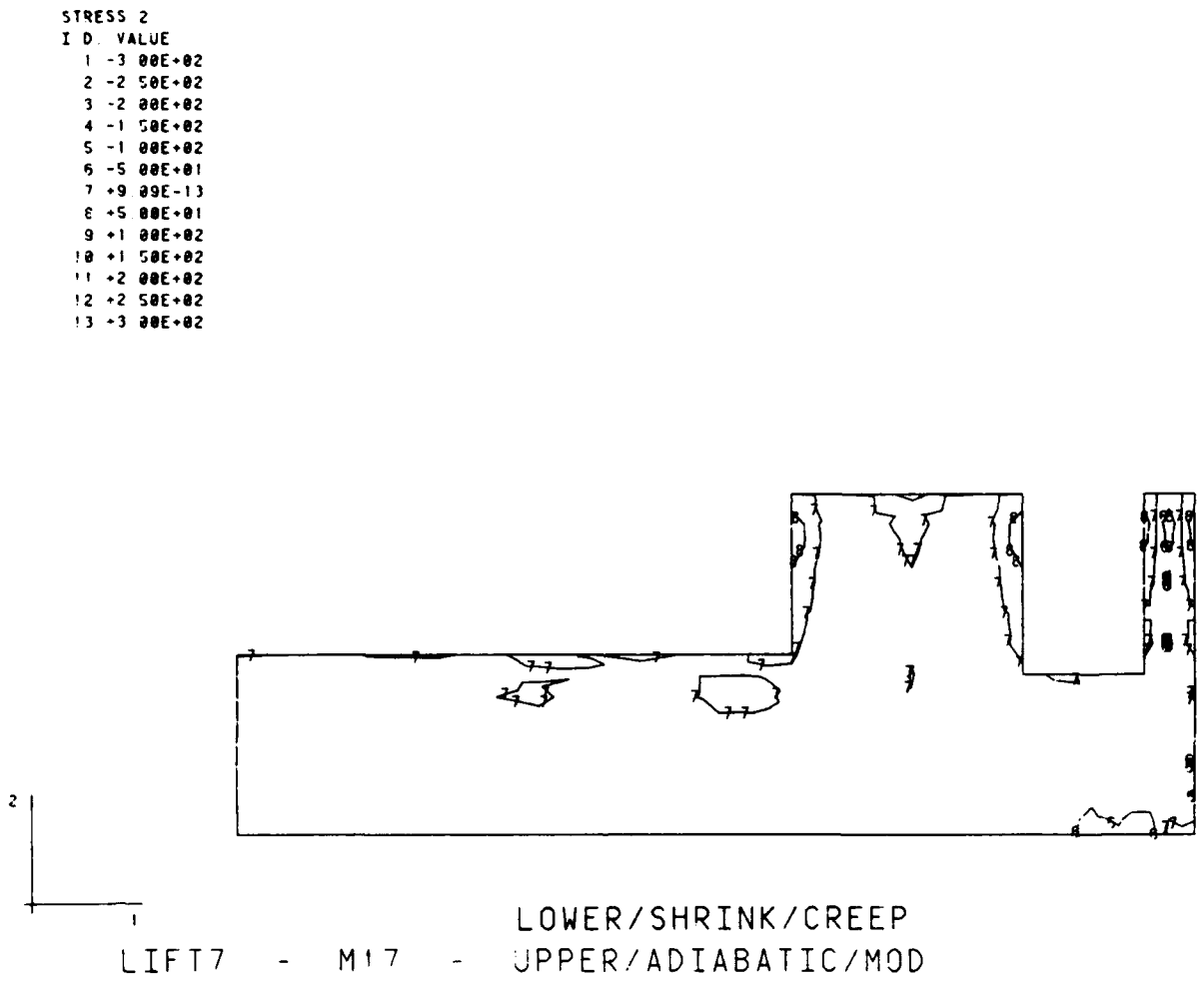

Figure 45b - Vertical stress contours in L-17, 5 days after lift 7 is placed, Gravity & thermal loadings, Lower creep/shrinkage

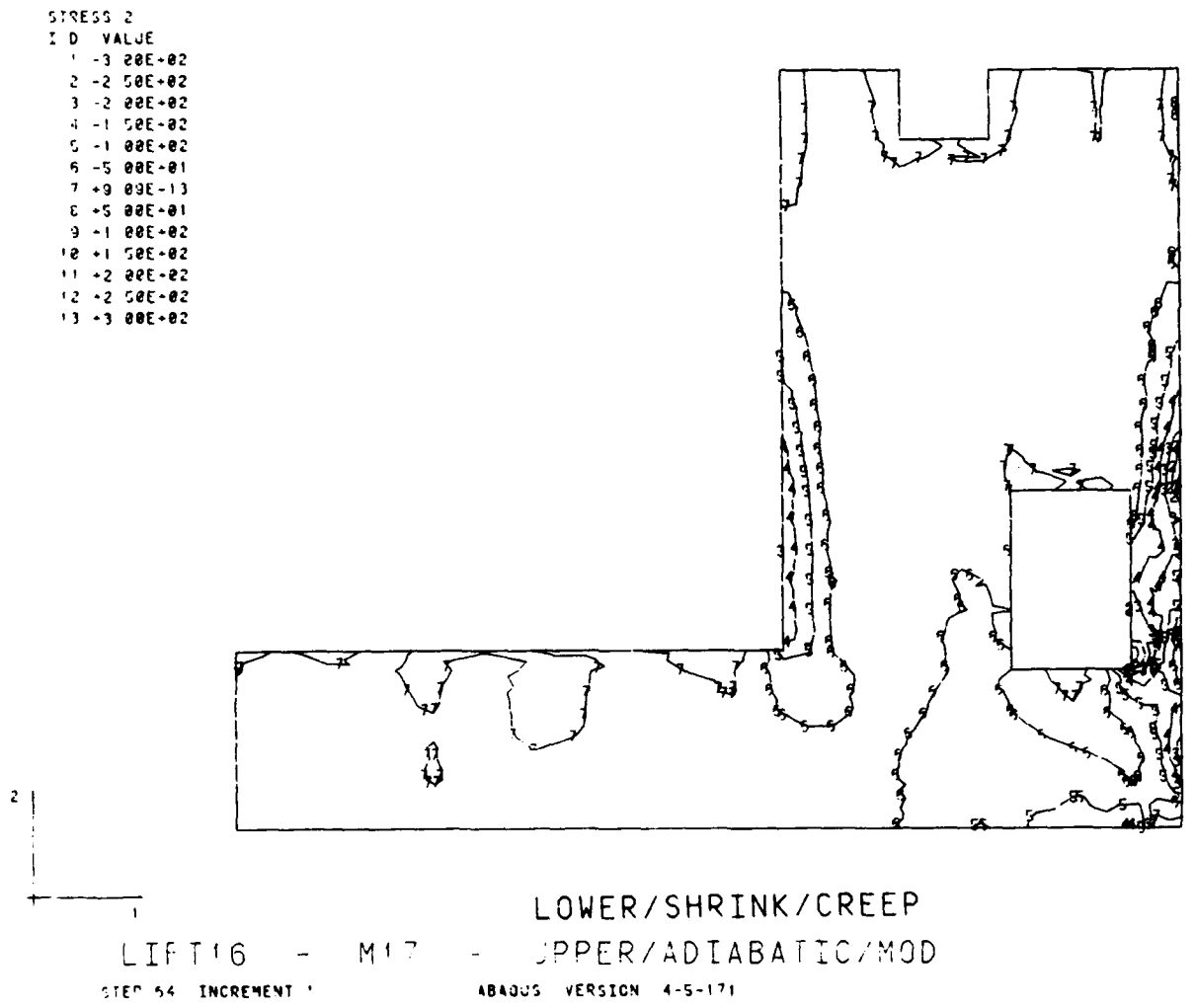

Figure 45c - Vertical stress contours in L-17, 5 days after lift 16 is placed, Gravity & thermal loadings, Lower creep/shrinkage

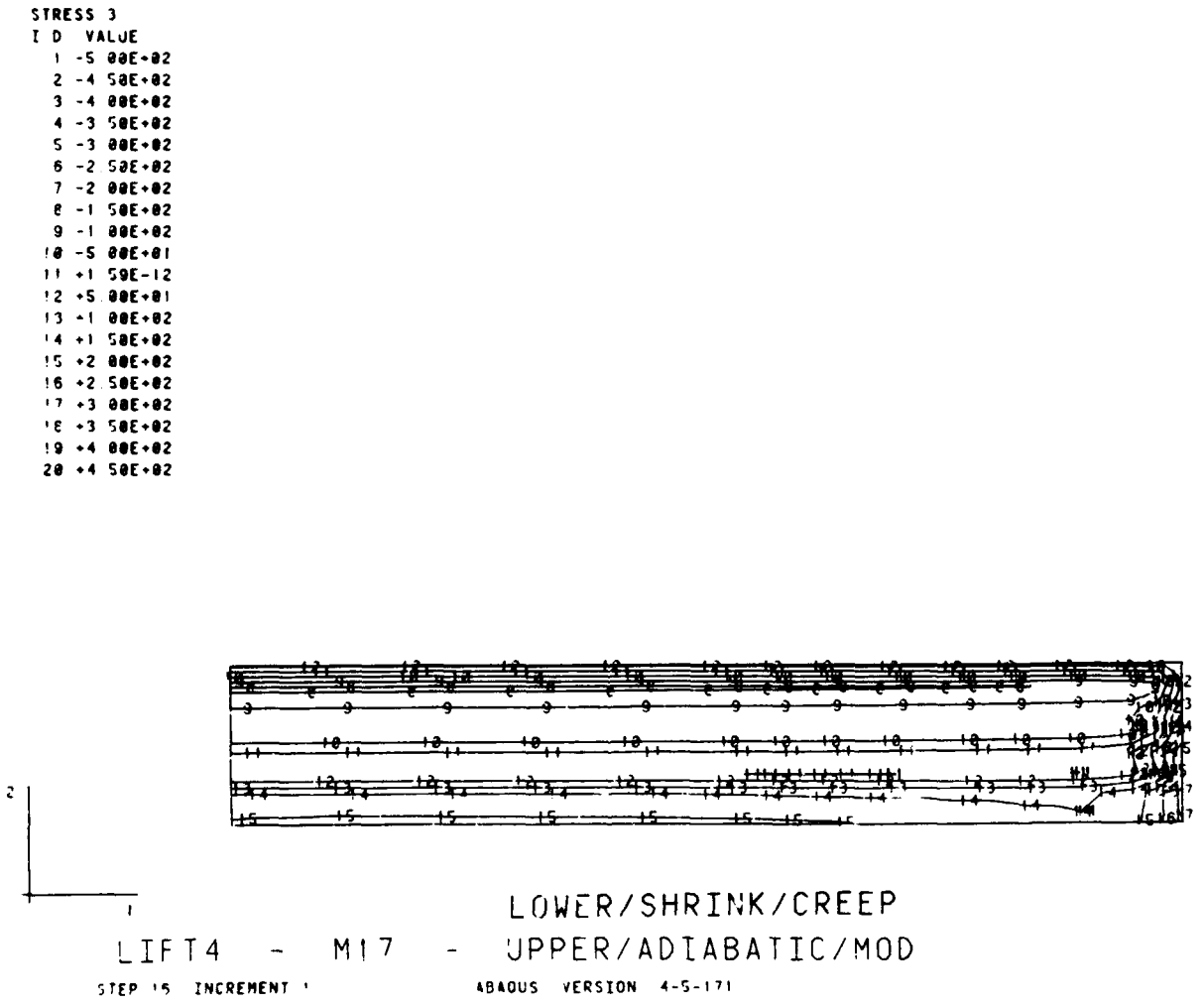

Figure 46a - Out-of-plane stress contours in L-17, 5 days after lift 4 is placed, Gravity & thermal loadings, lower creep/shrinkage

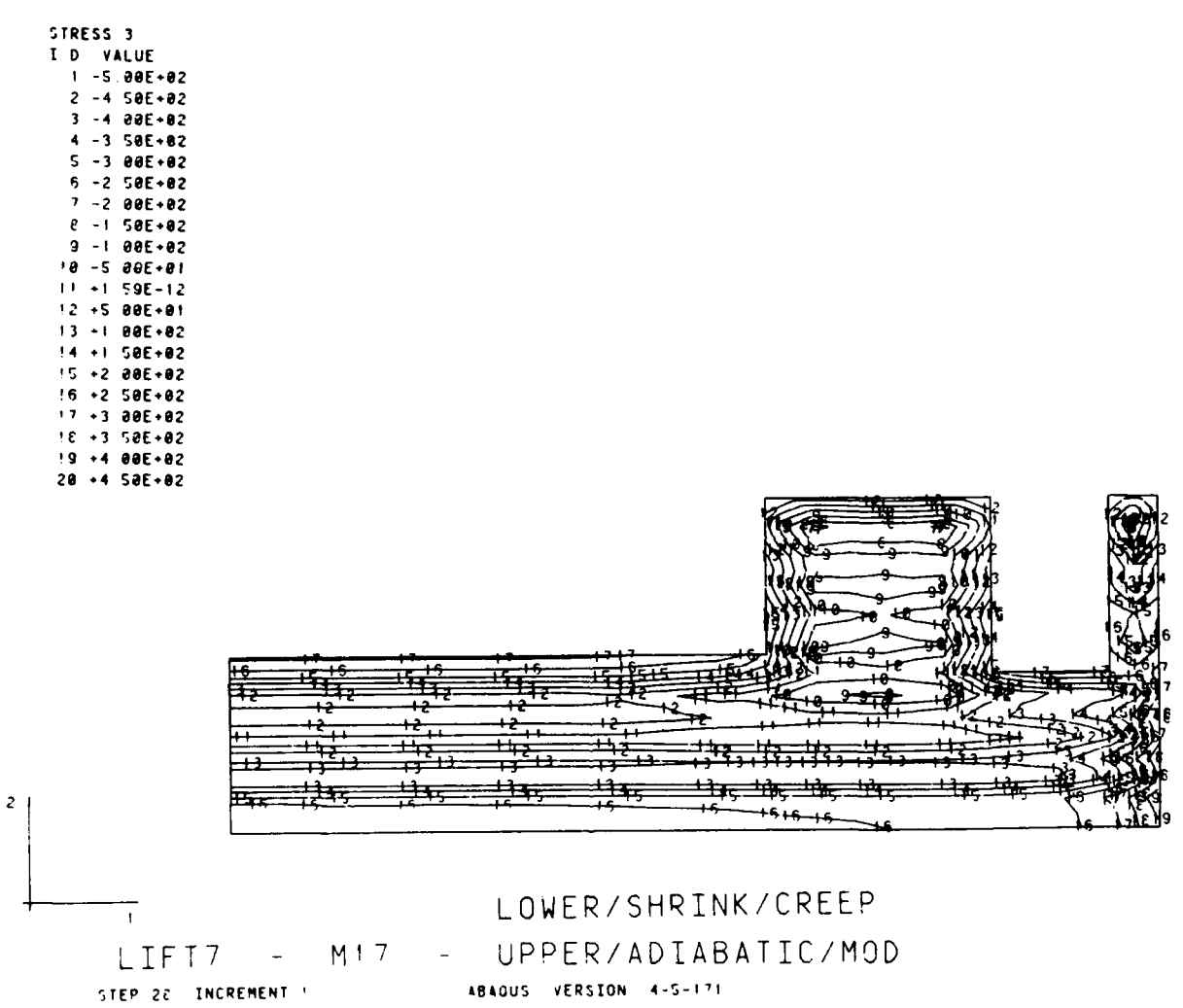

Figure 46b - Out-of-plane stress contours in L-17,
5 days after lift 7 is placed,
Gravity & thermal loadings, Lower creep/shrinkage

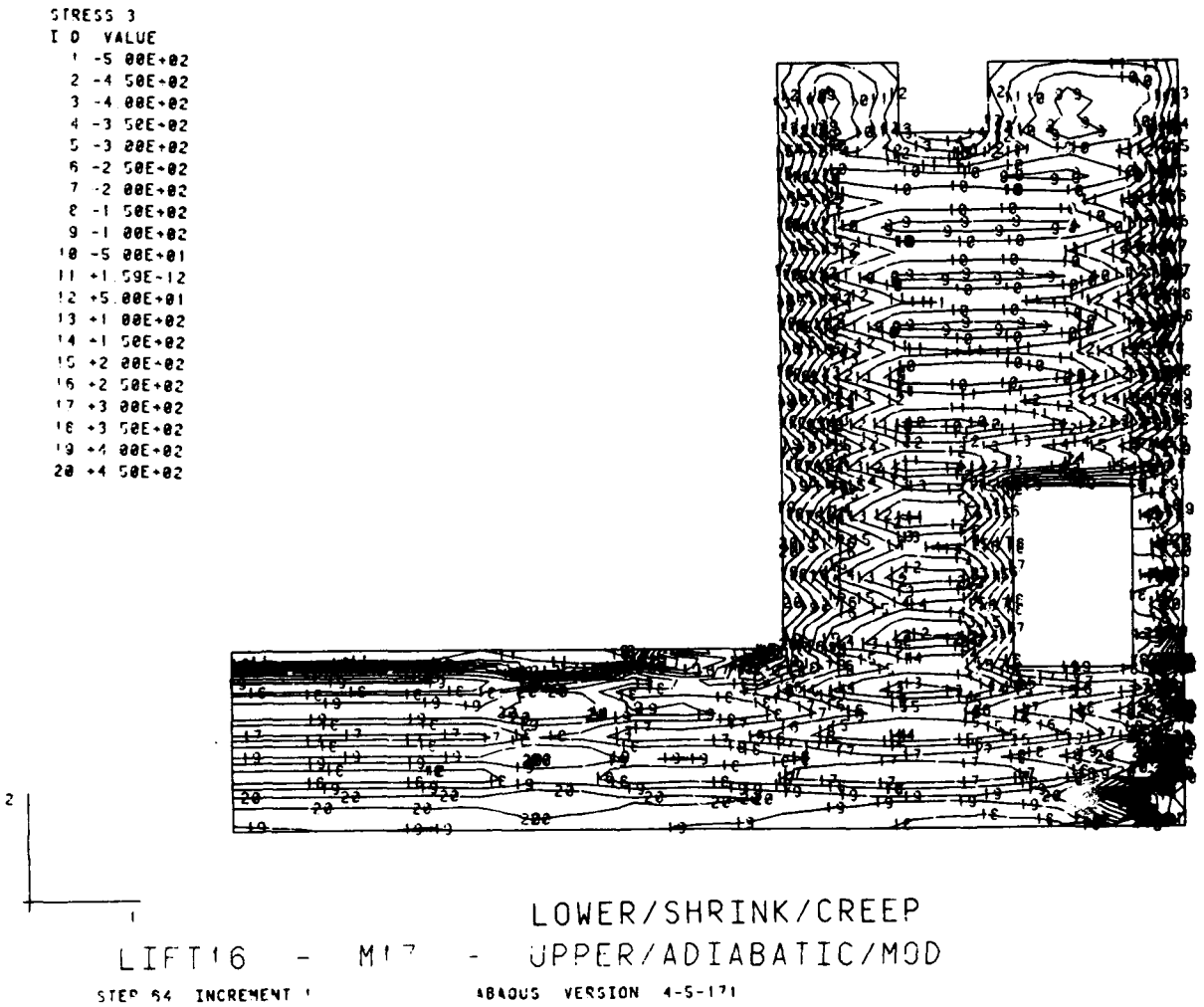

Figure 46c - Out-of-plane stress contours in L-17, 5 days after lift 16 is placed, Gravity & thermal loadings, Lower creep/shrinkage

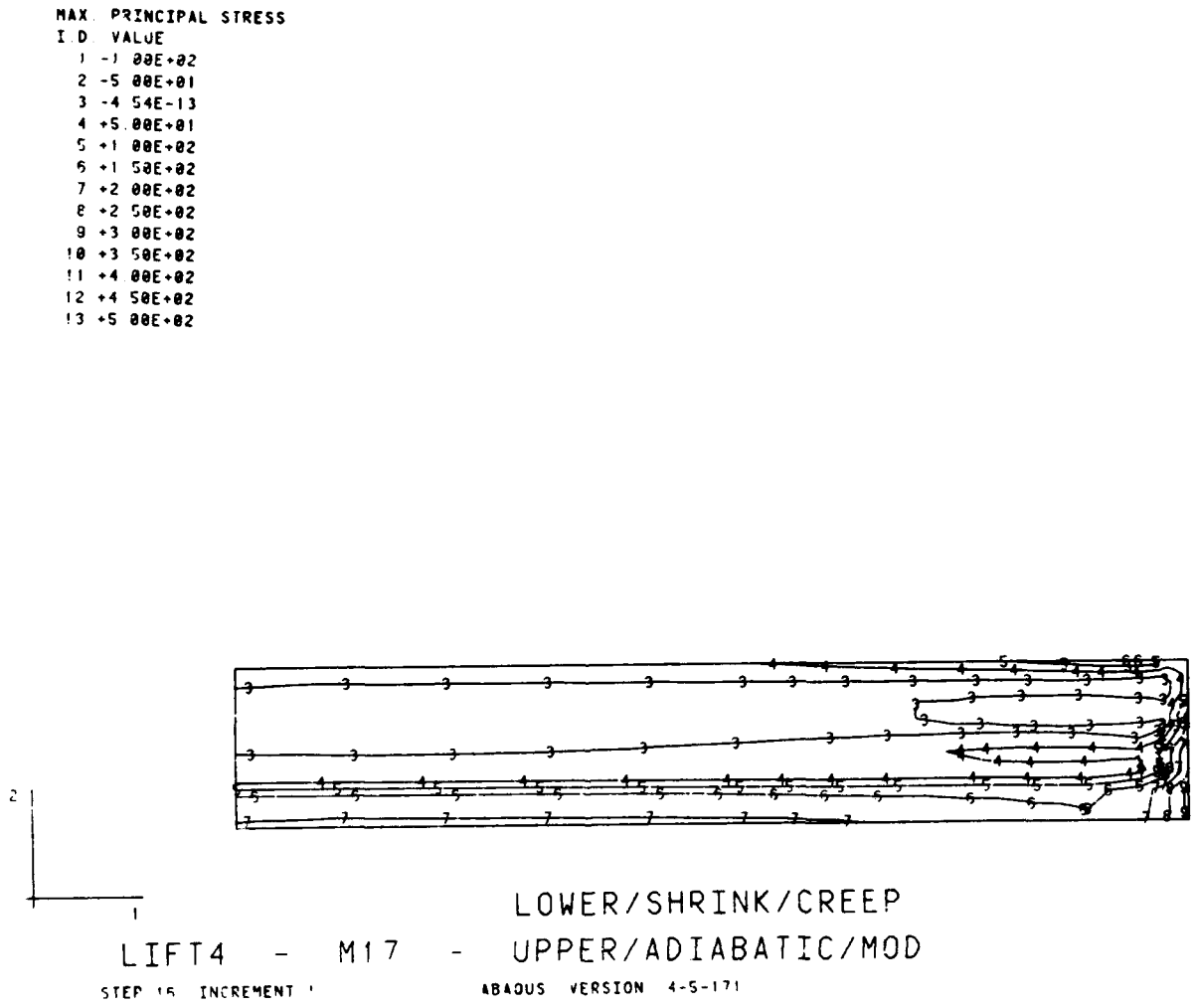

Figure 47a - Max. Principal stress contours in L-17, 5 days after lift 4 is placed, Gravity & thermal loadings, Lower creep/shrinkage

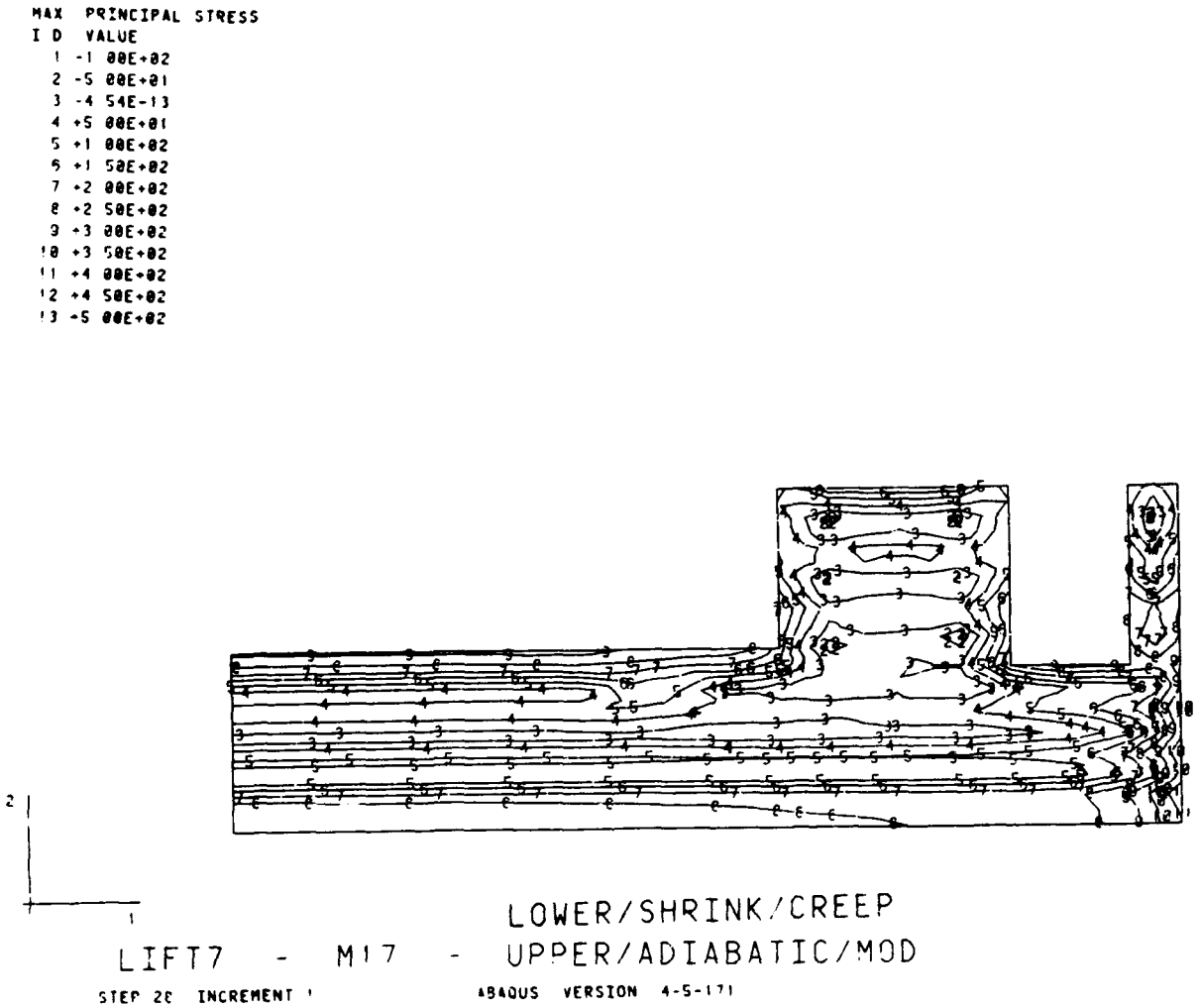

Figure 47b - Max. Principal stress contours in L-17, 5 days after lift 7 is placed, Gravity & thermal loadings, Lower creep/shrinkage

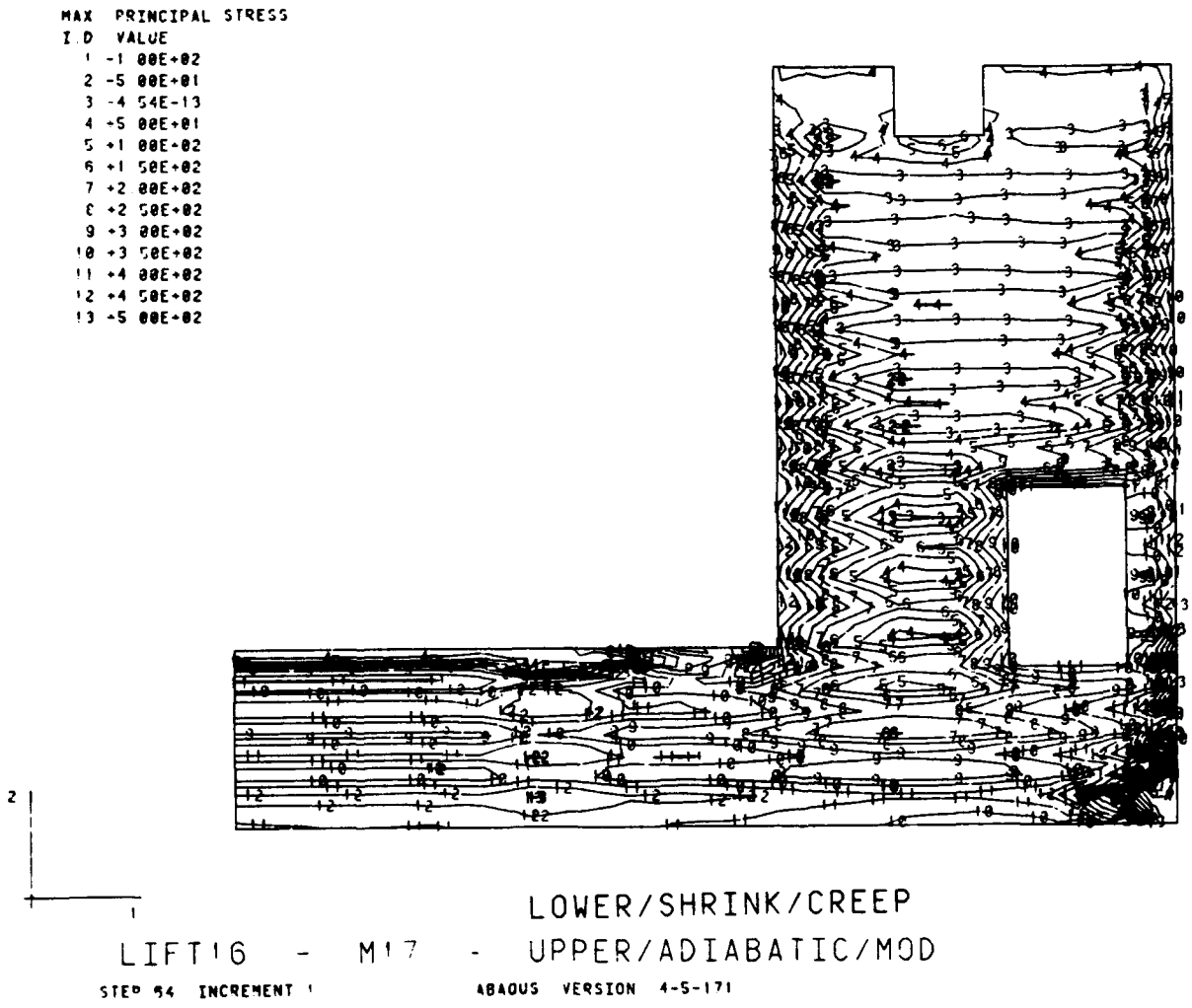

Figure 47c - Max. Principal stress contours in L-17, 5 days after lift 16 is placed, Gravity & thermal loadings, Lower creep/shrinkage

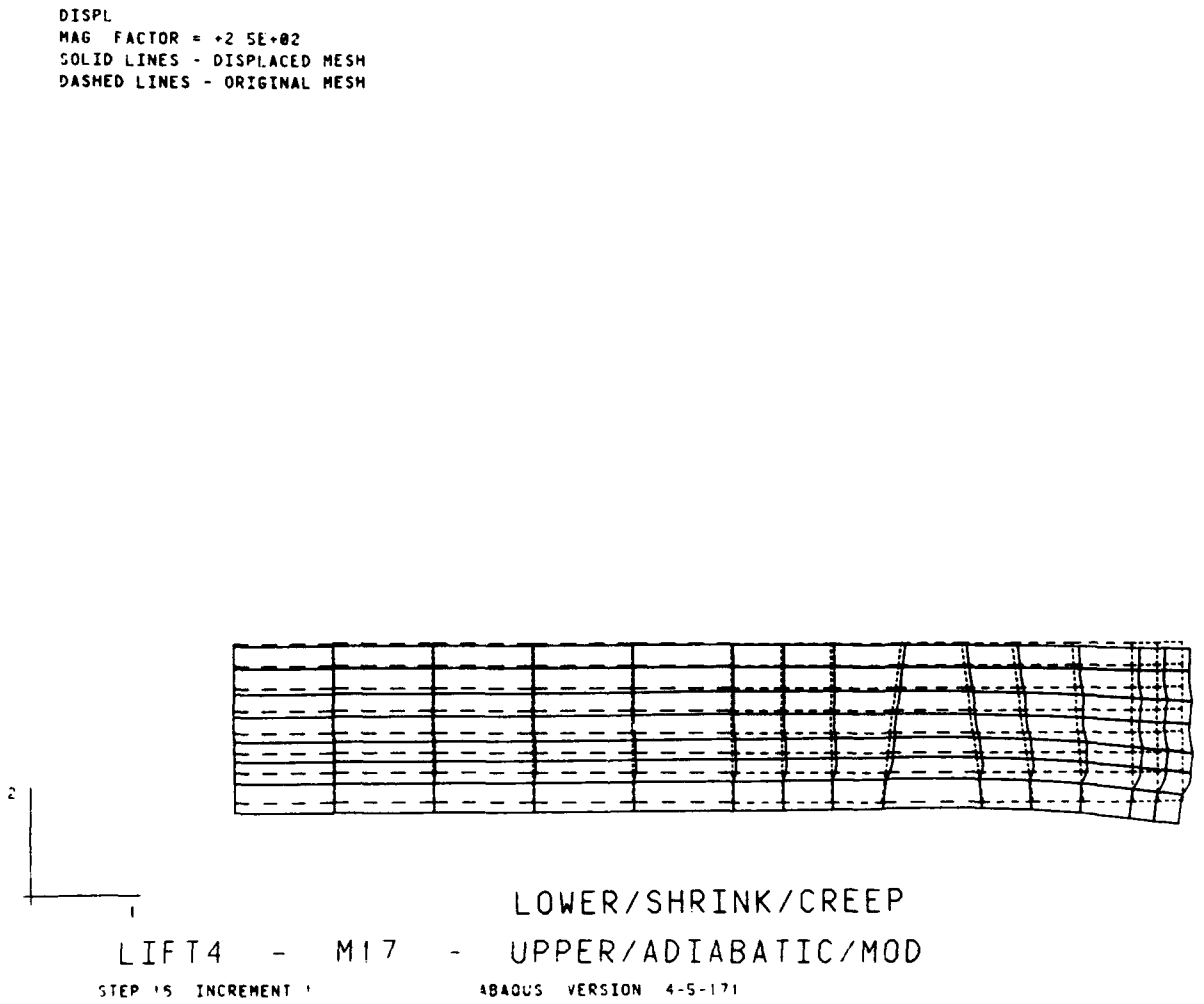

**Figure 48a - Displaced shape of L-17,
5 days after lift 4 is placed,
Gravity + thermal loadings, Lower creep/shrinkage**

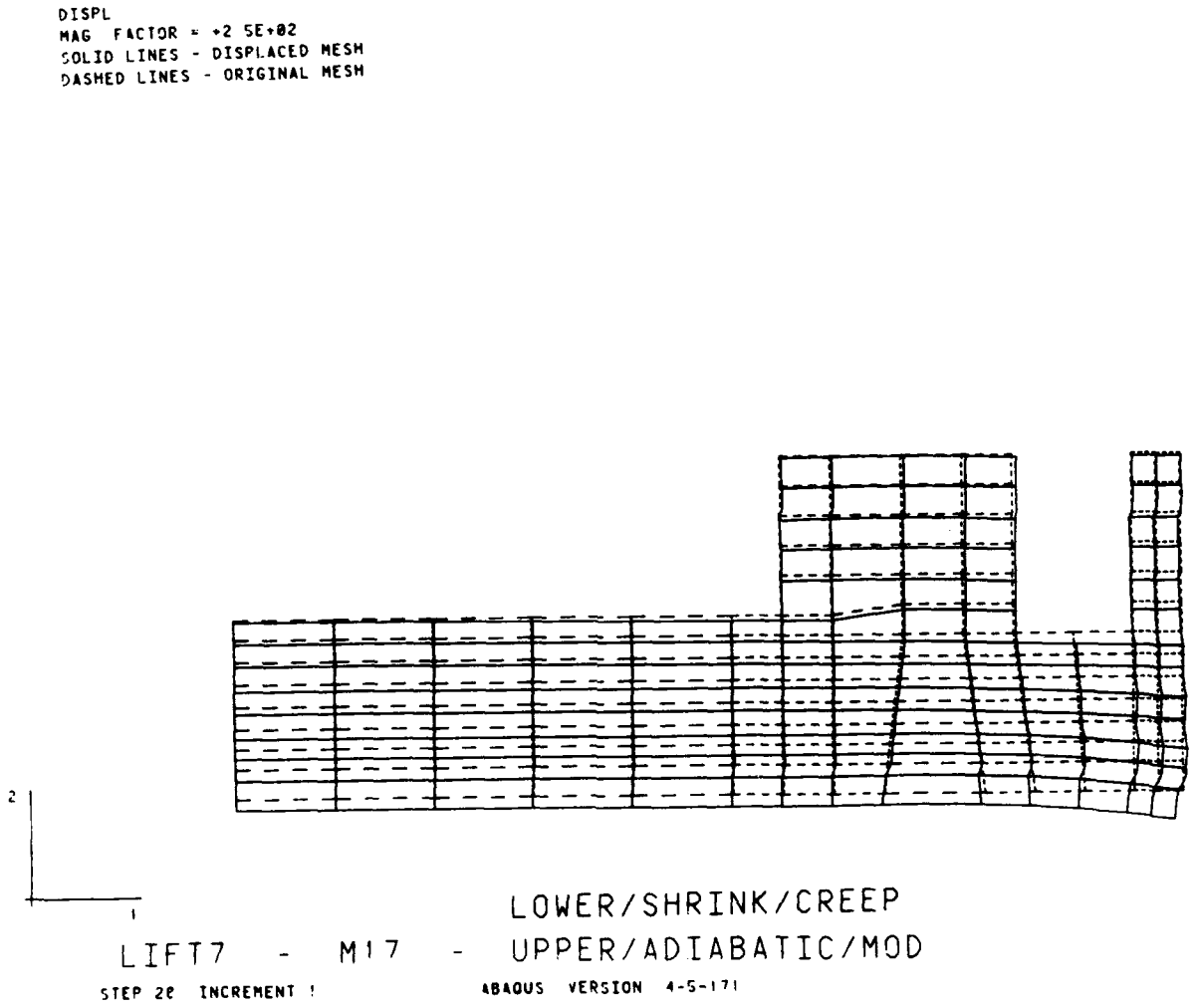

**Figure 48b - Displaced shape of L-17,
5 days after lift 7 is placed,
Gravity & thermal loadings, Lower creep/shrinkage**

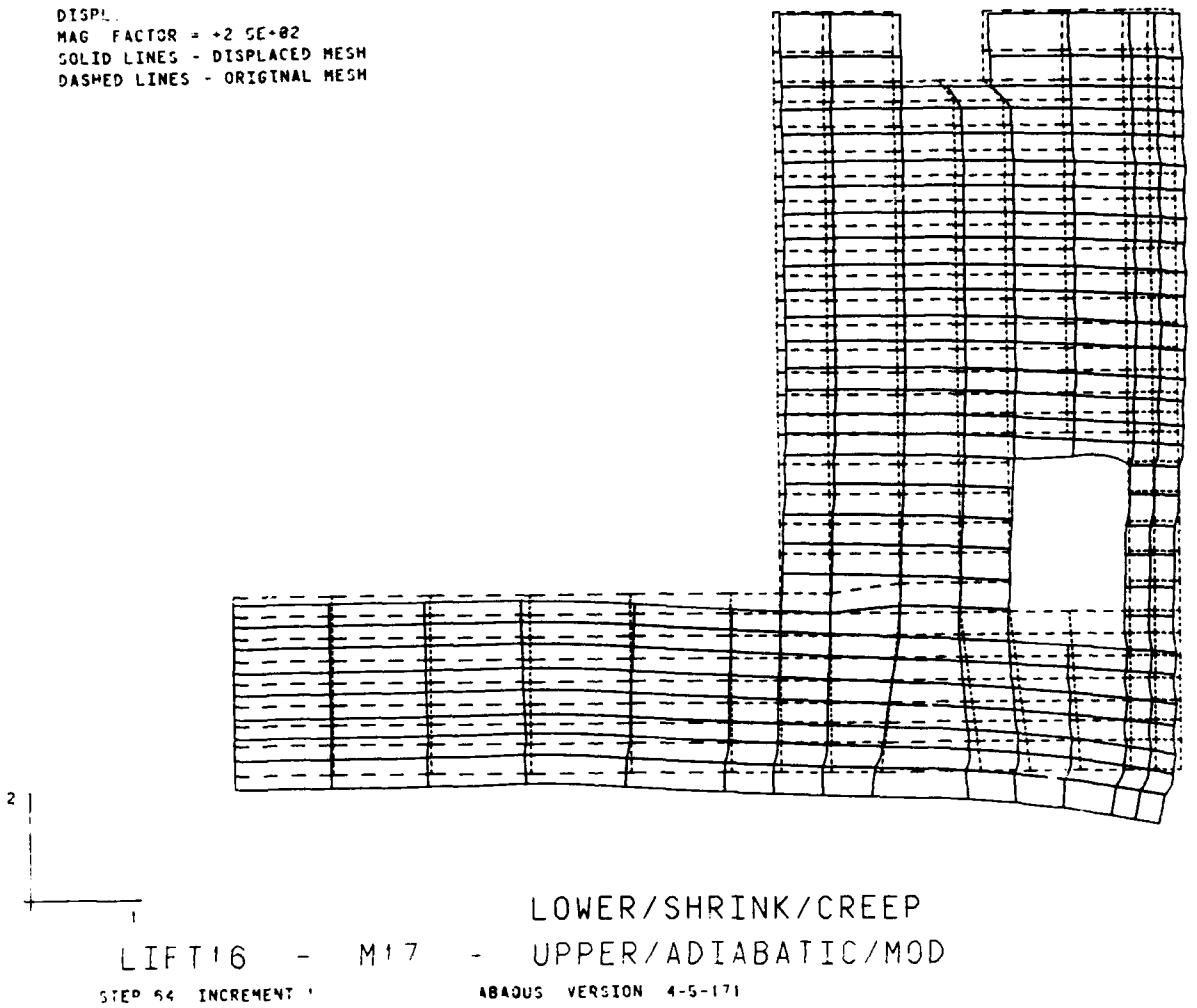

**Figure 48c - Displaced shape of L-17,
5 days after lift 16 is placed,
Gravity & thermal loadings, Lower creep/shrinkage**

Appendix A
Revised Material Input Parameters for Monolith L-17

REVISED MATERIAL INPUT PARAMETERS
FOR MONOLITH L-17

```
*MATERIAL,ELSET=LIFT1
*USER MATERIAL,CONSTANTS=10
2.718E06,0.17,1000.,1.0E-04,4.5E-06,0.25,1.1,0.618,
70.,0.0001
*DEPVAR
60
*MATERIAL,ELSET=LIFT2
*USER MATERIAL,CONSTANTS=10
2.718E06,0.17,1000.,1.0E-04,4.5E-06,0.25,1.1,0.618,
70.,5.0001
*DEPVAR
60
*MATERIAL,ELSET=LIFT3
*USER MATERIAL,CONSTANTS=10
2.718E06,0.17,1000.,1.0E-04,4.5E-06,0.25,1.1,0.618,
70.,10.0001
*DEPVAR
60
*MATERIAL,ELSET=LIFT4
*USER MATERIAL,CONSTANTS=10
2.718E06,0.17,1000.,1.0E-04,4.5E-06,0.25,1.1,0.618,
70.,15.0001
*DEPVAR
60
*MATERIAL,ELSET=LIFT5
*USER MATERIAL,CONSTANTS=10
2.718E06,0.17,1000.,1.0E-04,4.5E-06,0.25,1.1,0.618,
70.,20.0001
*DEPVAR
60
*MATERIAL,ELSET=LIFT6
*USER MATERIAL,CONSTANTS=10
2.718E06,0.17,1000.,1.0E-04,4.5E-06,0.25,1.1,0.618,
70.,25.0001
*DEPVAR
60
*MATERIAL,ELSET=LIFT7
*USER MATERIAL,CONSTANTS=10
2.718E06,0.17,1000.,1.0E-04,4.5E-06,0.25,1.1,0.618,
70.,30.0001
*DEPVAR
60
*MATERIAL,ELSET=LIFT8
*USER MATERIAL,CONSTANTS=10
2.718E06,0.17,1000.,1.0E-04,4.5E-06,0.25,1.1,0.618,
70.,35.0001
*DEPVAR
60
```

```
*MATERIAL,ELSET=LIFT9
*USER MATERIAL,CONSTANTS=10
2.718E06,0.17,1000.,1.0E-04,4.5E-06,0.25,1.1,0.618,
70.,40.0001
*DEPVAR
60
*MATERIAL,ELSET=LIFT10
*USER MATERIAL,CONSTANTS=10
2.718E06,0.17,1000.,1.0E-04,4.5E-06,0.25,1.1,0.618,
70.,45.0001
*DEPVAR
60
*MATERIAL,ELSET=LIFT11
*USER MATERIAL,CONSTANTS=10
2.718E06,0.17,1000.,1.0E-04,4.5E-06,0.25,1.1,0.618,
70.,50.0001
*DEPVAR
60
*MATERIAL,ELSET=LIFT12
*USER MATERIAL,CONSTANTS=10
2.718E06,0.17,1000.,1.0E-04,4.5E-06,0.25,1.1,0.618,
70.,55.0001
*DEPVAR
60
*MATERIAL,ELSET=LIFT13
*USER MATERIAL,CONSTANTS=10
2.718E06,0.17,1000.,1.0E-04,4.5E-06,0.25,1.1,0.618,
70.,60.0001
*DEPVAR
60
*MATERIAL,ELSET=LIFT14
*USER MATERIAL,CONSTANTS=10
2.718E06,0.17,1000.,1.0E-04,4.5E-06,0.25,1.1,0.618,
70.,65.0001
*DEPVAR
60
*MATERIAL,ELSET=LIFT15
*USER MATERIAL,CONSTANTS=10
2.718E06,0.17,1000.,1.0E-04,4.5E-06,0.25,1.1,0.618,
70.,70.0001
*DEPVAR
60
*MATERIAL,ELSET=LIFT16
*USER MATERIAL,CONSTANTS=10
2.718E06,0.17,1000.,1.0E-04,4.5E-06,0.25,1.1,0.618,
70.,75.0001
*DEPVAR
60
```

Waterways Experiment Station Cataloging-in-Publication Data

Jones, H. Wayne.
Refined stress analysis of Melvin Price Locks and Dam / by H. Wayne Jones ; prepared for U.S. Army Engineer District, St. Louis.
192 p. : ill. ; 28 cm. — (Technical report ; ITL-92-7)
Includes bibliographic references.
1. Dams — Illinois — Alton — Testing. 2. Melvin Price Locks and Dam (Ill.) 3. Thermoelastic stress analysis. 4. Piling (Civil engineering) — Evaluation. I. United States. Army. Corps of Engineers. St. Louis District. II. U.S. Army Engineer Waterways Experiment Station. III. Computer-aided Structural Engineering Project. IV. Title. V. Series: Technical report (U.S. Army Engineer Waterways Experiment Station) ; ITL-92-7.
TA7 W34 no.ITL-92-7

WATERWAYS EXPERIMENT STATION REPORTS PUBLISHED UNDER THE COMPUTER-AIDED STRUCTURAL ENGINEERING (CASE) PROJECT

	Title	Date
Technical Report K-78-1	List of Computer Programs for Computer-Aided Structural Engineering	Feb 1978
Instruction Report O-79-2	User's Guide: Computer Program with Interactive Graphics for Analysis of Plane Frame Structures (CFRAME)	Mar 1979
Technical Report K-80-1	Survey of Bridge-Oriented Design Software	Jan 1980
Technical Report K-80-2	Evaluation of Computer Programs for the Design/Analysis of Highway and Railway Bridges	Jan 1980
Instruction Report K-80-1	User's Guide: Computer Program for Design/Review of Curvilinear Conduits/Culverts (CURCON)	Feb 1980
Instruction Report K-80-3	A Three-Dimensional Finite Element Data Edit Program	Mar 1980
Instruction Report K-80-4	A Three-Dimensional Stability Analysis/Design Program (3DSAD)	
	Report 1: General Geometry Module	Jun 1980
	Report 3: General Analysis Module (CGAM)	Jun 1982
	Report 4: Special-Purpose Modules for Dams (CDAMS)	Aug 1983
Instruction Report K-80-6	Basic User's Guide: Computer Program for Design and Analysis of Inverted-T Retaining Walls and Floodwalls (TWDA)	Dec 1980
Instruction Report K-80-7	User's Reference Manual: Computer Program for Design and Analysis of Inverted-T Retaining Walls and Floodwalls (TWDA)	Dec 1980
Technical Report K-80-4	Documentation of Finite Element Analyses	
	Report 1: Longview Outlet Works Conduit	Dec 1980
	Report 2: Anchored Wall Monolith, Bay Springs Lock	Dec 1980
Technical Report K-80-5	Basic Pile Group Behavior	Dec 1980
Instruction Report K-81-2	User's Guide: Computer Program for Design and Analysis of Sheet Pile Walls by Classical Methods (CSHTWAL)	
	Report 1: Computational Processes	Feb 1981
	Report 2: Interactive Graphics Options	Mar 1981
Instruction Report K-81-3	Validation Report: Computer Program for Design and Analysis of Inverted-T Retaining Walls and Floodwalls (TWDA)	Feb 1981
Instruction Report K-81-4	User's Guide: Computer Program for Design and Analysis of Cast-in-Place Tunnel Linings (NEWTUN)	Mar 1981
Instruction Report K-81-6	User's Guide: Computer Program for Optimum Nonlinear Dynamic Design of Reinforced Concrete Slabs Under Blast Loading (CBARCS)	Mar 1981
Instruction Report K-81-7	User's Guide: Computer Program for Design or Investigation of Orthogonal Culverts (CORTCUL)	Mar 1981
Instruction Report K-81-9	User's Guide: Computer Program for Three-Dimensional Analysis of Building Systems (CTABS80)	Aug 1981
Technical Report K-81-2	Theoretical Basis for CTABS80: A Computer Program for Three-Dimensional Analysis of Building Systems	Sep 1981
Instruction Report K-82-6	User's Guide: Computer Program for Analysis of Beam-Column Structures with Nonlinear Supports (CBEAMC)	Jun 1982

(Continued)

WATERWAYS EXPERIMENT STATION REPORTS PUBLISHED UNDER THE COMPUTER-AIDED STRUCTURAL ENGINEERING (CASE) PROJECT

(Continued)

	Title	Date
Instruction Report K-82-7	User's Guide: Computer Program for Bearing Capacity Analysis of Shallow Foundations (CBEAR)	Jun 1982
Instruction Report K-83-1	User's Guide: Computer Program with Interactive Graphics for Analysis of Plane Frame Structures (CFRAME)	Jan 1983
Instruction Report K-83-2	User's Guide: Computer Program for Generation of Engineering Geometry (SKETCH)	Jun 1983
Instruction Report K-83-5	User's Guide: Computer Program to Calculate Shear, Moment, and Thrust (CSMT) from Stress Results of a Two-Dimensional Finite Element Analysis	Jul 1983
Technical Report K-83-1	Basic Pile Group Behavior	Sep 1983
Technical Report K-83-3	Reference Manual: Computer Graphics Program for Generation of Engineering Geometry (SKETCH)	Sep 1983
Technical Report K-83-4	Case Study of Six Major General-Purpose Finite Element Programs	Oct 1983
Instruction Report K-84-2	User's Guide: Computer Program for Optimum Dynamic Design of Nonlinear Metal Plates Under Blast Loading (CSDOOR)	Jan 1984
Instruction Report K-84-7	User's Guide: Computer Program for Determining Induced Stresses and Consolidation Settlements (CSETT)	Aug 1984
Instruction Report K-84-8	Seepage Analysis of Confined Flow Problems by the Method of Fragments (CFRAG)	Sep 1984
Instruction Report K-84-11	User's Guide for Computer Program CGFAG, Concrete General Flexure Analysis with Graphics	Sep 1984
Technical Report K-84-3	Computer-Aided Drafting and Design for Corps Structural Engineers	Oct 1984
Technical Report ATC-86-5	Decision Logic Table Formulation of ACI 318-77, Building Code Requirements for Reinforced Concrete for Automated Constraint Processing, Volumes I and II	Jun 1986
Technical Report ITL-87-2	A Case Committee Study of Finite Element Analysis of Concrete Flat Slabs	Jan 1987
Instruction Report ITL-87-1	User's Guide: Computer Program for Two-Dimensional Analysis of U-Frame Structures (CUFRAM)	Apr 1987
Instruction Report ITL-87-2	User's Guide: For Concrete Strength Investigation and Design (CASTR) in Accordance with ACI 318-83	May 1987
Technical Report ITL-87-6	Finite-Element Method Package for Solving Steady-State Seepage Problems	May 1987
Instruction Report ITL-87-3	User's Guide: A Three Dimensional Stability Analysis/Design Program (3DSAD) Module	Jun 1987
	Report 1: Revision 1: General Geometry	Jun 1987
	Report 2: General Loads Module	Sep 1989
	Report 6: Free-Body Module	Sep 1989

(Continued)

WATERWAYS EXPERIMENT STATION REPORTS PUBLISHED UNDER THE COMPUTER-AIDED STRUCTURAL ENGINEERING (CASE) PROJECT

(Continued)

	Title	Date
Instruction Report ITL-87-4	User's Guide: 2-D Frame Analysis Link Program (LINK2D)	Jun 1987
Technical Report ITL-87-4	Finite Element Studies of a Horizontally Framed Miter Gate Report 1: Initial and Refined Finite Element Models (Phases A, B, and C), Volumes I and II Report 2: Simplified Frame Model (Phase D) Report 3: Alternate Configuration Miter Gate Finite Element Studies–Open Section Report 4: Alternate Configuration Miter Gate Finite Element Studies–Closed Sections Report 5: Alternate Configuration Miter Gate Finite Element Studies–Additional Closed Sections Report 6: Elastic Buckling of Girders in Horizontally Framed Miter Gates Report 7: Application and Summary	Aug 1987
Instruction Report GL-87-1	User's Guide: UTEXAS2 Slope-Stability Package; Volume I, User's Manual	Aug 1987
Instruction Report ITL-87-5	Sliding Stability of Concrete Structures (CSLIDE)	Oct 1987
Instruction Report ITL-87-6	Criteria Specifications for and Validation of a Computer Program for the Design or Investigation of Horizontally Framed Miter Gates (CMITER)	Dec 1987
Technical Report ITL-87-8	Procedure for Static Analysis of Gravity Dams Using the Finite Element Method – Phase 1a	Jan 1988
Instruction Report ITL-88-1	User's Guide: Computer Program for Analysis of Planar Grid Structures (CGRID)	Feb 1988
Technical Report ITL-88-1	Development of Design Formulas for Ribbed Mat Foundations on Expansive Soils	Apr 1988
Technical Report ITL-88-2	User's Guide: Pile Group Graphics Display (CPGG) Post-processor to CPGA Program	Apr 1988
Instruction Report ITL-88-2	User's Guide for Design and Investigation of Horizontally Framed Miter Gates (CMITER)	Jun 1988
Instruction Report ITL-88-4	User's Guide for Revised Computer Program to Calculate Shear, Moment, and Thrust (CSMT)	Sep 1988
Instruction Report GL-87-1	User's Guide: UTEXAS2 Slope-Stability Package; Volume II, Theory	Feb 1989
Technical Report ITL-89-3	User's Guide: Pile Group Analysis (CPGA) Computer Group	Jul 1989
Technical Report ITL-89-4	CBASIN–Structural Design of Saint Anthony Falls Stilling Basins According to Corps of Engineers Criteria for Hydraulic Structures; Computer Program X0098	Aug 1989

(Continued)

WATERWAYS EXPERIMENT STATION REPORTS PUBLISHED UNDER THE COMPUTER-AIDED STRUCTURAL ENGINEERING (CASE) PROJECT

(Concluded)

	Title	Date
Technical Report ITL-89-5	CCHAN–Structural Design of Rectangular Channels According to Corps of Engineers Criteria for Hydraulic Structures; Computer Program X0097	Aug 1989
Technical Report ITL-89-6	The Response-Spectrum Dynamic Analysis of Gravity Dams Using the Finite Element Method; Phase II	Aug 1989
Contract Report ITL-89-1	State of the Art on Expert Systems Applications in Design, Construction, and Maintenance of Structures	Sep 1989
Instruction Report ITL-90-1	User's Guide: Computer Program for Design and Analysis of Sheet Pile Walls by Classical Methods (CWALSHT)	Feb 1990
Technical Report ITL-90-3	Investigation and Design of U-Frame Structures Using Program CUFRBC Volume A: Program Criteria and Documentation Volume B: User's Guide for Basins Volume C: User's Guide for Channels	May 1990
Instruction Report ITL-90-6	User's Guide: Computer Program for Two-Dimensional Analysis of U-Frame or W-Frame Structures (CWFRAM)	Sep 1990
Instruction Report ITL-90-2	User's Guide: Pile Group–Concrete Pile Analysis Program (CPGC) Preprocessor to CPGA Program	Jun 1990
Technical Report ITL-91-3	Application of Finite Element, Grid Generation, and Scientific Visualization Techniques to 2-D and 3-D Seepage and Groundwater Modeling	Sep 1990
Instruction Report ITL-91-1	User's Guide: Computer Program for Design and Analysis of Sheet-Pile Walls by Classical Methods (CWALSHT) Including Rowe's Moment Reduction	Oct 1991
Instruction Report ITL-87-2 (Revised)	User's Guide for Concrete Strength Investigation and Design (CASTR) in Accordance with ACI 318-89	Mar 1992
Technical Report ITL-92-2	Fiinite Element Modeling of Welded Thick Plates for Bonneville Navigation Lock	May 1992
Technical Report ITL-92-4	Introduction to the Computation of Response Spectrum for Earthquake Loading	Jun 1992
Instruction Report ITL-92-3	Concept Design Example, Computer Aided Structural Modeling (CASM) Report 1: Scheme A Report 2: Scheme B Report 3: Scheme C	 Jun 1992 Jun 1992 Jun 1992
Instruction Report ITL-92-4	User's Guide: Computer-Aided Structural Modeling (CASM) - Version 3.00	Apr 1992
Instruction Report ITL-92-5	Tutorial Guide: Computer-Aided Structural Modeling (CASM) - Version 3.00	Apr 1992
Contract Report ITL-92-1	Optimization of Steel Pile Foundtions Using Optimality Criteria	Jun 1992
Technical Report ITL-92-7	Refined Stress Analysis of Melvin Price Locks and Dam	Sep 1992